# THE PERFORMANCE OF CEMENTITIOUS BINDER SYSTEMS IN AGGRESSIVE MUNICIPAL WASTEWATER INFRASTRUCTURE

By

**Olasunkanmi Daniel Ilori**


Thesis submitted in fulfilment of the requirements for the degree
of
**Doctor of Philosophy**
at
University of KwaZulu-Natal, Durban

(Civil Engineering)

Supervisor
**Dr Moses Wopicho Kiliswa**

Co-supervisor
**Dr Surabhi Srivastava**

December 2023

# DECLARATION

I, Olasunkanmi Daniel Ilori, declare that,

i) The research reported in this thesis, except where otherwise indicated, is my original work.

ii) This thesis has not been submitted for any degree or examination at any other University.

iii) This thesis does not contain other persons' data, pictures, graphs or other information, unless specifically acknowledged as being sourced from other persons.

iv) This thesis does not contain other persons' writing, unless specifically acknowledged as being sourced from other researchers. Where other written sources have been quoted, then:

   a. Their words have been re-written, but the general information attributed to them has been referenced;
   b. Where their exact words have been used, their writing has been placed inside quotation marks, and referenced.

v) Where I have reproduced a publication of which I am an author, co-author or editor, I have indicated in detail which part of the publication was written by myself alone, and I have fully referenced such publications.

vi) This thesis does not contain text, graphics or tables copied and pasted from the internet, unless specifically acknowledged, and the source being detailed in the thesis and in the references section.

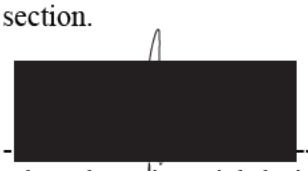

Olasunkanmi Daniel Ilori — 16-12-2023 (Date)

Received and approved:

Dr Moses Wopicho Kiliswa — 29 December 2023 (Date)

**Supervisor**

Dr Surabhi Srivastava — 29-12-2023 (Date)

**Co-supervisor**

# ABSTRACT

Globally, municipal wastewater infrastructure is faced with a common problem known as Microbially Induced Concrete Corrosion (MICC). MICC is deterioration caused by the activities of microorganisms, mainly sulphur-reducing bacteria (SRB) and sulphur-oxidizing bacteria (SOB). Through the activities of SRB, sulphate, contained in wastewater in sewer systems, is anaerobically reduced to hydrogen sulphide ($H_2S$). The $H_2S$ is eventually released into the sewer headspace in gaseous form and is absorbed onto the exposed moist concrete walls where it is aerobically oxidised thus establishing acidic environments for growth of SOB. Through the activities of SOB, the absorbed $H_2S$ is further oxidised to sulphuric acid ($H_2SO_4$), which gradually attacks and destroys the acid-soluble components in the concrete matrix. However, the rate of destruction or corrosion depends on several factors, such as the relative humidity in the sewer headspace, the amount of the acid-soluble components in the concrete matrix, and more significantly, the nature of the binder hydrates.

The aim of the current research was to study the performance of two binder systems in an aggressive wastewater environment, by exposure of various mortar samples; these systems were calcium aluminate cement (CAC)-based and Portland cement (PC)-based. For this study, the newly built Mahatma Gandhi Wastewater Pump Station (MGWWPS) in Durban, South Africa, was chosen as the exposure site for the samples, since it is categorised as an 'aggressive' environment based on the extent of MICC within the first few years of commissioning. To achieve the objectives of study, three different types of mortar samples were produced—CAC-based mortars ($CAC_m$), PC-based mortars ($PC_m$), and PC-based mortar with a crystalline waterproofing admixture, ($PCA_m$). The waterproofing was intended to keep the oxygen from SOB, within the concrete matrix, thus suppressing their acid-generating activities. These mortar samples were installed in the MGWWPS, after 28 days of water-curing in the laboratory, and were continually monitored for over twelve months, prior to undertaking further laboratory testing.

After a 12-month exposure period, total mass loss of about 0.87%, 2.84% and 25.6% was observed on the $CAC_m$, $PC_m$ and $PCA_m$ samples respectively. This translated into a corrosion rate of approximately 0.02 mm/year, 0.7 mm/year and 0.6 mm/year for $CAC_m$, $PC_m$ and $PCA_m$ samples respectively. In addition, backscattered images were taken using the scanning electron microscopy (SEM) technique, and analysed to reveal the microstructural changes that had taken place due to MICC, such as the decrease in the quantities of the products of hydration in the matrix of the mixtures.

Findings from this research showed that of the three cementitious binder systems, CAC-based samples showed the greatest resistance to MICC. Also, the SEM images showed that the binding system of the CAC matrix, which is mainly alumina-based, was still intact, unlike the PC-based samples ($PC_m$), which had its binding system—portlandite, $Ca(OH)_2$ and calcium-silicate-hydroxide gel (C-S-H)—being partially destroyed. Despite incorporating a waterproofing admixture, the modified PC-based samples ($PCA_m$) also had its binding system partially destroyed, although to lesser extent than the $PC_m$. This implies that the corrosion-rate controlling parameter during MICC is the nature of the binder used in concrete mixtures.

# DEDICATION

This thesis is dedicated to my wife, Esther Ehinome, and our daughter, Oluwaloniitan Danielle.

# ACKNOWLEDGEMENT

I would like to express by profound gratitude to my supervisor, Dr Moses Kiliswa, and my co-supervisor, Dr Surabhi Srivastava, for their immense support and guidance towards the success of this work.

My gratitude also goes to the technical staff at the department of Civil Engineering, UKZN: Logan, Ishaan, Lingis, Fathima, Boysie and Linda; my office colleagues: Sam, Janet, Naomi, Nobel, Braimah, Justine, Adekunle, and Abayomi; and the workers at Mahatma Gandhi Pumping Station, for all their contributions.

I also appreciate the Global-Harvest-Church-Akobo family and the New-Life-Church-Durban family, for their prayers and support.

I would also like to extend my gratitude to all my 'sons' and 'daughters': Ayomide, Chidera, Dami, Esther, Favour, Fimidara, Gideon, Glory, Glory, Grace, Jadesola, Jomiloju, Joshua, Marvellous, Michael, Nballu, Ore, Paul, Pelumi, Precious, Precious, Princess, Rere, Simi, Smart, Timi, Tofoye, Tofunmi, Tofunmi, Zainab, and others.

With all my heart, I sincerely appreciate my friends, Fikayo and Anthonia; my siblings, Bukola, Tunde, and Tobi; and my parents, Mr & Mrs Ilori for all their support prior to, and during this work, may God tremendously reward you all.

# TABLE OF CONTENTS

# LIST OF TABLES

# LIST OF FIGURES

# GLOSSARY

| | |
|---|---|
| Acidophilic | Microorganisms that survive in environments with pH below 4. |
| Aerobic | Condition of cellular respiration in the presence of oxygen. |
| Anaerobic | Condition of cellular respiration in the absence of oxygen. |
| Binder | A material used to form materials into a cohesive whole, as a means of providing structural stability. |
| Biofilm | A densely packed community of microbial cells that grow on living or inert surfaces and surround themselves with secreted polymers. Also known as slime. |
| Biogenic | Generated by living organisms or biological processes. |
| Biotic | Derived from or related to living organisms (involves biological mechanisms). |
| Carbonation | A process by which the atmosphere reacts with hydrated cement products to form calcium carbonate thereby reducing the alkalinity of the concrete. |
| Colonization | The presence of bacteria on a surface. |
| Corrosion | Deterioration of a material due to interaction with its environment. |
| Cast-in-situ | Cast on site. |
| Daily flow | This is the total waste volume generated over a 24-hour period |
| Effluent | Waste from domestic, agricultural, or industrial sources conveyed in sewers. |
| Flocculation | process by which a chemical coagulant added to the water acts to facilitate bonding between particles, creating larger aggregates which are easier to separate |
| Hydrophobic | Property of a substance that repel water |
| Microbially | Formed by the interaction of single-cell organisms. |
| Neutrophilic | Microorganisms that survive in environments with a pH range of approximately 6 to 9. |
| pH | A measure of the acidity or alkalinity of a solution, with neutrality represented by a value of 7, with increasing acidity represented by increasingly smaller values and with increasing alkalinity represented by increasingly larger values. |
| Polythionic | A thionic acid containing more than two sulphur atoms in the molecule. |

| | |
|---|---|
| Precast | Construction product produced by casting concrete in a reusable mould or "form" which is then cured in a controlled environment, transported to the construction site and lifted into place. |
| Sewage | See ‘Effluent’. |
| Sewer | An underground conduit for carrying off drainage water and waste matter. Also known as drainage. |
| Siliceous | Containing silica |
| Slime | See ‘Biofilm’. |
| Stoichiometry | Calculation of the relative quantities of reactants and products in chemical reactions. |
| Substrate | These are nutrients required for the growth, metabolism, and activity of microbial cells. |
| Thionic | Relating to or containing sulphur. |
| Tributary area | This is the area that serves a certain sewer segment. |
| Wastewater | See ‘Effluent’. |

# ABBREVIATIONS & ACRONYMS

| | |
|---|---|
| AC | Asbestos cement |
| AE | Auger electrons |
| AIOB | Acidophilic iron-oxidizing bacteria |
| AP | Acrylic polymer |
| APB | Acid-producing bacteria |
| ASOB | Acidophilic sulphur-oxidizing bacteria |
| ATP | Adenosine triphosphate |
| BOD | Biochemical oxygen demand |
| BSA | Biogenic sulphuric acid |
| BSE | Backscattered electrons |
| CAC | Calcium aluminate cement |
| $CAC_m$ | CAC-based mortar |
| CCN | Cement chemistry notation |
| COD | Chemical oxygen demand |
| CL | Cathodoluminescence |
| CWA | Crystalline waterproofing admixture |
| DNA | Deoxyribonucleic acid |
| DO | Dissolved oxygen |
| EDS | Energy dispersive spectroscopy |
| EPS | Extracellular polymeric substances |
| EWS | eThekwini Water and Sanitation |
| FISH | Fluorescence in-situ hybridisation |
| FOG | Fats, oils, and grease |
| FS | Fixed solid |
| FSS | Fixed suspended solid |

| | |
|---|---|
| HDPE | High-density polyethylene |
| ICP | Inductively Coupled Plasma |
| ISA | Ionic strength adjuster |
| ISE | Ion selective electrode |
| MGWWPS | Mahatma Gandhi wastewater pumping station |
| MICC | Microbially induced concrete corrosion |
| MOA | Mode of action |
| MMU | Microscopy and Microanalysis Unit |
| NC | Neutralisation capacity |
| NPC | Natal Portland Cement |
| NSOB | Neutrophilic sulphur-oxidizing bacteria |
| PC | Portland cement |
| $PC_m$ | PC-based mortar |
| $PCA_m$ | PC-based mortar modified with CWA |
| PVC | Polyvinyl chloride |
| QS | Quorum sensing |
| RDO | Relative Dissolved Oxygen |
| RH | Relative humidity |
| SA | styrene-acrylic ester polymer |
| SANS | South African National Standard |
| SBR | Styrene butadiene polymer |
| SE | Secondary electrons |
| SEM | Scanning Electron Microscopy |
| SF | Silica fume |
| SOB | Sulphur-oxidizing bacteria |
| SOM | Sulphur-oxidizing microorganism |
| SRB | Sulphur-reducing bacteria |

| | |
|---|---|
| SRM | Sulphur-reducing microorganism |
| TDS | Total dissolved solids |
| TS | Total solids |
| TSS | Total suspended solids |
| UKZN | University of KwaZulu-Natal |
| VPV | Vinyl copolymer |
| VS | Volatile solid |
| VSS | Volatile suspended solid |
| XRF | X-ray fluorescence |

# NOTATIONS

## CHEMICAL NOTATIONS

| | |
|---|---|
| $3CaO.Al_2O_3.3CaSO_4.32H_2O$ | Ettringite |
| $CaSO_4$ | Calcium sulphate |
| $CaSO_4.2H_2O$ | Gypsum (calcium sulphate dihydrate) |
| $CO_2$ | Carbon dioxide |
| $Fe$ | Iron |
| $H_2S$ | Hydrogen sulphide |
| $H_2SO_4$ | Sulphuric acid |

## CEMENT CHEMISTRY NOTATIONS (CCN)

| CCN | Oxide formula | Compound name |
|---|---|---|
| A | $Al_2O_3$ | Aluminium oxide (a.k.a. Alumina) |
| C | $CaO$ | Calcium oxide |
| $\bar{C}$ | $CO_2$ | Carbon dioxide |
| F | $Fe_2O_3$ | Ferric oxide |
| f | $FeO$ | Ferrous oxide |
| H | $H_2O$ | Water |
| K | $K_2O$ | Potassium oxide |
| M | $MgO$ | Magnesium oxide |
| N | $Na_2O$ | Sodium oxide |
| P | $P_2O_5$ | Phosphorus hemi-pentoxide |
| S | $SiO_2$ | Silicon dioxide (a.k.a. Silica) |
| $\bar{S}$ | $SO_3$ | Sulphur trioxide / Sulphate |
| T | $TiO$ | Titanium dioxide |
| $C_3S$ | $3CaO.SiO_2$ | Tricalcium silicate |

| | | |
|---|---|---|
| $C_2S$ | $2CaO.SiO_2$ | Dicalcium silicate |
| $C_3A$ | $3CaO.Al_2O_3$ | Tricalcium aluminate |
| $C_4AF$ | $4CaO.Al_2O_3.Fe_2O_3$ | Tetracalcium aluminoferrite |
| CH | $CaO.H_2O$ | Calcium hydroxide |
| $C\bar{S}H_2$ | $CaO.SO_4.2H_2O$ | Calcium sulphate dihydrate |
| C-S-H | $3CaO.2SiO_2.3H_2O$ | Calcium silicate hydrate |
| CA | $CaO.Al_2O_3$ | Monocalcium aluminate |
| $C_2A$ | $2CaO.Al_2O_3$ | Dicalcium aluminate |
| $C_2AS$ | $2CaO.Al_2O_3.SiO_2$ | Dicalcium aluminosilicate |
| $C_{12}A_7$ | $12CaO.7Al_2O_3$ | Dodecacalcium hepta-aluminate |
| $CAH_{10}$ | $CaO.Al_2O_3.10H_2O$ | Calcium aluminate decahydrate |
| $C_2AH_8$ | $2CaO.Al_2O_3.8H_2O$ | Dicalcium aluminate octahydrate |
| $C_3AH_6$ | $3CaO.Al_2O_3.6H_2O$ | Tricalcium aluminate hexahydrate |
| $AH_3$ | $Al_2O_3.3H_2O$ | Aluminium trihydrooxide (a.k.a. Alumina hydrate) |
| AFm ($C_2A\bar{S}H_{12}$) | $3CaO{\cdot}Al_2O_3{\cdot}3CaSO_4{\cdot}nH_2O$ | Calcium monosulfoaluminate |
| AFt ($C_3A\bar{S}_3H_{30\text{-}32}$) | $3CaO{\cdot}Al_2O_3{\cdot}3CaSO_4{\cdot}32H_2O$ | Calcium trisulfoaluminate hydrate |

# CHAPTER 1
# INTRODUCTION

## 1.1 General Background

Over the years, methods of disposing sewage have evolved from using 'cat holes', pit privies (also known as earth closets or out houses) and chamber pots to the use of sewer networks as we have today. A sewer network is a well-designed layout of pipelines interconnected for the purpose of draining and collecting domestic, agricultural, and industrial wastewater and conveying them to treatment facilities or a receiving water system (Hvitved-Jacobsen et al., 2013).

From historical records, sewer networks can be traced back to the days of urban revolution which started at about 7000 BC following the establishment of the first urban settlement. The development moved from Ancient Rome to European cities of the medieval period (Middle Ages). However, it was not until about the seventeenth century, that large European and some American cities started developing underground sewer networks as we have it today (Hvitved-Jacobsen et al., 2013).

In constructing sewer pipelines, different materials have been used over the years, such as clay, bricks, polyvinyl chloride (PVC), high-density polyethylene (HDPE), cast iron, ductile iron, asbestos cement (AC), concrete, and steel. However, today, from all these materials, while PVC, ductile iron, and HDPE may be used for small to medium sewer pipelines, concrete is mostly used for large sewer pipelines due to its versatility and cost of production, among other advantages (Taylor, 1997; Jiang et al., 2015; Kaushal et al., 2020).

Since the inception of industrialisation at around late eighteenth and nineteenth centuries, concrete has been the most widely used construction material (WCA, 2016). Concrete is a cohesive mass made up of hard, granular substances known as aggregates (fine and coarse aggregates), glued together by a binder, in the presence of water; this is achieved through chemical process called hydration. Concrete is well known for its high compressive strength and for its durability. In fact, record shows that the life span of structures built using concrete doubles or triples the life span of structures built with other common building materials such as clay, wood and PVC. Nevertheless, like all other construction materials, concrete is still subject to deterioration, degradation, or damage.

In sewer applications, the most common type of deterioration is a special type of corrosion known as Microbially Induced Concrete Corrosion (MICC). MICC is caused by the activities of microorganisms present in the wastewater within the sewer system, and it mostly occurs on the internal wall of the concrete sewer pipe due to the acidic nature of the environment (Jana & Lewis, 2005; House & Weiss, 2014). This problem is not peculiar to some countries but is a global concern, as concrete sewer pipes are being used worldwide. At Hamburg sewage system, Germany, after about 4 – 6 years of operation, it was observed that the concrete matrix had deteriorated to a depth of about 60 mm, while it was also noticed that the corroded concrete consisted of about 50% gypsum and the pH ranged from 1 to 2 (Diercks et al., 1991). In China, the frequent road collapse in recent years were linked to the corroded underground sewer pipes which have been in service for over 40 years. It was discovered that these 50 mm thick concrete pipe had only about 20 mm left (Kong et al., 2017). Reports from various studies indicates that corrosion rate can be within the range of about 1 mm/year up to 12 mm/year depending on how aggressive environment is (Wells et. al, 2012; Lines et al., 2021).

Consequent to the structural damages caused by MICC, the municipality and national budgets are seriously impacted. In the year 1996, over 520 million US dollars was spent in Los Angeles County,

California USA, on the rehabilitation of sewer systems damaged by MICC (Joseph et al., 2012), while in the year 2002, 390 billion US dollars was estimated in USA as the amount needed to repair and rehabilitate existing sewer system for the next 20 years (Gutiérrez-Padilla et al., 2010). In Sydney, Australia, 40 million AUS dollar was estimated to be spent annually to rehabilitate nearly 900km of concrete sewer pipe (Sydney Water, 2012-2013; Sydney Water, 2014), while in Belgium, 4 million Euro was estimated as the annual cost of sewer corrosion (Vincke et al., 2002).

Generally, internal corrosion of concrete sewer pipes has two major causes: conventional acid attack caused by low pH industrial wastes which are discharged directly into the sewer system, and the presence and high activity of biogenic sulphuric acid (BSA), which is microbially induced (Kienow & Kienow, 1991; St. John, et al., 1998). Hydrogen sulphide ($H_2S$) is the most corrosive agent that leads to MICC in sewer network, as attacks the concrete in both the sewer and the wastewater treatment plants (USEPA, 1991).

MICC is a multistage process which can be summarized into four stages (Parker, 1945a; Parker, 1945b; Vollertsen et al., 2008; Chaudhari et al., 2022):

i) Concrete surface initiation
ii) Formation of hydrogen sulphide ($H_2S$),
iii) Production of sulphuric acid ($H_2SO_4$), and
iv) Corrosion of concrete.

Microbial growth is hindered on the surface of fresh concrete due to its high alkalinity; hence, in the first stage MICC the pH of the fresh concrete is reduced to 9 from around 11 to 13. This drop in pH occurs due to carbonation and $H_2S$ acidification (Islander et al., 1991; Joseph et al., 2012; Lines et al., 2021).

The formation of $H_2S$ gas is set into motion by the decomposition of sulphur compounds, and conversion of sulphates and other oxidized sulphur compounds into sulphide (Cayford, et al., 2012), by the action of sulphur-reducing bacteria (SRB), which are anaerobic in nature, and are situated in sewage effluent or slime found in the submerged portion, as shown in Figure 1-1.

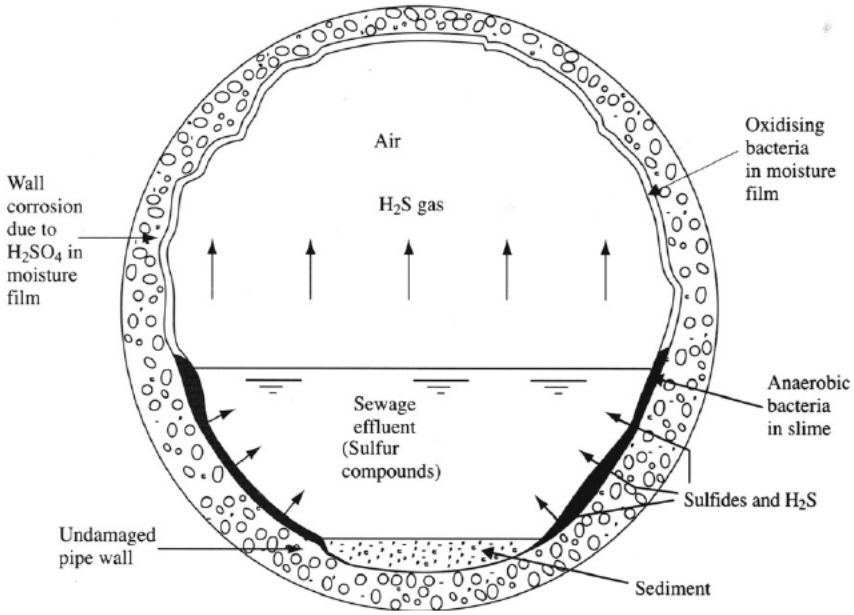


Figure 1-1: Schematic diagram showing the mechanism of sulphuric acid attack in concrete sewage pipe (Jana & Lewis, 2005)

In the third stage of MICC, the $H_2S$ gas diffuses through the sewage and escapes into the sewer atmosphere above the effluent, as shown in Figure 1-1. These gases dissolve into the moisture film that coats the portion of the internal pipe wall above the wastewater line (Okabe et al., 2007), and is rapidly oxidized into dilute sulphuric acid ($H_2SO_4$), and polythionic acids by the action of aerobic neutrophilic sulphur-oxidizing bacteria (NSOB), such as *Thiobacillus species* and *Thiomonas species* (Roberts et al., 2002; Lines et al., 2021; Chaudhari et al., 2022), that colonizes at the crown of the pipe i.e., the exposed arch (Kulpa & Baker, 1990).

Sulphur oxidation is continued by the action of acidophilic sulphur-oxidizing bacteria (ASOB) such as *Acidithiobacillus thiooxidans* which produces high amounts of sulphuric acid that decreases the pH to a range of 1.0 – 2.0 (Diercks et al., 1991; Wei et al., 2013; Lines et al., 2021; Chaudhari et al., 2022). The produced acid dissolves the hydrated binder paste from the crown and the portion of the wall surface above the effluent, and this leads to preferential leaching of paste relative to the siliceous aggregates and corrosion of the inner wall of the pipe.

There are two most common product of sulphuric acid attack: calcium sulphate dehydrates or gypsum ($CaSO_4 \cdot 2H_2O$) and ettringite ($3CaO \cdot Al_2O_3 \cdot 3CaSO_4 \cdot 32H_2O$) (O'Connell et al., 2010; Jiang, 2014; Lines et al., 2021), and this was the case of Hamburg sewage system briefly discussed above (Diercks et al., 1991). Gypsum usually occurs as a white mass on the inner aerated surface of the liner and acts as a protective shield to the interior pipe from further penetration of acid. This gypsum is sometimes washed out by intermittent high flow which adversely exposes 'new' surfaces for further acid attack. (Jana & Lewis, 2005). The formation of gypsum and ettringite weakens the structural integrity of the concrete pipe; this reduces the load-bearing capacity of the concrete and can result in the eventual collapse of the sewer. (Parande et al., 2006; Wells & Melchers, 2015; Lines et al., 2021; Chaudhari et al., 2022).

Corrosion rates of several millimetres per year are reported for sewer pipes (Vollertsen et al., 2008). However, the severity of corrosion depends on several inter-related factors such as the sulphur content of the effluent, the rate and amount of $H_2S$ gas generation, the type and concentration of bacteria causing the $H_2S$-to-$H_2SO_4$ conversion, sewage temperature, pH, and the flow rate of the effluent (Kulpa & Baker, 1990). And in terms of bacteria, the most significant are those that produce acidic sulphur compounds as a result of their metabolic processes.

In the last few decades, several attempts have been made to protect concrete against MICC and the strategies have been based upon two main approaches: (1) modification of the local environment and (2) modification of concrete structure. The former focuses on the optimization of the environmental parameter (e.g. pH and sulphate level) to minimize the microbial activity (Zhang et al., 2008), while the latter approach focuses on the production of more resistant concrete structure through (i) the use of protective materials like polymer linings (Liu & Vipulanandan, 2001; Berndt, 2011); (ii) incorporation of antimicrobial agents such as biocides into concrete mix or the coating systems (Yamanaka, 2002; Do et al., 2005; De Muynck et al., 2010; Scarfato et al., 2012); and (iii) modification of the concrete mixture through the use or incorporation of alternative cementitious materials or special cements (Caballero et al., 2000; Aydin et al., 2007; Goyal et al., 2009; Polder, 2012; Saucier & Kaitano, 2018; Lines et al., 2021; Zapata et al., 2022).

Over decades, calcium aluminate cement has been seen to have the potential to resist conditions supporting MICC. In 1991, after an inspection was carried out in Cairo Egypt, it was discovered that calcium aluminate pipes laid in the 1980's were still in a good condition after many years. It was also discovered that centrifuged Portland cement (PC) concrete pipes lined with CAC mortar laid in the 1950's were still in use (Dumas, 1990). Also, in Florida USA, two installed concrete pipelines,

protected with 100% CAC mortar were observed to have a relatively stable surface pH within the range 3 to 4 for many years despite high $H_2S$ concentration of 100 $ppm$ and above (Saucier & Lamberet, 2009).

Though CAC is four to five times as expensive as PC, which performs well in general applications and applications demanding high strength concrete, it is appreciably considered in sewer applications because of its great acid-attack resistivity, due to its unique chemistry; hence, resulting into a much more improved durability compared to PC-based concrete sewers (Scrivener et al., 1999). And this why it's also being considered in this study.

## 1.2 Research motivation and knowledge contribution

Record shows that most of the sewage pipelines in South Africa were installed late 19th century and 20th century and presently most of them are due for rehabilitation or replacement, as they have deteriorated due MICC, as explained in Section 1.1; this is an existing problem in South Africa, which in fact is a worldwide concern (Metcalf & Eddy, 1922).

In South Africa, polymer linings, such as epoxy, are used as a rehabilitation method; however due to high failure rate in recent time, despite the costs, efforts are being made to have a better and more reliable solution to the problem of $H_2S$ corrosion and the use of cementitious linings such as calcium aluminate cement (CAC) is one of such (Saucier & Kaitano, 2018).

One of the contributions of this study is that while most studies on CAC have been on its use within a concrete mixture, this study focuses on its use within mortar mixture. This is to study its performance in sewer environment as compared with the performance of Portland cement-based mortars, in view of using it as a rehabilitation method.

Another contribution of this study is that a wet-dry scenario is considered during this study for the exposure of mortars, as this better depicts a real-life situation in which sections of pipe wall above the wastewater line are exposed to water during high turbulence or flood.

## 1.3 Aims and objectives of study

The main aims of this research are:

1. To study the performance of two cement systems—calcium aluminate cement (CAC)-based system and Portland cement (PC)-based systems—in an aggressive wastewater environment.

2. To investigate the effect of a crystalline waterproofing admixture (CWA) in a PC-based mortar exposed to MICC.

To achieve the aims of this study as stated above, the objectives of this study are given as follows:

i. To assess the state, in terms of degradation, of the Mahatma Gandhi Wastewater Pumping Station (MGWWPS), Durban, eThekwini municipality, after about 9 years of functioning.

ii. To identify the parameters influencing the rate of MICC of the in-situ sewer environment within MGWWPS and relate this to our understanding of the sewer environment and material properties.

iii. To study how the rate of MICC is affected by three different mortar mixtures—calcium aluminate cement (CAC)-based mortars ($CAC_m$), Portland cement (PC)-based mortars ($PC_m$), and PC-based mortars modified with CWA ($PCA_m$), after a 12-month exposure period.

## 1.4 Scope and Limitations of Study

As briefly explained in Section 1.1, MICC is a complex phenomenon which involves several sewer processes taking place within and across the different phases, and affected by several factors, which can be independently studied. This study, however, focuses on the resulting corrosion rate due to the unique conditions existing in MGWWPS.

This scope was, however, limited by the following:

i. Due to the site used, the samples were not within an enclosed part of the sewer environment, which reduces the concentration of $H_2S$ gas within the sewer atmosphere. This site also had an opening above, which gave room for the escape of sewer gases and ingress of atmospheric gases. This reduces the potential corrosion that would have taken place if it were enclosed, as it is in a sewer pipe.

ii. A wet-dry scenario is considered in this study, which comes with an implication—the mass loss or loss in the dimension of mortar samples may not be totally due to MICC; it may also be attributed to abrasion and collision due to water action during flood or increased volume of flow; however, this was neglected.

## 1.5 Outline of the thesis document

This thesis consists of five chapters.

*Chapter One* presents the general background on the MICC, the main corrosion that takes place in sewer facilities, and how it affects concrete materials. This chapter also covers the research motivation and knowledge contribution, the aim and objectives of study, and the scope and limitation of this study.

*Chapter Two* is divided into four parts. The first part presents a literature review on the components that make up the sewer environment like the sewer pipe (solid phase), the wastewater (liquid phase), and the headspace (gaseous phase), and their characteristics. Also, in this part is a brief discussion on the sewer hydraulics and the sewer design. The second of this chapter dwells on MICC, the mechanism it, the biological and chemical agents involved, and the factors affecting it. The third part focuses on the effect of MICC on PC-based concrete/mortar and CAC-based concrete/mortar. The fourth part of this chapter reviews the recent studies that has been carried out in view of mitigating MICC or the effect it has on concrete sewer.

*Chapter Three* covers all the activities carried during this study which includes, the production of specimens, geographical data on the sewer environment used, assessment carried out on the aggressiveness of sewer, and the investigations carried out on the specimens during the exposure period. This chapter also presents the activities carried out in the environmental laboratory and the other laboratory analytical techniques used during this study.

*Chapter Four* presents and discusses the results gathered from the investigations carried out during the exposure period of specimens and the results obtained from the advanced analytical techniques used.

*Chapter Five* presents the conclusions drawn from the study, while recommendations were also tabled for further work, based on the current study.

## 1.6 References


Aydın, S., Yazıcı, H., Yiğiter, H. and Baradan, B., 2007. Sulfuric acid resistance of high-volume fly ash concrete. *Building and Environment*, *42*(2), pp.717-721.

Berndt, M.L., 2011. Evaluation of coatings, mortars and mix design for protection of concrete against sulphur oxidising bacteria. *Construction and Building Materials*, *25*(10), pp.3893-3902.

Caballero, C.E., Sanchez, E., Cano, U., Gonzalez, J.G. and Castano, V., 2000. On the effect of fly ash on the corrosion properties of reinforced mortars. *Corrosion Reviews*, *18*(2-3), pp.105-112.

Cayford, B.I., Dennis, P.G., Keller, J., Tyson, G.W. and Bond, P.L., 2012. High-throughput amplicon sequencing reveals distinct communities within a corroding concrete sewer system. *Applied and environmental microbiology*, *78*(19), pp.7160-7162.

Chaudhari, B., Panda, B., Šavija, B. and Chandra Paul, S., 2022. Microbiologically Induced Concrete Corrosion: A Concise Review of Assessment Methods, Effects, and Corrosion-Resistant Coating Materials. *Materials*, *15*(12), p.4279.

De Muynck, W., De Belie, N. and Verstraete, W., 2010. Antimicrobial mortar surfaces for the improvement of hygienic conditions. *Journal of applied microbiology*, *108*(1), pp.62-72.

Diercks, M., Sand, W. and Bock, E., 1991. Microbial corrosion of concrete. *Experientia*, *47*(6), pp.514-516.

Do, J., Song, H., So, H. and Soh, Y., 2005. Antifungal effects of cement mortars with two types of organic antifungal agents. *Cement and concrete research*, *35*(2), pp.371-376.

Dumas, T., 1990. Calcium aluminates cementitious binders: an answer to bacterial corrosion. *Int. Sym. On" Corrosion/Degradation of Building Material", Strasbourg, Nov*.

Goyal, S., Kumar, M., Sidhu, D.S. and Bhattacharjee, B., 2009. Resistance of mineral admixture concrete to acid attack. *Journal of Advanced Concrete Technology*, *7*(2), pp.273-283.

Gutiérrez-Padilla, M.G.D., Bielefeldt, A., Ovtchinnikov, S., Hernandez, M. and Silverstein, J., 2010. Biogenic sulfuric acid attack on different types of commercially produced concrete sewer pipes. *Cement and Concrete Research*, *40*(2), pp.293-301.

House, M. and Weiss, W.J., 2014. Review of microbially induced corrosion and comments on needs related to testing procedures.

Hvitved-Jacobsen T., Vollertsen J., & Nielsen, A. H., 2013. *Sewer Processes: Microbial and Chemical Process Engineering of Sewer Networks.* CRC Press, Taylor & Francis group. Pages 1-24.

Islander, R.L., Devinny, J.S., Mansfeld, F., Postyn, A. and Shih, H., 1991. Microbial ecology of crown corrosion in sewers. *Journal of Environmental Engineering*, *117*(6), pp.751-770.

Jana, D. and Lewis, R.A., 2005. Acid attack in a concrete sewer pipe–a petrographic and chemical investigation. In *Proc 27th Int. Conf on Cement Microscopy*.

Jiang, G., Keller, J. and Bond, P.L., 2014. Determining the long-term effects of $H_2S$ concentration, relative humidity and air temperature on concrete sewer corrosion. *Water research*, *65*, pp.157-169.

Jiang, G., Sun, X., Keller, J. and Bond, P.L., 2015. Identification of controlling factors for the initiation of corrosion of fresh concrete sewers. *Water research*, *80*, pp.30-40.

Joseph, A.P., Keller, J., Bustamante, H. and Bond, P.L., 2012. Surface neutralization and $H_2S$ oxidation at early stages of sewer corrosion: Influence of temperature, relative humidity and $H_2S$ concentration. *Water research*, *46*(13), pp.4235-4245.

Kaushal, V., Najafi, M., Love, J. and Qasim, S.R., 2020. Microbiologically induced deterioration and protection of concrete in municipal sewerage system: Technical review. *Journal of Pipeline Systems Engineering and Practice*, *11*(1), p.03119002.

Kienow, K.K. and Kienow, K.E., 1991. Corrosion below: sewer structures. *Civil Engineering*, *61*(9), p.57.

Kong, L., Zhang, B. and Fang, J., 2017. Study on the applicability of bactericides to prevent concrete microbial corrosion. *Construction and Building Materials*, *149*, pp.1-8.

Kulpa, C.F. and Baker, C.J., 1990. Involvement of sulfur-oxidizing bacteria in concrete deterioration. *Special Publication*, *122*, pp.313-322.

Lines, S.J., Rothstein, D.A., Rollins, B. and Alt, C.C., 2021. Microbially Induced Corrosion of Concrete. *Concrete International*, *43*(5), pp.28-32.

Liu, J. and Vipulanandan, C., 2001. Evaluating a polymer concrete coating for protecting non-metallic underground facilities from sulfuric acid attack. *Tunnelling and underground space technology*, *16*(4), pp.311-321.

Metcalf, L. and Eddy, H.P., 1922. *Sewerage and sewage disposal: A textbook*. McGraw-Hill Book Company, Incorporated.

O'Connell, M., McNally, C. and Richardson, M.G., 2010. Biochemical attack on concrete in wastewater applications: A state of the art review. *Cement and Concrete Composites*, *32*(7), pp.479-485.

Okabe, S., Odagiri, M., Ito, T. and Satoh, H., 2007. Succession of sulfur-oxidizing bacteria in the microbial community on corroding concrete in sewer systems. *Applied and environmental microbiology*, *73*(3), pp.971-980.

Parande, A.K., Ramsamy, P.L., Ethirajan, S., Rao, C.R.K. and Palanisamy, N., 2006, March. Deterioration of reinforced concrete in sewer environments. In *Proceedings of the Institution of Civil Engineers-Municipal Engineer* (Vol. 159, No. 1, pp. 11-20). Thomas Telford Ltd.

Parker, C.D., 1945a. The corrosion of concrete: 1. The isolation of a species of bacterium associated with the corrosion of concrete exposed to atmospheres containing hydrogen sulphide. *Australian Journal of Experimental Biology and Medical Science*, *23*(2), pp.81-90.

Parker, C.D., 1945b. The corrosion of concrete: 2. The function of thiobacillus concretivorus (nov. Spec.) In the corrosion of concrete exposed to atmospheres containing hydrogen sulphide. *Australian Journal of Experimental Biology and Medical Science*, *23*(2), pp.91-98.

Polder, R.B., 2012. Effects of slag and fly ash on reinforcement corrosion in concrete in chloride environment: Research from the Netherlands. *Heron, 57 (2012) 3*.

Roberts, D.J., Nica, D., Zuo, G. and Davis, J.L., 2002. Quantifying microbially induced deterioration of concrete: initial studies. *International Biodeterioration & Biodegradation*, *49*(4), pp.227-234.

Saucier, F. & Kaitano, T. (2018). $H_2S$ Biogenic Corrosion – Why using calcium aluminate concrete and mortars to rehabilitate corroded sewer infrastructures. *Imesa Conference*. Port Elizabeth, South Africa.

Saucier, F. & Lamberet, S., 2009. Keynote paper: Calcium aluminate concrete for sewers: going from qualitative to quantitative evidence of performance. *Concrete in aggressive aqueous environments-Performance, Testing, and Modeling*, pp.398-407.

Scarfato, P., Di Maio, L., Fariello, M.L., Russo, P. and Incarnato, L., 2012. Preparation and evaluation of polymer/clay nanocomposite surface treatments for concrete durability enhancement. *Cement and Concrete Composites*, *34*(3), pp.297-305.

Scrivener, K.L., Cabiron, J.L. and Letourneux, R., 1999. High-performance concretes from calcium aluminate cements. *Cement and concrete research*, *29*(8), pp.1215-1223.

Shook, W.E. and Bell, L.W., 1998. Corrosion control in concrete pipe and manholes. In *Proc., Int. Conf. Water Environment federation, Orlando, Fa*.

St John, D.A., Poole, A.B. and Sims, I., 1998. *Concrete petrography: a handbook of investigative techniques*.

Stanaszek-Tomal, E. and Fiertak, M., 2016. Biological corrosion in the sewage system and the sewage treatment plant. *Procedia engineering*, *161*, pp.116-120.

Sydney Water. Sydney Water's Annual Report 2012–2013; *Sydney Water:* Sydney, Australia, 2013.

Sydney Water. Sydney Water Annual Report 2014; *Sydney Water*: Sydney, Australia, 2014.

Taylor, H.F., 1997. *Cement chemistry* (Vol. 2, p. 459). London: Thomas Telford.

USEPA., 1991. *Hydrogen Sulphide Corrosion in Wastewater Collection and Treatment System (Technical Report).* United States Environmental Protection Agency, Office of Water (WH-595), Washington, DC.

Vincke, E., Van Wanseele, E., Monteny, J., Beeldens, A., De Belie, N., Taerwe, L., Van Gemert, D. and Verstraete, W., 2002. Influence of polymer addition on biogenic sulfuric acid attack of concrete. *International biodeterioration & biodegradation*, *49*(4), pp.283-292.

Vollertsen, J., Nielsen, A.H., Jensen, H.S., Wium-Andersen, T. and Hvitved-Jacobsen, T., 2008. Corrosion of concrete sewers—the kinetics of hydrogen sulfide oxidation. *Science of the total Environment*, *394*(1), pp.162-170.

Wei, S., Jiang, Z., Liu, H., Zhou, D. and Sanchez-Silva, M., 2013. Microbiologically induced deterioration of concrete: a review. *Brazilian Journal of Microbiology*, *44*, pp.1001-1007.

Wells, T., Melchers, R., Joseph, A., Bond, P., Vitanage, D., Bustamante, H., De Grazia, J., Kuen, T., Nazimek, J. and Evans, T., 2012, May. A collaborative investigation of the microbial corrosion of concrete sewer pipe in Australia. In *Proceedings of OzWater-12 Australia's National Water Conference and Exhibition* (pp. 8-10).

Wells, T. and Melchers, R.E., 2015. Modelling concrete deterioration in sewers using theory and field observations. *Cement and Concrete Research*, *77*, pp.82-96.

World Cement Association, (WCA), 2016. *Concrete: The most widely used material in the world.* Available from https://www.worldcement.com/special-reports/07122016/concrete-the-most-widely-used-material-in-the-world/. (Accessed June 2019).

Yamanaka, T., Aso, I., Togashi, S., Tanigawa, M., Shoji, K., Watanabe, T., Watanabe, N., Maki, K. and Suzuki, H., 2002. Corrosion by bacteria of concrete in sewerage systems and inhibitory effects of formates on their growth. *Water Research*, *36*(10), pp.2636-2642.

Zapata, J.F., Azevedo, A., Fontes, C., Monteiro, S.N. and Colorado, H.A., 2022. Environmental Impact and Sustainability of Calcium Aluminate Cements. *Sustainability*, *14*(5), p.2751.

Zhang, L., De Schryver, P., De Gusseme, B., De Muynck, W., Boon, N. and Verstraete, W., 2008. Chemical and biological technologies for hydrogen sulfide emission control in sewer systems: a review. *Water research*, *42*(1-2), pp.1-12.

# CHAPTER 2
# LITERATURE REVIEW

## 2.0 Outline

This chapter has been divided into four parts based on focus area:

*Part One* presents a review on the sewer environment and the characteristics of the various active phases that make up the environment—the solid phase, the liquid phase, and the gaseous phase. In addition, this part also presents information on the hydraulics design of sewers as they affect the sewer environment.

*Part Two* presents a review on microbially induced concrete corrosion (MICC), as it is crucial that one understands the mechanism behind its occurrence, how it affects concrete materials, and the factors that promotes it. This knowledge can then be used in making accurate engineering decisions.

*Part Three* presents a review on PC-based concrete/mortars and CAC-based concrete/mortars in sewer facilities and how they affect MICC while highlighting their respective inherent properties that are actively involved in MICC.

*Part Four* presents a review of the recent studies that has been carried out in view of mitigating MICC while also highlighting the methodology used and findings. This is important to reveal progress and ensure that the present study also presents a platform for further studies.

## 2.1 Sewer Environment

### 2.1.1 Introduction

The sewer environment is made of three phases: the liquid phase, which contains the wastewater, biofilm and sewer sediment; the gas phase, i.e., the sewer headspace, which predominantly contain gases associated with the several processes that take place in the sewer environment; and the solid phase, which is the sewer conduit wall and, in this case, the concrete sewer pipe wall which houses the liquid and gas phases. This means that the sewer pipe is affected by the physical, chemical and biological processes in both phases, and the main effect is corrosion caused by the activities of microbial organisms known as Microbially Induced Concrete Corrosion (MICC).

### 2.1.2 Solid phase

The solid phase comprises mainly of the sewer pipe which can be made from different material, as briefly discussed in the earlier part of Chapter 1 and as summarised in Table 2-1 below; however, focus will be on concrete pipes.

Table 2-1: Description of the various types of sewer pipes (Adapted from Davis, 2010)

| Types | Diameter* | Common Material used[#] | Main Function |
|---|---|---|---|
| Lateral | Small | PVC | Collects wastewater from buildings and convey it to main sewers |
| Main | Medium | PVC, VCP, DIP | Conveys wastewater to trunk or intercepting sewers |
| Force main | Medium | HDPE, DIP | Conveys wastewater from pumping stations to trunk or intercepting sewers |
| Trunk | Large | RCP | Conveys wastewater from to intercepting sewers or pumping stations or treatment facilities |
| Interceptor | Large | RCP | Conveys wastewater from to pumping stations or treatment facilities |

*Diameter: Small: 10mm -150mm; Medium: 200mm - 1.5m; Large: 2m - 5m
[#]PVC: Polyvinyl Chloride Pipe; VCP: Vitrified Clay Pipe; DIP: Ductile Iron Pipe; HDPE: High-Density Polyethylene; RCP: Reinforced Concrete Pipe

RCP are mostly trunk sewers and they are often produced with bells and spigot; this is used to connect to other concrete sewer pipes as shown in Figure 2-1 below. A typical trunk sewer also has an invert, which is where most sediments are found, and a crown, where corrosion is most severe, as also shown in Figure 2-2.

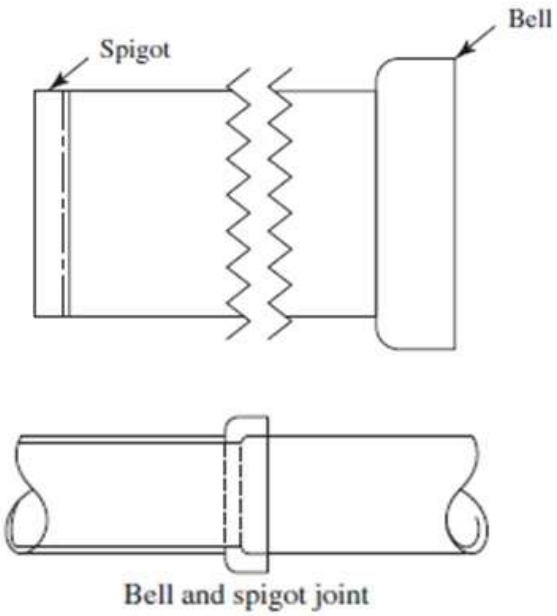


Figure 2-1: Parts of a typical trunk sewer (Davis, 2010)

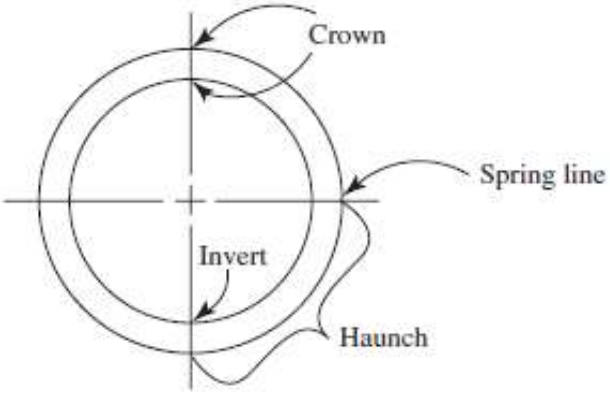


Figure 2-2: Parts of a typical trunk sewer (sectional view) (Davis, 2010)

### 2.1.3 Liquid phase

The liquid phase of the sewer environment consists of the wastewater and the processes that take place within it which includes cycles of carbon, nitrogen, and sulphur.

#### 2.1.3.1 Constituent of wastewater

Municipal wastewater is predominantly water (99.9% by volume) and a relatively small amounts of solids (0.1%), which can be classified as dissolved and suspended or fixed and volatile. Table 2-2 shows the general constituents of municipal wastewater—physical, chemical, and biological

constituents—and their main sources given, while Table 2-3 shows a typical composition of an untreated domestic wastewater.

Table 2-2: General constituents of a typical wastewater (Adapted from Tchobanoglous et al., 2003; Von Sperling, 2007; Kumar, n.d.)

| Constituents | Sources |
|---|---|
| Physical constituents | |
| Solids | Domestic water supply, domestic and industrial wastes, soil erosion, inflow-infiltration |
| Chemical constituents (organic) | |
| Carbohydrates | Domestic, commercial and industrials wastes |
| Fats, oils, and grease | Domestic, commercial and industrials wastes |
| Pesticides | Agricultural wastes |
| Phenols | Industrial wastes |
| Proteins | Domestic, commercial and industrials wastes |
| Surfactants | Domestic, commercial and industrials wastes |
| Others | Natural decay of organic materials |
| Chemical constituents (Inorganic) | |
| Chlorides | Domestic wastes, domestic water supply, ground water infiltration, water softeners |
| Heavy metals | Industrial wastes |
| Nitrogen | Domestic and agricultural wastes |
| Phosphorus | Domestic and Industrials wastes, natural runoff |
| Sulphur | Domestic water supply, domestic and industrial wastes |
| Toxic compounds | Industrial wastes |
| Chemical constituents (gases) | |
| Hydrogen sulphide | Decomposition of domestic wastes |
| Methane | Decomposition of domestic wastes |
| Oxygen | Domestic water supply, surface water infiltration |
| Biological constituents | |
| Animals | Open watercourses and treatment plants |
| Plants | Open watercourses and treatment plants |
| Protista | Domestic wastes and treatment plants |
| Viruses | Domestic wastes |

Table 2-3: Typical composition of untreated domestic waste (Davis, 2010)

| | Concentration ($mg/L$) | | |
|---|---|---|---|
| Constituent | Weak | Medium | Strong |
| Alkalinity (as $CaCO_3$) | 50 | 100 | 200 |
| Ammonia (free) | 10 | 25 | 50 |
| $BOD_5$ (as $O_2$) | 100 | 200 | 300 |
| Chloride | 30 | 50 | 100 |

| Constituent | Concentration ($mg/L$) | | |
|---|---|---|---|
| | Weak | Medium | Strong |
| COD (as $O_2$) | 250 | 500 | 1,000 |
| Total suspended solids (TSS) | 120 | 210 | 400 |
| Volatile suspended solids (VSS) | 95 | 160 | 315 |
| Fixed suspended solids (FSS) | 25 | 50 | 85 |
| Settleable solids, $mL/L$ | 5 | 10 | 20 |
| Sulphate | 20 | 30 | 50 |
| Total dissolved solid (TDS) | 200 | 500 | 1,000 |
| Total Kjeldahl nitrogen (TKN) (as $N$) | 20 | 40 | 80 |
| Total organic carbon (TOC) (as $C$) | 75 | 150 | 300 |
| Total phosphorus (as $P$) | 5 | 10 | 20 |

### 2.1.3.2 Characteristics of wastewater

Municipal wastewater possesses physical, chemical, and microbiological characteristics, and they are described in Table 2-4, Table 2-5, and Table 2-6 respectively. The physical characteristics of wastewater include the colour, odour, temperature, specific gravity, and turbidity; the chemical characteristics include pH value, chloride content, sulphur content, dissolved oxygen, biochemical oxygen demand, chemical oxygen demand, total Kjeldahl nitrogen, and total phosphorus; while the microbiological characteristics include aerobic processes, anaerobic processes, and anoxic processes.

Table 2-4: Physical characteristics of wastewater (Adapted from Von Sperling, 2007; Davis, 2010; Hvitved-Jacobsen et al., 2013; Malay, 2018)

| Physical characteristics | Description |
|---|---|
| Colour | Fresh sewage possesses a light brown, grey or yellowish colour while stale sewage possesses black or dark brown colour, as it has attained septic stage. |
| Odour | Fresh sewage could be musty but as it putrefies, its odour becomes offensive. However, at septic stage, the sewage possesses a rotten-egg smell due to the presence of hydrogen sulphide ($H_2S$) and other compounds formed during the decomposition of sewage. |
| Temperature | This normally ranges from 10℃ to 20℃, and fluctuations occur due to the discharge of hot or warm wastes from households or industries. |
| Specific gravity | This is slightly higher than that of potable water, but it is mostly taken as the same, 1 |
| Turbidity | This is directly dependent on the quantity of suspended particles in the wastewater. |

Table 2-5: Main chemical characteristics of wastewater (Adapted from Von Sperling, 2007; Davis, 2010; Hvitved-Jacobsen et al., 2013; Malay, 2018)

| Chemical characteristics | Description |
|---|---|
| pH value | This is the logarithm of the reciprocal of hydrogen ion ($H^+$) concentration. pH value varies between 1.0 to 14.0, with a neutral value of 7.0. And generally, pH value of a fresh sewage is greater than 7.0, and so alkaline, while pH value of septic sewage is less than 7.0, and so acidic. |
| Chloride | An average chloride content of 120 $mg/L$ is present in domestic sewage, while a higher value could be due to the sea water infiltration or chloride-rich industrial waste. |
| Sulphur | This includes sulphates (${SO_4}^{2-}$), sulphide ion ($S^{2-}$), bisulphide ion ($HS^-$), and hydrogen sulphide ($H_2S$). A fresh sewage often contains a high concentration of sulphate which after decomposition is converted to sulphide species ($S^{2-}, HS^-$ & $H_2S$) with their respective concentrations, dependent on pH.<br><br>Hvitved-Jacobsen et al. (2013) suggested that sewers with wastewater $H_2S$ concentrations level < 0.5, $0.5 - 2$ and > 2 $mg/L$ are respectively, at a low, average and high risk of $H_2S$-related problems like MICC. |
| Dissolved Oxygen (DO) | This is the concentration of dissolved oxygen (DO) present in the wastewater. Generally, fresh sewage has a DO concentration of around 6.5 - 7.0 $mg/L$. It is suggested that with DO > $0.1 - 0.5$ $mg/L$, sulphide build-up should not occur. |
| Biochemical oxygen demand ($BOD_5$) | This gives the oxygen equivalent of the organic matter that can be biochemically oxidized in 5 days at a temperature of 20°C. This is an indicator of the sewage strength. |
| Chemical oxygen demand (COD) | This gives the oxygen equivalent of the organic matter that can be oxidized chemically over 3 hours with the use of a strong oxidizing agent (potassium dichromate, $K_2Cr_2O_7$) in an acid medium. |
| Total Kjeldahl nitrogen (TKN) | This is a measure of the total organic and ammonia nitrogen present in the wastewater. It presents a measure of the availability of nitrogen for microbial cell-building and potential nitrogenous oxygen demand that will have to be satisfied. A fresh sewage usually has a high amount of organic nitrogen and low amount of free ammonia, while the reverse is the case in stale sewage. It should be noted that total nitrogen includes nitrates and nitrites which is not a part of TKN, as they are not always present in fresh sewage, and if present, they are always in low concentration; however, they are present in high concentrations in treated wastewater. |

| Chemical characteristics | Description |
|---|---|
| Total phosphorus (as P) | This includes orthophosphates, polyphosphates, and organic phosphate. |

Table 2-6: Microbiological characteristics of wastewater (Adapted from Hvitved-Jacobsen et al., 2013)

| Microbiological characteristics | Description |
|---|---|
| Aerobic processes | This is characterized by the presence of dissolved oxygen under which organic matter (substrate) in the wastewater is broken down (oxidized) to inorganic substances through the activity of aerobic microorganisms. These processes are predominant in aerated pressure sewers and partly filled gravity sewers. |
| Anaerobic processes | This is characterized by the absence of dissolved oxygen or nitrate ($NO_3^-$) under which sulphate ($SO_4^{2-}$) becomes the primary electron acceptor thereby leading to the formation of $H_2S$. Fermentation is another process that takes place within anaerobic conditions which results into the formation of malodours. These processes are predominant in pressure sewers, full flowing gravity sewers and gravity sewers with low slope and deposits. |
| Anoxic processes | This is characterized by the presence of $NO_3^-$ and absence of DO in the wastewater. Hence, nitrate is used as a terminal electron acceptor. Anoxic processes are not as common as aerobic and anaerobic processes, as most sewage do not contain nitrate; however, when it is present anoxic processes mostly occur within pressure sewers. |

### 2.1.3.3 Redox reactions

The liquid phase of the sewer environment is also characterized by redox reactions i.e., reduction-oxidation reactions. In the presence of an electron acceptor, like DO, $NO_3^-$, and $SO_4^{2-}$, there is a transfer of electrons from the electron donors (the substrates) to the electron acceptors which results into the reduction of these compounds to water ($H_2O$), molecular nitrogen ($N_2$), $H_2S$, respectively, and a corresponding oxidation of the electron donors. The electron donors are the organic substances which are the carbon sources needed for microbial growth. Hence, redox reactions are largely dependent on the microbial condition or microbiological processes, as discussed in Table 2-6, above (Hvitved-Jacobsen et al., 2013).

A simple redox reaction is presented in Equation 2-1 (a), (b), and (c) below, where A represents the electron donor and C the product formed after its oxidation; B represents the electron acceptor and D the product formed after its reduction (Hvitved-Jacobsen et al., 2013).

$$A \rightarrow C + e^- \quad \text{(oxidation half equation)} \qquad (2\text{-}1a)$$

$$B + e^- \rightarrow D \quad \text{(reduction half equation)} \qquad (2\text{-}1b)$$

$$A + B \rightarrow C + D \quad \text{(redox equation)} \qquad (2\text{-}1c)$$

### 2.1.4 Gaseous phase

This phase refers to the sewer headspace or atmosphere which contains gases such as carbon dioxide ($CO_2$), hydrogen sulphide ($H_2S$), ammonia ($NH_3$), oxygen ($O_2$), nitrogen ($N_2$), and sulphur dioxide ($SO_2$).

Table 2-7: Main gases found in sewer headspace (Adapted from Kiliswa, 2016)

| Sewer gases | Description |
|---|---|
| Oxygen ($O_2$) | Just as $O_2$ is found naturally in the atmosphere, it is also found in the sewer atmosphere and depending on the concentration of DO in the liquid phase, $O_{2(g)}$ can flux into the liquid phase where it can be used up by microorganisms. In addition to this, the $O_2$ in the sewer atmosphere can also be influenced by the flow speed, flow depth and temperature. |
| Carbon dioxide ($CO_2$) | Besides the $CO_2$ found in air, this is also generated through the activities of microorganisms in the sewer environment. $CO_2$, in the presence of water, dissolves to form carbonic acid ($H_2CO_3$), which is a weak acid that reacts with the binder hydrates to form calcium carbonate ($CaCO_3$) through a process called carbonation. |
| Ammonia ($NH_3$) | Ammonia is produced within the liquid phase and unlike other sewer gases, it is basic in nature and noncorrosive; however, when it reacts with sulphuric acid, $H_2SO_4$, the resulting compounds— ammonium sulphate ($NH_4HSO_4$) and ammonium bisulphate ($(NH_4)_2SO_4$)— promote MICC. |
| Sulphur dioxide ($SO_2$) | This is produced within the liquid phase during the decomposition of sulphur-based organic matter by microorganisms. It is later released into the sewer atmosphere as $SO_2$ gas, which in the presence of moisture forms sulphurous acid ($H_2SO_3$) and can react with $H_2S$ to form polythionic acids and eventually sulphuric acid, $H_2SO_4$. |
| Hydrogen sulphide ($H_2S$) | Unlike most of the other gases discussed here, $H_2S$ is not naturally found in air; it is produced within the liquid phase as $H_2S_{(aq)}$ and released into the atmosphere as $H_2S_{(g)}$. It is a toxic and corrosive gas with a characteristic rotten-egg odour; it is the most prevalent |

| Sewer gases | Description |
|---|---|
| | odorous gas of all. It is also the most significant gas for MICC to take place. |

### 2.1.5 Gas-Liquid interface

The occurrence of a substance or compound A at the gas-liquid interface is due to its relative occurrence in the gas phase and liquid phase. In the gas phase, it can be described to have a partial pressure, $p_A$, measured in atmosphere (atm) or volumetric expressed parts per million ($ppm$), while in the liquid-phase, it can be described to have a concentration, $c_A$, measured in $gm^{-3}$ or $molL^{-1}$

Another way of describing the concentration of compounds within these phases is using the mole fraction of the compound in the gas phase, denoted by $y_A$, and in the water phase, denoted by $x_A$.

In a two-compound system,

$$y_A = \frac{N_A}{N_A + N_B} \tag{2-2}$$

where:

$y_A =$ mole fraction of compound A ($mol\ mol^{-1}$)
$N_A =$ moles of compound A ($mol$)
$N_B =$ moles of compound B ($mol$)

Consequently, in a two-compound system,

$$y_A + y_B = 1 \tag{2-3}$$

It should be noted that Dalton's law, which states that the sum of the partial pressures of all compounds of a gas mixture equals the total pressure, though valid for an ideal gas, it can also be used for sewer atmosphere of gravity sewers due to its low pressure. Hence, in relation with Dalton's law:

$$y_A = \frac{p_A}{P} \tag{2-4}$$

where:

$p_A =$ partial pressure of compound A in the gas phase ($atm$)
$P =$ total pressure of the gas phase ($atm$)

Also, $y_A$ can be expressed as:

$$y_A = \frac{C_{GA}}{C_{air}} \tag{2-5}$$

where:

$C_{GA} =$ molar concentration of compound A in the air phase
$C_{air} =$ molar concentration of air

Similarly, the mole fraction of compound A in the liquid-phase, $x_A$, can be expressed as:

$$x_A = \frac{C_{LA}}{C_{H_20}} \tag{2-6}$$

where:

$x_A$ = mole fraction of compound A in the water phase ($mol\ mol^{-1}$)
$C_{LA}$ = molar concentration of compound A in water ($mol\ L^{-1}$)
$C_{H_20}$ = molar concentration of water ($mol\ L^{-1}$)

However,

$$C_{H_20} = \frac{density\ of\ water\ (g\ L^{-1})}{molar\ weight\ of\ water\ (g\ mol^{-1})} \tag{2-7}$$

$$= \frac{1000\ g\ L^{-1}}{(2+16)\ g\ mol^{-1}}$$

$$= \frac{1000\ g\ L^{-1}}{18\ g\ mol^{-1}}$$

$$= 55.56\ mol\ L^{-1}$$

Hence, Equation 2-6 becomes

$$x_A = \frac{C_{LA}}{55.56} \tag{2-8}$$

Another widely used principle used to describe the relationship between the gas and liquid phase when at equilibrium is the Henry's law given in Equation 2-9 below.

$$p_A = y_A P = H_A x_A \tag{2-9}$$

where:

$p_A$ = partial pressure of a compound A in the gas phase (atm)
$P$ = total pressure in the gas phase (atm)
$H_A$ = Henry's law constant for A (atm)
$x_A$ = mole fraction of compound A in the liquid phase ($mol\ mol^{-1}$)
$y_A$ = mole fraction of compound A in the gas phase ($mol\ mol^{-1}$)

(Hvitved-Jacobsen et al., 2013)

## 2.2 Hydraulic design of sewers

Just like any other structure, sewers are carefully designed to meet its designed purpose. This is carried out with the knowledge that maximum erosion occurs near the wastewater line and sewer crown, which also are the regions with maximum bending moments (Snaterse, 2013).

### 2.2.1 Design criteria

Critical to the design of sewer are some important criteria, which include design wastewater flow, design period and life expectancy.

### 2.2.1.1 Design wastewater flow

The quantity of wastewater must be determined before embarking on the design of a sewer segment for a tributary area. This is mainly a function of the domestic or sanitary wastewater flow, contributing industrial wastewater flow, extraneous infiltration/inflow (Guyer, 2018).

Domestic or sanitary wastewater flow includes discharges from residences; commercial facilities, such as banks and restaurants; and institutional facilities, such as schools and hospitals. Once the tributary area is known, the contributing population from these facilities must be determined which should include the residents or non-residents. This will help to calculate the average daily flow, average hourly flowrate, peak diurnal flowrate and the extreme peak flowrate. Figure 2-3 presents the daily average flow as a function of the daily minimum flow and the daily peak flow (Davis, 2010; Guyer, 2018).

As for the industrial wastewater flow, which includes wastewater from plants, technical laboratories, laundries, factories, etc., the type and extent of activities must be known; and the peak industrial flow determined.

Extraneous inflow includes wastewater from cooling water discharges, yard drains, foundation drains, roof drains, and storm sewers, while extraneous infiltration includes wastewater from groundwater infiltration which enters the sewer through defective pipes, joints, fittings, and manhole walls (Davis, 2010; Guyer, 2018).

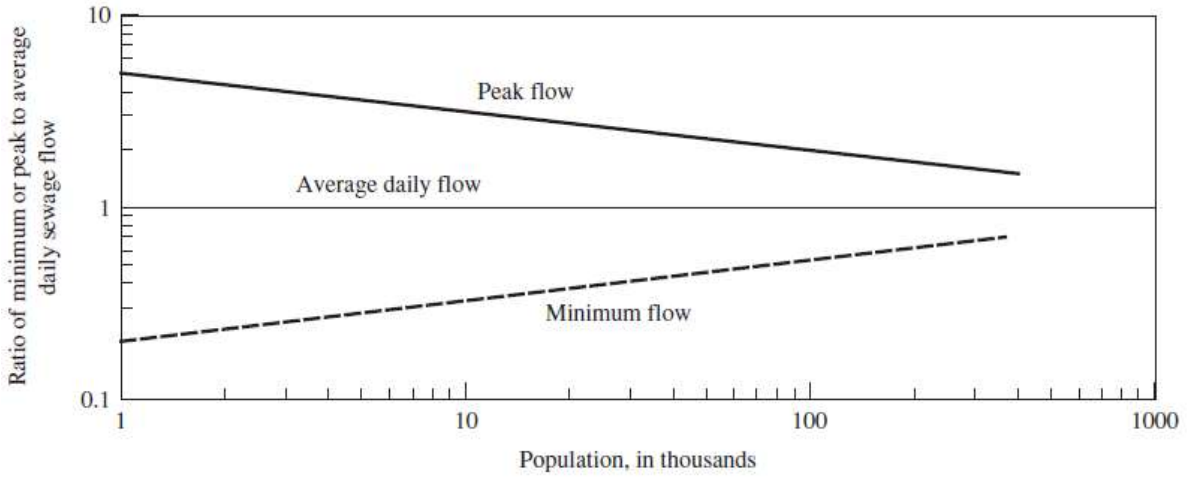


Figure 2-3: Relationship between the flow rates (Davis, 2010)

### 2.2.1.2 Design Period and Life Expectancy

Design Period is also called the Design Life and it is the period over which the sewer facility is expected to meet demand. And generally, sewers are designed to meet future demands to avoid replacement when there is a higher wastewater flow, perhaps due to increase in population in the tributary area (Davis, 2010).

Life Expectancy on the other hand is the period over which the sewer facility is expected to function structurally (Davis, 2010). This is often affected by overloads from external sources or corrosion, commonly caused by hydrogen sulphide. Hydrogen sulphide corrosion is discussed in the second part of this chapter.

Table 2-8: Design periods and life expectancy of sewer (Adapted from Davis, 2010)

| Type of sewer | Characteristics | Design period (yr) | Life Expectancy (yr) |
|---|---|---|---|
| Large pipelines | Difficult and expensive to enlarge or replace | 40-60 | 100+ |
| Mains > 60 cm | Replacement is expensive and difficult | 20-25 | 60+ |
| Laterals and mains ≤ 30 cm | Easy to refurbish or replace | To full development* | 40-50 |

*This means that the tributary area is completely occupied by houses and/or commercial and institutional facilities, and so has no room for population increase.

### 2.2.2 Design Equations

The two main equations used in the design of sewers are the Hazen-Williams equation and the Manning's equation (Manning, 1890) though the latter is used more often due to its flexibility, in that it can be used for both full and partially full sewer designs (Davis, 2010; Guyer, 2018).

Hazen-William's equation:

$$Q = 0.278\, C D^{2.63} S^{0.54} \tag{2-10}$$

where:

$Q$ = flow rate, $m^3/s$
$C$ = Hazen-William's coefficient of roughness
$D$ = diameter of pipe, m
$S$ = slope of energy line, m/m

Given below is the Manning's formula, which is often used for the design of gravity sewers:

$$v = \left(\frac{1}{n}\right)\left(R^{2/3}\right)\left(S^{1/2}\right) \tag{2-11}$$

where:

$v$ = velocity in $m\ s^{-1}$
$n$ = Manning's roughness coefficient of pipe, unitless
$R$ = hydraulic radius, $m$
$S$ = slope of energy line, $m$

Additional useful equations are given below with some derived from the Manning's formula:

$$R = \frac{\text{cross sectional area of flow, m}^2}{\text{wetted perimeter, m}} \tag{2-12}$$

$$S = \frac{(v^2)(n^2)(6.3448)}{(D^{1.333})} \tag{2-13}$$

$$Q = vA = \left(\frac{1}{n} R^{2/3} S^{1/2}\right) A \tag{2-14}$$

where:

$R$ = hydraulic radius, $m$
$S$ = slope of energy line, $m$
$v$ = velocity in $m\ s^{-1}$
$n$ = Manning's roughness coefficient of pipe, unitless
$D$ = diameter of pipe, $m$
$Q$ = flow rate, $m^3/s$
$A$ = cross-sectional area of flow, $m^2$

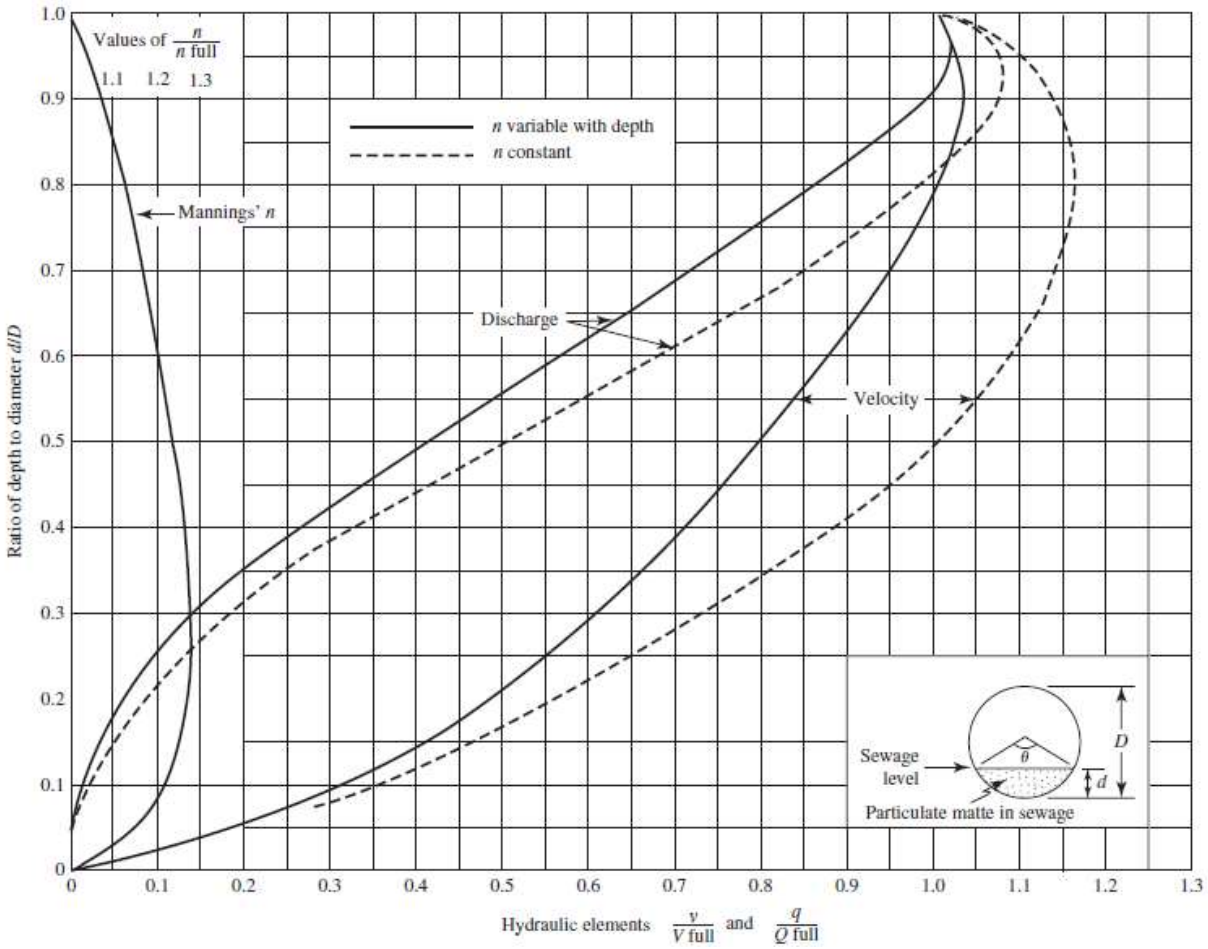


Figure 2-4: Hydraulic properties of circular sewers (Davis, 2010)

The above figure is called Camp's graph, as it was developed by Camp (1946), and it shows the nonlinear behaviour of the parameters in the Manning's equation, and it should be noted that the use of upper-case letters (D, V, and Q) depicts when the pipe is flowing full while lower-case letters (d, v, and q) represents when the pipe is flowing partially full.

### 2.2.3 Design Parameters

Some of the main parameters used in the design of sewer, especially gravity sewers, include pipe size, pipe slope, depth of invert and cover, roughness coefficient, flow velocity, and critical flow.

#### 2.2.3.1 Pipe size

A minimum diameter of 200 $mm$ is used for gravity sewer pipes to minimize clogging when extraneous materials enter the sewer (Lake & Board, 2004). Some engineers design sewers pipes to flow half full at the design capacity to provide a factor of safety; however, according to Steel and McGhee (1979), this practice is justifiable for laterals or branches, as this will give room for future growth in the tributary area, but not for mains, trunk lines, or interceptors.

#### 2.2.3.2 Pipe slope

Pipe slopes must be sufficient to provide the required minimum velocities and depths of cover. Though there is reduced excavation and construction costs on flat slopes, this will result into low flows which will promote the accumulation of solids and the generation of $H_2S$. Assuming uniform flow, the value of '$S$' in the Manning's formula, as given in Equation 2-11 above, is equivalent to the sewer invert slope (Tchobanoglous et al., 2003; Guyer, 2018).

#### 2.2.3.3 Depth

When basements are present, a minimum depth to invert of 3.0 to 3.5 $m$ is recommended or 0.6 $m$ below the lowest basement, and in cases where there are no basements, a minimum of 1.8 to 2.4 $m$ is used, while a maximum depth to invert of 8 to 9 m is recommended (Davis, 2010).

In general, it must be ensured that sufficient depth of cover is provided is protect the sewer from frost. This is because when there is a deep penetration of frost from the earth surface over a long time, the earth surrounding the pipe soon gets cool giving room for the build-up of ice films inside the pipe. And besides frost protection, an adequate depth of cover must also be provided to protect the pipe against structural damage in the event of a superimposed load from the surface (Guyer, 2018).

#### 2.2.3.4 Roughness coefficient

For concrete pipes, the roughness coefficient, '$n$', assumes a value between 0.013 to 0.015. The lower value, 0.013, is used for new pipe or relatively new pipes, in sections greater than 1.5 m, with smooth interior surfaces and in a good condition, while 0.015 is applied to older pipes with rough interior surfaces and in a fair to bad condition (Davis, 2010; Guyer, 2018).

#### 2.2.3.5 Flow velocity

Sewers are often designed to provide a minimum velocity of 0.60 $m\ s^{-1}$ at the average daily flow, or average hourly flowrate, and a minimum velocity of 0.75 to 1.05 $m\ s^{-1}$ at the peak diurnal flowrate. This is important to help flush out organic solids, sand and grits that might have settled at the sewer base during low flows when velocity drops below 0.30 $m\ s^{-1}$. And in case of situations whereby there is high accumulation of grits, sewers are designed with a maximum velocity of 2.50 to 3.00 $ms^{-1}$ (Tchobanoglous et al., 2003; Guyer, 2018).

### 2.2.3.6 Critical flow

Ordinarily, gravity sewers are designed for subcritical flow conditions throughout the normal range of design flow. However, there are times when super critical flow conditions are justified and must be provided for. For instance, in cases when a small to medium sized pipe is required to discharge unusually large flows, a super critical slope is necessitated. Also, the natural topography and ground condition of the route may demand greater slopes (Guyer, 2018).

## 2.2.4 Hydrogen sulphide ($H_2S$) consideration in sewer design

The two major problems related to wastewater sewers are (i) the corrosion of sewers and (ii) the propagation and emission of odorous and toxic gases, which can both be attributed to the generation of $H_2S$ in the sewer; however, with proper design it can be reduced by limiting its concentration below 1.0 $mg/L$ (1.0 $ppm$) (Guyer, 2018).

Given below is a table containing helpful guidelines in designing against $H_2S$ build-up.

Table 2-9: Factors affecting the build-up of $H_2S$ (Adapted from Hvitved-Jacobsen et al., 2013; Guyer, 2018; Saucier & Kaitano 2018)

| Factors | Details |
|---|---|
| Pipe size | Small-sized sewers designed to maintain a flow of 0.6 $ms^{-1}$ and above with adequate air-to-wastewater contact generally experience no significant $H_2S$ build-up, while larger sized sewers are more susceptible to $H_2S$ build-up. |
| Shear stress | This is important to prevent the growth of slime layer and deposits at the sewer invert. To achieve this, shear stress should have minimum value not less than 2 to 4 $Nm^{-2}$. |
| Self-cleaning | As much as possible, sewers should be designed to be self-cleaning in order to prevent the accumulation of deposits on the bottom and build-up of slime layer on the walls. |
| Stagnant water | The sewer must always be designed to flow and not retain water; however, in sewer facilities where this is unavoidable like wet wells and detention tanks, a good ventilation system must be provided to keep enough oxygen in the sewer headspace/atmosphere. |
| Detention time | Detention time in wet wells and detention tanks should be as short as possible to prevent the development of anaerobic conditions that favour $H_2S$ generation. |
| Ventilation | The provision of a good ventilation for the sewer network system will help to release $H_2S$ gas to the natural atmosphere while also allowing for reaeration of the sewer system. These reduces the potential of the occurrence of $H_2S$ corrosion. |

| Factors | Details |
| --- | --- |
| Discharge points | Discharge points on the upstream part of gravity sewers should be avoided except in situations where the discharged anaerobic flow can be immediately diluted by fresh wastewater flow. |

# Microbially Induced Concrete Corrosion (MICC)

## 2.3 Introduction

In a study carried out by Olmstead and Hamlin (1900), it was observed that a white pasty material was formed from a concrete sewer pipe after 5 years. After investigation, it was discovered that it was a result of sulphuric acid attack which led to the formation of expansive gypsum. This was physical evident with cracks and fractures. Parker (1945), a chemist and bacteriologist, also researched into sewer corrosion wherein five strains of sulphur-oxidizing microorganisms (SOM) known as *Thiobacillus* were discovered on the surface of the corroded concrete. Consequently, it was seen that the SOMs were responsible for the conversion of sulphur into $H_2SO_4$ through chemical oxidation. This event led to the term "Microbially Induced Concrete Corrosion, MICC". Other terms are also used to describe this corrosion like "$H_2S$ corrosion" and "Biogenic corrosion", with variations. From records, MICC has the potential to reduce the 100-years expected life span of a sewer to around 30 to 50 years and in extreme cases to 10 years (Jensen, 2009).

## 2.4 Stages of MICC

MICC can be summarized into five stages and stated below, and as depicted in Figure 2-5.

- Initiation stage
- Formation of hydrogen sulphide, $H_2S_{(aq)}$
- Generation of hydrogen sulphide gas, $H_2S_{(g)}$
- Production of sulphuric acid, $H_2SO_4$
- Corrosion of concrete

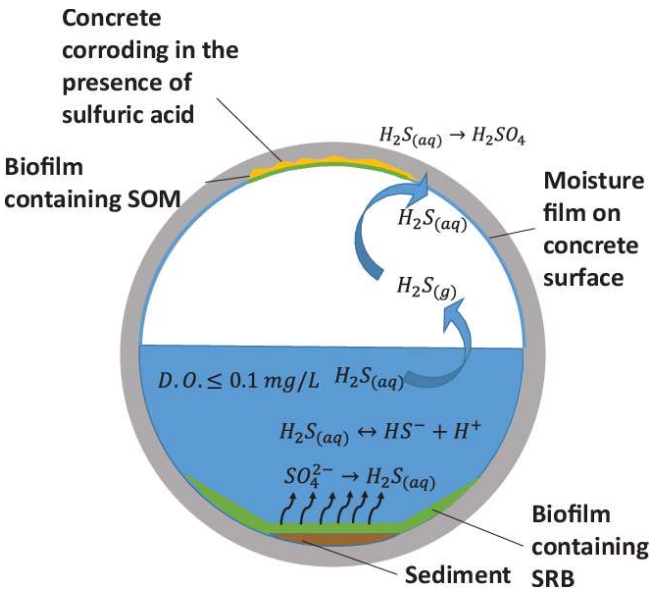


Figure 2-5: Schematic representation of MICC mechanism (House &Weiss, 2014)

### 2.4.1 Initiation stage

As mentioned in Section 2.4, MICC is possible due to the presence of hydrogen sulphide ($H_2S$) and the activity of microorganisms; however, the role of the sulphur-reducing bacteria (SRB) is key, as it is responsible for the formation of $H_2S$. By nature, SRB are slow-growing anaerobe which cannot possibly be in large population within the bulk wastewater; however, the presence of a biofilm (usually at the bottom of the sewer) creates a niche with all the right conditions needed for the growth of SRB (Ito et al., 2002; Chen et al., 2003; Jensen et al., 2016). Therefore, the presence of sewer biofilms plays a very significant role in MICC (Tanaka & Hvitved-Jacobsen, 1998; Vollertsen & Hvitved-Jacobsen, 1998; Abdul-Talib et al., 2002; Zhang et al., 2018; Lines et al., 2021). For this reason, biofouling and the formation of biofilm is discussed here.

Biofilm is a three-dimensional biostructure which adhere to substratum (carrier surface) and contains organized communities of slimy microorganisms, held together and protected by a sticky complex polymer called extracellular polymeric substances (EPS) (Flemming, 1993; George et al., 2000; Vaughn, 2007; Satoh et al., 2009; Cao et al., 2011; Alexander et al., 2013; Liu et al., 2016; Lai et al. 2018). The EPS matrix is secreted by bacteria, and it help to attract and glues microbes and particles to one another and onto surfaces; consequently, a biofilm is gradually formed as shown in Figure 2-6. The biofilm houses different types of microorganisms—bacteria, fungi, algae, etc.—which interact together to benefit one another and ensure survival. Also, the biofilm provides a relatively stable environment for the microorganisms within it compared to bacteria outside the biofilm i.e., in the bulk wastewater (Costeron et al., 1995; O'Toole et al., 2000; Watnick & Kolter, 2000; Cayford et al., 2012; Boltz et al., 2017; Huang et al., 2019). A typical biofilm has a thickness that varies from few micrometres to few centimetres, and besides the microbes, it is made up of $70 - 90\%$ water and $50 - 90\%$ organic matter (Hvitved-Jacobsen et al., 2013).

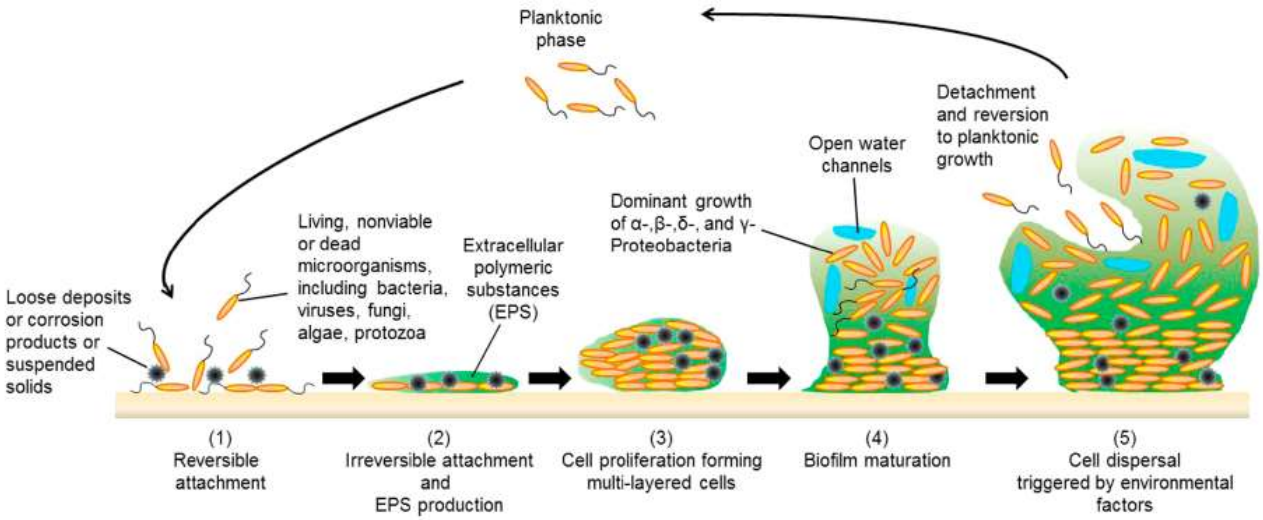


Figure 2-6: Formation and development of biofilm (Liu et al., 2016)

Biofilm formation begins with the transportation of macromolecules, like protein and starch, from the bulk wastewater to the substratum (concrete surface) where some of them are adsorbed, thereby creating a 'conditioned substratum.' This is followed by a reversible attachment of planktonic microbial cells, but some of the cells become irreversibly adsorbed. These adsorbed microbes produce EPS on the surfaces which helps to attract other planktonic microbial cell and particles, leading to an increase in population and biofilm accumulation. The EPS also provides an environment for the

growth of the cells. Gradually, a mature biofilm is made, and soon after maturity, detachment and desorption takes place (Videla & Characklis, 1992). The structure of a mature biofilm often includes microcolonies, aerial hyphae and fruiting bodies and channels to allow the supply of water, oxygen, and nutrients to the microorganisms within (O'Toole et al., 2000; Stoodley et al., 2002).

The development of biofilm is affected by several factors like the wastewater flowrate, which tends to affect the strength of the biofilm; higher flow rate promotes the development of stronger and denser biofilms which could be smaller but more compact (Liu et al., 2016). Other factors that affect the development of biofilm includes temperature, pH, presence of organic matters, and nitrogen-based compounds (Villaverde et al., 1997; Cresson et al., 2006; Gilbert et al., 2015; Liu et al., 2016; Young et al., 2017).

Within the biofilm are aerobes which depend on $O_2$ for respiration and anaerobes which do not depend on $O_2$ for respiration. Due to this, aerobes are found on the uppermost part of the biofilm where they can easily assess the dissolved oxygen (DO) in the bulk wastewater. As a result of this, the uppermost part of the biofilm becomes an aerobic zone as seen in Figure 2-7; consequently, in the absence of DO, an anaerobic zone is created under the aerobic zone as seen in Figure 2-7, which helps to build the anaerobe community (Vaughn, 2007; Snaterse, 2013; Natarajan, 2018).

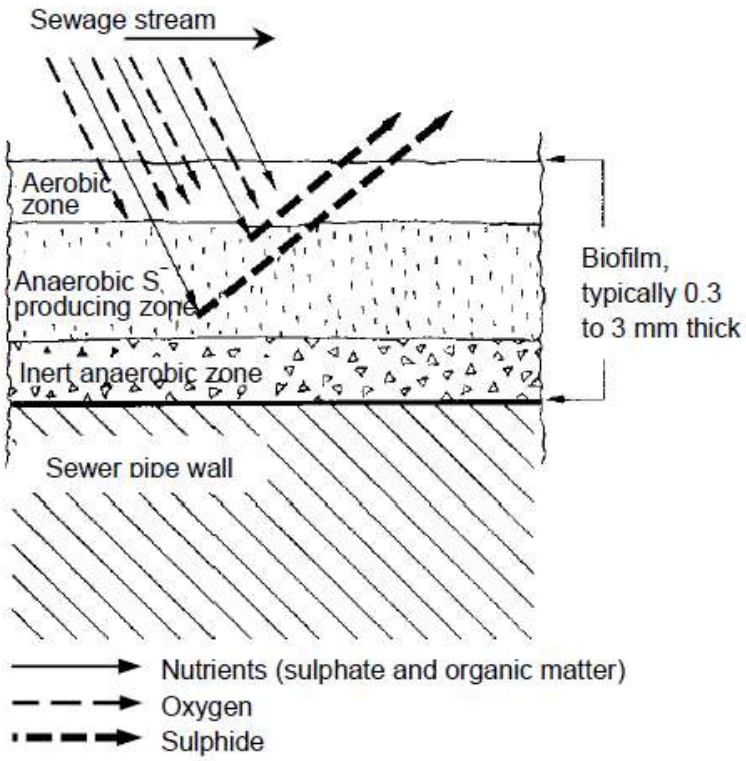


Figure 2-7: Schematic of the layers and activity within a typical biofilm (Boon & Pomeroy, 1990)

### 2.4.2 Formation of hydrogen sulphide, $H_2S_{(aq)}$

On the average, municipality domestic sewage has a sulphate ($SO_4{}^{2-}$) concentration of 40—200 mg/$L$ (Zhang et al., 2008). The sulphate and sulphur compounds are of importance in the formation of hydrogen sulphide within the wastewater. Sulphate, which is the main source of sulphide, is reduced in the presence of sulphur-reducing bacteria (SRB) (Taylor, 1997; Li et al., 2001; Dinh et al., 2004;

Hvitved-Jacobsen et al., 2013; Wu et al., 2018). In a low dissolved oxygen (DO) condition, organic substances (present in the sewage or the ones being formed through the process of fermentation of proteins, carbohydrates, and lipids, etc.) are decomposed by anaerobic SRB (within the biofilm) which uses it as a source of energy (electron donor), while sulphate is used as a terminal electron acceptor (House & Weiss, 2014; Natarajan, 2018; Lines et al., 2021; Chaudhari et al., 2022). These is summarized in Equation 2-15 below.

$$SO_4{}^{2-} + 2C \text{ (organic matter)} + 2H_2O \xrightarrow{SRB} 2HCO_3{}^{-} + H_2S_{(aq)} \quad (2\text{-}15)$$

The common SRB found in municipal sewer pipes, as reported in most studies, are *Desulfovibrio desulfuricans* and *Desulfotomaculum* spp*,* which are obligate anaerobes that depend on sulphate as electron acceptors for respiration (Muyzer & Stams, 2008; Barton & Fauque, 2009; Jensen et al., 2009, 2011; House & Weiss, 2014; Lines et al., 2021; Chaudhari et al., 2022).

Besides the DO content being a contributing factor at this stage, there are other factors that can either accelerate or retard the formation of $H_2S_{(aq)}$ in the wastewater. These conditions include biological oxygen demand (BOD), flow velocity, detention times, turbulence, and wastewater temperature among others (Norsker et al., 1995; Hvitved-Jacobsen et al., 2002; Vaughn, 2007; Sharma et al., 2008; House & Weiss, 2014; Hvitved-Jacobsen et al., 2013; Grengg et al., 2016; Lin et al., 2018; Sun et al., 2018a, 2018b; Qian et al., 2019).

In general, it should be noted that there are three major sources of sulphide. Firstly, the source can be autogenic in which the sulphide is generated within the pipe, as explained in this section. Secondly, the source can be allogeneic, in which sulphide is generated from another source and transferred to the pipe under consideration, for instance $H_2S$ can be generated within a pressure pipe while its emission takes place in the gravity sewer pipe. Thirdly, the source can be exogenous in which sulphide is generated from an external source, for instance the discharge of a sulphide-rich industrial wastewater into the sewer pipe (Snaterse, 2013).

### 2.4.3 Generation of hydrogen sulphide gas, $H_2S_{(g)}$

At this stage, the $H_2S_{(aq)}$ formed from the previous stage is converted into gaseous state resulting into its release as $H_2S_{(g)}$ through diffusion into the sewer headspace (above the wastewater line). This conversion is, however, dependent on some factors which includes (1) wastewater pH, (2) gas-liquid interphase equilibrium condition, (3) temperature, and (4) turbulence of flow (House & Weiss, 2014).

Starting with the first mentioned factor, pH of wastewater, Figure 2-8 shows a relationship between the pH of wastewater and the concentration of sulphide species— hydrogen sulphide ($H_2S$), bisulfide ion ($HS^-$), and sulfide ($S^{2-}$). The figure reveals that at a neutral pH of 7, there is a 1:1 concentration of $H_2S$ and $HS^-$, while in an alkaline environment of a pH of 12, there is a 1:1 concentration of $HS^-$ and $S^{2-}$ (Vaughn, 2007, Kiliswa & Alexander, 2014). More specifically, Figure 2-8 reveals that the more acidic the environment, the more the production of $H_2S_{(aq)}$. It should follow that the higher the production of $H_2S_{(aq)}$, the higher the production of $H_2S_{(g)}$; however, this hypothesis may not be completely true as there are other factors that governs the generation of $H_2S_{(g)}$ as earlier mentioned, which leads us to the second factor. Equation 2-16 & 2-17 shows the ionic reversible reactions involving these sulphide species (Zhang et al., 2008; House & Weiss, 2014; Kiliswa & Alexander, 2014).

$$S^{2-}{}_{(aq)} + H^{+}{}_{(aq)} \longleftrightarrow HS^{-}{}_{(aq)} \quad (2\text{-}16)$$

$$HS^{-}{}_{(aq)} + H^{+}{}_{(aq)} \longleftrightarrow H_2S_{(aq)} \quad (2\text{-}17)$$

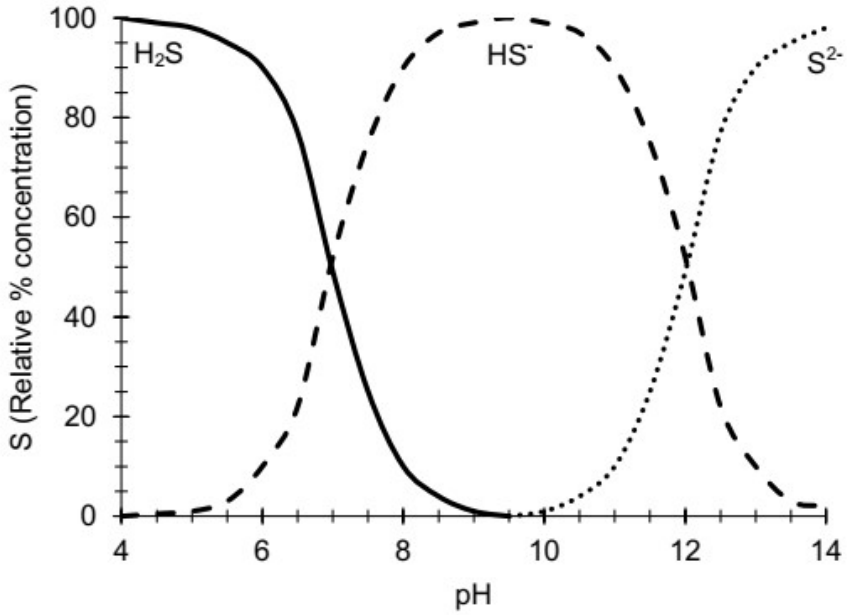


Figure 2-8: Relationship between pH and sulphide species distribution (Morel, 1983)

In addition, at a temperature above 15℃, $H_2S$ is formed as $HS^-$ reacts with $H_2O$. Bisulphide ion acidifies the water resulting into an increasing concentration of hydrogen ion ($H^+$), which in turn accelerates the formation of more bisulphide ion and $H_2S$ (Ehrich & Book, 1996; Snaterse, 2013; Stanaszek-Tomal & Fiertak, 2016).

$H_2S$ escapes into the sewer atmosphere as a gas through diffusion, and if the sewer is running full, as in the case of pressure mains, the gas stays in the bulk water. This conversion of $H_2S_{(aq)}$ to $H_2S_{(g)}$ also depends on the equilibrium with the partial pressure of the gas in the atmosphere. This is governed by Henry's law, which states: "At a constant temperature, the amount of a given gas that dissolves in a given type and volume of liquid is directly proportional to the partial pressure of that gas in equilibrium with that liquid." Equation 2-18 gives the mathematical presentation of the law (Vaughn, 2007; Snaterse, 2013).

$$p_A = y_A P = H_A x_A \quad (2\text{-}18)$$

where,

$p_A$ = partial pressure of compound $A$ (which in this case is $H_2S$) in the gas phase ($atm$)
$P$ = total pressure in the gas phase ($atm$)
$H_A$ = Henry's law constant for compound A (which in this case is $H_2S$) ($mL^- atm^-$)
$x_A$ = mole fraction of compound A (which in this case is $H_2S$) in the liquid phase (mol mol$^{-1}$)
$y_A$ = mole fraction of compound A (which in this case is $H_2S$) in the gas phase (mol mol$^{-1}$)

However, the henry's constant, $H_A$, as stated in the law, depends on temperature (Smith & Harvey, 2007), which in this case will be the sewer temperature. Hence, this suggests also that temperature is a factor that determines the rate of $H_2S$-release. In addition, as seen in the Henry's law equation, the concentration of $H_2S$ in the liquid phase is another factor that contributes to the generation of $H_2S$. Figure 2-9 shows the relationship between these two factors (temperature and $H_2S_{(aq)}$ concentration) and how they affect the concentration of $H_2S_{(g)}$ (House & Weiss, 2014).

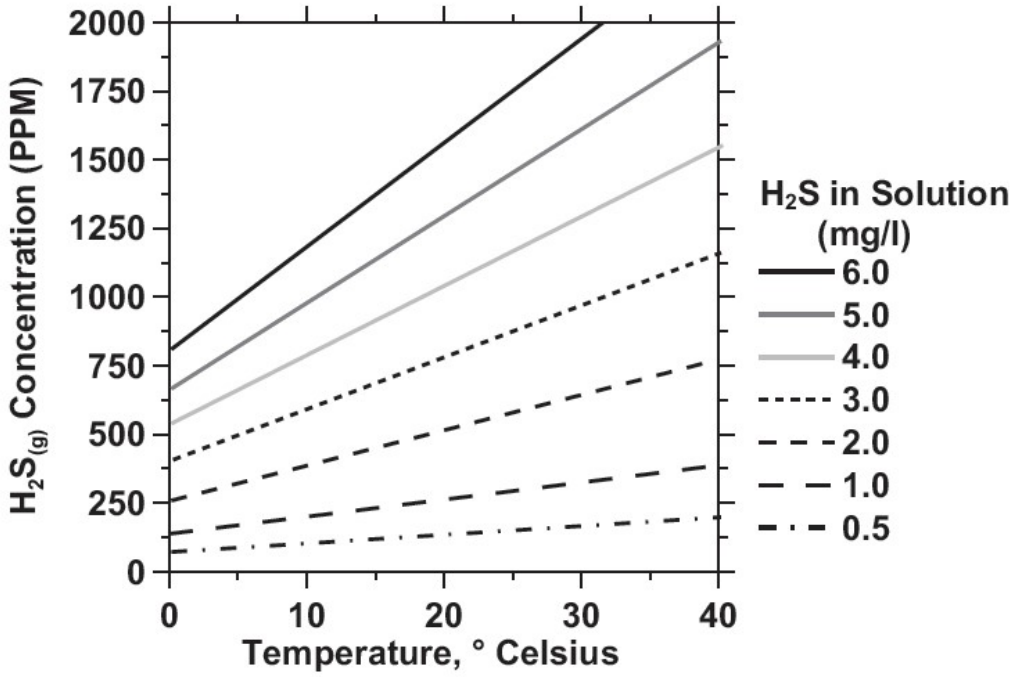


Figure 2-9: Relationship between $H_2S_{(aq)}$ concentration, temperature & $H_2S_{(g)}$ concentration (USEPA, 1985)

Besides the equilibrium, the flux is also dependent turbulence in the flow of wastewater which increases the concentration of $H_2S$ gas in the sewer atmosphere due to an increase in the surface area of the liquid-gas interface. Hence, areas within the sewer network system where this occurs like, manholes, junction boxes, and pumping stations, usually have higher $H_2S$-gas reading. Turbulence within the wastewater sewer system can be due to high wastewater-flow rate, hydraulic jump, sudden drops, or poor construction (Snaterse, 2013; House & Weiss, 2014).

### 2.4.4 Formation of sulphuric acid, $H_2SO_4$

This stage can be further broken down into three phases which dictates the level of microbial activity.

First, it should be noted that fresh concretes are alkaline in nature with a pH range of around 12—13 (Alexander et al., 2013; Kiliswa & Alexander, 2014; Vollpracht et al., 2015). However, this pH range hinders the activity of sulphur-oxidizing bacteria (SOB) until the pH is dropped to around 9. One of the ways this can be achieved is through carbonation of concrete surfaces (Taylor, 1997; Richardson, 2002; Roberts et al., 2002). $CO_2$ in the sewer atmosphere dissolves into the concrete pore water solution of the concrete to form carbonic acid ($H_2CO_3$), a weak acid, as shown in Equation 2-19 (Melchers & Wells, 2010; Yuan et al., 2015). Carbonic acid later dissociates to form carbonate ${CO_3}^{2-}$ which reacts with calcium ion ($Ca^{2+}$), a product of the partial dissociation of calcium hydroxide

($Ca(OH)_2$), as shown in Equation 2-20, to form calcium carbonate ($CaCO_3$) also known as portlandite, as shown in Equation 2-21.

$$CO_2 + H_2O \longrightarrow H_2CO_3 \quad (2\text{-}19)$$

$$Ca(OH)_2 \longrightarrow Ca^{2+} + 2OH^- \quad (2\text{-}20)$$

$$Ca^{2+} + {CO_3}^{2-} \longrightarrow CaCO_3 \quad (2\text{-}21)$$

Besides carbonation, the reaction of $H_2S_{(g)}$ with concrete surfaces also lowers the concrete surface pH (Kaushal et al., 2020).

As soon as the concrete surface pH drops to ~9, neutrophilic sulphur-oxidizing bacteria (NSOB) become very active, which announces the second phase. They form a colony on the surface of the concrete (as seen in Figure 2-5) from where the oxidization of hydrogen sulphide takes place (Equations 2-22, 2-23 & 2-24) (Okabe et al., 2007; Joseph et al., 2012; Natarajan, 2018; Lines et al., 2021; Chaudhari et al., 2022). NSOB use up the $H_2S_{(g)}$ which has diffused into the condensed film on the concrete surface, as electron donor (Islander et al., 1991; Jensen et al., 2011; Yuan et al., 2015). As the pH continues to drop, different species of the genus *Thiobacillus,* as shown in Figure 2-10, continue to oxidize $H_2S_{(g)}$ to form elemental sulphur ($S^0$), thiosulfate ion (${S_2O_3}^{2-}$) or polythionates (${S_nO_6}^{2-}$, where n assumes value from $1-60$) depending on pH conditions. These products eventually form weaker forms of sulphuric acid which further causes the pH of the concrete to drop (Okabe et al., 2007; Satoh et al., 2009; Gomez-Alvarez et al., 2012; Snaterse, 2013; Sun et al., 2015; Stanaszek-Tomal & Fiertak, 2016; Grandclerc et al., 2017; Lines et al., 2021; Chaudhari et al., 2022).

$$2\,H_2S + 2\,O_2 \longrightarrow H_2S_2O_3 + H_2O \quad (2\text{-}22)$$

$$5\,Na_2S_2O_3 + 8\,O_2 + H_2O \longrightarrow 5\,Na_2SO_4 + H_2SO_4 + 4\,S \quad (2\text{-}23)$$

$$4\,S + 6\,O_2 + 4\,H_2O \longrightarrow 4\,H_2SO_4 \quad (2\text{-}24)$$

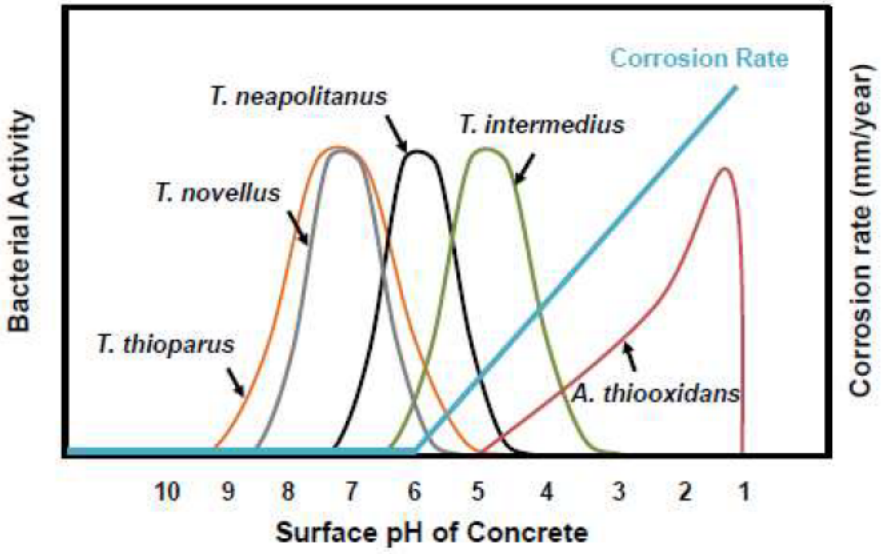


Figure 2-10: Ecological succession of Thiobacillus sp. on the surface of fresh concrete exposed to hydrogen sulphide (Islander, 1991)

The third phase begins at a pH of $\sim 4-5$. Here, the activity of the NSOB decreases while the activity of acidophilic sulphur-oxidizing bacteria (ASOB), like *Acidithiobacillus thiooxidans,* increases (Alexander & Fourie, 2011; Jiang et al., 2016; Li et al., 2017). Like NSOB, ASOB also colonize the concrete surface; however, unlike NSOB, they are able to oxidize $H_2S_{(g)}$ to form sulphuric acids ($H_2SO_4$) directly without any intermediate ($S^0, {S_2O_3}^{2-}, {S_nO_6}^{2-}$). In addition, ASOB also oxidize the intermediates deposited on the concrete walls by the activity of NSOB to produce more sulphuric acid (Islander et al., 1991; Jensen et al., 2008, 2011; Lines et al., 2021; Chaudhari et al., 2022). $H_2SO_4$ is the main agent that causes serious damage to concrete surfaces. As the activity of ASOB, the concrete pH drops to $\sim 1-2$ (House, 2013; Kiliswa & Alexander, 2014; Wu et al., 2018).

Some of the conditions favouring these oxidization processes includes, $H_2S$ gas concentration greater than 2 $ppm$, high RH and high atmospheric oxygen content (Vaughn, 2007).

### 2.4.5 Corrosion of concrete sewer

This MICC stage occurs simultaneously with the previous stage due to the formation of sulphuric acid. First, it should be noted that concretes are alkaline after production so, its durability will be threatened in an environment that is acidic; the more acidic the environment, the more threat the concrete is exposed to. During the hydration of Portland cement in the production of concrete, two main products are formed—portlandite, $Ca(OH)_2$ (simply denoted as CH) and calcium-silicate-hydroxide gel (C-S-H gel)—which forms the binding system of concrete (Mehta & Monteiro, 2013). Sulphuric acid ($H_2SO_4$) formed by the activity of ASOB as explained in Section 2.4 reacts with portlandite and other calcium salts through acid-base reaction (neutralisation) to form calcium sulphate, $CaSO_4$, as represented in Equations 2-25, 2-26 & 2-27 (Guitierrez et al., 2016). Upon further hydration, calcium sulphate dihydrate is form, which is known as gypsum ($CaSO_4.2H_2O$). Consequently, gypsum reacts with the calcium aluminate hydrates to form ettringite ($3CaO.Al_2O_3.3CaSO_4.32H_2O$), as given in Equation 2-28, which is the main product that causes the spalling of concrete and aggregate particles. (Snaterse, 2013; Kiliswa & Alexander, 2014; Guitierrez et al., 2016; Stanaszek-Tomal & Fiertak, 2016).

$$H_2SO_4 + Ca(OH)_2 \longrightarrow CaSO_4.2H_2O \quad (2\text{-}25)$$

$$H_2SO_4 + CaCO_3 \longrightarrow CaSO_4 + H_2CO_3 \quad (2\text{-}26)$$

$$H_2SO_4 + CaOSiO_2.2H_2O \longrightarrow CaSO_4 + Si(OH)_4 + H_2O \quad (2\text{-}27)$$

$$3CaSO_4.6H_2O + 4CaO.Al_2O_3.12H_2O + 14H_2O \longrightarrow 3CaO.Al_2O_3.3CaSO_4.32H_2O \quad (2\text{-}28)$$

Both gypsum and ettringite are expansive in nature. Gypsum is a white mushy substance that has no cohesive properties, so it can be washed away easily. It has a volume expansivity factor of 1.2—2.2 (Harrison, 1984; Wafa, 1994; Wu et al., 2020; Lines et al., 2021). Ettringite, on the other hand, is much more expansive in nature, as it has a volume expansivity factor of 2.3—7 (Monteny et al., 2000; Parande et al., 2006; Chaudhari et al., 2022). During crystallization, expansion takes place which causes an increase in internal pressure, thereby inducing tension resulting into crack formation facilitating disintegration. As seen in Figure 2-11, ettringite occupies an internal layer and as a result of its high expansivity, it leads to bulging and eventually bursting (Roberts et al., 2002; Jiang et al., 2013, Snaterse, 2013; Stanaszek-Tomal & Fiertak, 2016; Lines et al., 2021; Chaudhari et al., 2022).

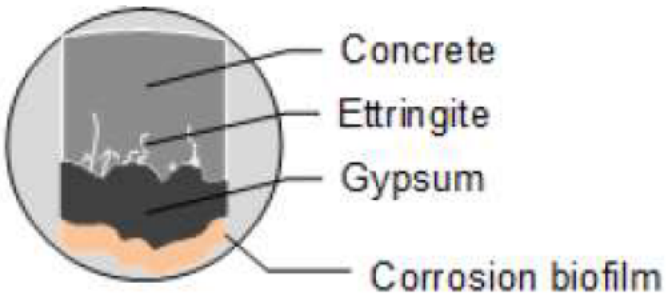


Figure 2-11: Layer within a corroded concrete (Guitierrez et al., 2016)

In the event of high level of wastewater flow or flood, there is a washing away of gypsum from the top layer of concrete, due to its expansion and lack of cohesive properties, which exposes fresh surfaces to the penetration of moisture, acid and microorganism, leading to much more deterioration. Moreover, erosion is maximum at the crown of the sewer and near the wastewater line which are regions with the highest bending moment; hence, the sewer pipe is weakened, it gets unstable, and depending on load conditions, it may eventually lead to collapse if adequate measures are not taken. In fact, so far as the ASOB are present, there will be a continuous production of sulphuric acids on the concrete walls which makes MICC an active deterioration process (Yamanaka, 2002; House, 2013; Snaterse, 2013; Wu et al., 2018).

In general, conditions that will favour corrosion of concrete sewer pipes includes the kind, concentration and strength (pH value) of acid, frequency and duration of concrete exposure, temperature, flow rates, etc. For flow rates, as explained earlier, the acid attack is accelerated as corroded surfaces are continually removed, which exposes fresh surfaces to corrosion. As this cycle continues to repeat, the thickness of concrete pipe is gradual reduces. However, in the case of no-flow conditions, the acid attack is controlled since it has been neutralised through the acid-base reaction and so it stays neutralised. Also, there is reduced amount of $H_2S$ for more production of sulphuric acid (Stanaszek-Tomal & Fiertak, 2016).

## 2.5 Microorganism Involvement

The role of microorganisms in MICC cannot be undermined, and so the remaining subsections in this part of the review focuses on understanding microorganism and why they are so important in MICC.

### 2.5.1 General MICC microorganisms

In general microorganisms can be classified based on their energy or carbon source, their relationship with oxygen and temperature requirement. Table 2-10 show the different classifications.

Table 2-10: Main classification of microorganisms based on energy or carbon source, oxygen, and temperature (Adapted from Davis, 2010)

| Classification based on | Types | Description |
|---|---|---|
| Energy or carbon source | Autotrophs | Require only $CO_2$ as their carbon source |
| | Heterotrophs | Use organic matter as source of carbon |
| | Mixotrophs | Can use different energy and carbon source. |
| | Phototrophs | Rely on light as their source of energy |
| | Chemotrophs | Extract energy by the oxidation of reduced organic molecules (chemoorganotrophs) or inorganic molecules (chemolithotrophs) |
| Oxygen ($O_2$) | Aerobes | Grow in the presence of $O_2$ or may require it to survive. Obligate aerobes can only survive in the presence of $O_2$ while facultative aerobes (may also be called facultative anaerobes) can use $O_2$ or can survive in the presence or absence of $O_2$. |
| | Anaerobes | Obligate anaerobes cannot survive in the presence of oxygen while facultative anaerobes (may also be called facultative aerobes) can use $O_2$ or survive in the presence or absence of $O_2$. |
| Temperature | Psychrophiles | Grow best at a temperature below 20°C |
| | Mesophiles | Grow best within a temperature range of 20°C to 40°C |
| | Thermophiles | Grow best within a temperature range of 45°C to 60°C |
| | Hyperthermophiles | Grow best at a temperature above of 60°C |

The microorganisms involved in MICC are mostly extremophiles, as they show tolerance to extreme variation in temperature, pressure, pH, and metal concentrations (Natarajan, 2018). Table 2-11 shows the classification of the common microorganisms involved in MICC.

Table 2-11: Classification of the main microorganisms involved in MICC (Natarajan, 2018)

| Microorganisms | Classification |
|---|---|
| Bacteria | • Sulphur-oxidizing bacteria (*Acidithiobacillus spp*)<br>• Acid-producing bacteria (inorganic sulphuric acid by *Acidithiobacillus,* organic acid by *Bacillus spp.*)<br>• Sulphur-reducing bacteria (*Desulfovibrio*, *Desulfotomaculum*, *Desulfobacter*)<br>• Iron-oxidizing bacteria or metal-oxidizing bacteria and metal-depositing bacteria (*Gallionella*, *Crenothrix*, *Leptothrix*, *Sphraerotilus*)<br>• Metal-reducing bacteria (*Pseudomonas*, *Shewanella*)<br>• Slime-producing bacteria (*Bacillus*, *Flavobacterium*, *Aerobacter*, *Pseudomonas*) |
| Fungi | • *Clasdosporium resinae*<br>• *Paecilomyces varioti*<br>• *Aspergillus niger*<br>• *Penicillium cyclospium*<br>All fungi produce organic acids |
| Algae | • Blue green algae |
| Microbial consortia | Mutualism among different groups of microorganisms |

As revealed in Table 2-11 above, quite a number of microorganisms are involved in MICC, which adds to the complexity of the mechanism (Javaherdashti, 2009); however, the focus here will be on bacteria, as they have the highest population and greatest influence on MICC due to nature, and in particular sulphur-reducing bacteria (SRB) and sulphur-oxidizing bacteria (SOB), which are also acid-producing bacteria (APB) as they are responsible for the production of inorganic acids (sulphuric acids).

SOB is further classified into two groups: neutrophilic sulphur-oxidizing bacteria (NSOB) and acidophilic sulphur-oxidizing bacteria (ASOB). The NSOB grow and develop within the pH range of around $4-10$ and temperature range of $8-42$℃ while the ASOB grow and develop within the pH range of $0.5-6$ and temperature range of $10-37$℃, as shown in Table 2-12.

### 2.5.2 Sulphur-reducing and sulphur-oxidizing bacteria

While sulphur-reducing bacteria (SRB) and sulphur-oxidizing bacteria (SOB) are not the only microorganisms involved in MICC, as discussed in Section 2.5.1, they are, in no doubt, the main microorganisms involved due to their nature and relevance to sulphur cycle, as shown in Figure 2-12.

Under anaerobic conditions, characterised by low redox potentials due to the absence of dissolved oxygen (DO) and nitrates, at the bottom of the sewer pipe, sulphate ($SO_4{}^{2-}$) contained in sewage is reduced to $H_2S$ through an esoteric reaction by sulphate-reducing bacteria (SRB) e.g., *Desulfovibrio*

*spp* and *Desulfomaculum spp,* which are obligate anaerobic species (Dinh et al., 2004; Vaughn, 2007; Hvitved-Jacobsen et al., 2013; Snaterse, 2013; Lines et al., 2021).

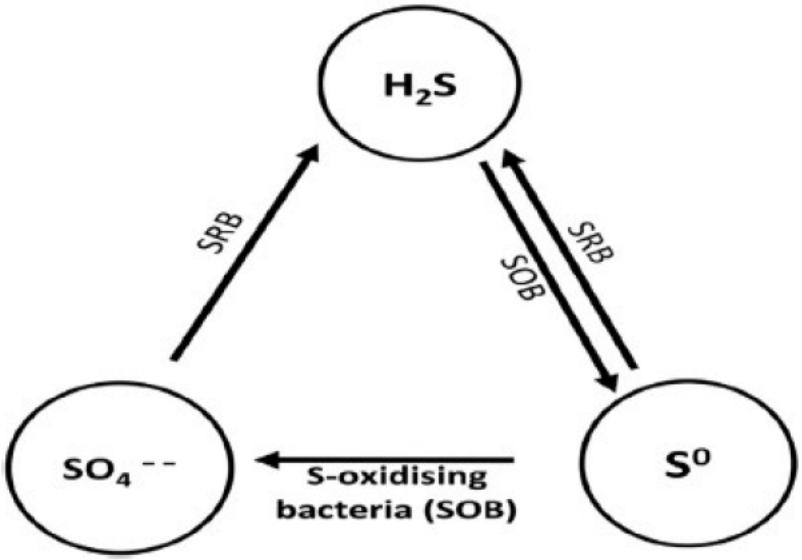


Figure 2-12: Sulphur-bacteria cycle relevant to MICC (Natarajan, 2018)

As the pH of the concrete surface reduces to around 9.5 due to the abiotic chemical reaction with $CO_2$ and acidification of the $H_2S$ gas (present in the sewer atmosphere) to thiosulphate ion ($S_2O_3^{2-}$) and polythionic acid ($H_2S_nO_6$) like trithionic acid ($H_2S_3O_6$) and tetrathionic acid ($H_2S_4O_6$, an environment favourable for bacterial growth is created which permits the growth of NSOB, and the most commonly occurring NSOB in sewer is of the genus *Thiobacillus* (Islander et al., 1991; Sawyer et al., 2003; Stanaszek-Tomal & Fiertak, 2016), which are described in Table 2-12 below.

During high flows, NSOB are taken to the wall and crown of the sewer where they stick to and remain even after the high flow recedes. Under favourable condition, these NSOB grow, and a microbial colony is formed. They use up the $H_2S$ gas emitted from the wastewater as a source of energy (substrate); consequently, elemental sulphur ($S^0$) and polythionic acids like thiosulphate ($S_2O_3^{2-}$) are produced, which further reduces the pH of the concrete and also acts as a substrate for many *Thiobacilli* species like *Acidithiobacillus thiooxidans, Thiomonas intermedius, Halothiobacillus neopolitanus, Thiobacillus novellus*, and *Thiobacillus thioparus* (Kelly et al., 2000; Roberts et al., 2002), as given in Table 2-12.

At a concrete surface pH reduces to around 4, the growth of NSOB is truncated; however, this ushers in the acidophilic sulphur-oxidizing bacteria (ASOB), *Acidithiobacillus thiooxidans* (Figure 2-13), which grows under the pH of 4. The ASOB metabolize the elemental sulphur and thiosulphate into $H_2SO_4$ which result into a further reduction of the concrete pH to around 2, where it may be sustained depending on how severe the aggressiveness of the sewer is (Vincke et al., 2002).

Table 2-12: Sulphur-oxidizing bacteria (*Thiobacillus*) species involved in MICC and their characteristics (Guitierrez et al., 2016)

| Species | Growth pH | Temp. (°C) | Lifestyle | Sulphur substrates |
|---|---|---|---|---|
| *Thiobacillus thioparus* | 4.5-10 | 15-42 | Autotrophic aerobe | Thiosulphate, sulphide, thiocyanate |
| *Starkeya novella (Thiobacillus novellus)* | 5-9.2 | 10-37 | Mixotroph | Thiosulphate |
| *Halothiobacillus neopolitanus* | 4.5-8.5 | 8-39 | Autotroph | Thiosulphate, sulphur, sulphide |
| *Thiomonas intermedia* | 5-7.5 | 15-37 | Mixotroph | Thiosulphate, sulphide |
| *Thiobacillus plumbophilus* | 4-6.5 | 9-41 | Autotroph | Sulphide |
| *Thiothrix spp.* | Neutral pH | 10-30 | Mixotroph | Thiosulphate, sulphide |
| *Thiobacillus intermedius (Thiomonas intermedia)* | 1.7-9 | 15-37 | Mixotroph | Thiosulphate |
| *Acidithiobacillus thiooxidans* | 0.5-5.5 | 10-37 | Autotroph | Thiosulphate, Sulphur |
| *Acidiphilum acidophilum* | 1.5-6.0 | 10-37 | Heterotroph | Thiosulphate, Sulphur |

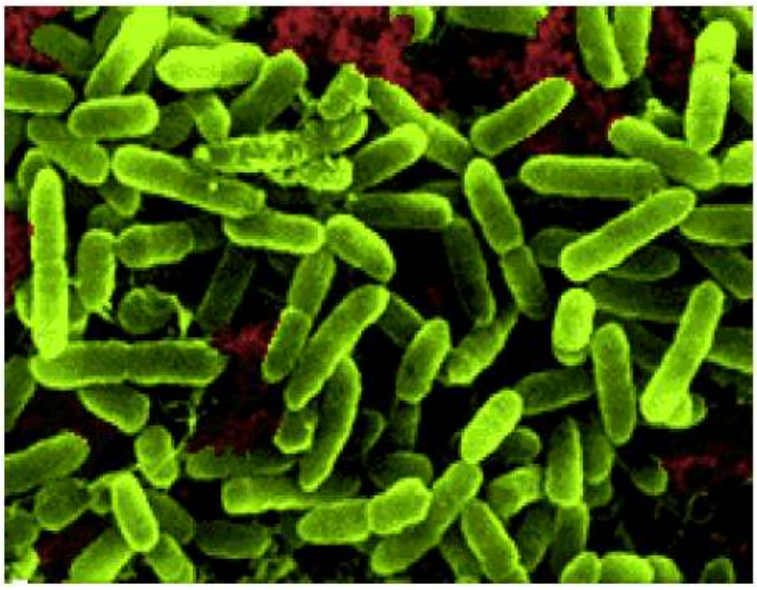

Figure 2-13: Electron microscope picture of *Acidithiobacillus thiooxidans* (Khan et al., 2012)

### 2.5.3 Conditions that favour the activities of SRB and SOB

There are several factors that favour the metabolic activities of SRB and SOB, some of which have been mentioned in previous sections. The factors include DO content, sulphate concentration, $H_2S$ concentration, relative humidity (RH), temperature; and design-influenced factors like slope, flow speed, retention duration, and ventilation. How these factors favour the activities of SRB and SOB is described in Table 2-13 below.

Table 2-13: Conditions favouring the activities of SRB and SOB within the sewer (Adapted from Vaughn, 2007; Davis, 2010; Joseph et al., 2012; Wells et al., 2012; Hvitved-Jacobsen et al., 2013; Wei et al., 2013; Romanova et al., 2014; Stanaszek-Tomal & Fiertak, 2016; Saucier & Kaitano, 2018)

| Condition | Description |
|---|---|
| Low DO content. | This promotes the activities of SRB, as it creates an anaerobic condition, suitable for their growth, within the liquid phase. |
| Sulphate-rich wastewater | This promotes the metabolic activities of SRB who use sulphate as a source of energy, leading to their growth. |
| Low ventilation | This reduces the amount of $O_2$ that enter the sewer network to replace the depleted dissolved oxygen (DO) while also reducing the amount of $H_2S$ gas that can escape from the sewer atmosphere into the natural atmosphere. |
| Long retention times | This gives room for the development of biofilm at the bottom of the pipe and hence, promoting the growth of SRB community. |
| Low flow speed | This also encourages the development of biofilm and hence, the SRB community, thereby promoting their activity and growth. |
| Little slope | This also encourages the accumulation of deposits at the bottom of the sewer pipe leading to anaerobic conditions below the wastewater line. |
| Elevated temperatures | This promotes the release of $H_2S$ gas into the sewer atmosphere making more $H_2S$ gas available for the use of SOB |
| Turbulence | This also promotes the release of $H_2S$ gas from the liquid phase of the sewer thereby increasing the concentration of $H_2S$ gas in the sewer atmosphere. |
| High $H_2S$ gas concentration | High concentration of $H_2S$ gas in the sewer headspace promotes the activities of both NSOB and ASOB, who use it up as a source of energy. |
| High relative humidity (RH) | This ensures that the sewer walls remain moist; hence, more $H_2S$ gases are able to dissolve into the condensed moisture film, where it can be used for the metabolic activities of SOB. |

## 2.6 PC-based concrete

Most concrete infrastructures are Portland cement (PC)-based, as the binder used in the mixture is Portland cement (PC).

### 2.6.1 Introduction

PC has lime ($CaO$) and silica ($SiO_2$) as its main oxides, as shown in Table 2-14, in the form of tricalcium silicate ($C_3S$) and dicalcium silicate ($C_2S$), as shown in Table 2-15, which when in reaction with water ($H_2O$) predominantly forms amorphous calcium silicate hydrate ($CSH$) and crystalline calcium hydroxide ($CH$) (Scrivener et al., 1999). More details on the process are given later in this chapter.

Table 2-14: Typical oxide composition of Portland cement (Adapted from Neville & Brooks, 1987)

| Oxide | CCN | Oxide formula | % by mass |
|---|---|---|---|
| Lime | C | $CaO$ | 63 – 69 |
| Silica | S | $SiO_2$ | 19 – 24 |
| Alumina | A | $Al_2O_3$ | 4 – 7 |
| Ferric oxide | F | $Fe_2O_3$ | 1 – 6 |
| Ferrous oxide | f | $FeO$ | 0 |
| Sulphate | $\bar{S}$ | $SO_3$ | 1.3 – 3.0 |
| Magnesium oxide | M | $MgO$ | 0.5 – 3.6 |
| Titanium oxide | T | $TiO_2$ | 0 |
| Alkalis | N, K | $(Na_2O, K_2O)$ | 0.2 – 0.8 |

Table 2-15: Typical proportion of the major mineral components of cement clinker (Adapted from Neville & Brooks, 1987)

| Mineral name | Phase | % by mass |
|---|---|---|
| Alite | $C_3S$ | 55 – 65 |
| Belite | $C_2S$ | 15 – 25 |
| Celite | $C_3A$ | 8 – 14 |
| Ferrite | $C_3AF$ | 8 – 12 |
| | $CA$ | 0 |

### 2.6.2 Hydration of PC

The hydration of PC is an exothermic reaction set in place when PC combines with water ($H$), which occurs rapidly in the early stage and slowly thereafter. The two main products of PC hydration are a

complex and poorly crystalline calcium-silicate-hydroxide gel, also known as C-S-H gel, and a highly crystalline calcium hydroxide ($CH$) also known as portlandite (CNCI, 2009).

Hydration of PC is a complex process that is better understood when broken down into the reactions of the silicate phases ($C_3S$ and $C_2S$) and aluminate phases ($C_3A$ and $C_3AF$). In the presence of water, alite ($C_3S$) is hydrated to produce $CSH$ and portlandite as given in Equation 2-29. $CSH$ contributes greatly to the initial strength of PC while portlandite does not, it however helps to maintain a pH of about 12.5 in the pore water, which helps to protect rebars against corrosion (Mindess & Young, 2002; CNCI, 2009).

$$2C_3S + 6H \longrightarrow C_3S_2H_3 + 3CH + \text{Heat (120 cal/g)} \quad (2\text{-}29)$$

Belite ($C_2S$) also reacts with water to form $CSH$ and portlandite, but a lesser heat is released. And like the in the hydration of alite, the C-S-H gel produced contributes to the strength; however, this occurs at a slow rate. Hence, it is responsible for the long-term strength of PC concrete (Mindess & Young, 2002).

$$C_2S + 4H \longrightarrow C_3S_2H_3 + CH + \text{Heat (62 cal/g)} \quad (2\text{-}30)$$

Ferrite ($C_4AF$) in the presence of water react with gypsum to form ettringite, portlandite and alumina hydroxides as shown in Equation 2-31. Progressively, ferrite further reacts with the produced ettringite to form garnet (Equation 2-32), which only takes space and does not contribute to the strength on PC paste (Mindess & Young, 2002).

$$C_4AF + 3C\bar{S}H_2 + 3H \longrightarrow C_6(A,F)\bar{S}_3H_{32} + (A,F)H_3 + CH \quad (2\text{-}31)$$

$$C_4AF + C_6(A,F)\bar{S}_3H_{32} + 2CH + 23H \longrightarrow 3C_4(A,F)\bar{S}H_{18} + (A,F)H_3 \quad (2\text{-}32)$$

Lastly, celite ($C_3A$) reacts with gypsum ($C\bar{S}H_2$) to produce ettringite ($C_2A\bar{S}_3H_{30-32}$), which are only stable in the presence of gypsum; however, when gypsum is used up, it becomes unstable and so reacts with the remaining celite in the PC to produce monosulphate aluminate hydrate crystal as given in Equation 2-34 (Mindess & Young, 2002).

$$C_3A + 3C\bar{S}H_2 + 26H \longrightarrow C_6A\bar{S}_3H_{32} + \text{Heat (207 cal/g)} \quad (2\text{-}33)$$

$$2C_3A + 3C_6A\bar{S}_3H_{32} + 22H \longrightarrow 3C_4A\bar{S}H_{18} \quad (2\text{-}34)$$

These crystals are generally stable except in the presence of sulphate, wherein they are converted back to ettringite; however, now with a much larger crystal size (about 2.5 times larger), which is the main product in the corrosion of sewer facilities, as explained in Section 2.4.5 (Mindess & Young, 2002).

### 2.6.3 PC in an acidic environment

In the presence of acid, calcium hydroxide $Ca(OH)_2$, also known as portlandite, contained in PC dissolves. Consequently, the concrete pores open which gives room for further acid attack. As these process repeats, there is an increasing depth of attack over time. Besides the dissolution of $Ca(OH)_2$, the calcium contained in the C-S-H gel also dissolves which leaves a structureless silica gel (Scrivener et al., 1999). Due to this attack, PC concrete surfaces become very rough, it loses thickness and weight, and the aggregate pops out.

### 2.6.4 Neutralisation capacity of PC

The neutralisation capacity (NC), also known as alkalinity, of any material is the amount of acid required to neutralise a certain amount of material; in other words, it reveals the amount of acid that can be neutralised by a certain amount of material. These amounts are not fixed, as it depends on the material being used. The neutralisation capacity of PC is, therefore, its capacity to react with and neutralise acid (in this case, biogenic $H_2SO_4$ acid).

Within an acidic environment, two things take place: firstly, the materials in PC binder system are 'attacked' therefore causing an alteration, and secondly, the 'attacking' acid, itself, is consumed i.e., neutralised, by the material, which, in fact, is the primary indicator of MICC (Kiliswa, 2016).

$$nH^+ + \text{material} \longrightarrow Ca^{2+} + \text{altered material} \tag{2-35}$$

As shown in Equation 2-35, the consumption of a certain amount of acid is directly proportional to the destruction of a certain amount of acid. Hence, neutralisation capacity can be expressed as given in Equation 2-36 below.

$$\text{NC (milliMoles/grams(mM/g))} = \frac{\text{No of acid H atom (mM)}}{\Delta \text{ mass of material (g)}} \tag{2-36}$$

With Equation 2-36 and stoichiometry, one can calculate the potential neutralisation capacity of PC and any other material once the chemical composition is known (Kiliswa, 2016).

The NC of PC is later compared with that of CAC in Section 2.7.4.

### 2.6.5 PC-based concrete modified with CWA

Admixtures are substances, besides water, aggregate and cement, used in the production of concrete to enhances cementing properties; hence, they are added to improve a certain property in the concrete. Waterproofing admixtures—most of which are crystalline—are targeted towards reducing permeability in concrete, and its commonly used to control crack development within the concrete, which is one of the most common structural defects in concrete structures (Nataadmadja & Runtuwene, 2018).

Crystalline waterproofing admixtures (CWA) consist of PC, treated quartz and a number of active chemicals which manufacturers present as confidential information. The waterproofing effect is achieved due to the chemical reactions that take place within the solution when combined with concrete matrix (Rahhal et al., 2009; Pazderka & Hájková, 2016). They react with calcium hydroxide ($CH$) and other product of cement hydration to form insoluble hydrophobic crystals, which fills the existing microcracks, pores, and capillaries in the concrete and resist external water. Equation 2-37 shows a simplified chemical reaction between cement and water in a conventional concrete (without admixture), while Equation 2-38 describes the effect of adding CWA to the mix (Biparva & Gupta, 2010; Garcia-Vera et al., 2019; Figmig, 2020).

$$\text{Cement} + \text{water} = \text{calcium silicate hydrate } (CSH) + \text{calcium hydroxide } (CH) \tag{2-37}$$

$$\text{Cement} + \text{water} + \text{CWA} = CSH + CH + \text{pore blocking crystals} \tag{2-38}$$

Several studies have shown and verified that CWA are, indeed, effective in waterproofing; hence, they improve the durability of concrete (Dao et al., 2010; Wang et al., 2012; Reiterman & Bäumelt, 2014; Cappellesso et al., 2016; Pazderka & Hájková, 2016; Garcia-Vera et al., 2019; Figmig, 2020; Matar & Barhoun, 2020). However, its effect on strength is not yet well established; some studies have reported increase in compressive strength (Cappellesso et al., 2016; Matar & Barhoun, 2020), while some have reported that it has no significant effect on compressive strength (Pazderka & Hájková, 2016; Garcia-Vera et al., 2019; Gojević et al., 2021).

## 2.7 CAC-based concrete

For decades now, in some parts of the world, calcium aluminate cement (CAC) is being used in the place of PC for sewer infrastructures due to its durability. This section throws more light into CAC and why it is more durability in sewer environments.

### 2.7.1 Introduction

Calcium aluminate cement (CAC) is produced when calcium aluminate clinker, a partially or completely fused product consisting of hydraulic calcium aluminates, is pulverized. However, unlike PC, CAC has lime ($CaO$) and alumina ($Al_2O_3$) as its main oxides, as shown in Table 2-17, which combine to form monocalcium aluminate ($CA$) as the main active phase, as shown in Table 2-18; this reacts with water ($H_2O$) to give calcium aluminate hydrates (Scrivener et al., 1999; Zapata et al., 2022). More details on the process are given later in this chapter.

Table 2-16:Typical oxide composition of CAC (Taylor, 1997)

| Oxide | CCN | Oxide formula | % by mass |
|---|---|---|---|
| Lime | C | $CaO$ | 37 – 39 |
| Silica | S | $SiO_2$ | 3 – 5 |
| Alumina | A | $Al_2O_3$ | 38 – 40 |
| Ferric oxide | F | $Fe_2O_3$ | 15 – 18 |
| Ferrous oxide | f | $FeO$ | 3 – 6 |
| Sulphate | $\bar{S}$ | $SO_3$ | 0 – 0.2 |
| Magnesium oxide | M | $MgO$ | 0 – 1.5 |
| Titanium oxide | T | $TiO_2$ | 2 – 4 |
| Alkalis | N, K | $(Na_2O, K_2O)$ | 0 – 0.4 |

Table 2-17: Typical proportion of the major mineral components of CAC (Clarke, 1997)

| Mineral name | Phase | % by mass |
|---|---|---|
| Alite | $C_3S$ | 0 |
| Belite | $C_2S$ | 0 – 10 |
| Celite | $C_3A$ | 0 |
| Ferrite | $C_3AF$ | 10 – 40 |
| | $CA$ | 40 – 50 |

### 2.7.2 Hydration of CAC

Monocalcium aluminate ($CA$), formed by the combination of lime and silica, reacts with water to form calcium aluminate decahydrate ($CAH_{10}$) at low temperature, dicalcium aluminate octahydrate ($C_2AH_8$) and alumina hydrate ($AH_3$) at a medium temperature, or/and tricalcium aluminate hexahydrate ($C_3AH_6$) and $AH_3$ at a high temperature as shown in Figure 2-14 below (Scrivener et al., 1999; Zapata et al., 2022).

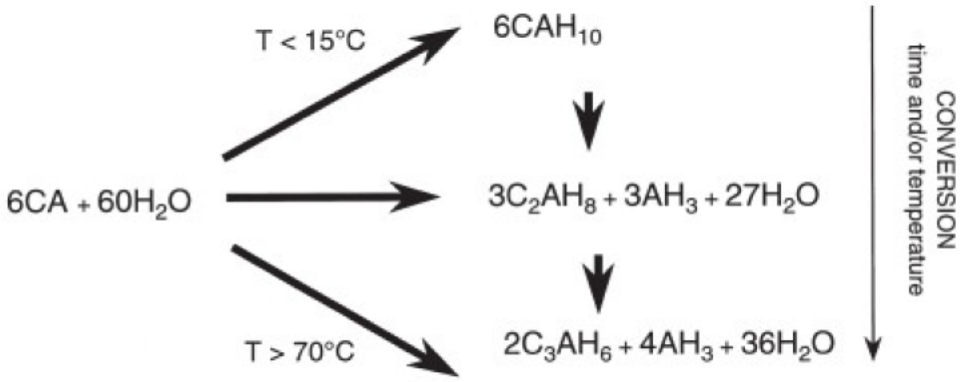


Figure 2-14: Hydration reactions of monocalcium aluminate (Scrivener et al., 1999)

However, of all these hydrates, $C_3AH_6$ and $AH_3$ are the stable phases while others are metastable (Heikal et al., 2005). Due to this instability of these phases, they are eventually converted to $C_3AH_6$ and $AH_3$ through process/reaction called Conversion, which dependent on the temperature and moisture (Scrivener et al., 1999; Mehta & Monteiro, 2006). The released water further hydrates the unhydrated phases within the matrix resulting into a stable and denser $C_3AH_6$ (Sakai et al., 2010).

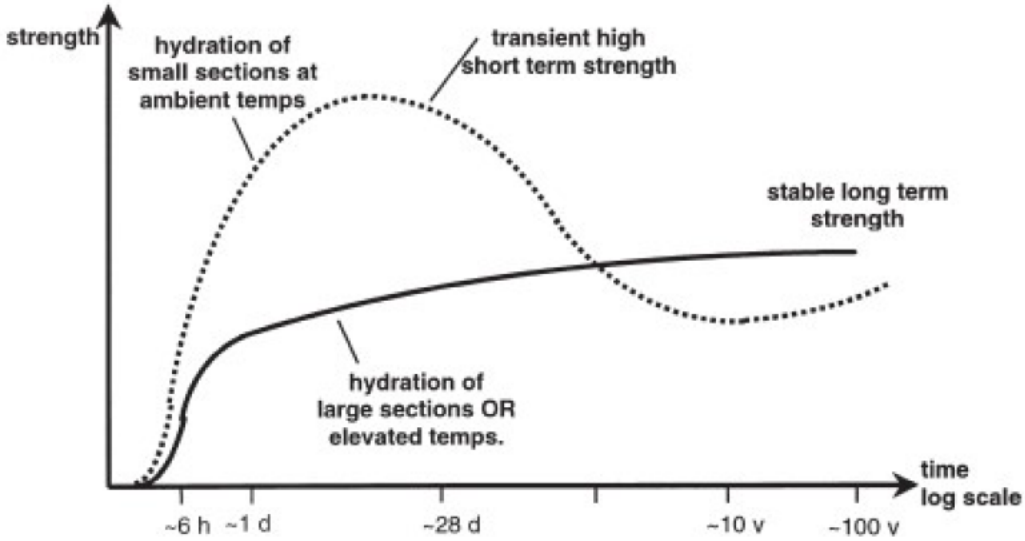


Figure 2-15: Schematic strength development of calcium aluminate cements at a water cement ratio of about 0.4 (Scrivener et al., 1999)

From the hydration of CAC, as discussed, it should be noted that $Ca(OH)_2$ is not produced as it is in the case of the hydration of PC; hence, it should be expected that CAC will perform differently in an acidic environment, which is discussed in the next section.

### 2.7.3 CAC in an acidic environment

Depending on how acidic the environment is, alumina hydrate ($AH_3$) remains stable down to a pH of about 3 or 4. However, the other hydrates as mentioned in Section 2.7.2 are dissolved by the acid leading to the formation of additional quantities of alumina hydrates as shown in Equation 2-39. These additional hydrates fill the concrete pores thereby shielding the concrete from further acidic attack and generally giving a smoother attacked surface with less aggregate loss (Scrivener et al., 1999).

$$C_3AH_6 + 6H^+ \longrightarrow 3Ca^{2+} + 2Al(OH)_3\downarrow + 6H_2O \quad (2\text{-}39)$$

However, at a lower pH of around 3.5, the alumina hydrates eventually dissolve, but in so doing neutralises more acid as shown in Equation 2-40 below.

$$AH_3 + 6H^+ \longrightarrow 2Al^{3+} + 6H_2O \quad (2\text{-}40)$$

The overall neutralisation reaction is given thus:

$$C_3AH_6 + 2AH_3 + 24H^+ \longrightarrow 3Ca^{2+} + 6Al^{3+} + 24H_2O \quad (2\text{-}41)$$

The figure below shows the microstructure of a 30-year-old sewer lining which has been extensively decalcified resulting into higher concentration of $AH_3$ which in turn created a dense microstructure with low porosity.

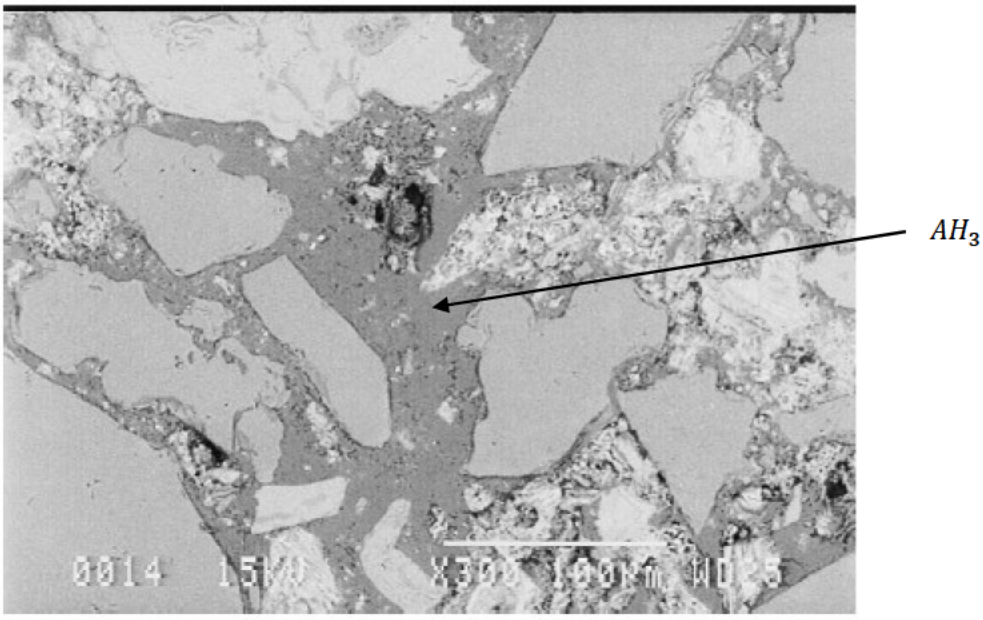


Figure 2-16: $AH_3$ dominated microstructure of 30-year-old sewer lining (Scrivener et al., 1999)

### 2.7.4 Neutralisation capacity of CAC

As explained in Section 2.6.4, neutralisation capacity reveals the amount of acid (in this case, biogenic $H_2SO_4$ acid) that can be neutralised by a certain amount of material. While both PC and CAC can neutralise biogenic acid, research shows that 1 $g$ of CAC can neutralise around 40% more acid than 1 $g$ of PC (Saucier & Kaitano, 2018). This reveals that CAC has a larger neutralisation capacity compared to PC, which explains why CAC-based concrete performs better than PC-based concrete in aggressive environments; however, it should be noted that while $C$ (calcium oxide) is the major contributor to the NC of PC, $A$ (Alumina) is the major contributor to the NC of CAC (Kiliswa, 2016).

### 2.7.5 Bacteriostatic effect of CAC

As discussed in Section 2.7.3, $AH_3$ is stable down to a pH of 3 to 4; however, it dissolves at a lower pH resulting into the release of aluminium ion $Al^{3+}$, which besides helping to neutralise more acids, as discussed in Section 2.7.3, also produces a bacteriostatic effect on bacterial metabolism, i.e., it stops bacteria from being active. Hence, bacteria are no longer able to oxidize sulphur from emitted $H_2S$ gas to produce more acids. This puts a stop in the pH-decrease and puts a hold to the corrosion process (Saucier & Kaitano, 2018).

## 2.8 Mitigation of MICC

In the past decades, several studies have been carried out in order to address microbially-induced concrete corrosion (MICC), few of which are presented in this section. These studies have been geared towards addressing one or more of the causal/promoting factors, inhibiting the activity of microorganisms, treating the concrete surface treatment or/and coating, or making use of special cements other than Portland cement.

However, the approaches employed in these studies have been categorised into three, namely:

a. mechanical-based mitigation approach
b. chemical-based mitigation approach
c. material-based mitigation approach

### 2.8.1 Mechanical-based mitigation approach

These are mitigation methods that are carried out mechanically within the sewer infrastructure. To remain effective, they are also conducted periodically. In most cases, these methods most have been considered during the design stage of the sewer system.

Some of the mechanical-based approaches include surface washing and crown spraying.

#### 2.8.1.1 Concrete surface washing

Sun et al., (2016) in their study investigated the effect of high-pressure surface washing on MICC. This study was conducted in the lab and to simulate real-life sewer environment, concrete coupons were produced and exposed to the gas phase of the controlled laboratory corrosion chamber containing domestic sewage for specified periods.

The concrete coupons used were of two types—fresh coupons cut out from a new concrete sewer and pre-corroded coupons cut out from a 70-year-old concrete sewer wall. These were exposed to the gaseous phase of four different chambers controlled at four different $H_2S$ concentration—5 $ppm$, 10 $ppm$, 25 $ppm$ and 50 $ppm$. The 5 $ppm$ and 50 $ppm$ chambers were used to monitor the corrosion recovery after samples are washed. Here, the coupons were removed on a weekly to monthly basis, washed with a high-pressure washer and returned to the chamber. At each removal, the $H_2S$ uptake rate (SUR), surface pH and sulphur species in the corrosion layers were measured. The 10 $ppm$ and 25 $ppm$ chambers were used to determine the concrete loss of washed and unwashed samples—washed at 6 to 10 months interval—over an exposure period of 54 months, and this was measured by the difference in dimension.

Sun et al., (2016) found that high-pressure surface washing affected the rate of corrosion by increasing the surface pH and decreasing the SUR; however, SUR recovery back to the level prior to washing took place within 60 to 140 days. For the concrete loss, it was found that there was no significant difference between the outcome of washed and unwashed coupons after the 54-month exposure.

### 2.8.1.2 Crown spray process

As covered in Section 2.4.4, there is a gradual decrease in the surface pH of the concrete sewer wall above the wastewater line due to the formation of acids through the activity of SOB; Sydney et al. (1996) based their mitigation method on this fact. This method involves the spraying of a high-pH mixture to the sewer crown to neutralize existing acid and gradually increasing the concrete surface pH. Consequently, this creates an unfavourable condition for the growth and colonization of SOB. It should be noted that though utilized by Sydney et al. (1996), this technology was invented by Edward Esfandi (Esfandi, 1986).

Sydney et al. (1996), after a screening process to identify potential mixtures, used six different chemical mixtures—24% sodium hydroxide ($NaOH$), 15% sodium carbonate ($Na_2CO_3$), 45% potassium carbonate ($k_2CO_3$), 50% magnesium hydroxide ($Mg(OH)_2$), 10% benzalkonium chloride, and 15% sodium carbonate + 1,000 $ppm$ benzalkonium chloride. Fresh concrete coupons were produced and exposed to highly corroded active sewer until the surface pH reduced to 2, after which they were moved to the lab where the chemical mixtures were applied.

It was found that of all the chemical mixtures used, 50% magnesium hydroxide performed a lot much better. Coupons sprayed with 50% $Mg(OH)_2$ immediately raised the surface pH to as high as 9 and remained at the level for the 7-week evaluation period. This resulted into a large decrease of SOB population by six orders of magnitude below control level. With the results from this stage, Sydney et al. (1996) proceeded into a full-scale spraying of the highly corroded sewer. The result obtained affirmed the deactivating and biocidal properties of 50% $Mg(OH)_2$ which in this case maintained a surface pH of 9 throughout the evaluation period of 9 months.

This study shows not only the effectiveness of the crown spray process but also the potential in the use $Mg(OH)_2$ in mitigating MICC.

## 2.8.2 Chemical-based mitigation approach

Chemical-based mitigation approach are methods that employ the use of a chemical compound, in one way or the other, in order to inhibit the growth of microorganisms or prevent the formation of $H_2S$ gas. Hence, the last discussed method in Section 2.8.1 also falls into this category.

Some of the chemicals used in studies include calcium formate, magnesium hydroxide, bactericides, anti-microbial compounds, and antibacterial nanoparticles.

### 2.8.2.1 Use of calcium formate to inhibit bacteria growth

As explained in Section 2.4, MICC is caused by the activity of bacteria; it, however, becomes pronounced due to the development of microcolonies inside the biofilm, in the case of SRB, and on the concrete surface above the wastewater line (especially at the crown), in the case of SOB. Based on this knowledge, Yamanaka et al. (2002), in their study, tried to inhibit the growth of bacteria using a growth inhibitory compound, calcium formate $Ca(HCOO)_2$.

Corroded concrete from the sewerage system was pulverized. The presence of SOB was confirmed by a detected decrease in pH decrease and increase in ATP (Adenosine triphosphate) after a mixture of pulverized corroded concrete sample and S6 medium was shaken in the Sakaguchi flask at 30℃. Similarly, the presence of acidophilic iron-oxidizing was confirmed by the increase in ferric ion after

a mixture of pulverized corroded concrete sample and 9K medium was shaken in the Sakaguchi flask at 30℃.

A sulphur-oxidizing bacterium was isolated by plating on solidified S6 media, while an acidophilic iron-oxidizing bacterium was isolated by plating on a solidified 9K media. These isolates were cultivated, their DNA (deoxyribonucleic acid) were extracted and purified (Marmur, 1961) and the G+C content of DNA was determined (Marmur & Doty, 1962). In order to see the effect of calcium formate, its salt was added to the culture media of sulfur-oxidizing bacteria (SOB) and acidophilic iron-oxidizing bacteria (AIOB). This resulted into growth inhibition though at varying concentration which was dependent on the source of the corroded concrete from whence the bacteria was extracted. The inhibitory effect was achieved with a calcium concentration of 10 $mM$ for bacteria from a site, 20 $mM$ from a second site and 50 $mM$ from a third site. This inhibitory effect was detected as there was no significant decrease in pH or increase in ATP at these concentrations.

Besides the test carried out on the corroded concrete product from the sewerage system, Yamanaka et al. (2002) went further to produce concrete pieces of mass around 570 $g$ in which calcium formate solution was used instead of water. These concrete pieces were suspended in the sewerage system where they were exposed to $H_2S_{(g)}$ at a concentration greater than 600 $ppm$. After a period of 8 months, the corroded portion of the concrete pieces were washed off and it was discovered that the pH of the wash water from the concrete pieces produced with only water (without calcium formate) were around 2.4 while those produced with calcium formate solution were around 4.4. Also, it was discovered that mass of the remaining portion of concrete piece after the wash-off of the control samples and the test samples was around 47 $g$ and 149 $g$ respectively. Hence, this shows that the presence of calcium formate protected the concrete pieces, though not completely, through its inhibitory properties.

### 2.8.2.2 Use of magnesium hydroxide to inhibit bacteria growth

Mathews et al., (2020) in their study utilized magnesium hydroxide, $Mg(OH)_2$ as a chemical dosing treatment to reduce $H_2S_{(g)}$ generation within the sewer infrastructure. In addition, the effectiveness of two biological dosing compounds (Bioproducts A and B), with different modes of action (MOA) was also investigated. The compound $Mg(OH)_2$ raises the pH of the wastewater; thereby, reducing the release of $H_2S$; bioproduct A creates an interruption in microbial communication by means of quorum sensing (QS) while bioproduct B scours sewers of fats, oils, and grease (FOGs), which later become adhesion point for microbial attachment; hence, development of biofilm is prevented, and wastewater-flow retention time is also reduced.

In carrying out the study, a switchable diversion was constructed to the existing sewer infrastructure. This gave room for close monitoring within a designated sewer section, in which dosing took place upstream and the monitoring took place downstream.

After the study, it was observed that while both Bioproducts A and B did not show any positive result, magnesium hydroxide showed as promising result. The release of $H_2S_{(g)}$ was reduced by 61.7% and 60.4% at two different trials. In addition, it was found, through microbiological methods and statistical analysis, that microbial activity within the system was also reduced. This may also be a result of the suppression of $H_2S_{(g)}$. Hence, the use of magnesium hydroxide did not only reduce the release of $H_2S_{(g)}$ but also had an inhibitory effect on bacteria.

Other studies (Jefferson et al., 2002; Gutierrez et al., 2011; Ganigué et al., 2011, 2016; Liu et al., 2013; Sudarjanto et al., 2013) also confirm the effectiveness of $Mg(OH)_2$ in the sewer environment.

### 2.8.2.3 Use of nanoparticles surface treatment to inhibit bacteria growth

Noeiaghaei et al. (2017), in their study to examine the inhibitory properties of antibacterial nanoparticles (NPs) on cementitious materials, used zinc oxide ($ZnO$) NPs and silver ($Ag$) NPs of particle size ranging from $25$ to $30$ $nm$.

The test was carried out in two stages. The first stage was the monitoring stage, in which the growth of two model bacteria—gram-positive *Bacillus cereus* and gram-negative *Escherichia coli*— was monitored after being placed in nano-treated mortar disks; Kirby-Bauer disk diffusion test was used here.

In the second stage of the study, the inhibitory properties of zinc oxide ($ZnO$) NPs and silver ($Ag$) NPs was more intensively studied under different surface pH of treated mortars and under different concentration of bacterial cells. To study the effect of mortar alkalinity, a mixture of crushed mortar and deionized water was prepared and enriched with nutrient to facilitate the bacterial growth while to achieve a decreasing-pH effect, the pH of the mixture was adjusted with the use of sulphuric acid. The mixture samples were sterilized, and supplementary pre-sterilized NPs were added, followed by inoculation, then incubation. To study the effect of bacterial density, a similar set of experiments was conducted; however, here, the mixtures were inoculated after sterilization, while the NPs were applied during the logarithmic growth phases of bacterial isolates.

Noeiaghaei et al. (2017) found that at all pH values, there was more than 60% reduction in the bacterial cell population when a starting concentration of $250$ $mg/L$ was used. However, a higher concentration resulted into a lesser growth inhibition. By comparison, it was found that $Ag$ NPs exhibited more inhibitory properties due to uniformity in particle size and high degree of nanoparticle stability while $ZnO$ Nps were found to be susceptible to pH change and aggregation which resulted into its lower inhibitory performance. And in terms of the bacteria cells, it was found that gram-negative *Escherichia coli* was more sensitive to the used nanoparticles.

### 2.8.2.4 Use of bactericides to sterilize bacteria

In order to protect concrete from bacteria, Kong et al. (2017), in their study, incorporated bactericides in the production of concrete at different proportions. Five different types of bactericides were used—sodium bromide ($NaBr$), sodium tungstate ($Na_2WO_4$), zinc oxide ($ZnO$), copper phthalocyanine ($C_{32}H_{16}CuN_8$), and dodecyl dimethyl benzyl ammonium chloride ($C_{21}H_{38}NCl$). An artificial sewage was produced to resemble typical sewage in a live sewer and the specimens were immersed for 3 months.

After this duration, through DNA sequencing of sewage from each sample with bactericides and without bactericide (control), it was found that the microbial population was greatly reduced for all bactericides especially copper phthalocyanine ($C_{32}H_{16}CuN_8$) and sodium bromide ($NaBr$). Copper phthalocyanine ($C_{32}H_{16}CuN_8$) had bactericidal rate of 90.82% and 64.25% on Bacteroidetes and Proteobacteria respectively. These are the main microorganisms responsible for corrosion in concrete. On the other hand, sodium bromide ($NaBr$), though not as effective as copper phthalocyanine, has a bactericidal rate of 86.8% and 54.99% on Bacteroidetes and Proteobacteria respectively.

In addition, Kong et al. (2017) found that, of all the bactericides, only the concrete with copper phthalocyanine resulted into a significant increase in compressive strength with reference to the control specimen (sample without bactericide). At a concentration of 0.1% of copper phthalocyanine, there was an increase of about 60%.

In terms of retention of bactericide in the concrete, copper phthalocyanine had the highest retention rate of 99.69% after 120 days of immersion while sodium bromide had the least retention rate of 87.14%.

Hence, of all the bactericide used in the study, copper phthalocyanine showed the best result in all areas and so the most suitable for use in the production of anti-microbial corrosion concrete.

#### 2.8.2.5 Use of antimicrobial-compound admixtures and surface treatments

De Muynck et al. (2009) in their study to investigate the performance of different materials in protecting concrete from biogenic corrosion performed two series of microbiological simulation tests. In the first series, cores were drilled out from a new pipe and different surface treatments were applied: hydrous silicate admixture (SAC), epoxy coating (EC), polyurethane lining (PUL) and cementitious coating (CC). For the second series, fresh concrete specimens were produced in the laboratory: a reference concrete (RC), a mixture with an addition of silver-copper zeolites (ZC) and a mixture with the addition of antimicrobial fibres (FC).

After 8 cycles of accelerated microbiological simulation test, it was found that the epoxy coating (EC) and polyurethan lining (PUL) performed well in protecting the concrete from biogenic sulphuric acid corrosion as no degradation was observed after the 8 cycles, while CC was seen to have the worst performance. Samples with SAC treatment, silver-copper zeolites and antimicrobial fibres did not show any improved performance with respect to the reference concrete.

The potential in the use of epoxy was also confirmed by Berndt (2011).

### 2.8.3 Material-based mitigation approach

Mitigation of MICC has also be address through the modification of concrete mix write from the production stage. This may include the modification of mix with polymer, the partial replacement of Portland cement (PC) with cementitious materials like silica fume, or the total replacement of Portland cement (PC) with geopolymer or special cements like sulphate-resistant Portland cement and calcium aluminate cement (CAC).

#### 2.8.3.1 Use of silica fume or polymer to modify concrete properties

Vincke et al. (2002) in their study to investigate the influence on material on biogenic sulphuric acid attack produced concrete specimens with the addition of silica fume (SF) and polymer. Four types of polymers were used: styrene butadiene polymer (SBR), styrene-acrylic ester polymer (SA), acrylic polymer (AP) and vinyl copolymer (VPV).

This study was performed in the laboratory and so the corrosion process was simulated at a temperature of 28℃ for a duration for 68 days at 17-day cycles. To investigate the rate of corrosion, the thickness of samples was measured at the end of each cycle and the loss of substance at the end of the duration was also determined.

After the duration, Vincke et al. (2002) was found that mixtures with VPV showed no significant difference in thickness loss and mass loss with respect to the control mix which recorded a thickness loss of 2.7% and mass loss of 7.5%. Concrete specimens that were modified with AP and SF showed a negative influence as they had the largest loss in thickness of 4.4% reduction and 4.1% respectively while also having the largest mass loss of 9.3% and 8.4% respectively. Samples with SBR also showed

no significant difference in thickness loss; however, they recorded a better mass loss of 6.6%. Overall, samples with styrene-acrylic ester polymer (SA), which recorded a thickness loss of 1.7% and a mass loss of 6.5%, were found to perform better in resisting the biogenic acidic attack.

Monteny et al. (2001) also confirms the resisting capability of styrene-acrylic ester polymer (SA).

### 2.8.3.2 Use of special cements

Khan et al. (2019), in their study, investigated the performance of two special cements—sulphate resistant Portland cement (CEM-V) and calcium aluminate cement (CAC)—within an aggressive sewer environment and sulphuric acid; however, this review focuses on their study that relates to the sewer.

Mortars were produced from these cements and placed in two accessible overflow chambers, within a wastewater treatment plant, both connected to anaerobic digesters.

After an exposure period of 2 years, from visual inspection, Khan et al. (2019) found that SR had major degradation and loss of material compared to the CAC mortars. The SR mortars had a mass loss of about 19.2% and 7.5% in the two chambers while CAC mortars had a mass loss of about 3.8% and 4.3% respectively. In terms of strength, the SR mortars recorded a compressive strength reduction of around 67% and 43%, while CAC mortars recorded as reduction of 32% and 7% in the first and second chamber respectively.

From advanced analysis like SEM and EDX mapping, it was seen that the CAC mortars performed much better than the SR mortars due to its greater neutralization capacity. On both mortar-types, crystallized gypsum was evident in the deterioration zone which caused the development of microcracks. In addition, in the case of SR mortars, this was followed by the formation of secondary ettringite which gave room for more sulphate-ion penetration through the microcracks leading to further deterioration. However, in the case of CAC mortars, though secondary ettringite was formed, there was a significant amount of gibbsite ($AH_3$) also formed, which healed the existing microcracks, thereby preventing further deterioration.

In addition, studies by Kiliswa (2016) and Berndt (2011) also display the potential in the use of calcium aluminate cement in sewer facilities.

### 2.8.3.3 Coating of with geopolymer-based mortar and blended mix

Like the study by Khan et al. (2019), Roghanian & Banthia (2019) researched into the performance of binder alternatives for producing coating materials for use within an aggressive sewer environment. In their lab-based study, three base binders were used in the production of mortars: Portland cement, geopolymer and a blended mix of geopolymer and magnesium phosphate ($Mg_3(SO_4)_2$). To address bacteria, two approaches were used: direct addition of zinc oxide ($ZnO$) to the coating material and incorporation of zinc-doped clay particles in the mix. For the later, sodium bentonite clay ($Al_2H_2Na_2O_{13}Si_4$) was used, and to improve its properties, it was impregnated with zinc ions ($Zn^{2+}$); this impregnation was achieved through an ion-exchange process. In all, eight coating systems were studied: cement mortar binder (CF), cement mortar binder mixed with Zn particles (CZF), cement mortar binder mixed with Zn-doped clay particles (CCZF), geopolymer binder (GF), geopolymer binder mixed with Zn particles (GZF), geopolymer binder mixed with Zn-doped clay (GCZF), geopolymer-magnesium phosphate composite binder mixed with Zn particles (HM), and geopolymer-magnesium phosphate composite mixed with Zn-doped clay (HMCZ).

Arch-shaped cement mortar samples were produced to represent the top half of a typical sewer, and these were coated separately with the different coating mixes and placed in an accelerated bio-corrosion chamber for a duration of 6 months. This was the first stage aimed at investigating the performance of the coated systems in protecting the mortar samples, and in the second stage, coatings were applied on the uncoated cement mortars from Stage-1 to study their potential when used for repair purposes.

Roghanian & Banthia (2019) found that the multiphase composites (HM & HMCZ) were more stable to the attack with pH between 6 and 6.5. Next to these are the geopolymer-based samples (GF, GZF & GCZF) which ended up with a pH around 5 after 180 days. The blended and geopolymer-based samples were also found to experience a strength loss of about 35% compared to 52% from samples coated with cement-based mortars and 73% from uncoated samples. And for the second stage, it was found that the blended mix and geopolymer-based coatings were able to restore the strength of corroded samples by about 40%. However, from all the samples, based on results, HMCZ was found to be the most promising.

### 2.8.4 Conclusion- Past MICC-mitigation studies

This part of Literature review presents past studies aimed at mitigating MICC, most of which were focused on inhibiting the activity bacteria; this is not surprising as bacteria, as it were, can be referred to as the agent of MICC, as explained in the second part of this review.

The study by Sun et al. (2016) shows that a mechanical approach as simple as high-pressure surface washing can mitigate MICC as it causes an increase in the surface pH of the concrete sewer above the wastewater. However, this approach is most suited for recently new sewers or uncorroded sewer, and it also requires a regular or periodic implementation.

The use of magnesium hydroxide $Mg(OH)_2$ appears to be a very promising method as it was employed in the study by Mathews et al. (2020) and Sydney et al. (1996), among other studies, though in different ways which suggests that beyond the mode of application, the compound itself is highly effective mitigating MIC. Hence, I will recommend that various research be carried out to find out the best way to effectively utilize $Mg(OH)_2$ in the sewer environment and the optimum dosage.

In line with chemical compounds, copper phthalocyanine (Kong et al. 2017), styrene-acrylic ester polymer (Vincke et al., 2002) and calcium formate (Yamanaka et al., 2002; Monteny et al., 2001), as used in their studies proved to be very effective in protecting concrete from biogenic acidic attack. However, further research is needful to as ascertain long-term performance in resisting MICC and long-term effect on the environment. In addition, the effectiveness of the use of $Ag$ nanoparticles is seen in the study by Noeiaghaei et al. (2017); however, more research needs to be carried out in this area as application of nanotechnology is relatively new in the concrete industry.

Calcium aluminate cement as an alternative to Portland cement has been found to perform well in acidic environment while also performing better than sulphate resistant Portland cement (CEM-V) (Khan et al., 2019). Hence, while other mitigation approaches may be geared towards inhibiting $H_2S$ generation or activity of SRB/SOB, this approach presents a material upgrade capable of withstanding the acidic environment. This is also confirmed in other researchers like Kiliswa (2016) and Berndt (2011). However, though effective, this is an expensive method to implement on a large scale, hence this may be best suited for coating new sewer or repairing corroded sewers.

In line with coating systems, geopolymer-magnesium phosphate composite binder mixed with Zn particles (HM), and geopolymer-magnesium phosphate composite mixed with Zn-doped clay (HMCZ) performed well from the study carried out by Roghanian & Banthia (2019). Further research still needs to be done to ascertain its long-term applicability. Also, De Muynck et al. (2009), it was found that the epoxy coating (EC) and polyurethan lining (PUL) performed well in protecting the concrete from biogenic sulphuric acid corrosion as no degradation was observed after the 8 cycles

## 2.9 References


Abdul-Talib, S., Hvitved-Jacobsen, T., Vollertsen, J. and Ujang, Z., 2002. Anoxic transformations of wastewater organic matter in sewers–process kinetics, model concept and wastewater treatment potential. *Water science and technology*, *45*(3), pp.53-60.

Alexander, M., Bertron, A. and De Belie, N., 2013. *Performance of cement-based materials in aggressive aqueous environments* (Vol. 10). Berlin, Germany: Springer.

Alexander, M.G. and Fourie, C., 2011. Performance of sewer pipe concrete mixtures with portland and calcium aluminate cements subject to mineral and biogenic acid attack. *Materials and structures*, *44*(1), pp.313-330.

Barton, L.L. and Fauque, G.D., 2009. Biochemistry, physiology and biotechnology of sulfate-reducing bacteria. *Advances in applied microbiology*, *68*, pp.41-98.

Berndt, M.L., 2011. Evaluation of coatings, mortars and mix design for protection of concrete against sulphur oxidising bacteria. *Construction and Building Materials*, *25*(10), pp.3893-3902.

Biparva, A. and Gupta, R., 2010. *Smart waterproofing system: a review.* Unpublished manuscript. Downloaded from researchgate.net.

Boltz, J.P., Smets, B.F., Rittmann, B.E., Van Loosdrecht, M.C., Morgenroth, E. and Daigger, G.T., 2017. From biofilm ecology to reactors: a focused review. *Water Science and Technology*, *75*(8), pp.1753-1760.

Boon A.G. and Pomeroy, R.D., 1990. The problem of hydrogen sulphide in sewers. *Clay Pipe Development Association. Ltd., London, 2nd edition (edited by A. G. Boon), 1990, 24*.

Camp, T.R., 1946. Design of sewers to facilitate flow. *Sewage Works Journal*, *18*(1), pp.3-16.

Cao, B., Ahmed, B., Kennedy, D.W., Wang, Z., Shi, L., Marshall, M.J., Fredrickson, J.K., Isern, N.G., Majors, P.D. and Beyenal, H., 2011. Contribution of extracellular polymeric substances from Shewanella sp. HRCR-1 biofilms to U (VI) immobilization. *Environmental science & technology*, *45*(13), pp.5483-5490.

Cappellesso, V.G., dos Santos Petry, N., Dal Molin, D.C.C. and Masuero, A.B., 2016. Use of crystalline waterproofing to reduce capillary porosity in concrete. *Journal of Building Pathology and Rehabilitation*, *1*(1), pp.1-12.

Cayford, B.I., Dennis, P.G., Keller, J., Tyson, G.W. and Bond, P.L., 2012. High-throughput amplicon sequencing reveals distinct communities within a corroding concrete sewer system. *Applied and environmental microbiology*, *78*(19), pp.7160-7162.

Chaudhari, B., Panda, B., Šavija, B. and Chandra Paul, S., 2022. Microbiologically Induced Concrete Corrosion: A Concise Review of Assessment Methods, Effects, and Corrosion-Resistant Coating Materials. *Materials*, *15*(12), p.4279.

Chen, G.H., Leung, D.H. and Hung, J.C., 2003. Biofilm in the sediment phase of a sanitary gravity sewer. *Water Research*, *37*(11), pp.2784-2788.

Clarke J.N., 1997. Calcium Aluminate Cements in Construction: A re-assessment. *Concrete Society* (No 46).

CNCI, 2009. Cementitious materials for concrete- standards, selection and properties. *Cement & concrete institute*, Midrand.

Costerton, J.W., Lewandowski, Z., Caldwell, D.E., Korber, D.R. and Lappin-Scott, H.M., 1995. Microbial biofilms. *Annual review of microbiology*, *49*(1), pp.711-745.

Cresson, R., Carrère, H., Delgenes, J.P. and Bernet, N., 2006. Biofilm formation during the start-up period of an anaerobic biofilm reactor—Impact of nutrient complementation. *Biochemical Engineering Journal*, *30*(1), pp.55-62.

Dao, V.T., Dux, P.F., Morris, P.H. and Carse, A.H., 2010. Performance of permeability-reducing admixtures in marine concrete structures. *ACI Materials Journal*, *107*(3), p.291.

Davis, M.L., 2010. *Water and wastewater engineering: design principles and practice*. McGraw-Hill Education, New York, Pages 19(1-49) & 22(1-29).

De Muynck, W., De Belie, N. and Verstraete, W., 2009. Effectiveness of admixtures, surface treatments and antimicrobial compounds against biogenic sulfuric acid corrosion of concrete. *Cement and Concrete Composites*, *31*(3), pp.163-170.

Dinh, H.T., Kuever, J., Mußmann, M., Hassel, A.W., Stratmann, M. and Widdel, F., 2004. Iron corrosion by novel anaerobic microorganisms. *Nature*, *427*(6977), pp.829-832.

Ehrich, S. and Bock, E., 1996. Biogenic sulfuric acid corrosion test procedure for cement bound materials. *DECHEMA MONOGRAPHIEN*, pp.193-198.

Esfandi, E., 1986. Proposal to conduct research for control of sewer corrosion. *Internal Memorandum, County Sanitation Districts of Los Angeles County*.

Figmig, R., 2020. Efficiency of the crystallizing waterproofing admixture in lower-quality concrete. In *IOP Conference Series: Materials Science and Engineering* (Vol. 867, No. 1, p. 012007). IOP Publishing.

Flemming, H.C., 1993. Biofilms and environmental protection. *Water Science and Technology*, *27*(7-8), pp.1-10.

Ganigué, R., Gutierrez, O., Rootsey, R. and Yuan, Z., 2011. Chemical dosing for sulfide control in Australia: an industry survey. *Water research*, *45*(19), pp.6564-6574.

Ganigué, R., Jiang, G., Sharma, K., Chen, J., Vuong, L. and Yuan, Z., 2016. Online Control of magnesium hydroxide dosing for sulfide mitigation in sewers: algorithm development, simulation analysis, and field validation. *Journal of Environmental Engineering*, *142*(12), p.04016069.

García-Vera, V.E., Tenza-Abril, A.J., Saval, J.M. and Lanzón, M., 2019. Influence of crystalline admixtures on the short-term behaviour of mortars exposed to sulphuric acid. *Materials*, *12*(1), p.82.

George, R.P., Muraleedharan, P., Parvathavarthini, N., Khatak, H.S. and Rao, T.S., 2000. Microbiologically influenced corrosion of AISI type 304 stainless steels under freshwater biofilms. *Materials and Corrosion*, *51*(4), pp.213-218.

Gilbert, E.M., Agrawal, S., Schwartz, T., Horn, H. and Lackner, S., 2015. Comparing different reactor configurations for Partial Nitritation/Anammox at low temperatures. *Water research*, *81*, pp.92-100.

Gojević, A., Ducman, V., Netinger Grubeša, I., Baričević, A. and Banjad Pečur, I., 2021. The Effect of Crystalline Waterproofing Admixtures on the Self-Healing and Permeability of Concrete. *Materials*, *14*(8), p.1860.

Gomez-Alvarez, V., Revetta, R.P. and Santo Domingo, J.W., 2012. Metagenome analyses of corroded concrete wastewater pipe biofilms reveal a complex microbial system. *BMC microbiology*, *12*(1), pp.1-14.

Goyns A., 2008. *Design Manual for Concrete Pipe Outfall Sewers*. Design Manual, Pretoria: Concrete Pipe Manufactures Association (CMA) of South Africa.

Grandclerc, A., Guéguen-Minerbe, M., Nour, I., Dangla, P. and Chaussadent, T., 2017. Impact of cement composition on the adsorption of hydrogen sulphide and its subsequent oxidation onto cementitious material surfaces. *Construction and Building Materials*, *152*, pp.576-586.

Grengg, C., Mittermayr, F., Ukrainczyk, N., Koraimann, G., Kienesberger, S. and Dietzel, M., 2018. Advances in concrete materials for sewer systems affected by microbial induced concrete corrosion: A review. *Water research*, *134*, pp.341-352.

Gutierrez, O., Sudarjanto, G., Sharma, K.R., Keller, J. and Yuan, Z., 2011. SCORe-CT: a new method for testing effectiveness of sulfide-control chemicals used in sewer systems. *Water Science and Technology*, *64*(12), pp.2381-2388.

Guitierrez, O., Jiang, G., Sharma, K.R. and Yuan, Z., 2016. Biofilm development in sewer networks. *Aquatic Biofilms*, p.145.

Guyer, J.P., 2018. *An Introduction to Hydraulic Design of Sewers*. The Clubhouse Press, California.

Harrison Jr, A.P., 1984. The acidophilic thiobacilli and other acidophilic bacteria that share their habitat. *Annual review of microbiology*, *38*(1), pp.265-292.

Heikal, M., Radwan, M.M. and Darweesh, H.H.M., 2005. Hydration characteristics and durability of calcium aluminate cement containing some blended systems. *Silicates Ind Ceram Sci Technol*, *70*, pp.3-4.

House, M.W., 2013. *Using biological and physico-chemical test methods to assess the role of concrete mixture design in resistance to microbially induced corrosion*. Purdue University.

House, M. and Weiss, W.J., 2014. Review of microbially induced corrosion and comments on needs related to testing procedures.

Huang, H., Peng, C., Peng, P., Lin, Y., Zhang, X. and Ren, H., 2019. Towards the biofilm characterization and regulation in biological wastewater treatment. *Applied microbiology and biotechnology*, *103*(3), pp.1115-1129.

Hvitved-Jacobsen, T., Vollertsen, J., Yongsiri, C., Nielsen, A.H. and Abdul-Talib, S., 2002. Sewer microbial processes, emissions and impacts. In *3rd International Conference on sewer processes and networks, April* (pp. 15-17).

Hvitved-Jacobsen T., Vollertsen J., & Nielsen, A.H., 2013. *Sewer Processes: Microbial and Chemical Process Engineering of Sewer Networks.* CRC Press, Taylor & Francis group. Pages 1-24.

Islander, R.L., Devinny, J.S., Mansfeld, F., Postyn, A. and Shih, H., 1991. Microbial ecology of crown corrosion in sewers. *Journal of Environmental Engineering*, *117*(6), pp.751-770.

Ito, T., Nielsen, J.L., Okabe, S., Watanabe, Y. and Nielsen, P.H., 2002. Phylogenetic identification and substrate uptake patterns of sulfate-reducing bacteria inhabiting an oxic-anoxic sewer biofilm determined by combining microautoradiography and fluorescent in situ hybridization. *Applied and environmental microbiology*, *68*(1), pp.356-364.

Javaherdashti, R., 2009. A brief review of general patterns of MIC of carbon steel and biodegradation of concrete. *IUFS J. Biol*, *68*(6).

Jefferson, B., Hurst, A., Stuetz, R. and Parsons, S.A., 2002. A comparison of chemical methods for the control of odours in wastewater. *Process Safety and Environmental Protection*, *80*(2), pp.93-99.

Jensen, H.S., Nielsen, A.H., Hvitved-Jacobsen, T. and Vollertsen, J., 2008. Survival of hydrogen sulfide oxidizing bacteria on corroded concrete surfaces of sewer systems. *Water Science and Technology*, *57*(11), pp.1721-1726.

Jensen, H.S., 2009. *Hydrogen sulphide induced concrete corrosion of sewer networks*. PhD thesis, Aalborg University, Denmark.

Jensen, H.S., Nielsen, A.H., Hvitved-Jacobsen, T. and Vollertsen, J., 2009. Modeling of hydrogen sulfide oxidation in concrete corrosion products from sewer pipes. *Water Environment Research*, *81*(4), pp.365-373.

Jensen, H.S., Lens, P.N., Nielsen, J.L., Bester, K., Nielsen, A.H., Hvitved-Jacobsen, T. and Vollertsen, J., 2011. Growth kinetics of hydrogen sulfide oxidizing bacteria in corroded concrete from sewers. *Journal of hazardous materials*, *189*(3), pp.685-691.

Jensen, H., Biggs, C.A. and Karunakaran, E., 2016. The importance of sewer biofilms. *Wiley Interdisciplinary Reviews: Water*, *3*(4), pp.487-494.

Jiang, F., Liang, Z.S., Peng, G.L., Qian, J. and Chen, G.H., 2013. Nitrogen removal capacity of simultaneously autotrophic and heterotrophic denitrification in a sewer receiving nitrified source-separated urine. *Water Practice and Technology*, *8*(1), pp.33-40.

Jiang, G., Zhou, M., Chiu, T.H., Sun, X., Keller, J. and Bond, P.L., 2016. Wastewater-enhanced microbial corrosion of concrete sewers. *Environmental science & technology*, *50*(15), pp.8084-8092.

Joseph, A.P., Keller, J., Bustamante, H. and Bond, P.L., 2012. Surface neutralization and H2S oxidation at early stages of sewer corrosion: Influence of temperature, relative humidity and H2S concentration. *Water research*, *46*(13), pp.4235-4245.

Kaushal, V., Najafi, M., Love, J. and Qasim, S.R., 2020. Microbiologically induced deterioration and protection of concrete in municipal sewerage system: Technical review. *Journal of Pipeline Systems Engineering and Practice*, *11*(1), p.03119002.

Khan, S., Haq, F., Hasan, F., Saeed, K. and Ullah, R., 2012. Growth and biochemical activities of Acidithiobacillus thiooxidans collected from black shale. *J Microbiol Res*, *2*(4), pp.78-83.

Khan, H.A., Castel, A., Khan, M.S. and Mahmood, A.H., 2019. Durability of calcium aluminate and sulphate resistant Portland cement-based mortars in aggressive sewer environment and sulphuric acid. *Cement and Concrete Research*, *124*, p.105852.

Kiliswa, M.W., 2016. 'Composition and microstructure of concrete mixtures subjected to biogenic acid corrosion and their role in corrosion prediction of concrete outfall sewers', PhD thesis, University of Cape Town, South Africa.

Kiliswa, M.W. and Alexander, M.G., 2014, Biogenic corrosion of concrete sewer pipes: A review of the performance of cementitious materials. In *Proceedings of the XIII Conference Durab Build Mater Components, Sao Paulo, Brazil* (pp. 2-5).

Kley, G. & Caradot, N. 2013. *Review of sewer deterioration models*. Berlin: KWB

Kong, L., Zhang, B. and Fang, J., 2017. Study on the applicability of bactericides to prevent concrete microbial corrosion. *Construction and Building Materials*, *149*, pp.1-8.

Kumar, R., n.d. *Characteristics of Sewage: 3 Characteristics*. Environmental Pollution, viewed 20 April 2019, <http://www.environmentalpollution.in/waste-management/sewage/characteristics-of-sewage-3-characteristics-waste-management/5242/>

Lai, C.Y., Dong, Q.Y., Chen, J.X., Zhu, Q.S., Yang, X., Chen, W.D., Zhao, H.P. and Zhu, L., 2018. Role of extracellular polymeric substances in a methane-based membrane biofilm reactor reducing vanadate. *Environmental science & technology*, *52*(18), pp.10680-10688.

Lakes, G. and Board, U.M.R., 2004. Recommended Standards for Wastewater Facilities. *Health Education Services Division, Health Research Inc.: Menands, NY, USA*.

Li, S.Y., Kim, Y.G., Jeon, K.S., Kho, Y.T. and Kang, T., 2001. Microbiologically influenced corrosion of carbon steel exposed to anaerobic soil. *Corrosion*, *57*(9), pp.815-828.

Li, X., Kappler, U., Jiang, G. and Bond, P.L., 2017. The ecology of acidophilic microorganisms in the corroding concrete sewer environment. *Frontiers in microbiology*, *8*, p.683.

Lin, S., Mackey, H.R., Hao, T., Guo, G., van Loosdrecht, M.C. and Chen, G., 2018. Biological sulfur oxidation in wastewater treatment: a review of emerging opportunities. *Water research*, *143*, pp.399-415.

Lines, S.J., Rothstein, D.A., Rollins, B. and Alt, C.C., 2021. Microbially Induced Corrosion of Concrete. *Concrete International*, *43*(5), pp.28-32.

Liu, Y., Ganigué, R., Sharma, K. and Yuan, Z., 2013. Controlling chemical dosing for sulfide mitigation in sewer networks using a hybrid automata control strategy. *Water science and technology*, *68*(12), pp.2584-2590.

Liu, S., Gunawan, C., Barraud, N., Rice, S.A., Harry, E.J. and Amal, R., 2016. Understanding, monitoring, and controlling biofilm growth in drinking water distribution systems. *Environmental science & technology*, *50*(17), pp.8954-8976.

Malay, S., 2018. *3 Characteristics of Sewage: Physical, Chemical and Biological Characteristics*. Civil Engineering, viewed 20 June 2019, < https://www.civilnoteppt.com/2018/03/characteristics-of-sewage-physical-chemical-biological.html>

Manning, R., 1890. On the flow of water in open channels and pipes. Engineer Bd. 69 (1890) S. 80. *Trans. Inst. civ. Engr. Ireland Bd*, *12*, p.68.

Marmur, J., 1961. A procedure for the isolation of deoxyribonucleic acid from micro-organisms. *Journal of molecular biology*, *3*(2), pp.208-IN1.

Marmur, J. and Doty, P., 1962. Determination of the base composition of deoxyribonucleic acid from its thermal denaturation temperature. *Journal of molecular biology*, *5*(1), pp.109-118.

Matar, P. and Barhoun, J., 2020. Effects of waterproofing admixture on the compressive strength and permeability of recycled aggregate concrete. *Journal of Building Engineering*, *32*, p.101521.

Mathews, E.R., Wood, J.L., Phillips, D., Billington, N., Barnett, D. and Franks, A.E., 2020. Town-scale microbial sewer community and $H_2S$ emissions response to common chemical and biological dosing treatments. *Journal of Environmental Sciences*, *87*, pp.133-148.

Mehta, P.K.A.M. and Monteiro, P., 2014. *Concrete: microstructure, properties, and materials*. McGraw-Hill Education.

Melchers, R.E. and Wells, P.A., 2007. Modelling the long-term corrosion of reinforced concrete sewers. *Research Gate.net*.

Mindess, S. and Young, J.F., 2002. *Concrete*. Prentice Hall.

Monteny, J., De Belie, N., Vincke, E., Verstraete, W. and Taerwe, L., 2001. Chemical and microbiological tests to simulate sulfuric acid corrosion of polymer-modified concrete. *Cement and Concrete Research*, *31*(9), pp.1359-1365.

Monteny, J., Vincke, E., Beeldens, A., De Belie, N., Taerwe, L., Van Gemert, D. and Verstraete, W., 2000. Chemical, microbiological, and in situ test methods for biogenic sulfuric acid corrosion of concrete. *Cement and Concrete Research*, *30*(4), pp.623-634.

Morel, F., 1983. *Principles of aquatic chemistry* (Vol. 446). New York: Wiley.

Muyzer, G. and Stams, A.J., 2008. The ecology and biotechnology of sulphate-reducing bacteria. *Nature reviews microbiology*, *6*(6), pp.441-454.

Nataadmadja, A.D. and Runtuwene, J.A.P., 2018, December. Analysis of concrete permeability with additional waterproofing admixture. In *IOP Conference Series: Earth and Environmental Science* (Vol. 195, No. 1, p. 012002). IOP Publishing.

Natarajan, K.A., 2018. Biofouling and Microbially Influenced Corrosion. Chapter 12 in *Biotechnology of Metals,* Elsevier, pp. 355–393, doi: 10.1016/B978-0-12-804022-5.00012-8

Neville, A.M. and Brooks, J.J., 1987. *Concrete technology* (pp. 242-246). England: Longman Scientific & Technical.

Noeiaghaei, T., Dhami, N. and Mukherjee, A., 2017. Nanoparticles surface treatment on cemented materials for inhibition of bacterial growth. *Construction and Building Materials*, *150*, pp.880-891.

Norsker, N.H., Nielsen, P.H. and Hvitved-Jacobsen, T., 1995. Influence of oxygen on biofilm growth and potential sulfate reduction in gravity sewer biofilm. *Water Science and Technology*, *31*(7), pp.159-167.

Okabe, S., Odagiri, M., Ito, T. and Satoh, H., 2007. Succession of sulfur-oxidizing bacteria in the microbial community on corroding concrete in sewer systems. *Applied and environmental microbiology*, *73*(3), pp.971-980.

Olmstead, W. and Hamlin, H., 1900. Converting portions of the Los Angeles outfall sewer into a septic tank. *Engineering news*, *44*(19), pp.317-318.

O'Toole, G., Kaplan, H.B. and Kolter, R., 2000. Biofilm formation as microbial development. *Annual Reviews in Microbiology*, *54*(1), pp.49-79.

Parande, A.K., Ramsamy, P.L., Ethirajan, S., Rao, C.R.K. and Palanisamy, N., 2006, March. Deterioration of reinforced concrete in sewer environments. In *Proceedings of the Institution of Civil Engineers-Municipal Engineer* (Vol. 159, No. 1, pp. 11-20). Thomas Telford Ltd.

Parker, C.D., 1945a. The corrosion of concrete: 1. The isolation of a species of bacterium associated with the corrosion of concrete exposed to atmospheres containing hydrogen sulphide. *Australian Journal of Experimental Biology and Medical Science*, *23*(2), pp.81-90.

Parker, C.D., 1945b. The corrosion of concrete: 2. The function of thiobacillus concretivorus (nov. Spec.) In the corrosion of concrete exposed to atmospheres containing hydrogen sulphide. *Australian Journal of Experimental Biology and Medical Science*, *23*(2), pp.91-98.

Pazderka, J. and Hájková, E., 2016. Crystalline admixtures and their effect on selected properties of concrete. *Acta Polytechnica*, *56*(4), pp.306-311.

Qian, Z., Tianwei, H., Mackey, H.R., van Loosdrecht, M.C. and Guanghao, C., 2019. Recent advances in dissimilatory sulfate reduction: From metabolic study to application. *Water research*, *150*, pp.162-181.

Rahhal, V., Bonavetti, V., Delgado, A., Pedrajas, C. and Talero, R., 2009. Scheme of the Portland cement hydration with crystalline mineral admixtures and other aspects. *Silicates industriels*, *74*(11), p.347.

Reiterman, P. and Bäumelt, V., 2014. Long-term sorption properties of mortars modified by crystallizing admixture. In *Advanced Materials Research* (Vol. 1054, pp. 71-74). Trans Tech Publications Ltd.

Richardson, M.G., 2002. *Fundamentals of durable reinforced concrete*. CRC Press.

Roberts, D.J., Nica, D., Zuo, G. and Davis, J.L., 2002. Quantifying microbially induced deterioration of concrete: initial studies. *International Biodeterioration & Biodegradation*, *49*(4), pp.227-234.

Roghanian, N. and Banthia, N., 2019. Development of a sustainable coating and repair material to prevent bio-corrosion in concrete sewer and waste-water pipes. *Cement and Concrete Composites*, *100*, pp.99-107.

Sakai, E., Sugiyama, T., Saito, T. and Daimon, M., 2010. Mechanical properties and micro-structures of calcium aluminate based ultra-high strength cement. *Cement and Concrete Research*, *40*(6), pp.966-970.

Satoh, H., Odagiri, M., Ito, T. and Okabe, S., 2009. Microbial community structures and in situ sulfate-reducing and sulfur-oxidizing activities in biofilms developed on mortar specimens in a corroded sewer system. *Water research*, *43*(18), pp.4729-4739.

Saucier, F. & Kaitano, T., 2018. $H_2S$ Biogenic Corrosion – Why using calcium aluminate concrete and mortars to rehabilitate corroded sewer infrastructures. *Imesa Conference*. Port Elizabeth, South Africa.

Saucier, F. & Lamberet, S., 2009. Keynote paper: Calcium aluminate concrete for sewers: going from qualitative to quantitative evidence of performance. *Concrete in aggressive aqueous environments-Performance, Testing, and Modeling*, pp.398-407.

Sawyer, C.N., McCarty, P.L. and Parkin, G.F., 2003. *Chemistry for environmental engineering and science* (Vol. 5, p. 587590). New York: McGraw-Hill.

Scrivener, K.L., Cabiron, J.L. and Letourneux, R., 1999. High-performance concretes from calcium aluminate cements. *Cement and concrete research*, *29*(8), pp.1215-1223.

Sharma, K.R., Yuan, Z., de Haas, D., Hamilton, G., Corrie, S. and Keller, J., 2008. Dynamics and dynamic modelling of H2S production in sewer systems. *Water Research*, *42*(10-11), pp.2527-2538.

Smith, F.L. and Harvey, A.H., 2007. Avoid common pitfalls when using Henry's law. *Chemical engineering progress*, *103*(9), pp.33-39.

Snaterse, C., 2013. 'Wastewater applications: corrosion due to biogenic sulphides and other aggressive waters'. In *CeoCor (European Committee for the Study of Corrosion and Protection or Piping Systems)*, Brussels, Belgium.

Stanaszek-Tomal, E. and Fiertak, M., 2016. Biological corrosion in the sewage system and the sewage treatment plant. *Procedia engineering*, *161*, pp.116-120.

Steel, E.W. and McGhee, T.J., 1979. *Water Supply and Sewerage.* 5th ed., McGraw-Hill, New York, pp. 331, 381–382, 392–399, 418–425.

Stoodley, P., Sauer, K., Davies, D.G. and Costerton, J.W., 2002. Biofilms as complex differentiated communities. *Annual Reviews in Microbiology*, *56*(1), pp.187-209.

Sudarjanto, G., Gutierrez, O., Ren, G. and Yuan, Z., 2013. Laboratory assessment of bioproducts for sulphide and methane control in sewer systems. *Science of the total environment*, *443*, pp.429-437.

Sun, X., Jiang, G., Bond, P.L. and Keller, J., 2015. Impact of fluctuations in gaseous H2S concentrations on sulfide uptake by sewer concrete: the effect of high H2S loads. *Water Research*, *81*, pp.84-91.

Sun, X., Jiang, G., Chiu, T.H., Zhou, M., Keller, J. and Bond, P.L., 2016. Effects of surface washing on the mitigation of concrete corrosion under sewer conditions. *Cement and Concrete Composites*, *68*, pp.88-95.

Sun, J., Ni, B.J., Sharma, K.R., Wang, Q., Hu, S. and Yuan, Z., 2018a. Modelling the long-term effect of wastewater compositions on maximum sulfide and methane production rates of sewer biofilm. *Water research*, *129*, pp.58-65.

Sun, R., Zhang, L., Zhang, Z., Chen, G.H. and Jiang, F., 2018b. Realizing high-rate sulfur reduction under sulfate-rich conditions in a biological sulfide production system to treat metal-laden wastewater deficient in organic matter. *Water research*, *131*, pp.239-245.

Sydney, R., Esfandi, E. and Surapaneni, S., 1996. Control concrete sewer corrosion via the crown spray process. *Water environment research*, *68*(3), pp.338-347.

Tanaka, N. and Hvitved-Jacobsen, T., 1998. Transformations of wastewater organic matter in sewers under changing aerobic/anaerobic conditions. *Water science and technology*, *37*(1), pp.105-113.

Taylor, H.F., 1997. *Cement chemistry* (Vol. 2, p. 459). London: Thomas Telford.

Tchobanoglous, G., Burton, F.L. and Stensel, H.D., 2003. Wastewater engineering: treatment and reuse, Metcalf & Eddy Inc. *McGraw-Hill, Inc., New York. doi*, *10*, p.0070418780.

USEPA, 1985. *Design manual: Odor and corrosion control in sanitary sewerage systems and treatment plants.* United States Environmental Protection Agency, Cincinnati.

Vaughn, O., 2007. Understanding Biogenic Sulfide Corrosion. *Material Performance*, pp. 36-39.

Videla, H.A. and Characklis, W.G., 1992. Biofouling and microbially influenced corrosion. *International Biodeterioration & Biodegradation*, *29*(3-4), pp.195-212.

Villaverde, S., Garcia-Encina, P.A. and Fdz-Polanco, F., 1997. Influence of pH over nitrifying biofilm activity in submerged biofilters. *Water Research*, *31*(5), pp.1180-1186.

Vincke, E., Van Wanseele, E., Monteny, J., Beeldens, A., De Belie, N., Taerwe, L., Van Gemert, D. and Verstraete, W., 2002. Influence of polymer addition on biogenic sulfuric acid attack of concrete. *International biodeterioration & biodegradation*, *49*(4), pp.283-292.

Vollertsen, J. and Hvitved-Jacobsen, T., 1998. Aerobic microbial transformations of resuspended sediments in combined sewers—a conceptual model. *Water science and technology*, *37*(1), pp.69-76.

Vollpracht, A., Lothenbach, B., Snellings, R. and Haufe, J., 2016. The pore solution of blended cements: a review. *Materials and Structures*, *49*(8), pp.3341-3367.

Von Sperling, M., 2007. *Wastewater characteristics, treatment and disposal*. IWA publishing.

Watnick, P. and Kolter, R., 2000. Biofilm, city of microbes. *Journal of bacteriology*, *182*(10), pp.2675-2679.

Wafa, F.F., 1994. Accelerated sulfate attack on concrete in a hot climate. *Cement, Concrete and Aggregates*, *16*(1), pp.31-35.

Wang, K.L., Hu, T.Z. and Xu, S.J., 2012. Influence of permeated crystalline waterproof materials on impermeability of concrete. In *Advanced Materials Research* (Vol. 446, pp. 954-960). Trans Tech Publications Ltd.

Wei, S., Jiang, Z., Liu, H., Zhou, D. and Sanchez-Silva, M., 2013. Microbiologically induced deterioration of concrete: a review. *Brazilian Journal of Microbiology*, *44*, pp.1001-1007.

Wu, L., Hu, C. and Liu, W.V., 2018. The sustainability of concrete in sewer tunnel—A narrative review of acid corrosion in the city of Edmonton, Canada. *Sustainability*, *10*(2), p.517.

Wu, M., Wang, T., Wu, K. and Kan, L., 2020. Microbiologically induced corrosion of concrete in sewer structures: A review of the mechanisms and phenomena. *Construction and Building Materials*, *239*, p.117813.

Yamanaka, T., Aso, I., Togashi, S., Tanigawa, M., Shoji, K., Watanabe, T., Watanabe, N., Maki, K. and Suzuki, H., 2002. Corrosion by bacteria of concrete in sewerage systems and inhibitory effects of formates on their growth. *Water Research*, *36*(10), pp.2636-2642.

Young, B., Delatolla, R., Kennedy, K., Laflamme, E. and Stintzi, A., 2017. Low temperature MBBR nitrification: Microbiome analysis. *Water research*, *111*, pp.224-233.

Yuan, H., Dangla, P., Chatellier, P. and Chaussadent, T., 2015. Degradation modeling of concrete submitted to biogenic acid attack. *Cement and Concrete Research*, *70*, pp.29-38.

Zapata, J.F., Azevedo, A., Fontes, C., Monteiro, S.N. and Colorado, H.A., 2022. Environmental Impact and Sustainability of Calcium Aluminate Cements. *Sustainability*, *14*(5), p.2751.

Zhang, L., De Schryver, P., De Gusseme, B., De Muynck, W., Boon, N. and Verstraete, W., 2008. Chemical and biological technologies for hydrogen sulfide emission control in sewer systems: a review. *Water research*, *42*(1-2), pp.1-12.

Zhang, L., Zhang, Z., Sun, R., Liang, S., Chen, G.H. and Jiang, F., 2018. Self-accelerating sulfur reduction via polysulfide to realize a high-rate sulfidogenic reactor for wastewater treatment. *Water research*, *130*, pp.161-167.

# CHAPTER 3
# METHODOLOGY

## 3.1 Introduction

Most studies on biogenic corrosion are carried out in the laboratory, wherein a real sewer is simulated with the use of a corrosion chamber (Vincke et al., 2002; De Belie et al., 2004; De Muynck et al., 2009; Jiang et al., 2014; Sun et al., 2016); while other studies use the in-situ approach whereby a real and active sewer is used (Satoh et al., 2009; Kiliswa et al., 2019; Song et al., 2019). For this study, the in-situ approach was used, as this is seen to generate more natural results. In addition, since rehabilitation is the focus, mortar samples were produced rather than concrete samples; these were produced with materials of interest and exposed in a functioning sewer facility undergoing MICC. The samples were suspended in the aggressive environment for duration of 14-months during which regular monitoring and investigations were carried out on the sewer environment and on the mortar samples.

This chapter discusses all the lab work carried out during this research. This includes:

- the production of mortar samples,
- information on materials used,
- information on the exposure site,
- activities carried out before, during, and after the exposure of specimens, as summarized in Figure 3-1, below.

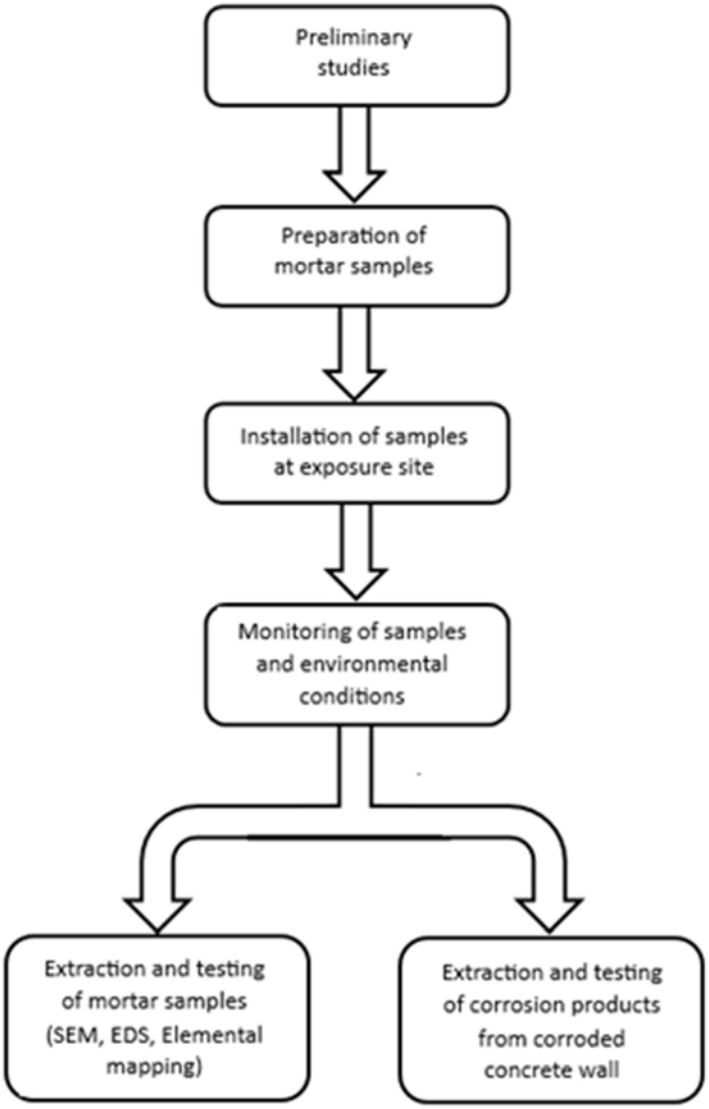


Figure 3-1: Flowchart showing a summary of activities carried out

## 3.2 Pre-exposure stage

This section presents all the activities that were carried out before the samples were exposed to the aggressive environment. During this stage, three different mortar samples were produced: calcium aluminate cement (CAC)-based mortars, denoted as $CAC_m$; Portland cement (PC)-based mortars, denoted as $PC_m$; and Portland cement (PC)-based mortars with CWA, denoted as $PCA_m$. Besides the production of mortar samples, relevant geographical information on the area and data on the sewer network is also provided.

### 3.2.1 Materials

The materials used for the production of mortar specimens are calcium aluminate cement (CAC) dry mortar, Portland cement (PC), crystalline waterproofing admixture (CWA), fine aggregates, and water.

#### 3.2.1.1 Calcium aluminate cement dry mortar

The CAC dry mortar used, as shown in Figure 3-2, produced by Kerneos Aluminate Technologies. It was manufactured by a fusion process, with bauxite and limestone used as raw materials. It is a combination of calcium aluminate cement, calcium aluminate aggregate, and additives. Its maximum particle size is 2.5 mm, and it has a wet density within the range of $2200 - 2300\ kg/m^3$ and bulk density, 1500-1600 $kg/m^3$. It has a 28-day compressive strength greater than 50 $MPa$ and flexural greater than 9 $MPa$. Its main constituents are given in Table 3-1 as supplied by the manufacturer. However, Khan et al. (2019), who also used this material, provides a more detailed constituent obtained through XRF (X-ray fluorescence) analysis; this is shown in Table 3-2.

Figure 3-2: Calcium aluminate cement dry mortar

Table 3-1: Chemical composition of CAC dry mortar (manufacturer)

| Main Constituents (%) | |
|---|---|
| Compounds | Usual range |
| $Al_2O_3$ | 40 – 46 |
| $CaO$ | 34 – 40 |
| $SiO_2$ | 4 – 9 |
| $Fe_2O_3$ | 9 – 15 |

Table 3-2: Chemical composition of CAC dry mortar by XRF analysis (Khan et al., 2019)

| Properties | % by mass |
|---|---|
| $SiO_2$ | 8.76 |
| $Al_2O_3$ | 43.27 |
| $CaO$ | 36.52 |
| $Fe_2O_3$ | 8.05 |
| $MgO$ | 0.7 |
| $MnO$ | 0.13 |
| $Na_2O$ | 0.21 |
| $K_2O$ | 0.18 |
| $P_2O_5$ | 0.112 |
| $TiO_2$ | 1.92 |
| $SO_3$ | 0.07 |
| LOI | 1.34 |
| Specific gravity | 3.34 |

### 3.2.1.2 Portland Cement

This is Portland cement of type CEM II/B-S 42.5N manufactured by Natal Portland Cement, NPC; this is shown in Figure 3-3. Since it is of the type CEM II/B-S 42.5N, it is a modified Portland cement as it contains an extender, blast furnace slag, which is a cementitious admixture. The main constituents are given in Table 3-3 below.

Table 3-3: Main constituents of CEM II/B-S 42.5N (SANS 50197-1)

| Main Constituents (%) | |
|---|---|
| Clinker | 65 – 79 |
| Blast furnace slag | 21 – 35 |

Figure 3-3: Portland cement (CEM II/B-S 42.5N)

### 3.2.1.3 Crystalline waterproofing admixture

Penetron Admix, a product of Penetron International Ltd, was used. It consist of Portland cement, very fine treated silica sand and various active proprietary chemicals (undisclosed). It is designed to form and generate a non-crystalline formation throughout the pores and capillary tracts in concrete, thereby sealing against the penetration of liquids. Figure 3-4 shows the admixture in its dry state and in its wet state, after the addition of water as stipulated.

(a) (b)

Figure 3-4: Penetron Admix (a) before the addition of water (b) after the addition of water

### 3.2.1.4 Aggregate

Natural fine aggregate sourced from Codmor quarry, Durban, was used in this study. The aggregate was sieved to remove the silt content, resulting into a fine aggregate with particle-size range of 600 $\mu m$ to 1180 $\mu m$, as shown in Figure 3-5.

Figure 3-5: Fine aggregate

### 3.2.1.5 Water

Tap water was used for the mortar production. This is portable water as supplied from eThekwini Water and Sanitation (EWS) department, Durban, with an average pH of 7.

## 3.2.2 Production of samples

For this study, three different samples were produced: calcium aluminate cement mortars ($CAC_m$), Portland cement mortars ($PC_m$), and Portland cement mortars with CWA ($PCA_m$). 100 $mm$ mortar cubes were produced which were later cored and sliced into 28 $mm$-long cores (average diameter of 48 $mm$) for exposure purpose. The entire production i.e., batching, mixing, casting, curing, coring, and slicing were all carried out at UKZN Civil Engineering lab, Howard college, Durban.

### 3.2.2.1 Mortar mixture batching

For $CAC_m$, since a pre-mixed dry mortar (calcium aluminate cement + calcium aluminate aggregate) was used, all that was left to complete the mortar mixture is the addition of water. And this was done as specified by the manufacturer.

In the case a $PC_m$, required quantities of constituents were weighed, as shown in Figure 3-6, and class-II mortars were produced in accordance with SANS 50197-1. Common cement (CEM II B-S 42.5N) was used as binder and this was combined with fine aggregate using the ratio 1:5. Water was added to complete the mixture.

Also, in the case of $PCA_m$, class-II mortars were produced in accordance with SANS 50197-1. The quantity of binder and fine aggregate used for $PC_m$ was maintained; however, for $PCA_m$, Penetron admix was added using the required quantity as specified by the manufacturer.

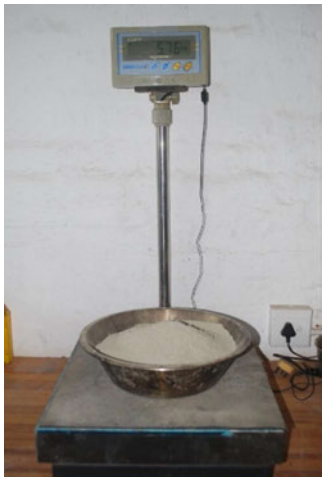

(a) Weighing of materials

(b) Batched materials ready for mixing

Figure 3-6: Batching of materials

### 3.2.2.2 Mixing, casting and curing of samples

After batching, the materials were mixed in accordance to SANS 5861-3. After a good mix was achieved, it was placed in $100 \times 100\ mm$ moulds, which were greased prior to placement to ensure easy demoulding. The filled moulds were vibrated on a vibrating table, in accordance with SANS 5861-3.

The mortars (in their respective moulds) were left to set for 24 hours, in accordance with SANS 5861-3, after which they were demoulded. The mortars were transferred into the curing tank for curing at a temperature of about 24℃ for 28 days.

### 3.2.2.3 Production of cylindrical specimens

After curing, each of the cubes were cored using Dymodrill coring machine with a 50 $mm$ diameter coring blade attached, as shown in Figure 3-7. Figure 3-7 (b) shows a cube sample firmly clamped into position ready for coring while Figure 3-8 shows the coring process. The coring resulted into core samples with average diameter of 48 $mm$ and an average height of 100 $mm$ (height of cube), as shown in Figure 3-9.

(a) (b)

Figure 3-7: Dymodrill coring machine (a) front view (b) auxiliary view

Figure 3-8: Coring of cube samples

Figure 3-9: Cored mortar cylindrical samples, $CAC_m$ (left), $PCA_m$ (middle), $PC_m$ (right)

### 3.2.2.4 Quality checks

Before the exposure specimens were produced, samples of each of the specimens, i.e., $CAC_m$, $PCA_m$, and $PC_m$, were tested for 28-days compressive strength in accordance with SANS 6255. The 100 $mm$ high cylindrical cores were used for this test as shown in the diagram Figure 3-12, prior to which

measurements were taken, using a vernier calliper and weighing scale, to calculate the density of each sample, as shown in Figure 3-10 below.

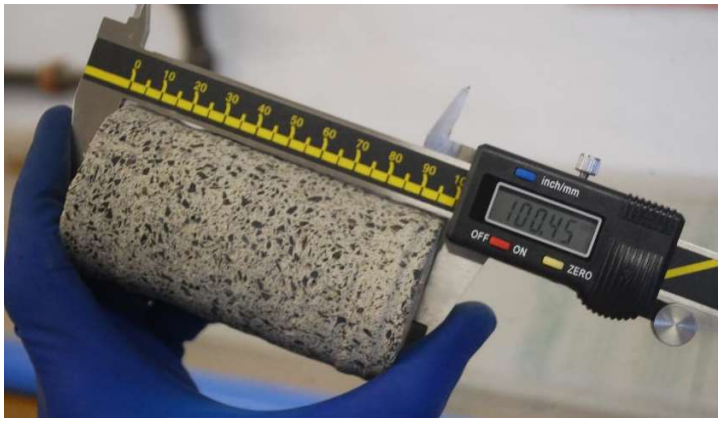


(a) Vernier calliper

(b) Weighing scale

Figure 3-10: Measuring of core specimen dimension and mass

Avery-Denison compression machine (Figure 3-11) was used which works on hydraulic system. Each cylindrical mortar sample was well centred in the compression machine, as shown in Figure 3-12 (a), after which the mortar was loaded at a loading rate of 0.3 $MPa/s$ $\pm 0.1$ $MPa/s$, in accordance to with SANS 5863, by the machine till failure occurred, as shown in Figure 3-12 (b). The maximum load in kilonewtons ($kN$) was obtained from the display screen of the machine, and this was used to calculate the compressive strength.


Figure 3-11: Avery-Denison compression machine

(a) Core sample during loading (b) Core sample after failure

Figure 3-12: Strength-testing of core samples

### 3.2.2.5 Production of Exposure specimens

To get the desired specimen size for exposure, the 100 $mm$ cylindrical cores was further cut into three smaller pieces, with the laitance layers discarded. This was achieved with the use of Clipper cutting machine (Figure 3-13), which uses water for easier cutting and reduction of dust. The machine was set to cut at 30 $mm$ away from the stopper, resulting into the production of $\pm 28$ $mm$-long cores, as shown in Figure 3-14. Three cores were obtained from each 100 $mm$-cylindrical specimen, as shown in Figure 3-14(b), while the remaining part was disposed. These cores were labelled for identification after which the dimensions of each core were measured with a vernier calliper, and their respective mass was also measured with the use of an electronic balance. These measurements were taken to serve as a reference point for these parameters during and after the exposure stage.

Figure 3-13: Clipper cutting machine

(a) Core samples during cutting

(b) Core samples after cutting

Figure 3-14: Cutting of core samples

### 3.2.3 Exposure site

The exposure site used for this study is Mahatma Gandhi Wastewater Pumping Station (MGWWPS). It is located in Durban, a city on the east coast of South Africa, as shown in Figure 3-15 and Figure 3-16. Durban has a warm temperate climate, which is characterized by hot and humid summers (average temperature of 21-29℃) and cool to mild winters (average temperature of 11-24℃), average humidity ranging from 73% to 83% throughout the year; and according to Saucier & Lamberet (2009), this is an accelerating factor for MICC even though it is not a needed factor.


Figure 3-15: Location of Durban within South Africa (Google map)

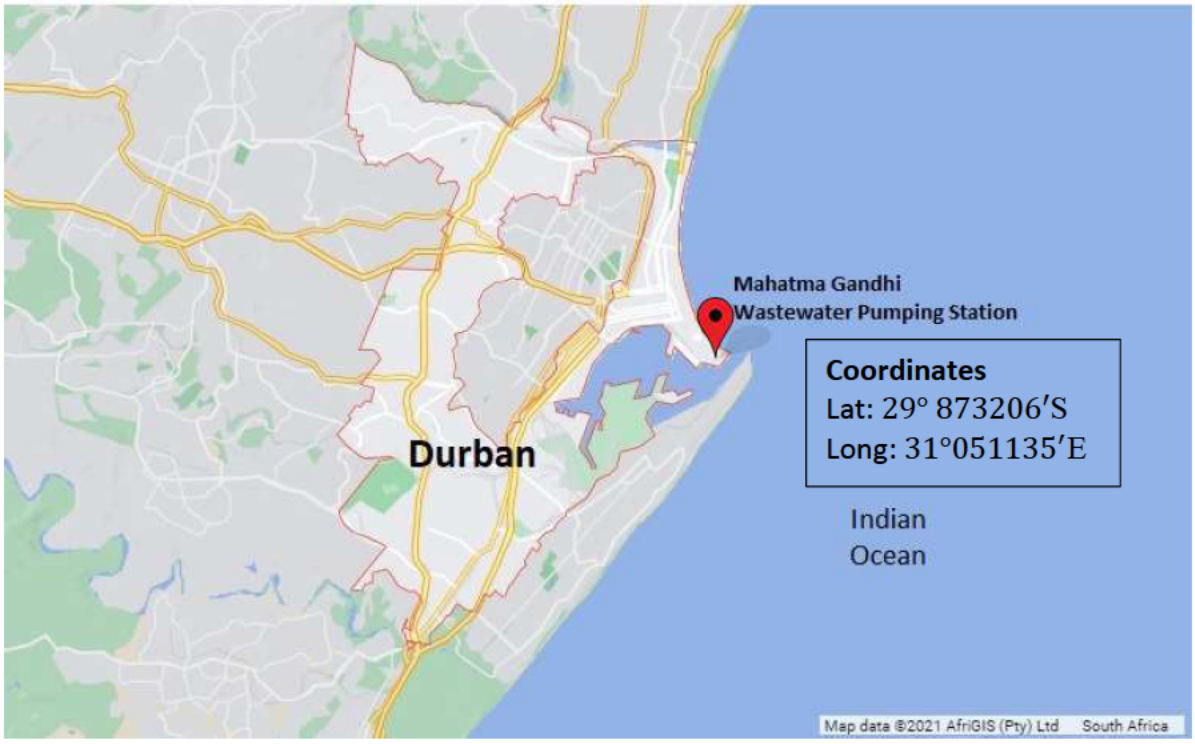


Figure 3-16: Location of MGWWPS within Durban (Google map)

MGWWPS is one of the main pumping stations in Durban, and like any other pumping station, it receives wastewater from underground gravity pipeline(s) with the main function of pumping the wastewater to an elevated height from whence it can freely flow under gravity to a designed destination. The pumping is through a pressurized pipe system while the destination is usually the treatment plant, which is the case at MGWWPS.

MGWWPS is made up of four main sections—the receiving well, the wet well, the pumps room, and the control rooms. MGWWPS is only one inlet gravity pipe through which the city sewage, and storm drains is received. This is transferred to the wet well which feeds the pumps. The wet well is equipped to always detect the level of wastewater. When wastewater level reaches a certain level, the pumps are triggered and a pressurized pumping takes place, lifting wastewater through pressure pipes which discharges into gravity pipes heading to the wastewater treatment plant.

## 3.3 Exposure stage

During this stage, the core samples produced in Section 3.2.2.5 were suspended within the aggressive environment for a period of 12 months during which they were being monitored.

### 3.3.1 Suspension of specimens

To expose the samples as desired within the aggressive environment while also ensuring easy access to the samples for monitoring purposes, a special cage, roughly in the form of a cuboid with dimensions $250 \times 180 \times 110\ mm$, was prepared to accommodate the samples. This cage was made using two perforated mini crates, as shown in Figure 3-17. Besides the existing side holes, more holes were created below the mini crates resulting into a sample cage with openings in all directions, as

shown in Figure 3-18. This modification was done to allow for easy entering of gases, giving room for $H_2S$ gas being emitted from the wastewater as discussed in Section 2.4.3. The cage was locked with cable ties while two ropes of the same length were tied to both handles of the cage for suspending the crate within the aggressive environment, as shown in Figure 3-19. The sample cage was transported to MGWWPS and suspended at the 'incoming' at a height of about 500 $mm$ from the average wastewater line, as shown in Figure 3-20.

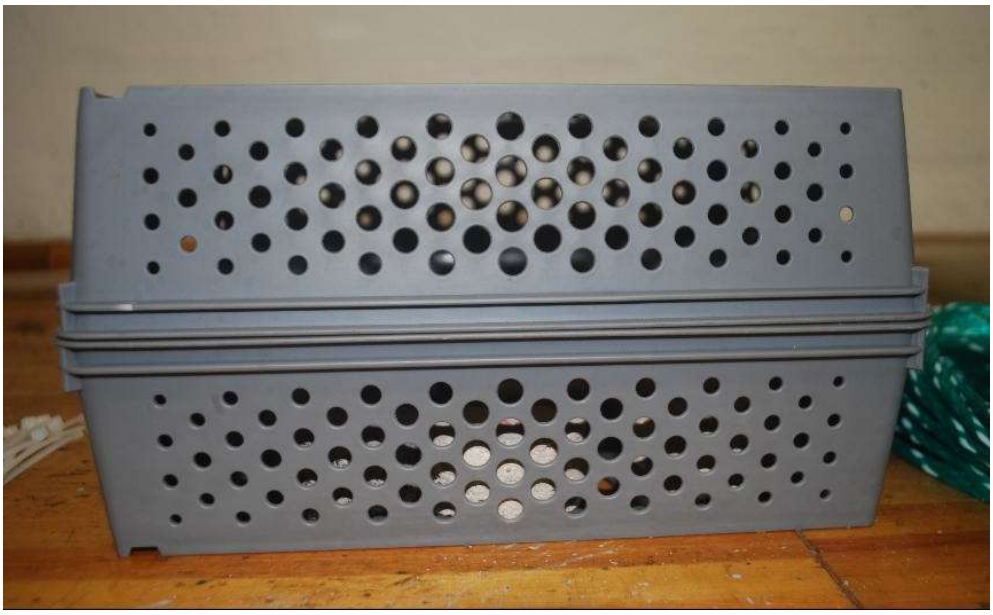

Figure 3-17 Sample cage for mortar samples

Figure 3-18: Mini crate (left) and modified mini crate (right)

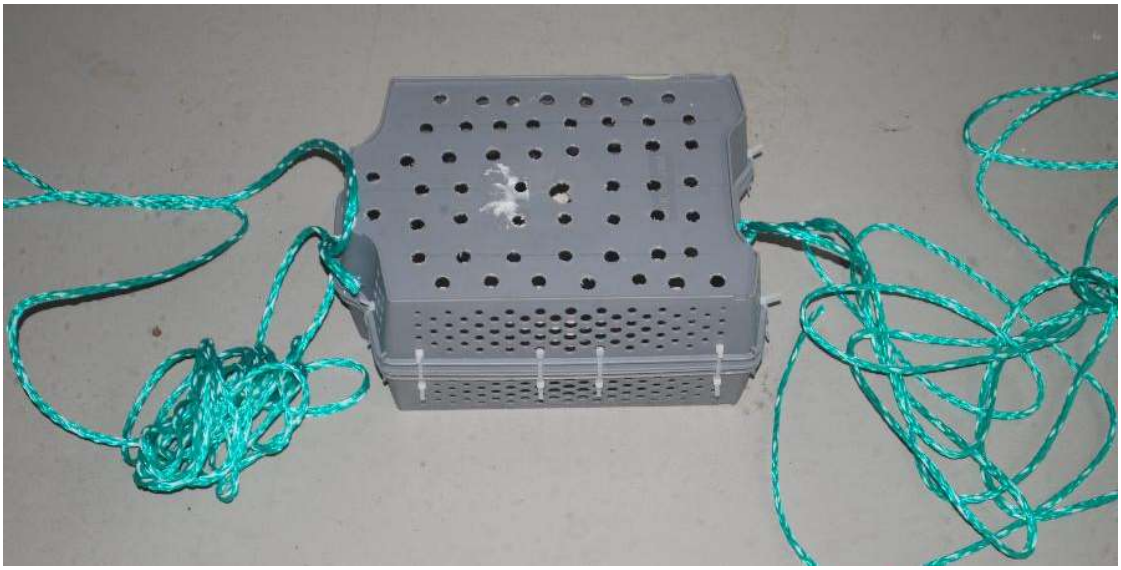

Figure 3-19: Prepared sample cage, ready to be transported to site

Figure 3-20: Suspended sample cage within the sewer environment

### 3.3.2 Assessment of sewer environment

The site was regularly assessed, every 30 days, visually and with the use of instrument. And as described in Section 2.4.5, MICC becomes more visible once concrete spalling sets in. The site atmospheric temperature was also being monitored; this was done with the use of Major Tech MT-630 digital thermometer (Figure 3-21(a)) which can also be used to measure the temperature of wastewater because of its metallic probe. MSA Altair 4X multigas detector (Figure 3-21(b)) was used to measure the $H_2S$ concentration in the atmosphere, which also measured simultaneously measured the levels of oxygen, methane ($CH_4$) and carbon monoxide ($CO$), at the same time.


(a) (b)

Figure 3-21: (a) Digital thermometer (b) Multigas detector

Samples of wastewater at the site was also being monitored and assessed regularly; this is covered in the next section, Section 3.3.3. Samples of corroded concrete were also taken from the site for advanced analysis; this is later discussed in Section 3.4.1.

### 3.3.3 Wastewater Analysis

Samples of wastewater was taken from the exposure site every month for wastewater characterization. These samples were stored in plastic bottles and were taken to the Civil Engineering Environmental lab for analysis. For lab analyses that were not conducted immediately, the wastewater samples were stored in the cold room till they were conducted. For analyses that could not be performed within the lab, the samples were prepped and stored in the freezer till they were transferred to the laboratories where these analyses were performed. The lab tests done within the Civil Engineering Environmental lab are pH, Temperature, RDO (Relative Dissolved Oxygen), Conductivity, Nitrate & Ammonia, Solids—Total Solids (TS), Volatile Solids (VS) and Fixed Solids (FS)—BOD (Biochemical Oxygen Demand), and COD (Chemical Oxygen Demand). The only test that was performed in an external lab

is the ICP (Inductively Coupled Plasma) analysis. All these tests were performed to assess the liquid phase of the sewer environment, over the duration of study, and draw inferences on the active MICC.

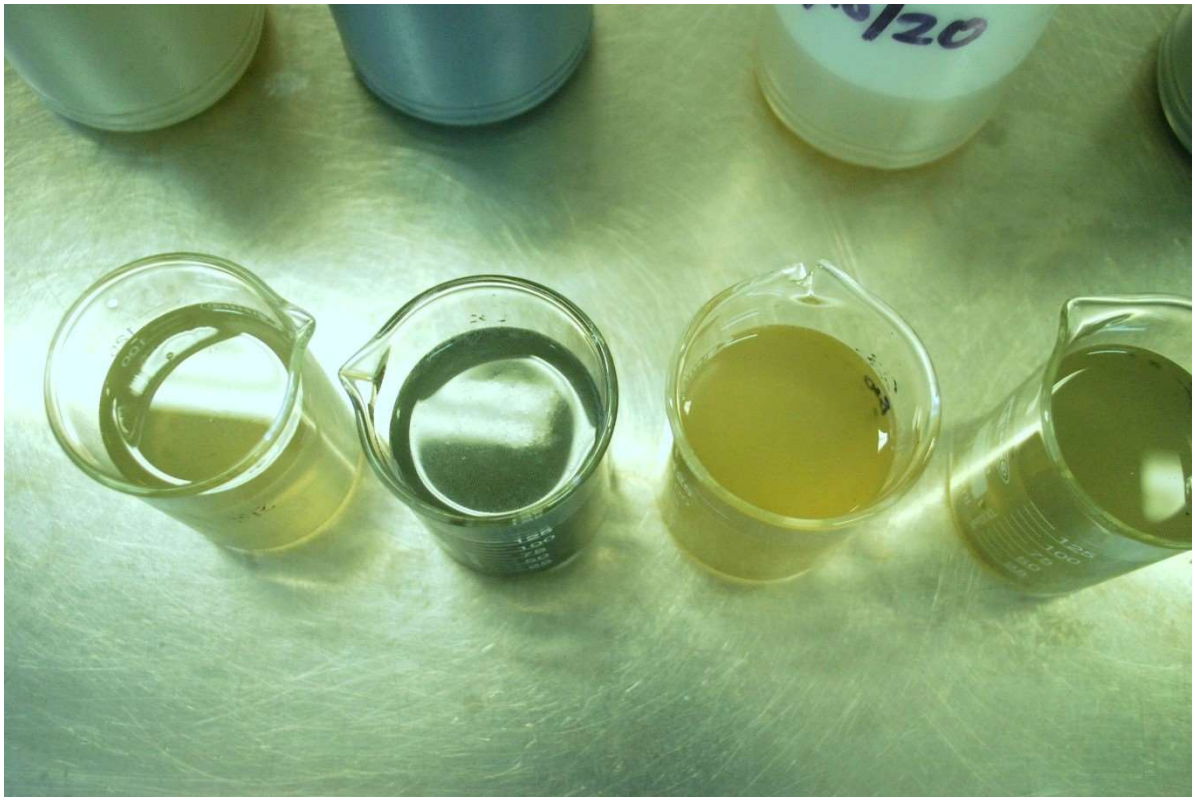

Figure 3-22: Wastewater samples made ready for liquid tests

### 3.3.3.1 pH and Temperature

As discussed in Section 2.4.3 and as shown in Figure 2-8, the pH of the wastewater determines the hydrogen sulphide species distributions. This in turn affects the amount of $H_2S$ gas released into the sewer headspace. Also, as explained in the same section (Section 2.4.3) and as shown in Figure 2-9, the wastewater temperature also affects the release of $H_2S$ gas following the Henry's Law (Equation 2-18).

This test was performed using Orion Thermo Scientific Meter with a pH electrode connected, as shown in Figure 3-23. The pH electrode also had, integrated into it, a temperature sensor, which made it possible for the two parameters to be measured at the same time.


Figure 3-23: Multimeter, pH electrode, pH standard solutions

The samples were prepared in triplicates using 50 $ml$ beakers. A magnetic stir bar was placed into each beaker which were placed on the magnetic stirrer and set to a moderate speed. This was done to ensure homogeneity. The pH electrode, in its stand, was carefully lowered the wastewater sample and the reading was taken. This was done for all samples.

### 3.3.3.2 RDO (Relative Dissolved Oxygen)

This test gives the amount oxygen present within the wastewater, which can give indications about the activity of SRB within liquid phase of the sewer environment (MGWWPS).

This test was also performed using the Orion Thermo Scientific Meter, however, with a dedicated probe, as shown in Figure 3-24. 50 $ml$ beakers were also used to hold the wastewater samples, in triplicates. Like in the previous test, the magnetic stirrer was also used to ensure homogeneity. The RDO probe was inserted into the wastewater sample and the reading was taken and recorded.


Figure 3-24: Multimeter and electrodes

### 3.3.3.3 Conductivity

Conductivity is the measure of how much a liquid can conduct electricity, which is a function of the ions present in the liquid such as sulphide ions like $S^{2-}$ and $HS^{-}$.

Like the pH & temperature testing and RDO testing, Conductivity test was also carried out using the Orion Thermo Scientific Meter, however, with a conductivity probe connected in the appropriate port. The experiment was also carried out on triplicate samples of wastewater. The magnetic stirrer was also used to ensure homogeneity of solution. The conductivity probe was inserted into the sample and the reading was taken and recorded.

### 3.3.3.4 Nitrate ion and Ammonia ion

Nitrate test and Ammonia test was carried out using HACH multimeter and performed in accordance with the manufacturer's guideline.

For Nitrate test, 25 $ml$ wastewater samples were prepared in triplicates. One pillow of nitrate ISA (ionic strength adjuster) powder (Figure 3-25), provided by the manufacturer, was added to the sample to ensure accurate reading. The powder, being a chemical coagulant, resulted into the coagulation and flocculation of particles, as shown in Figure 3-26(a). The nitrate ISE (ion selective electrode) was connected to the multimeter and lowered into the sample, as shown in Figure 3-26(b), and the reading was taken.

Figure 3-25: Ammonia and nitrate ion meter, electrodes, powder, and storage solution

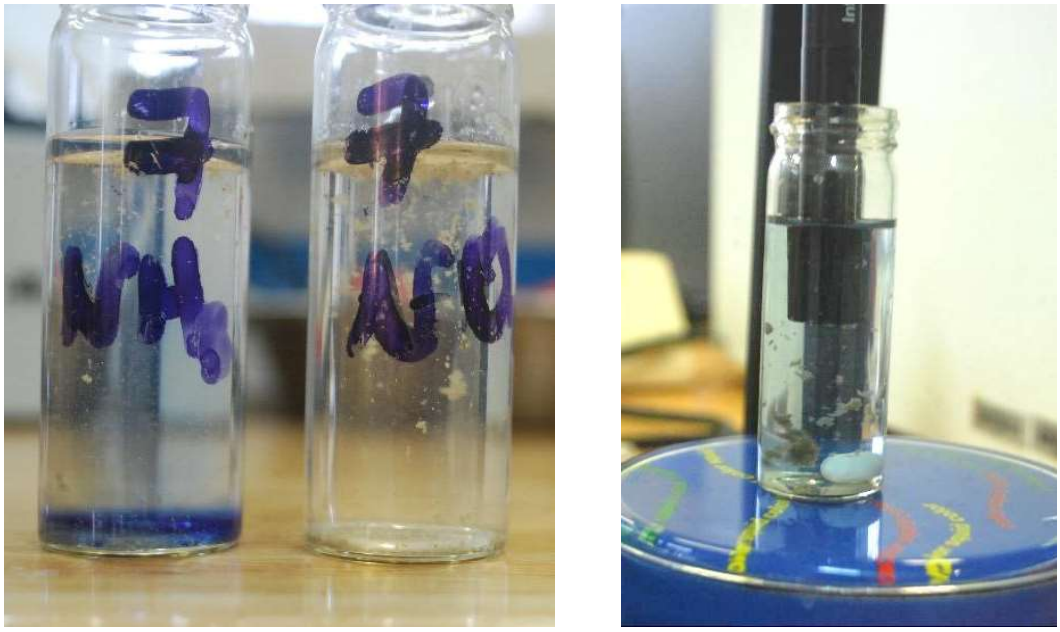

Figure 3-26: Wastewater sample (a) after the addition of powder (b) being tested

Similarly, for Ammonia test, 25 $ml$ wastewater samples were also prepared in triplicates. One pillow of ammonia ISA (ionic strength adjuster) powder was also added, which led to also resulted into coagulation and flocculation, as shown in Figure 3-26(a). 20 drops of Ammonia electrode storage

solution were released to the Ammonia probe cap after which the electrode was covered. The electrode was connected to the multimeter and lowered into the sample, and the reading was taken. This was done for all samples.

### 3.3.3.5 Total Solids, Volatile Solids and Fixed Solids

This experiment was performed to determine the amount of solid in the wastewater and further determine the volatile and the fixed solids.

The experiment was performed in accordance with the guidelines provided in the book written by Baird (2017). Empty crucibles were weighed using Scaltec high precision weighing balance (Figure 3-27) and the readings were recorded. The wastewater sample was stirred using a magnetic stirrer to ensure homogeneity while a micropipette was used to place 20 $g$ of sample into the crucible, still on the scale, as shown in Figure 3-28. The new reading was recorded, and the loaded crucible was carefully transferred to the oven tray using a crucible tong (Figure 3-27). This process was carried out thrice for each wastewater sample. The loaded tray was transferred into the oven (Figure 3-29) set at 105℃ and left for 24 hours. This was done to give enough room for evaporation to take place leaving behind the solid contents in the wastewater samples.


Figure 3-27: Apparatus for Total solids test

Figure 3-28: Measurement of wastewater sample into crucible


Figure 3-29: Wastewater sample being weighed (left) and placed inside the oven (right)

The next day, the tray was removed from the oven, and as expected the water content in the crucibles were all gone leaving behind the solids, as shown in Figure 3-31(b). The crucibles were all transferred to a desiccator to cool off while guarding off water moisture, as shown in Figure 3-30(a). After this, each crucible was weighed to determine the mass of the crucible and wastewater solid, which was used for further calculation; this is discussed in the next chapter. The crucibles were returned to the tray and transferred into a pre-ignited furnace, as shown in Figure 3-30(b). The furnace ignition level was increased to 550℃, and the samples was left to burn for 2 hours. This was done to get rid of the volatile solids leaving behind the fixed solids. After the 2-hour period, the samples were removed and allowed to cool in the desiccator after which they were weighed.

(a) (b)

Figure 3-30: Wastewater samples in (a) the desiccator (b) the furnace

(a) (b) (c)

Figure 3-31: Wastewater samples in its (a) wet state (b) dry state (c) fired state

### 3.3.3.6 Biochemical Oxygen Demand (BOD)

Biochemical Oxygen Demand (BOD) is an experiment used to determine the amount of oxygen consumed within a specified incubation period due to the activity of aerobic microorganisms (bacteria) within the wastewater. These organisms depend on oxygen $O_2$ as a source of energy, as shown in Equation 3-1, without which they cannot breakdown organic substances contained in the wastewater. Hence, high BOD value suggests high amount of organic matter.

$$\text{Organic matter} + \text{microorganism} + O_2 + \text{nutrients} \longrightarrow CO_2\uparrow + H_2O + \text{microorganism} \quad (3\text{-}1)$$

The experiment was also performed in accordance with the guidelines provided by the manufacturer, AQUALYTIC. The incubation period in this case was 5 days; hence, BOD is presented as $BOD_5$. To begin, the components of the BOD test kit were prepared, as shown in Figure 3-32, while the OxiTop heads (pressure sensor) were particularly checked using the OxiTop remote sensor to ensure that the battery level is sufficient. Based on the expected result range, 56 $ml$ of wastewater sample was used for this experiment. This was measured in triplicates using the measuring cylinder and poured into the BOD bottles, as shown in Figure 3-33. Three drops of N-allylthiourea (ATH), provided by the

manufacturer, were added to inhibit nitrification after which the bottle was sealed with a seal cup (also known as gasket). Ten drops of $KOH$ (provided by the manufacturer) were released into each seal cup and the bottles were closed by screwing the OxiTop heads (pressure sensor. The OxiTop remote sensor was used to 'start' each sample, as shown in Figure 3-34, after which they were transferred to the incubator pre-set to 20℃; this creates a conducive environment for the growth of aerobic microorganisms. The samples were left in the incubator for 5 days after which the readings were obtained from the OxiTop remote sensor.


Figure 3-32: BOD test apparatus and reagents

Figure 3-33: Wastewater sample being measured into BOD bottles

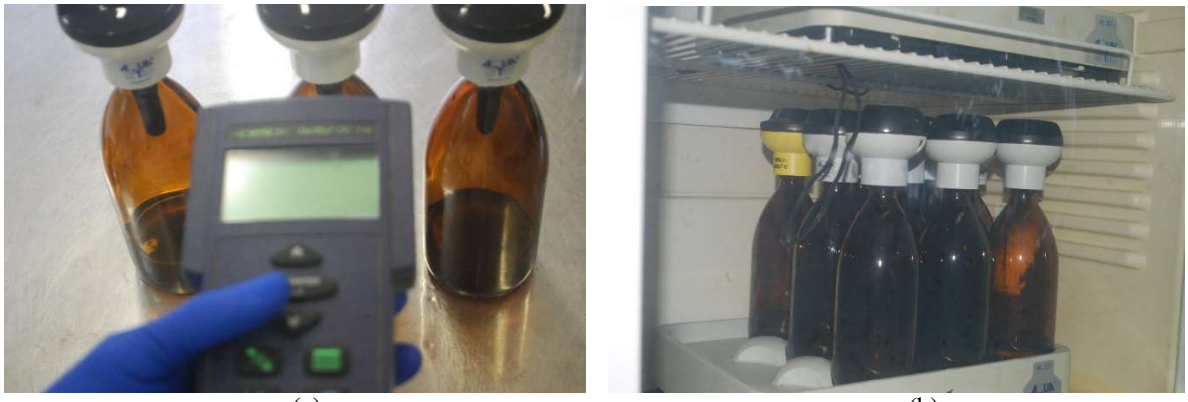

(a) (b)

Figure 3-34: Starting of BOD sample using the sensor remote (a) and placed in the incubator (b)

### 3.3.3.7 Chemical Oxygen Demand (COD)

Chemical Oxygen Demand (COD) is an experiment used to determine the amount of reduction that has taken place due to the reaction between an oxidant and organic matter within a given sample. In other words, it determines the amount of oxygen required for the chemical oxidation of organic matter present within a sample. The oxidant in this case is dichromate ion ($Cr_2O_7{}^{2-}$) which is reduced to chromic ion ($Cr^{3+}$) while the sample is wastewater.


Figure 3-35: Reagents used for COD test

The experiment was also performed in accordance with the guidelines provided in the book by Baird (2017); Figure 3-35 shows the reagents that were used during the experiment. For measurements, a micropipette due to the small quantities involved. 0.5 $ml$ of each wastewater sample was measured into vials in triplicates and diluted with 2.0 $ml$ of distilled water. 2.5 $ml$ of potassium hydrogen phthalate (KHP) standard was also measured into empty vials as well as blanks (distilled water), which served as control. 1.5 $ml$ of potassium dichromate ($K_2Cr_2O_7$) was added into all the prepared vials, as shown in Figure 3-36(a), followed by an addition of 3.5 $ml$ of concentrated sulphuric acid ($H_2SO_4$). The vials were closed with the lid and transferred to the COD reactor (Hach COD reactor), as shown in Figure 3-36(b). The reactor was set to 150℃ and the countdown timer was set to 2 hours.

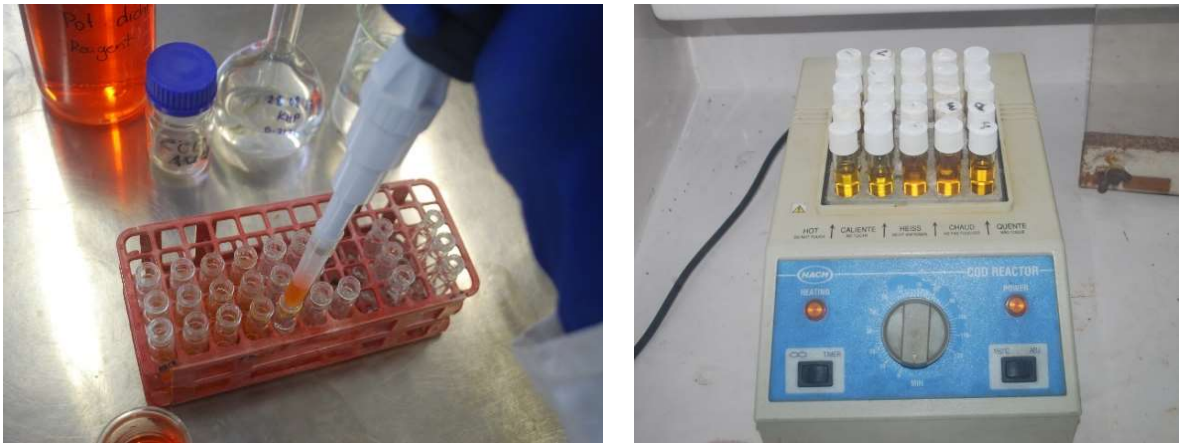


(a) (b)

Figure 3-36: (a) Preparation of COD test samples (b) Sample vials under COD reaction

After this duration, the vials were transferred into the rack and allowed to cool for about 15 minutes. Hach spectrophotometer was set and calibrated after which each vial was inserted, as shown in Figure 3-37, and the readings were recorded.

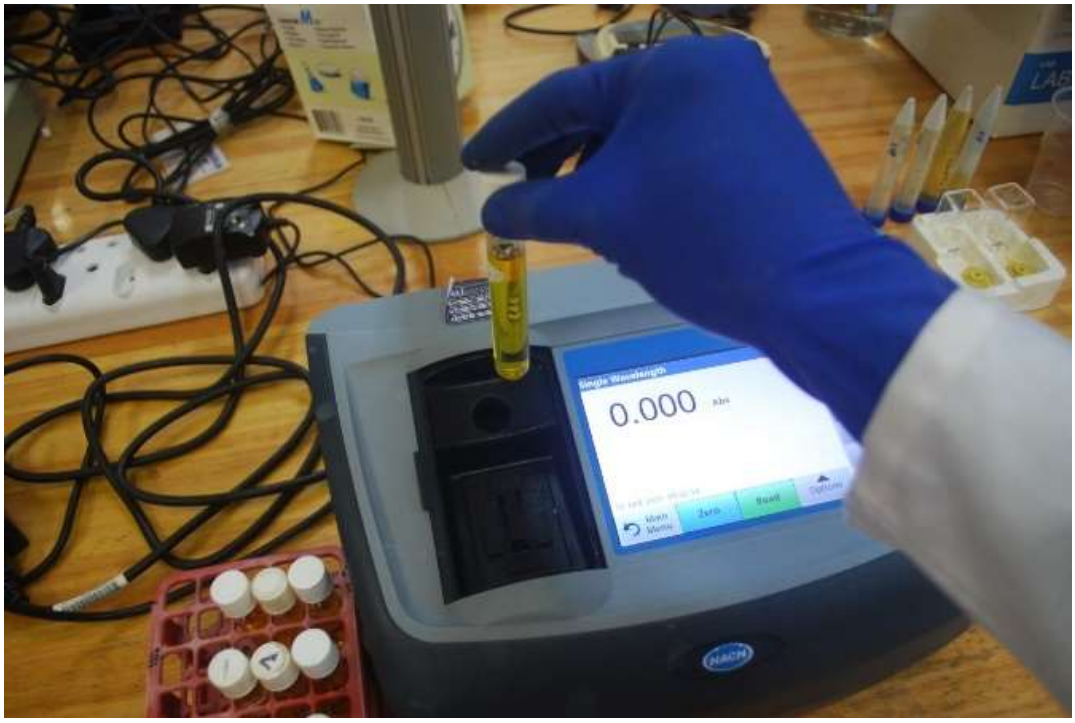


Figure 3-37: Sample vials being inserted in the spectrophotometer

### 3.3.3.8 Inductively Coupled Plasma-Mass Spectrometry (ICP-MS) Analysis

ICP-MS analysis is an elemental metal analysis performed on a liquid sample to determine the concentrations of elements contained in it.

This experiment is one of the few experiments that was sent to externals labs; however, the samples were prepped in duplicates. 50 $ml$ of wastewater was measured into 50 $ml$ conical tube and transferred into the centrifuge for centrifugation, as shown in Figure 3-38. This resulted into the sedimentation of particles at the bottom of the tube, as shown in Figure 3-39, after which the samples were carefully sieved with the use of a syringe and 0.25 $ml$ micro filter (Figure 3-38) to remove all tiny particles into the sample conical tubes. All prepped samples, as shown in Figure 3-40, were stored in the freezer till it was transfer to the testing lab.


Figure 3-38: Centrifuge (left), micro filter and syringe (right)

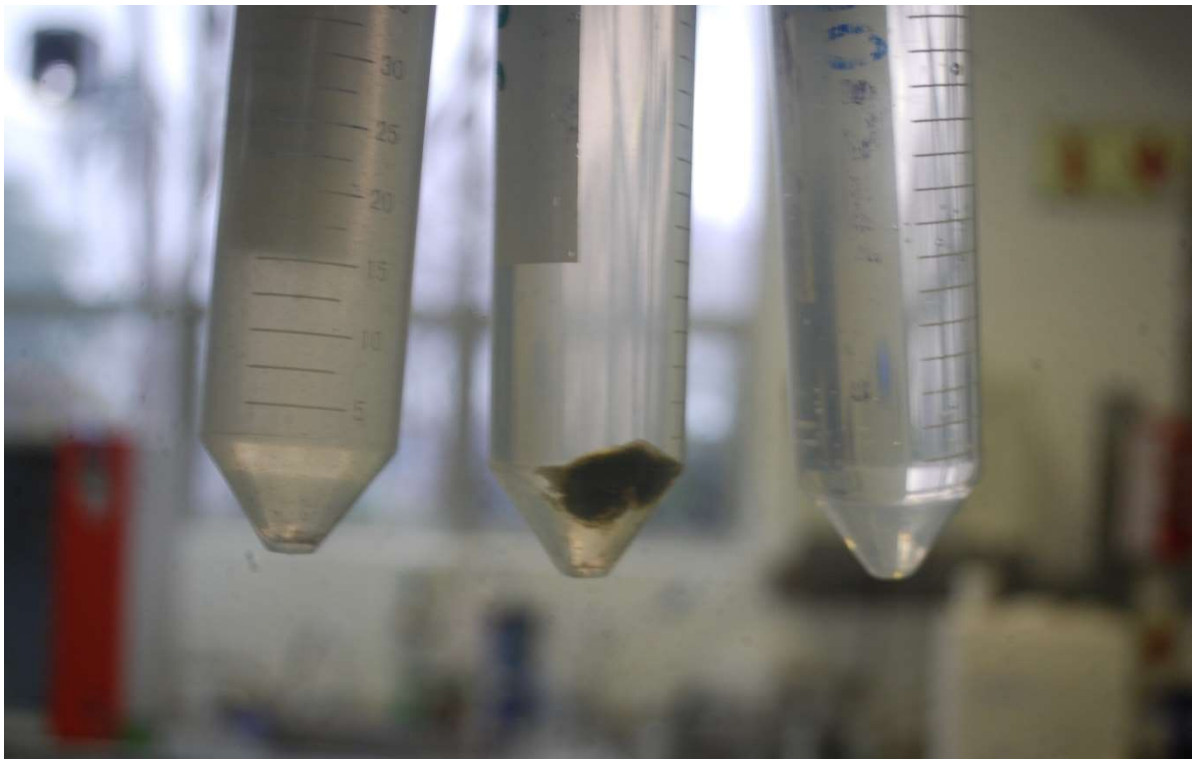

Figure 3-39: Wastewater sample in its raw state (left), after centrifugal separation (middle), and after microsieving (right)

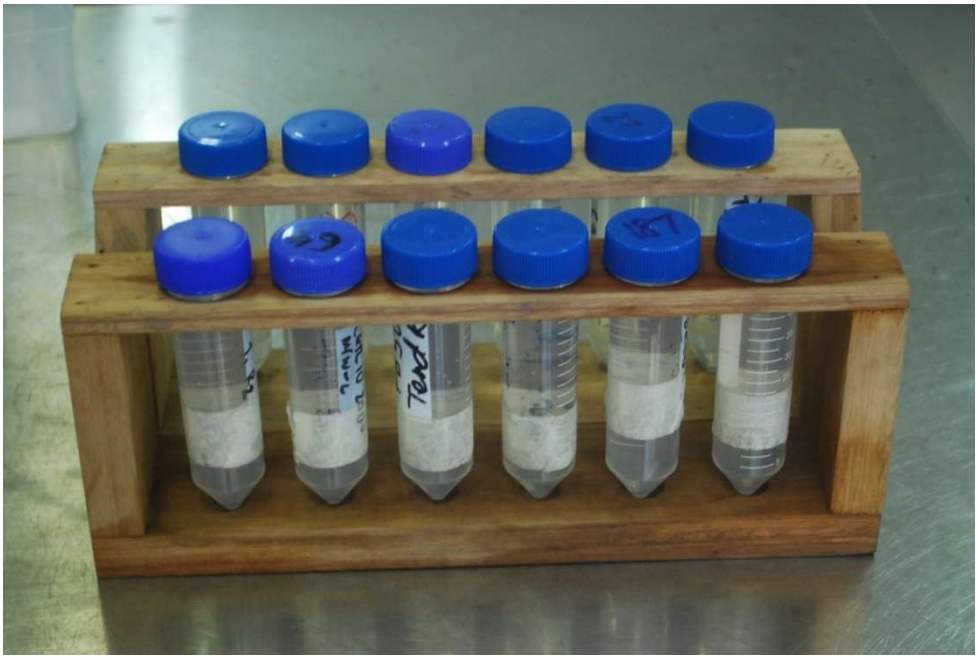

Figure 3-40: Wastewater samples prepped for ICP analysis

### 3.3.4 Specimen Monitoring

The exposed specimens are monitored every month. The suspended cage is pulled up and opened to access the mortars. The diameter and height of each sample is measured with the use of a digital vernier calliper (Mac Afric digital vernier caliper), as shown in Figure 3-41(a). The mass of each sample was also measured with the use of an electronic weighing scale (EPS-302 precision scale), as shown in Figure 3-41(b). These measurements were being taken to detect changes in the physical properties of the mortars for further investigations.


(a) (b)

Figure 3-41: Size and mass of mortar samples being monitored during the exposure period

## 3.4 Post-exposure stage

This section covers all the activities carried out off-site and after the exposure duration. It focuses on the advanced analysis technique used during this study—Scanning Electron Microscopy (SEM)—which took place at the Microscopy and Microanalysis Unit (MMU) at UKZN.

### 3.4.1 Scanning Electron Microscopy (SEM) and Energy Dispersive Spectroscopy (EDS)

Scanning Electron Microscopy (SEM) is an advanced technique used to produce images with a wide range of magnifications of up to about 100,000x while yet still retaining a very high resolution; hence, SEM images are very clear and detailed. It can be used to visualize the microstructural characteristics of materials or morphological characteristics of microorganisms (Gaylarde et al., 2003).

A scanning electron microscope targets the interested area on the sample with accelerated electrons referred to as the primary electron (PE). This results into the dissipation of multiple electron signals which are used for valuable for various analysis. The dissipated signals include auger electrons (AE), secondary electrons (SE), backscattered electrons (BSE), photons (characteristic and continuum X-rays), and visible light (cathodoluminescence, CL). However, for this study, three of these signals were used; the SE was used to produce SEM images, which gave details on topography and morphology; the BSE were used to produce the BSE micrographs, which gave details on composition/microstructural contrast; and the characteristic X-ray was used for EDS (Energy Dispersive Spectroscopy) analysis which is an elemental analysis.

For this study, three categories of samples were used with this technique: unexposed mortar samples, oven-dried exposed mortar samples and corroded concrete (product of corrosion) from the wall of the aggressive environment (MGWWPS). SEM was used to see the microstructural characteristics and investigate the elemental composition of the exposed and unexposed mortar samples, while it was also used to visualize the community of microbes on the corroded concrete samples. And unlike FISH (fluorescence in-situ hybridisation) analysis which gives a complete profile of bacteria, SEM can only be used to visualize, and not identify, the microorganisms (Gaylarde et al., 2003; Trejo et al., 2008).

Samples were prepared under safe laboratory conditions and thereafter dispatched for the analysis. For the mortar samples, they were oven dried and cut to the recommended size for proper analysis; while for the corroded samples, a very small amount of sample was taken from different spots on the corroded concrete wall. These tiny samples were kept inside a sample vial, as shown in Figure 3-42, which contained 25% glutaraldehyde ($C_5H_8O_2$) solution, after which they were kept in the cold room till the analysis was performed. 25% glutaraldehyde solution was used as a fixative, to preserve the microbial cells.

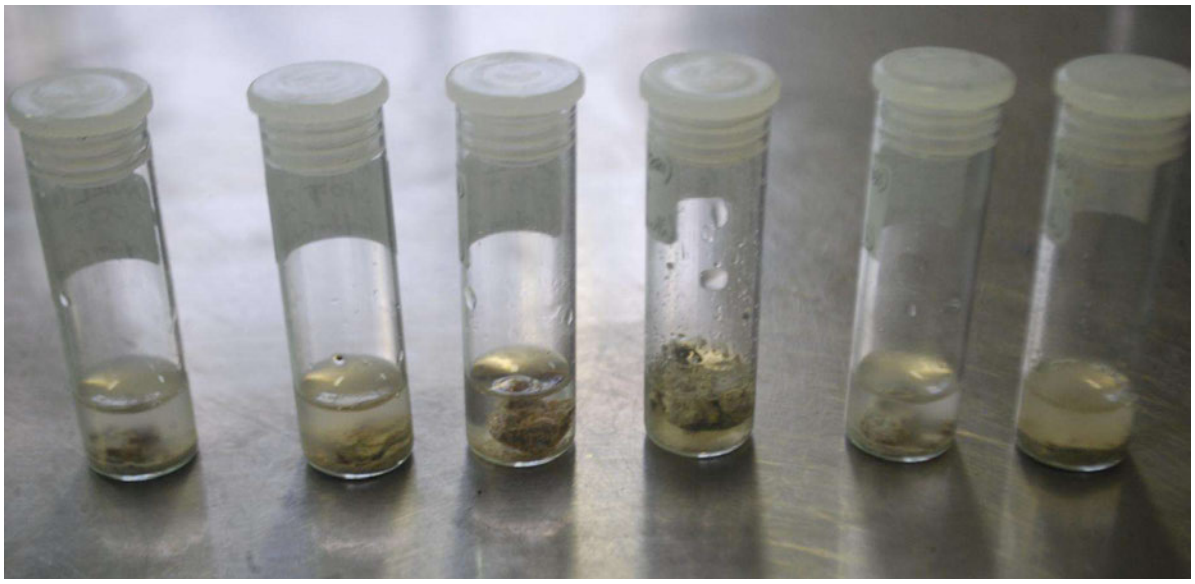

Figure 3-42: Samples of corroded concrete kept inside vial containing fixative

## 3.5 References


Baird, R.B., 2017. *Standard methods for the examination of water and wastewater, 23rd*. Water Environment Federation, American Public Health Association, American Water Works Association.

De Belie, N., Monteny, J., Beeldens, A., Vincke, E., Van Gemert, D. and Verstraete, W., 2004. Experimental research and prediction of the effect of chemical and biogenic sulfuric acid on different types of commercially produced concrete sewer pipes. *Cement and concrete research*, *34*(12), pp.2223-2236.

De Muynck, W., De Belie, N. and Verstraete, W., 2009. Effectiveness of admixtures, surface treatments and antimicrobial compounds against biogenic sulfuric acid corrosion of concrete. *Cement and Concrete Composites*, *31*(3), pp.163-170.

Gaylarde, C., Silva, M.R. and Warscheid, T., 2003. Microbial impact on building materials: an overview. *Materials and structures*, *36*(5), pp.342-352.

Jiang, G., Keller, J. and Bond, P.L., 2014. Determining the long-term effects of $H_2S$ concentration, relative humidity and air temperature on concrete sewer corrosion. *Water research*, *65*, pp.157-169.

Khan, H.A., Castel, A., Khan, M.S. and Mahmood, A.H., 2019. Durability of calcium aluminate and sulphate resistant Portland cement-based mortars in aggressive sewer environment and sulphuric acid. *Cement and Concrete Research*, *124*, p.105852.

Kiliswa, M.W., Scrivener, K.L. and Alexander, M.G., 2019. The corrosion rate and microstructure of Portland cement and calcium aluminate cement-based concrete mixtures in outfall sewers: A comparative study. *Cement and Concrete Research*, *124*, p.105818.

Saucier, F. & Lamberet, S., 2009. Keynote paper: Calcium aluminate concrete for sewers: going from qualitative to quantitative evidence of performance. *Concrete in aggressive aqueous environments-Performance, Testing, and Modeling*, pp.398-407.

South African National Standard (SANS) 5861-3, 2006. *Concrete tests: Making and curing of test specimens*. SABS Standards Division.

South African National Standard (SANS) 5863, 2006. *Concrete tests: Compressive strength of hardened concrete*. SABS Standards Division.

South African National Standard (SANS) 6255, 2006. *Mortar tests — Compressive strength of mortar*. SABS Standards Division.

South African National Standard (SANS) 50197-1, 2011. *Cement: Composition, Specifications and Conformity Criteria for Common Cements*. SABS Standards Division.

Satoh, H., Odagiri, M., Ito, T. and Okabe, S., 2009. Microbial community structures and in situ sulfate-reducing and sulfur-oxidizing activities in biofilms developed on mortar specimens in a corroded sewer system. *Water research*, *43*(18), pp.4729-4739.

Song, Y., Tian, Y., Li, X., Wei, J., Zhang, H., Bond, P.L., Yuan, Z. and Jiang, G., 2019. Distinct microbially induced concrete corrosion at the tidal region of reinforced concrete sewers. *Water research*, *150*, pp.392-402.

Sun, X., Jiang, G., Chiu, T.H., Zhou, M., Keller, J. and Bond, P.L., 2016. Effects of surface washing on the mitigation of concrete corrosion under sewer conditions. *Cement and Concrete Composites*, *68*, pp.88-95.

Trejo, D., de Figueiredo, P., Sanchez, M., Gonzalez, C., Wei, S. and Li, L., 2008. *Analysis and assessment of microbial biofilm-mediated concrete deterioration* (No. SWUTC/08/476660-00008-1). Southwest Region University Transportation Center (US).

Vincke, E., Van Wanseele, E., Monteny, J., Beeldens, A., De Belie, N., Taerwe, L., Van Gemert, D. and Verstraete, W., 2002. Influence of polymer addition on biogenic sulfuric acid attack of concrete. *International biodeterioration & biodegradation*, *49*(4), pp.283-292.

CHAPTER 4

# RESULT & ANALYSES

## 4.1 Introduction

To achieve the aim of this study, several assessments and experiments were conducted. While some of the assessments were done visually, some were carried out with the use of lab tools and equipment, and some were carried with the use of advanced technology equipment. Here, in this chapter, the results obtained from each test is presented and discussed.

## 4.2 Strength test

As discussed in Section 3-22, three kinds of mortar samples were produced— calcium aluminate cement (CAC)-based mortars, denoted as $CAC_m$; Portland cement (PC)-based mortars, denoted as $PC_m$; and Portland cement (PC)-based mortars with waterproofing admixture, denoted as $PCA_m$. After 28 days curing, these mortars were taken through a compression test using the Avery-Denison compression machine which has maximum load (crushing) value as its output reading. The readings were recorded and used with the cross-sectional area of each mortar sample to calculate the compressive strength in $MPa$. The average values of the resulting compressive strength of each mortar are given in Figure 4-1 below.

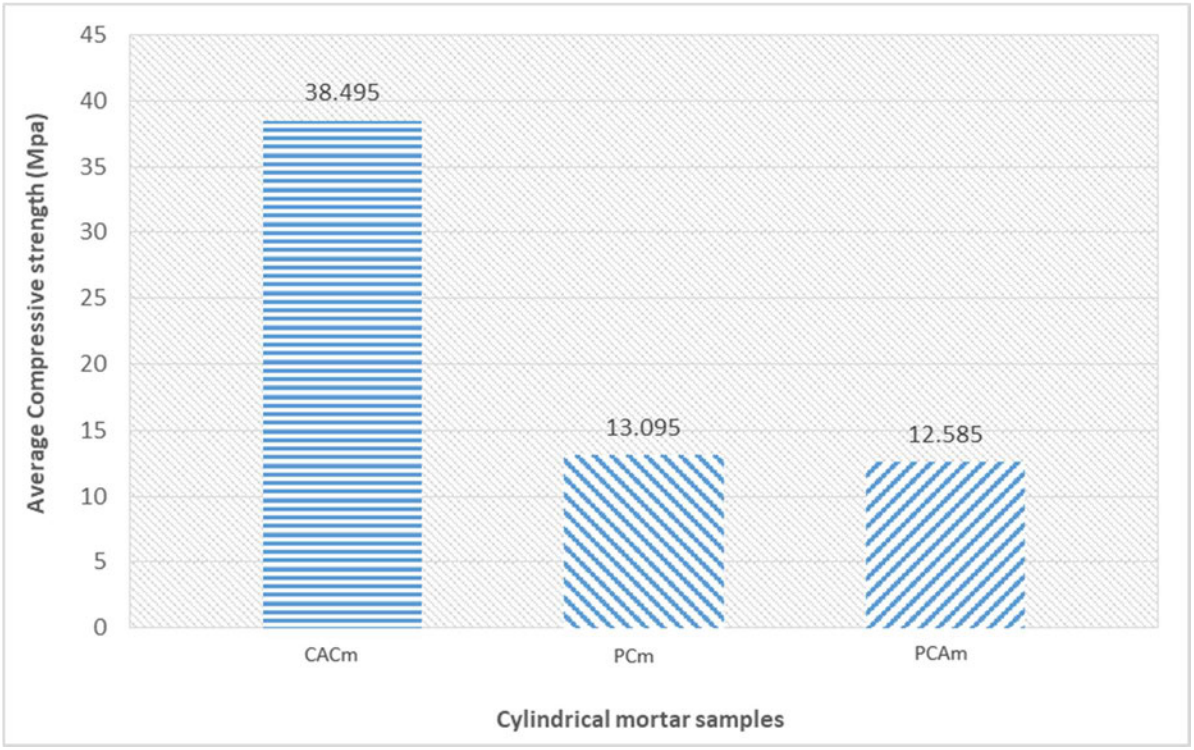


Figure 4-1: Average compressive strength of mortars with different mixtures

From the result presented in Figure 4-1, it can be seen that $CAC_m$ had a compressive strength of 38.5 $MPa$ which is roughly three times the compressive strength of the PC-based mixtures—$PC_m$ and $PCA_m$. There is no doubt that this is due to the different binders used in mixtures. $PC_m$ and $PCA_m$ have similar compressive strengths despite the addition of a crystalline waterproofing admixture (CWA). This suggests that CWA does not have any significant effect on the compressive strength of mortar mixtures; this agrees with the report from some other studies (Pazderka & Hájková, 2016; García-Vera et al., 2019; Gojević et al., 2021). For example, Pazderka and Hájková (2016), in their study on the effect of crystalline admixtures on the properties of concrete, found out that the compressive strength of the concrete with CWA and the compressive strength of the specimens from concrete without CWA were almost identical after 28 days.

The average density of $CAC_m$, $PC_m$ and $PCA_m$ was also calculated using their masses and volumes, and it was found to be 2715 $kg/m^3$, 2279 $kg/m^3$and 2353 $kg/m^3$respectively.

## 4.3 Site assessment

Prior to the exposure stage of this study, the site (MGWWPS) was assessed to confirm its suitability for this study, as an aggressive environment was the requirement. And by visual assessment, MGWWPS was indeed found to be suitable for the study, as MICC was obviously active, due to features like deteriorating concrete surface, expanded concrete cover, exposed aggregate. This can be seen in Figure 4-2, Figure 4-3, and Figure 4-4.

However, this assessment did not stop at the beginning of the study, it continued throughout the study. Figure 4-5(a) shows the state of a concrete-wall section at the beginning of the study, after about 8 years of service, while Figure 4-5(b) shows the state of the same wall section a year after, which shows progressive effect of MICC in the environment.

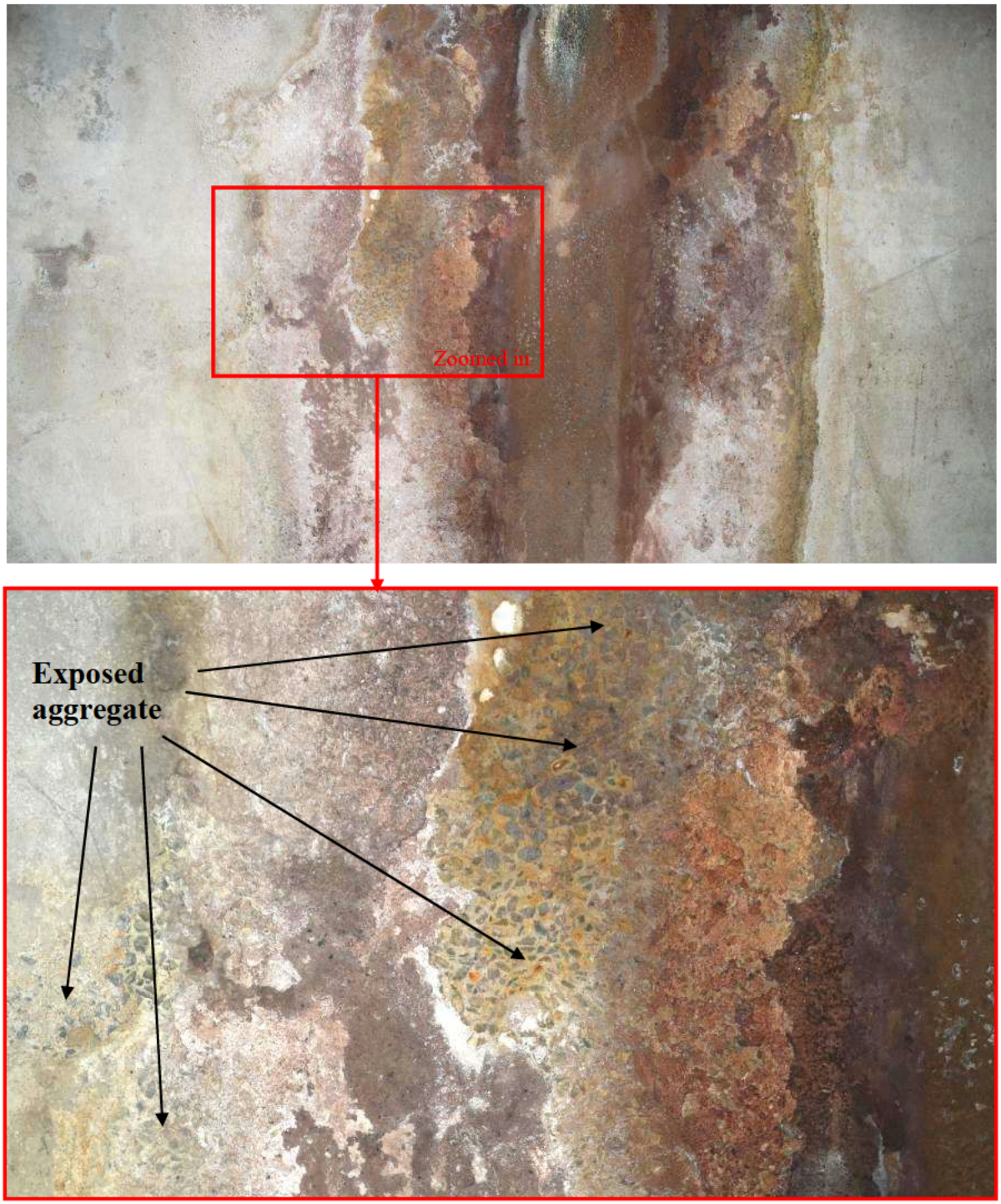


Figure 4-2: Corroded concrete wall


Figure 4-3: Corroded concrete wall

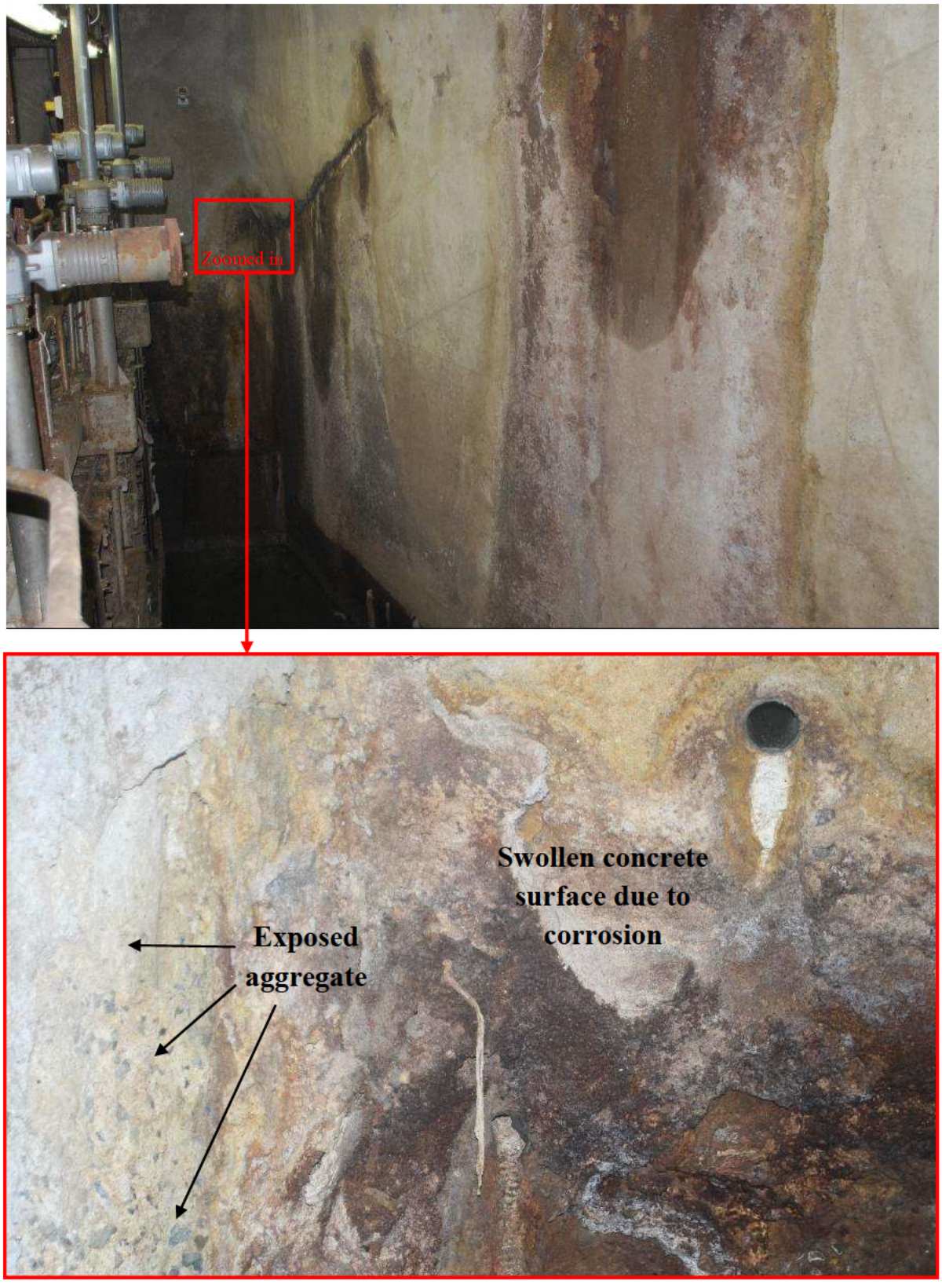


Figure 4-4: Corroded concrete wall


Figure 4-5: Progressive effect of MICC at the exposure site

Besides the visual assessment, the temperature and $H_2S$ gas concentration of the headspace was also being monitored with the use of a digital temperature and a gas detector, as shown in Figure 3-22. The average temperature of the environment was found to be 27°C, while the average $H_2S$ concentration was found to be 5 $ppm$. It should be noted that the site does not have an enclosed headspace, as one will have in a concrete sewer pipe; hence, gases are free to flow in, from the atmosphere beyond the site, and out from the headspace. This will greatly reduce the concentration of $H_2S$ and other sewer gases. Therefore, the warm temperature is seen as the main factor contributing to the MICC taking place in the environment.

## 4.4 Wastewater analysis

In order to understand more about the environment, 8 wastewater samples were taken from the site on different months (within the 12-month exposure duration of mortar samples) and were labelled A to G. This samples were taken through series of test as discussed in Section 3.3.3. Following are the results from these tests and analyses.

### 4.4.1 pH, Temperature, RDO & Conductivity

The pH, temperature, RDO and conductivity of the wastewater samples were measured separately but with the use of the same multimeter, and the results are presented in Figure 4-6, Figure 4-7, Figure 4-8 and Figure 4-9 respectively.

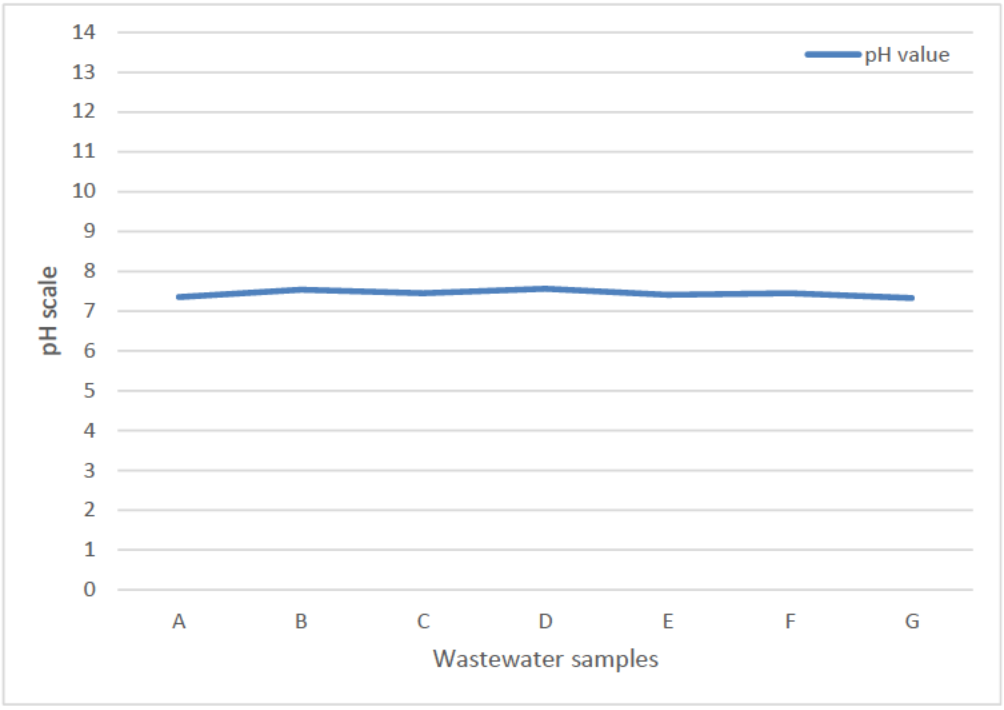


Figure 4-6: pH of wastewater samples

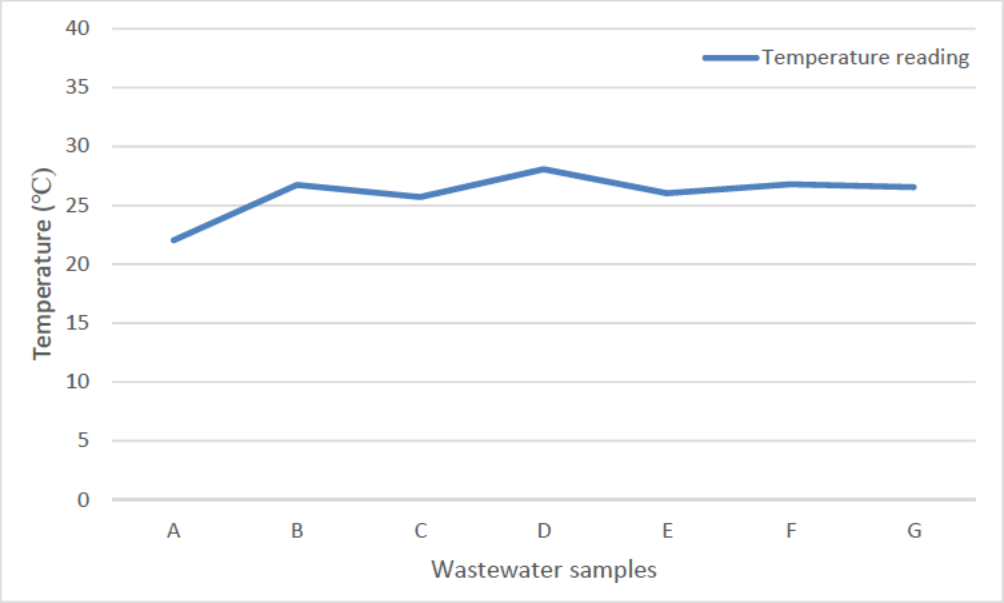


Figure 4-7: Temperature of wastewater samples

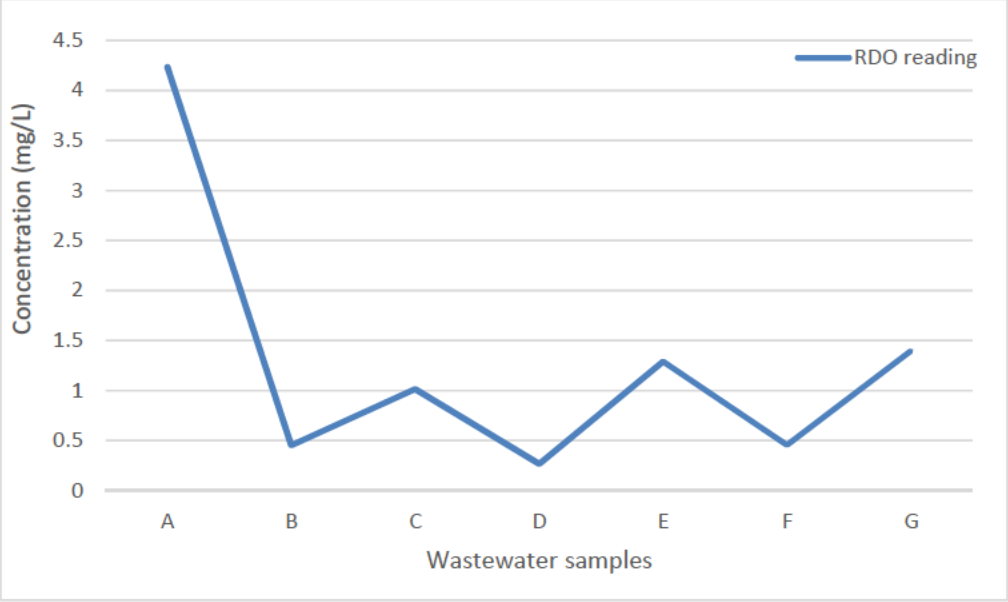


Figure 4-8: RDO concentration of wastewater samples

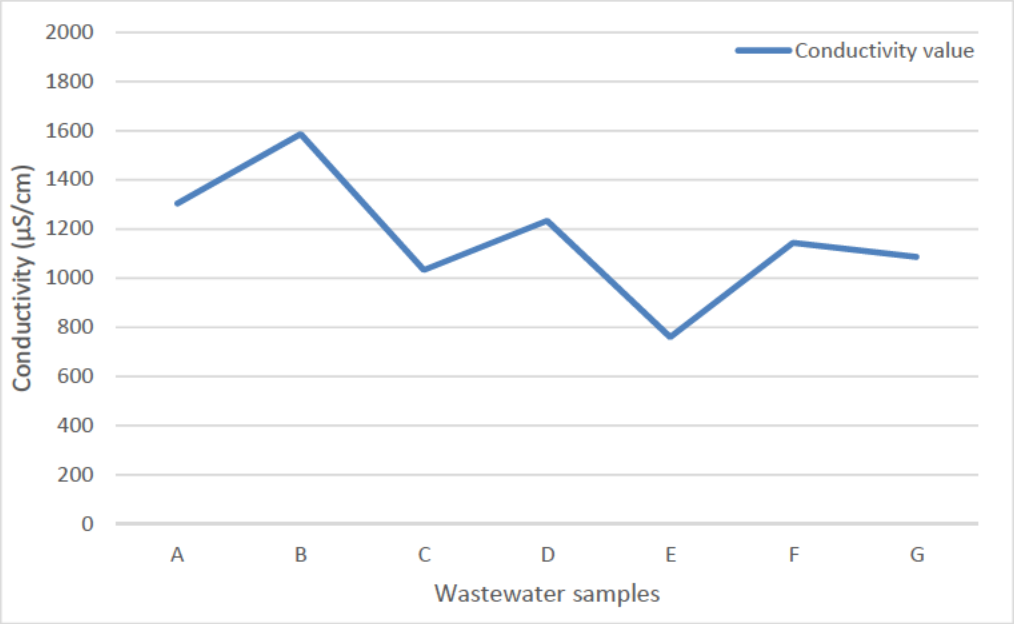


Figure 4-9: Conductivity of wastewater samples

Figure 4-6 shows that the pH of the wastewater (fresh wastewater) is relatively constant with an average pH of about 7.5; hence, the wastewater is alkaline in nature, which creates a conducive environment for SRB (Hao et al., 1996). In addition, Figure 4-7 reveals that the wastewater had temperature values within the range 22°C to 28°C, with an average of 26°C; this, also, is conducive for SRB. Okabe and Characklis (1992) reported that *Desulfovibrio desulficans* have a specific growth rate of 0.38/h at 25°C.

Figure 4-8 shows that the DO concentration of the wastewater is mostly within the range 0.3 – 1.4 $mg/L$, which is a relatively low DO concentration. This promotes the activity of SRB, which under low DO condition decompose organic substances leading to sulphide build-up within the liquid phase of the environment. In addition, this low DO conditions also promotes the formation of biofilm, as explained in Section 2.4.1, which helps to build the anaerobe (SRB) community; hence, increasing their activities, especially in the presence of sulphate-rich wastewater.

From Figure 4-9, it is seen that the wastewater had a least value of 750 µ$S/cm$, highest value of 1600 µ$S/cm$ and an average value of about 1165 µ$S/cm$, which when standardized (to a 25°C-temperature reading) is 1142 µ$S/cm$. This shows a low ion concentration from dissolved salts within the wastewater; hence, suggesting low or negligible concentration of anions like $SO_4^{2-}$, $S^{2-}$, $Cl^-$, $CO_3^{2-}$, and $NO_3^-$; and cations like $Ca^{2+}$, $Na^+$, $Mg^{2+}$ and $Al^{3+}$.

### 4.4.2 Nitrate ion & Ammonia ion

Similar to the previous tests, nitrate ion and ammonia ion test were carried out separately using the same multimeter, and Figure 4-10 and Figure 4-11 respectively shows the results.

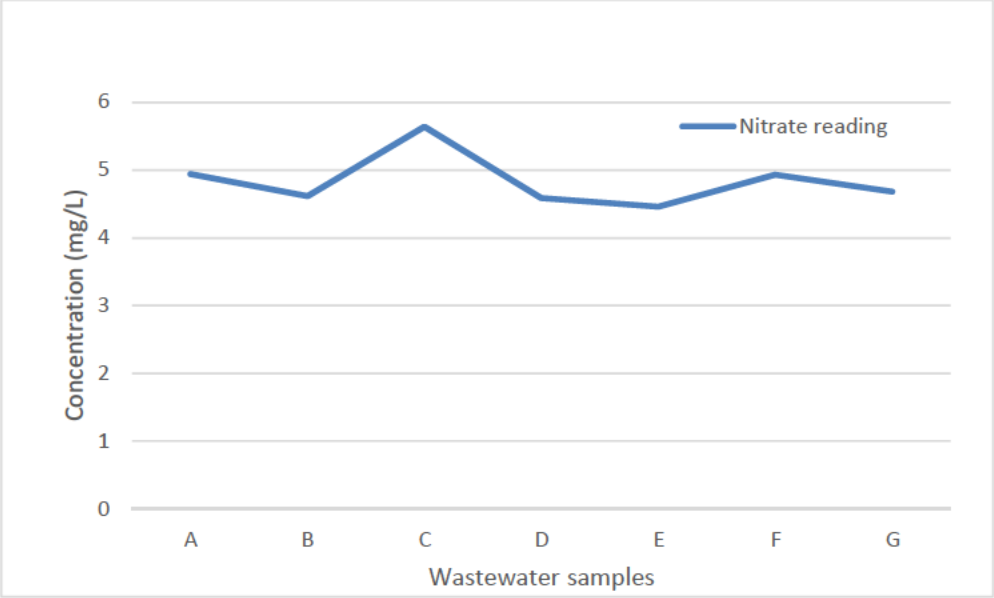


Figure 4-10: Nitrate ion concentration of wastewater samples

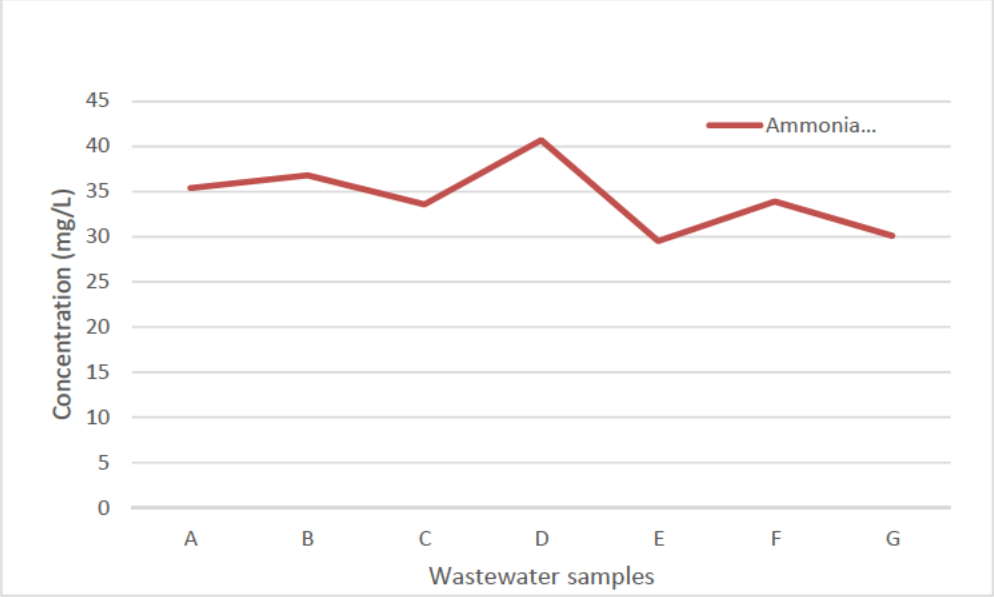


Figure 4-11: Ammonia ion concentration of wastewater samples

From Figure 4-10, the wastewater has nitrate ion concentrations within the range 4.5 – 5.6 $mg/L$ and an average concentration of 4.8 $mg/L$, while it has ammonia ion concentrations within 29.5 – 41 $mg/L$ and an average concentration of 34.3 $mg/L$, which is a moderately strong concentration based on Table 2-3. This, however, is an indication that active organic matter decomposition taking place within the liquid phase of the sewer environment through the activity of microorganisms; this decomposition leads to the formation of sulphide, as explained in Section 2.4.2.

### 4.4.3 TS, VS & FS

For this test, 20 g of each wastewater sample was used in triplicates, and going through the test procedure, as explained in Section 3.3.3.5, several masses were recorded. These masses were further used to calculate the percentage content of solid—total solid (TS), volatile solid (VS) and fixed solid (FS)—in each sample. The average of these results is presented in Figure 4-12.

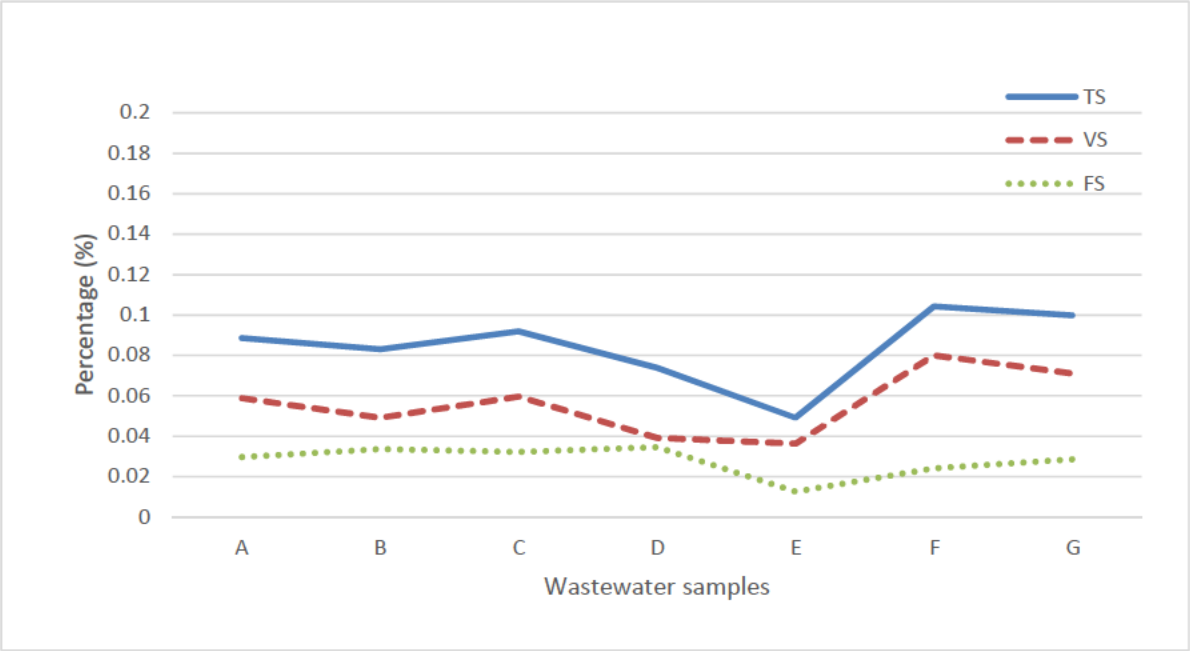


Figure 4-12: TS, VS & FS of wastewater samples

Figure 4-12 shows that TS content of the wastewater is generally less than 0.12% (1200 $mg/L$) with a higher VS content than FS content. The wastewater has an average TS concentration of 844 $mg/L$ which is a moderately strong concentration for wastewater, according to Table 2-3. This was expected, as visual assessment of the samples indicated high solid particle content. It should be noted that TS content comprises the total dissolved solids (TDS) and the total suspended solids (TSS). While TDS is mainly made of ions (calcium, chloride, nitrate, phosphorus, iron, sulphur and others), TSS is mainly made up of soil (silt, clay) particles, plankton, algae, fine organic debris, and other particulate matter.

### 4.4.4 BOD

The BOD experiment, as explained in Section 3.3.3.6, took place for 5 days. After the duration, the result of each sample was extracted from the sensor (OxiTop remote sensor), which also presented the graph for each sample. The graphs give information on what took place within the 5 days in each sample, and the nature of these graphs will suggest if the experiment needs to be rerun, as it could be that the concentration is beyond the expected range that was used at the beginning of the experiment; this is explained in Section 3.3.3.6. An example of the sensor generated graph is presented in Figure 4-13, while the average of the concentrations (amount of $O_2$ consumption), after all necessary reruns, of each wastewater sample is presented in Figure 4-14.

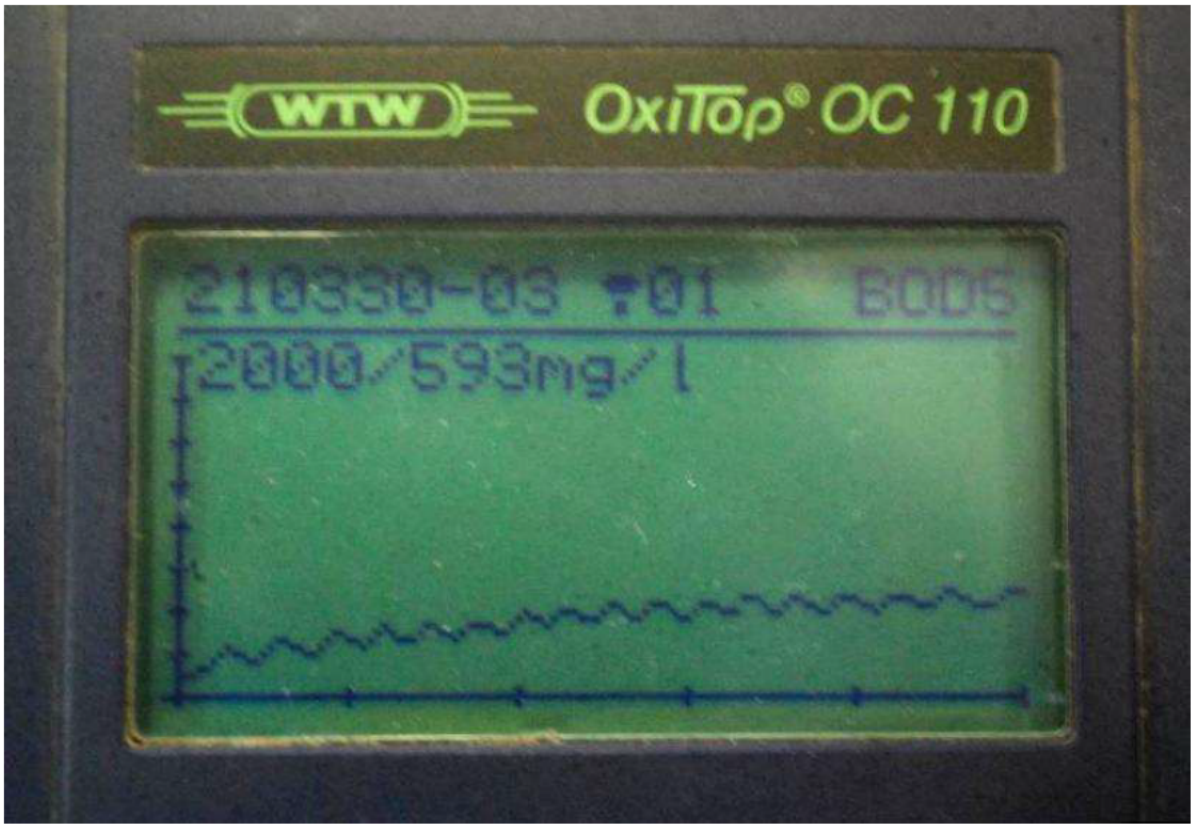


Figure 4-13: BOD sensor generated graph of a wastewater sample

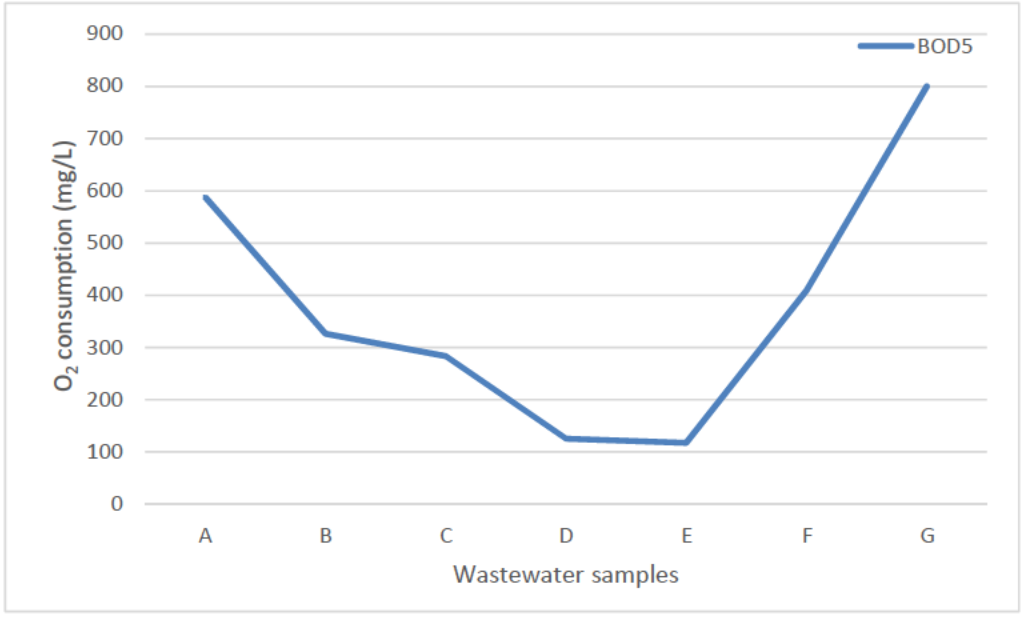


Figure 4-14: $BOD_5$ of wastewater samples

Figure 4-14 shows that the BOD values of the wastewater range between about $115 - 800\ mg/L$ with an average of about $380\ mg/L$ which is a strong concentration. Hence, the wastewater contains high amount of organic matter that is being biochemically consumed (oxidized) by SRB which

depends on it as a source of energy. While this keeps the DO concentration low or further reduces it, it also enhances the formation of sulphide within the wastewater as explained in Section 2.4.2.

### 4.4.5 COD

As explained in Section 3.3.3.7, the final stage of COD experiment involved the use of a spectrophotometer. Here, the amount of light absorbed by each sample is measured and the result is displayed on the screen in the unit of 'abs', which stands for absorbance. These results were used in further calculations to obtain the concentrations (amount of $O_2$ consumption) in $mg/L$. Figure 4-15 shows the final average concentrations of each wastewater sample.

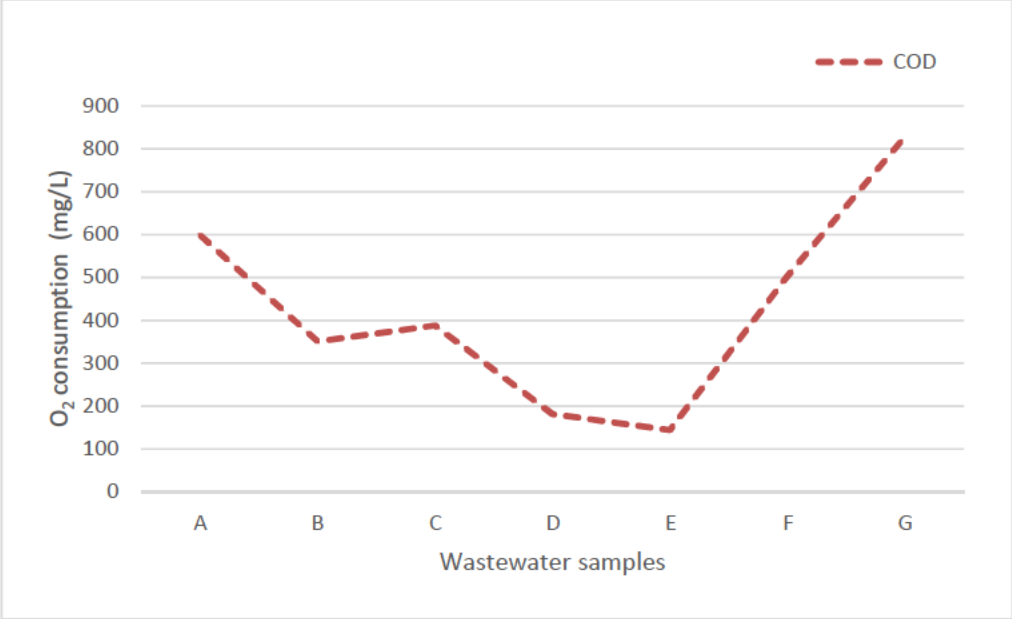


Figure 4-15: COD of wastewater samples

From Figure 4-15, we can be seen that the COD values of the wastewater range between about $150 - 830\ mg/L$ with an average of about $420\ mg/L$. This is a medium concentration according to Table 2-3 though it has a higher value than average BOD value. This also confirms that there is high amount of oxidization compounds in the wastewater; hence increasing the potential for the generation of sulphide within the wastewater.

BOD and COD may be similar in a number of ways; however, one of the major differences is that while BOD focuses on the organic matter contained in a sample, COD focuses on not only the organic matter but also the inorganic matter. Hence, COD value for every sample must be greater or equal to the $BOD_5$ value; therefore, the difference between the two (if any) reveals the amount of inorganic matter present in the sample. Figure 4-16 shows a combination of the $BOD_5$ and COD values for each wastewater sample for easier comparison.

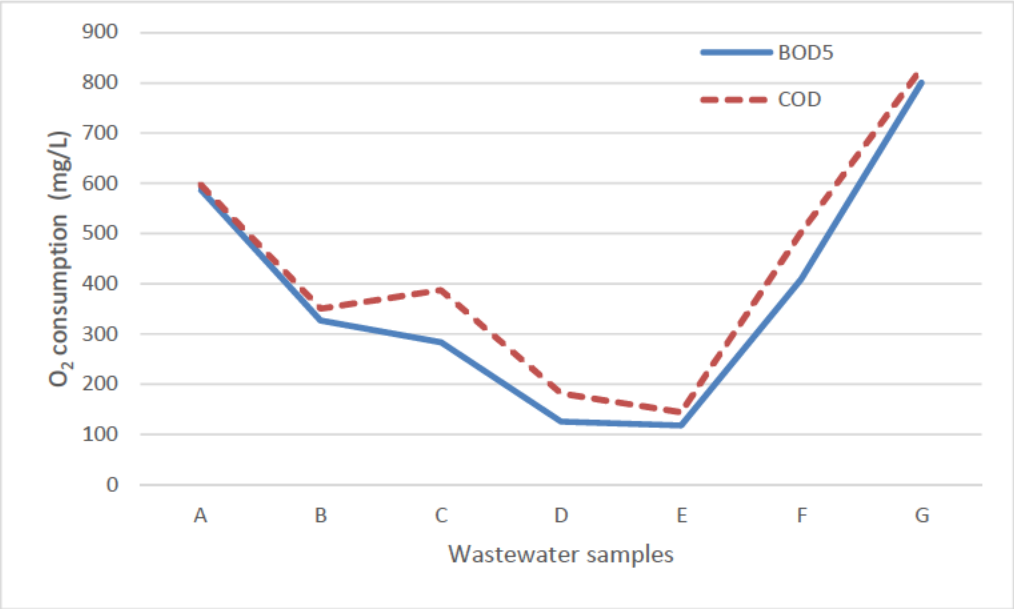


Figure 4-16: $BOD_5$ and COD of wastewater in comparison

As shown in Figure 4-16, the BOD and COD value followed the same trend and as expected, the COD values exceeded the BOD values for every sample; however, seeing that the difference between the COD and BOD values are not much, this indicates that there is a relatively low amount of inorganic compounds in the wastewater when compared with the organic compounds.

### 4.4.6 ICP-MS Analysis

As explained in Section 3.3.3.8, an elemental metal analysis was performed on the wastewater samples; this is to measure the amounts of metals present in each sample. The result is presented in Figure 4-17 below. Figure 4-18 is an enlargement of Figure 4-17, with focus on aluminium ($Al$), iron ($Fe$) and manganese ($Mn$), as they are 'lost' in the Figure 4-17 due to their relatively very slow concentrations which makes them almost negligible and so insignificant.

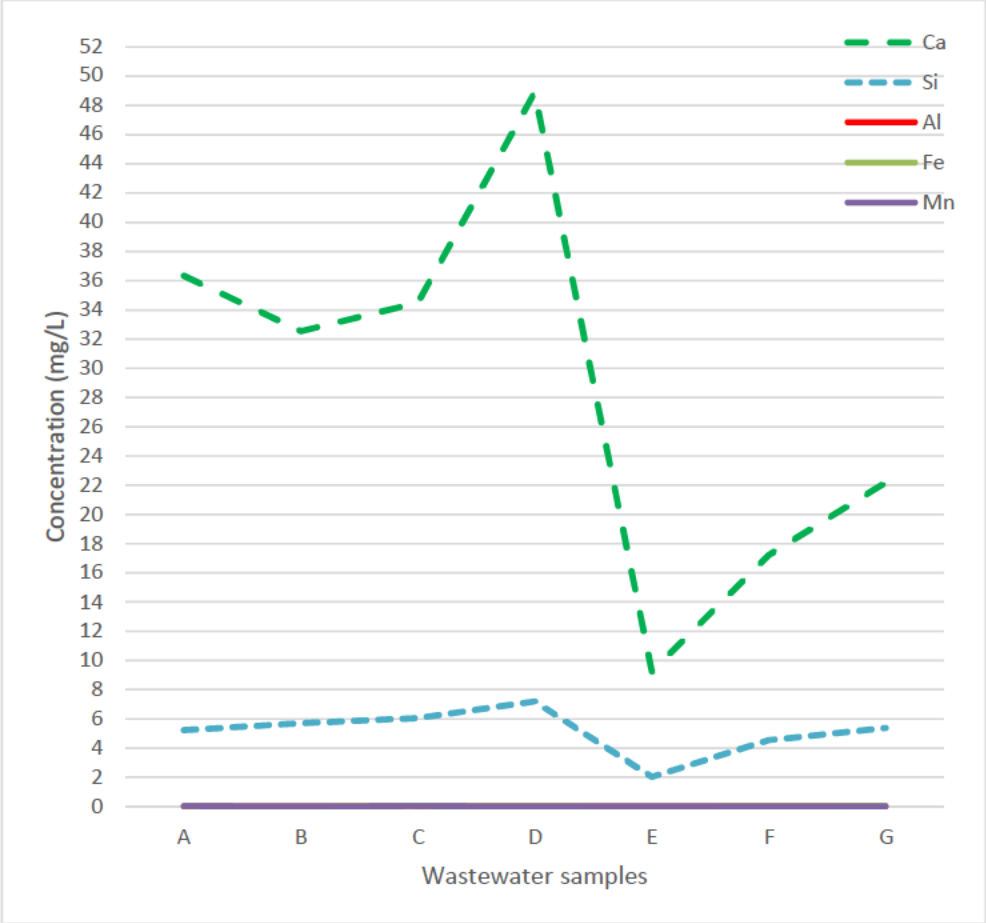


Figure 4-17: Concentration of metals on wastewater samples

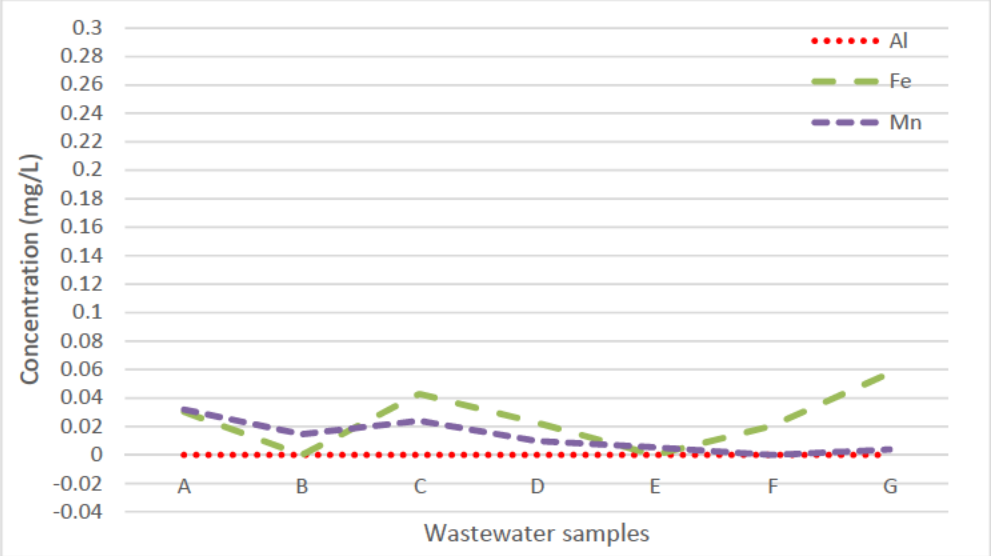


Figure 4-18: Concentration of ***Al***, ***Fe*** & ***Mn*** in wastewater samples

From Figure 4-17, it can be clearer seen that there is a greater abundance of $Ca$ and $Si$ in the wastewater, than any other metal. However, between these two metals, there is a wide difference in their concentrations, with the concentration of $Ca$ being 3 to 5 times that of $Si$.

The relatively very high concentration of Ca is an indication of the presence of cement hydration products like ettringite ($3CaO.Al_2O_3.3CaSO_4.32H_2O$) and gypsum ($CaSO_4.2H_2O$) within the liquid phase of the aggressive environment which must have been washed down following the attack of the concrete wall by sulphuric acid, as explained in Section 2.4.5, which is a stage in MICC. However, seeing that there is a negligible amount of $Al$, as clearly seen in Figure 4-18, the very high concentration must be because of washed-off gypsum (product of corrosion).

Since concrete is a combination of aggregates, cement and water, the high concentration of $Si$ (a representation of fine aggregate) found in the wastewater is also an indication of the active corrosion taking place within the environment. This leads to the exposure of coarse aggregate, as seen in Figures 4-2, 4-3, 4-4 and 4-5, because the concrete cover (cement and fine aggregate) has been literally consumed.

## 4.5 Assessment of mortar samples

As explained in Section 3.3.4, the mortar samples, after they were installed at the exposure site, were monitored monthly to observe changes in the physical properties and to take readings. Section 4.5.1 covers the changes observed visually while Section 4.5.2 covers observations gathered from the measurements taken.

### 4.5.1 Visual Assessment of mortar samples

It was observed that all the mortar samples had taken in water from the environment and no longer in a dry state. This must have been due to overflow or flooding of wastewater in the facility. While the rate of absorption of each mortar sample could not be determined, it is hypothesized that $PC_m$ must have absorbed moisture from much faster than the other two mixtures, as it was noticed that $PC_m$ samples got dry faster than the other two mixtures. This is an indication that moisture within $PC_m$ had easier passage out through the mixture compared to $PCA_m$, which had a waterproofing admixture, and $CAC_m$; hence, $PC_m$ appears to have the highest absorption rate and desorption rate, due to its permeability.

After the second month, minor changes in the physical properties of the PC-based mortars—$PC_m$ and $PCA_m$—were observed right. These changes include reduction in height and diameter, microcracks and pores becoming more pronounced. Though these changes increased over the subsequent months, the $CAC_m$ still retained its integrity, as shown in Figure 4-19, Figure 4-20, Figure 4-21 and Figure 4-22.


Figure 4-19: $CAC_m$ sample after 9-month exposure

Figure 4-20: $PC_m$ sample after 9-month exposure

Figure 4-21: $PCA_m$ sample after 9-month exposure

While Figure 4-19, 4-20 and 4-21 focused on each mortar mixture, Figure 4-22 shows them in comparison with each other, and it reveals the extent of material that had been lost in the PC-based mixtures after only 9 months.

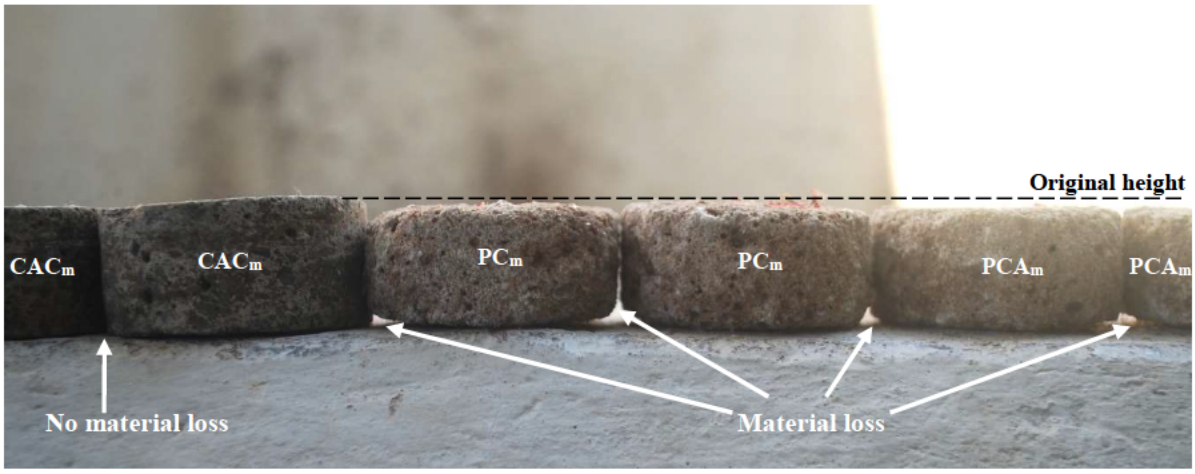


Figure 4-22: Mortar samples after 9-month exposure

### 4.5.2 Mass and volume changes in mortar samples

As explained in Section 3.3.4, the mortar samples were monitored over the 12-month exposure period on a monthly basis (every 30 days). The mass, diameter and height were measured and recorded. The measured heights and diameters were used to calculate the volume of each sample. The average of the volumes for each mixture is presented in Figure 4-23. These derived volumes were further used to calculate Δvolume (change in volume), with reference to volume before exposure, and this is presented in Figure 4-24. Similarly, the average of the masses of each mixture is presented in Figure 4-25, which

was used to calculate Δmass, with reference to mass before exposure, and this is presented in Figure 4-26.

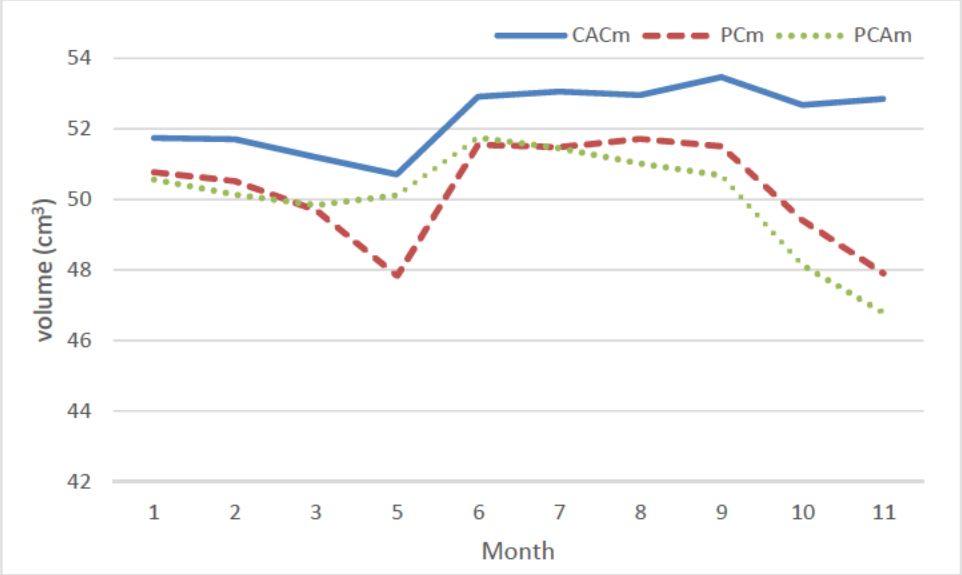


Figure 4-23: Volume of exposed mortar samples

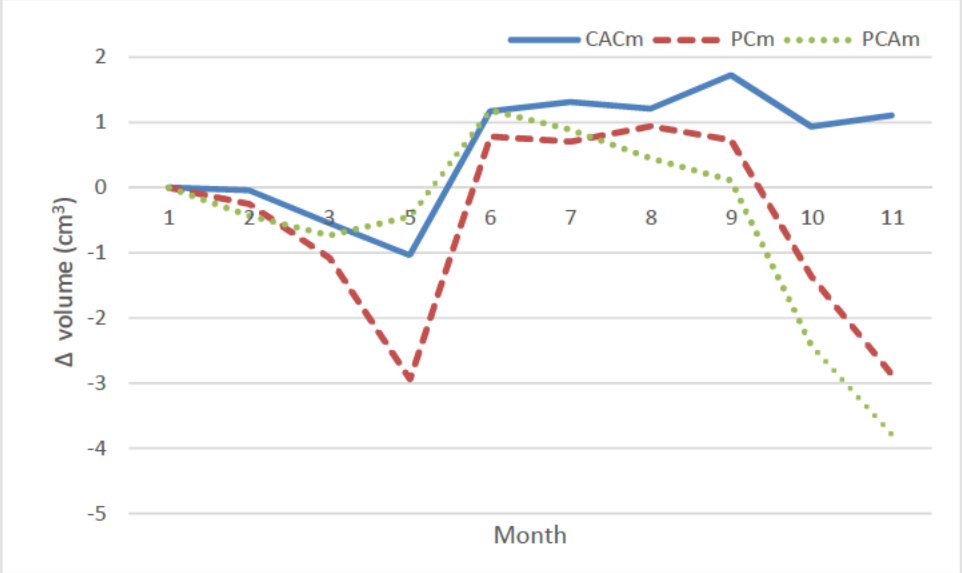


Figure 4-24: Change in volume of exposed mortar samples

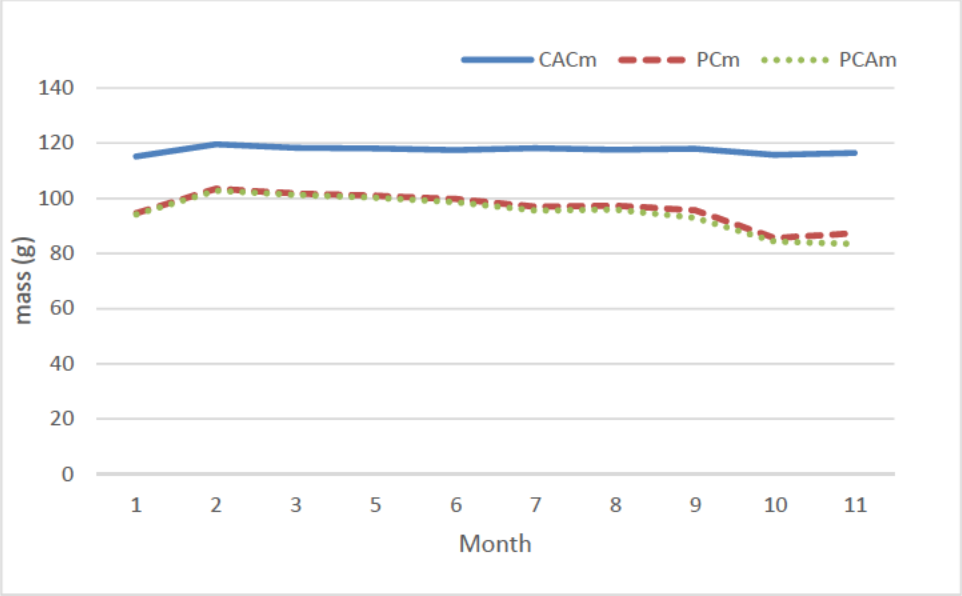


Figure 4-25: Mass of exposed mortar samples

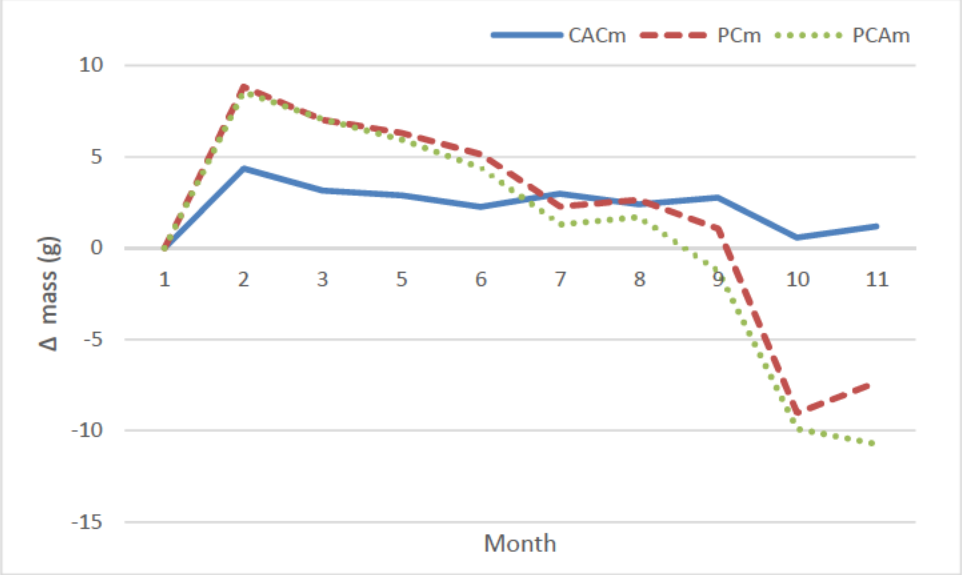


Figure 4-26: Change in mass of exposed mortar samples

Figure 4-24 and Figure 4-25 shows that the mortar samples ($CAC_m$, $PC_m$ and $PCA_m$) all experienced an initial contraction (shrinkage); this must be due to loss of moisture from the samples due to changes in the environment (these changes were not measured at the time of testing). This decrease is, however, more pronounced in $PC_m$ (and not $PCA_m$) which is an indication that moisture was easier lost to the environment in $PC_m$ than in $PCA_m$, due to the absence of CWA in $PC_m$.

Another decrease in volume is also observed in $PC_m$ and $PCA_m$ towards that last months while the volume of $CAC_m$ remained relatively constant. This decrease, unlike the initial one, must be due to gradual loss of material as shown in Figure 4-22.

Figure 4-25 shows an initial increase in mass of the samples (more obvious in Figure 4-26) in the first month. This increase in mass is mostly due to an initial moisture absorption from the sewer environment since the samples were initially in a dry state. However, the mass of $CAC_m$ remained relatively constant after this increment; this is not the case for the PC-based mortars ($PC_m$ and $PCA_m$) that both decreased in a similar manner, as shown in Figure 4-25 and Figure 4-26. This decrease also explains the latter decrease in volume as presented in Figure 4-23 and Figure 4-24 of $PC_m$ and $PCA_m$.

### 4.5.3 Corrosion rate

After the 12-month exposure duration, the samples were extracted from the aggressive environment and oven-dried after which the mass was measured. This was compared with the initial mass of the specimen before its exposure to the aggressive environment to get the total mass loss, without moisture, over the 12 months. This is presented in Figure 4-27 below.

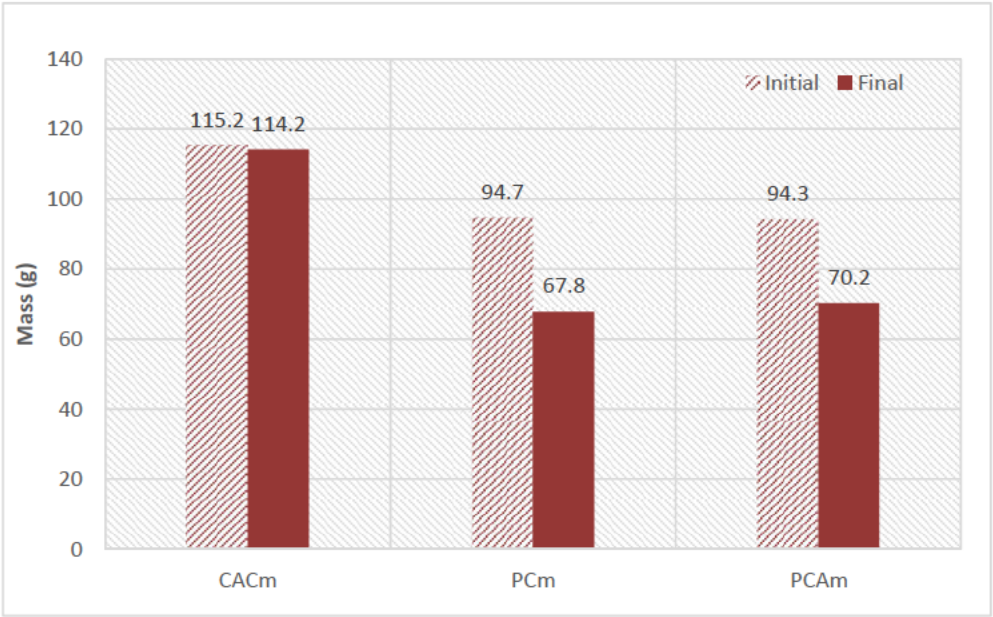


Figure 4-27: Mass of mortar samples before (initial) and after (final) a 12-month exposure period

From Figure 4-27, one can easily see that PC-based mixtures did not perform nearly as much as the CAC-based mixture despite been exposed to the same aggressive environment over the same period of time. $CAC_m$ had a total mass loss of 1 $g$ (0.87% loss), $PC_m$ had a total mass loss of 26.9 $g$ (28.4% loss), while $PCA_m$ had a total mass loss of 24.1 $g$ (25.6% loss). While $PC_m$ and $PCA_m$ may not have performed as good as $CAC_m$, it was, however, observed that $PCA_m$ performed slightly better than $PC_m$. This improved performance in the side of $PCA_m$ must have been because of the included CWA (crystalline waterproofing admixture) which is the only difference between the two PC-based mixtures.

Using the equation below, the corrosion rate of each mixture was calculated

$$c = \frac{m_1 - m_2}{d \times A \times \Delta t} \quad (4\text{-}1)$$

where:

c = corrosion rate ($mm/year$)
$m_1$ = initial mass ($g$)
$m_2$ = final mass after time $t$ ($g$)
d = density of mortar ($g/mm^3$)
A = surface area exposed to biogenic acid ($mm^2$)
$\Delta t$ = time lapse between measurement of $m_1$ and $m_2$ (years)

Using $m_1$ and $m_2$ values as presented in Figure 4-27, density of 2715 $kg/m^3$ ($2.715 \times 10^{-3}$ $g/mm^3$), 2279 $kg/m^3$ ($2.279 \times 10^{-3}$ $g/mm^3$) and 2353 $kg/m^3$ ($2.353 \times 10^{-3}$ $g/mm^3$) for $CAC_m$, $PC_m$ and $PCA_m$ respectively, as presented in Section 4.2, and total surface area of 16880 $mm^2$ for all mortars, since they have roughly the same dimension right from specimen production, as explained in Section 3.2.2.3 and Section 3.2.2.5, their corrosion rates was calculated. This was found to be approximately 0.02 $mm/year$ for $CAC_m$, 0.7 $mm/year$ for $PC_m$ and 0.6 $mm/year$ for $PCA_m$.

From the calculated corrosion rate, one can see how durable $CAC_m$ is compared to the PC-based mortars. Although $PC_m$ and $PCA_m$ did not perform nearly as good as $CAC_m$, $PCA_m$ still performed better than $PC_m$, due to the presence of CWA; this may not be obvious until after about 5 years due to its slightly lower corrosion rate (difference of 0.1 $mm/year$).

## 4.6 SEM Analysis

As explained in Section 3.4.1, three categories of samples were taken for SEM analysis: unexposed mortar samples, exposed mortar samples and product of corrosion from the concrete wall. The resulting images and data of the unexposed and exposed mortar samples are presented in Section 4.6.1 while that of the product of corrosion is presented in Section 4.6.2.

### 4.6.1 SEM analysis on mortar samples

This section presents the SEM images of the mortar samples (unexposed and exposed)—$CAC_m$, $PC_m$ and $PCA_m$— their EDS spectra and weight distribution of elements, and the mapping of elements present in each sample.

#### 4.6.1.1 SEM images of mortar samples

The SEM images of the unexposed and exposed mortar samples is discussed here. All images are presented in the linear scale of 250 $\mu m$, as indicated in the scale bar; this will only avail us some details.

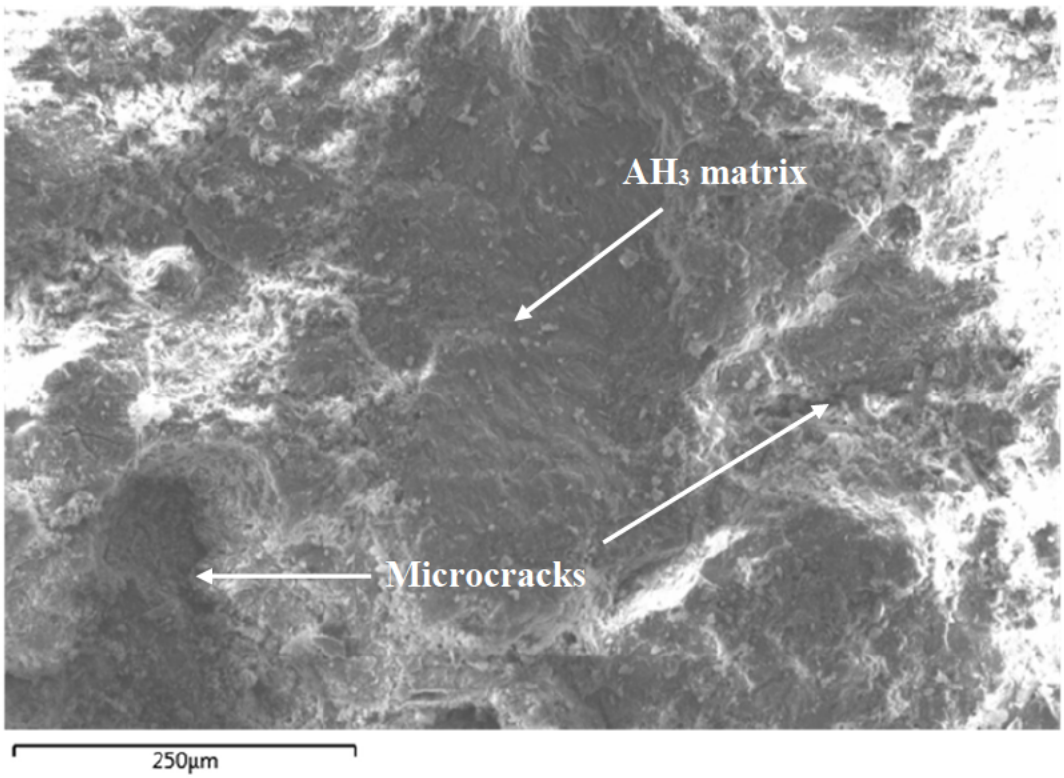


Figure 4-28: SEM image of an unexposed $CAC_m$ sample

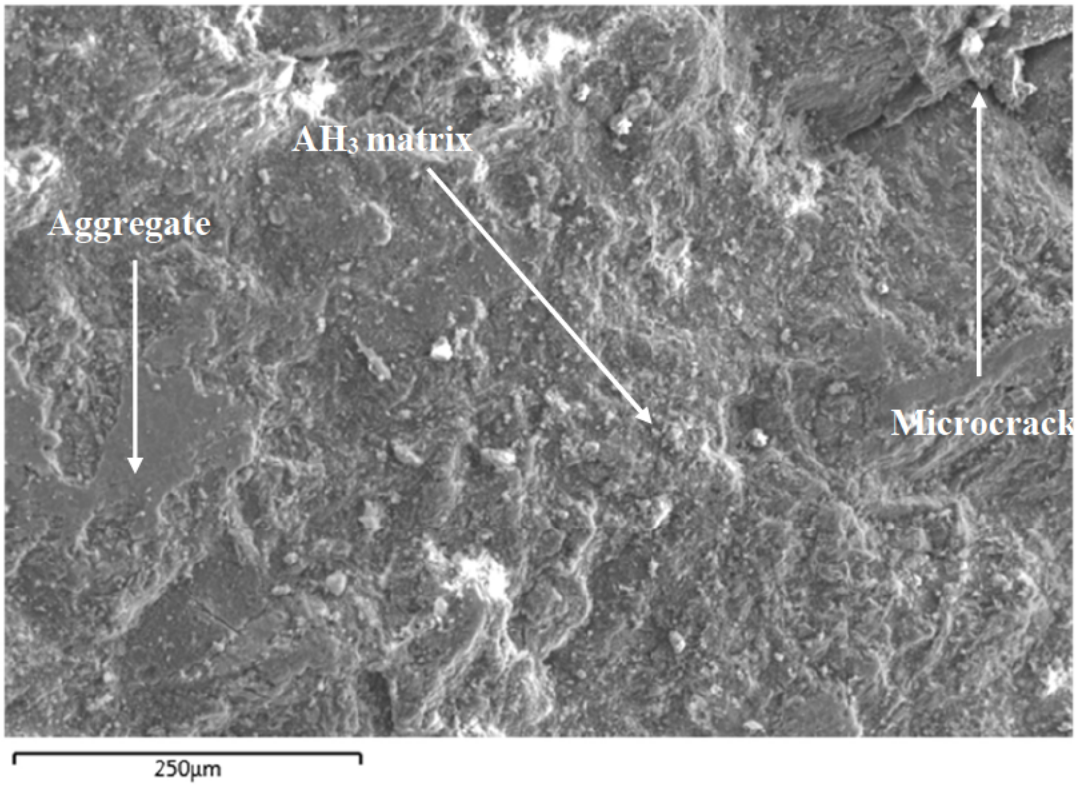


Figure 4-29: SEM image of an exposed $CAC_m$ sample

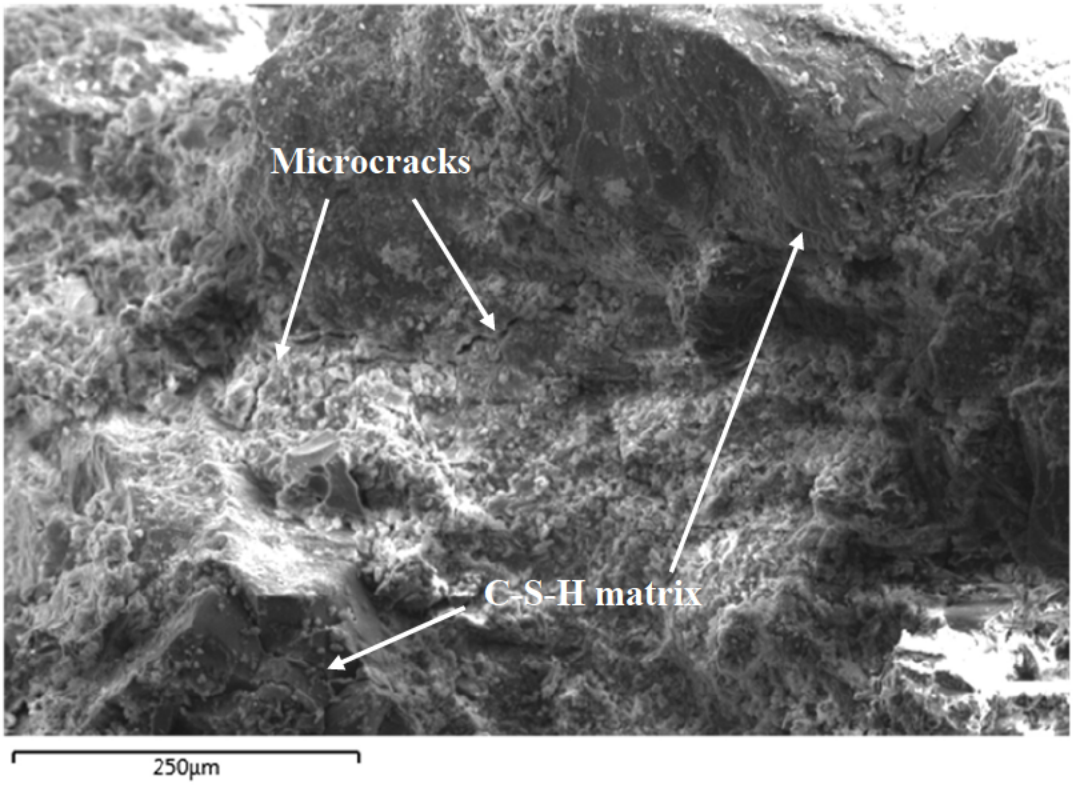


Figure 4-30: SEM image of an unexposed $PC_m$

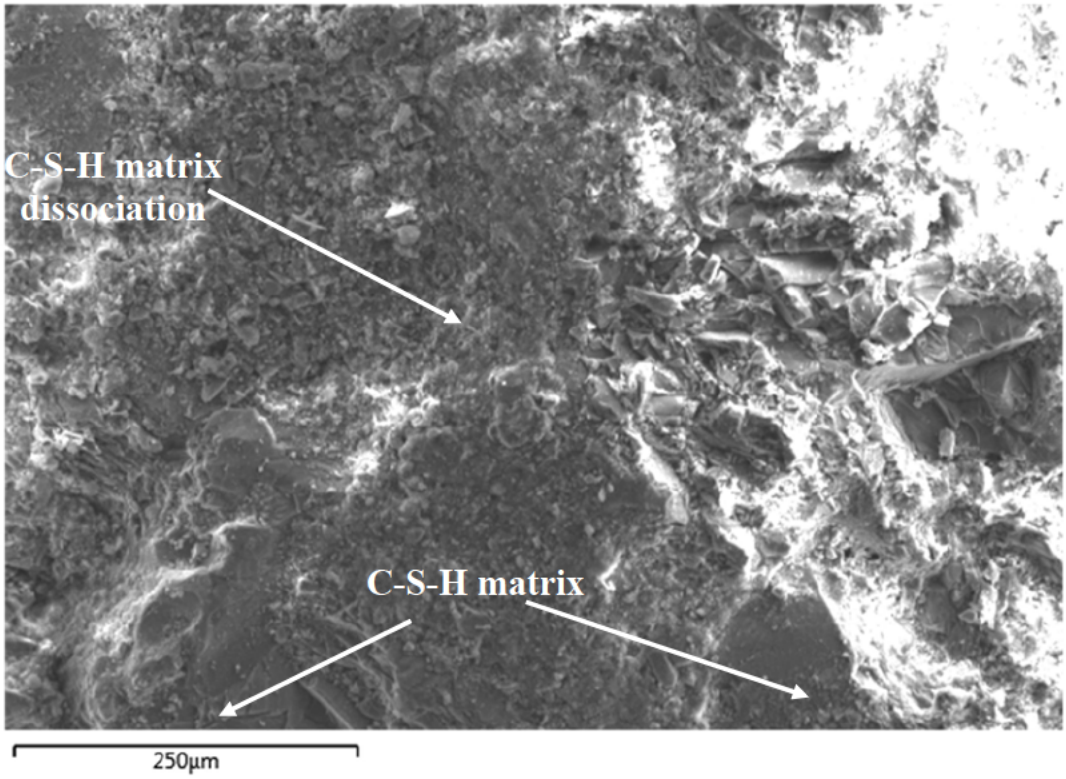


Figure 4-31: SEM image of an exposed $PC_m$ sample

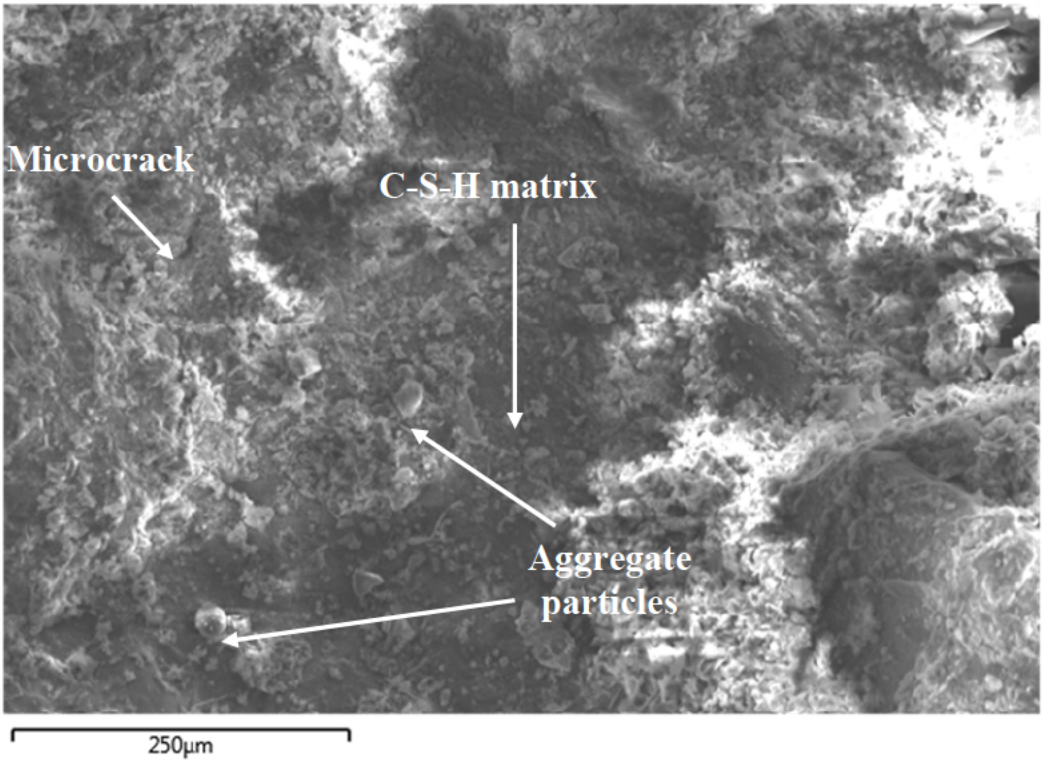


Figure 4-32: SEM image of an unexposed $PCA_m$ sample

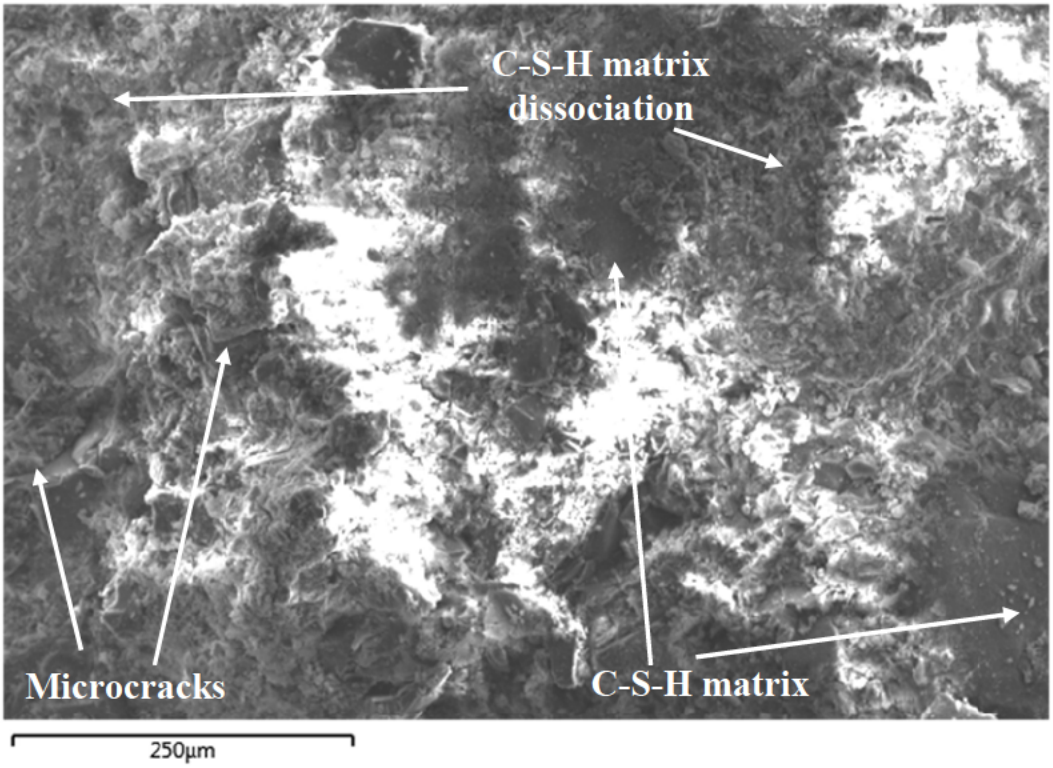


Figure 4-33: SEM image of an exposed $PCA_m$ sample

It can be seen from Figure 4-28 to Figure 4-33 that most of the mortar samples exhibit microcracks including the unexposed samples, though they are not visible to the human eyes. However, it may have occurred due to natural cement hydration processes, like heat of hydration or/and due to the mechanical processes employed during the production of the samples, like the coring process and slicing process.

It is also observed that $CAC_m$ (unexposed and exposed) have a denser matrix, as shown in Figure 4-28 and Figure 4-29, compared to $PC_m$ (Figure 4-30 & Figure 4-31) and $PCA_m$, (Figure 4-32 & Figure 4-33). This also reflects in their average density values are presented in Section 4.2.

Also, the SEM images of the exposed PC-based mortar (Figure 4-31 & Figure 4-33) display dissociation of C-S-H matrix, which is the binding system of PC-based mortars or concrete. This is an indication that the binding system of the mortar is being threatened due to the presence of sulphuric acid or other acidic compounds, as explained in Section 2.4.5. This is further discussed using the EDS spectra and elemental mapping in Section 4.6.1.2 and Section 4.6.1.3 respectively.

### 4.6.1.2 EDS spectra of mortar samples

EDS spectra, as presented in this section, revealed the elements present in in each sample, their intensity and their % weight distribution. It should be noted that while each spectrum shows the intensity of elemental peaks in $cps/ev$ (counts per second per electron voltage), is not necessarily an indication of weight % distribution.

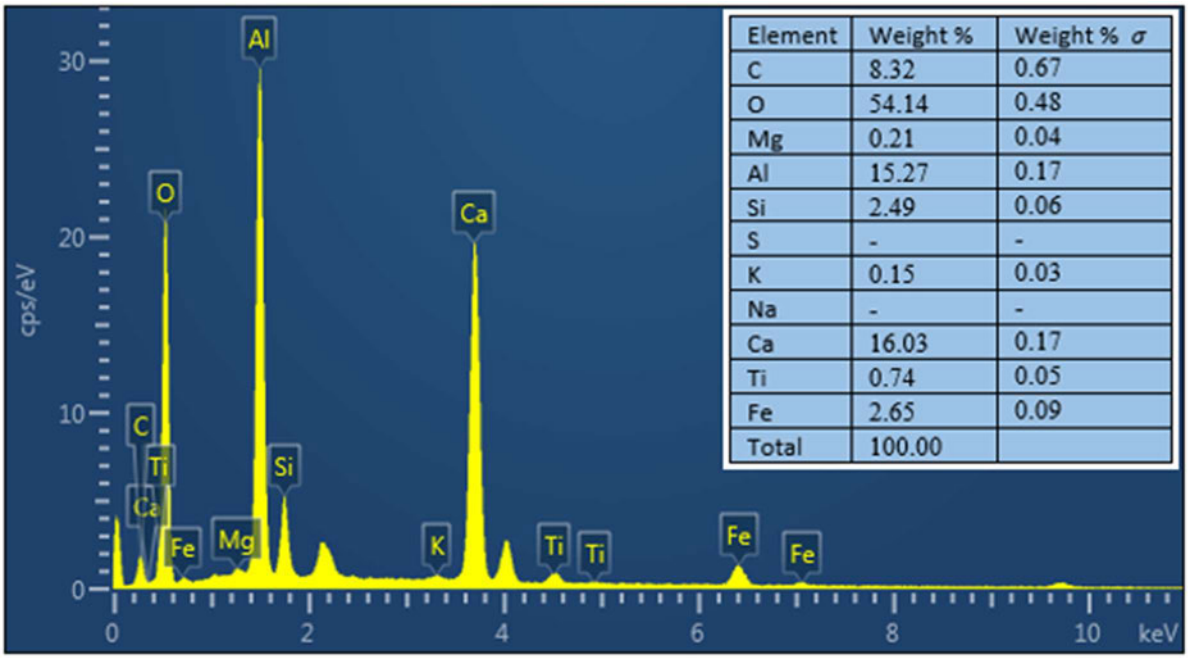


| Element | Weight % | Weight % σ |
|---|---|---|
| C | 8.32 | 0.67 |
| O | 54.14 | 0.48 |
| Mg | 0.21 | 0.04 |
| Al | 15.27 | 0.17 |
| Si | 2.49 | 0.06 |
| S | - | - |
| K | 0.15 | 0.03 |
| Na | - | - |
| Ca | 16.03 | 0.17 |
| Ti | 0.74 | 0.05 |
| Fe | 2.65 | 0.09 |
| Total | 100.00 | |

Figure 4-34: EDS Spectra of an unexposed $CAC_m$ sample

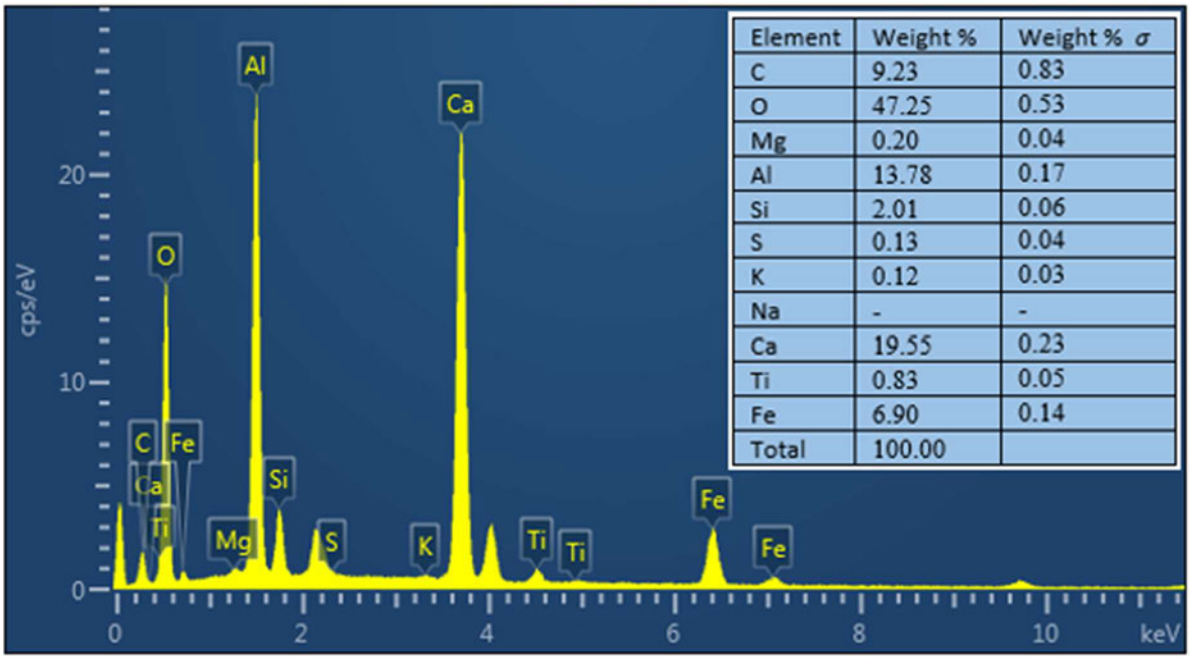


| Element | Weight % | Weight % σ |
|---|---|---|
| C | 9.23 | 0.83 |
| O | 47.25 | 0.53 |
| Mg | 0.20 | 0.04 |
| Al | 13.78 | 0.17 |
| Si | 2.01 | 0.06 |
| S | 0.13 | 0.04 |
| K | 0.12 | 0.03 |
| Na | - | - |
| Ca | 19.55 | 0.23 |
| Ti | 0.83 | 0.05 |
| Fe | 6.90 | 0.14 |
| Total | 100.00 | |

Figure 4-35: EDS spectra of an exposed $CAC_m$ sample

The EDS spectra in Figure 4-34 and Figure 4-35 indicates high presence of $Ca$ and $Al$; this is because of the binder used—calcium aluminate cement (CAC). O also has a high peak because most of the other elements exist in their oxides. For example, $Al$ existing in $Al_2O_3$ and $Ca$ existing in $CaO$. The weight distributions in both figures also show a higher weight distribution of $Ca$ and $Al$, besides $O$. In addition, the low level of $Si$ shows that a conventional fine aggregate was not used in the production of the pre-mixed dry mortar, as described in Section 3.2.1.1, rather a calcium aluminate aggregate was used.

Comparing Figure 4-34 and Figure 4-35, it is seen that there is no significant difference in the EDS spectra and weight distribution of an exposed $CAC_m$ and unexposed $CAC_m$; this is an indication that there are no or negligible MICC effects on the $CAC_m$ after the 12-month exposure, despite the aggressiveness of the environment.

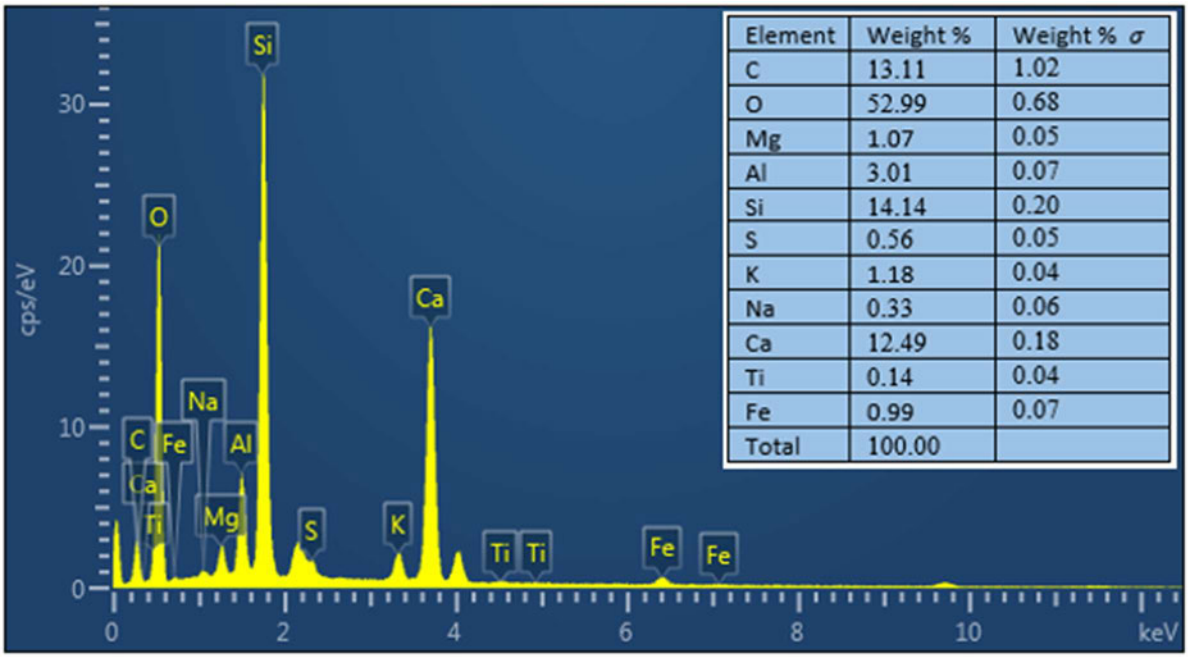


| Element | Weight % | Weight % σ |
|---|---|---|
| C | 13.11 | 1.02 |
| O | 52.99 | 0.68 |
| Mg | 1.07 | 0.05 |
| Al | 3.01 | 0.07 |
| Si | 14.14 | 0.20 |
| S | 0.56 | 0.05 |
| K | 1.18 | 0.04 |
| Na | 0.33 | 0.06 |
| Ca | 12.49 | 0.18 |
| Ti | 0.14 | 0.04 |
| Fe | 0.99 | 0.07 |
| Total | 100.00 | |

Figure 4-36: EDS spectra of an unexposed $PC_m$ sample

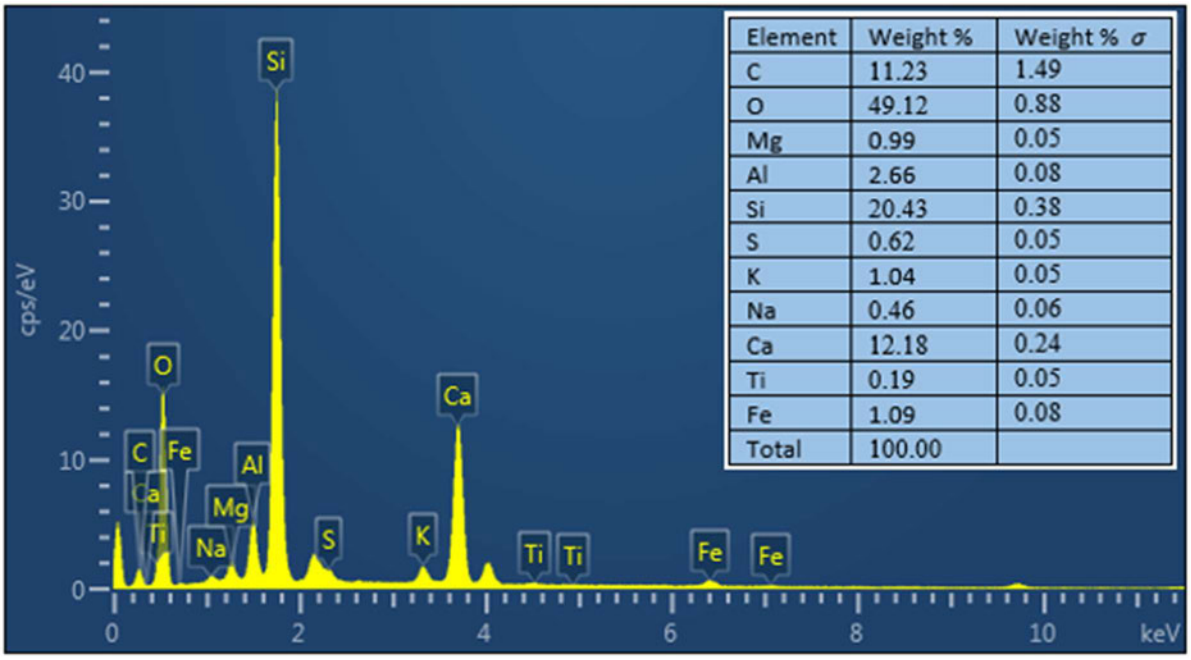


| Element | Weight % | Weight % σ |
|---|---|---|
| C | 11.23 | 1.49 |
| O | 49.12 | 0.88 |
| Mg | 0.99 | 0.05 |
| Al | 2.66 | 0.08 |
| Si | 20.43 | 0.38 |
| S | 0.62 | 0.05 |
| K | 1.04 | 0.05 |
| Na | 0.46 | 0.06 |
| Ca | 12.18 | 0.24 |
| Ti | 0.19 | 0.05 |
| Fe | 1.09 | 0.08 |
| Total | 100.00 | |

Figure 4-37: EDS spectra of an exposed $PC_m$ sample

The EDS spectra in Figure 4-38 and Figure 4-39 show peaks of $Si$, then $Ca$ and $O$. $Si$ is a representation of silica ($SiO_2$) mostly from the fine aggregate, then from the binder, while $Ca$ is a representation of lime ($CaO$) from the binder—Portland cement (PC). A slight drop in the $Ca$ and $O$ spectra can be

observed in the exposed $PC_m$ sample, as shown in Figure 4-36, compared to that of the unexposed $PC_m$ sample, as shown in Figure 4-37; this is most likely due to the biogenic attack.

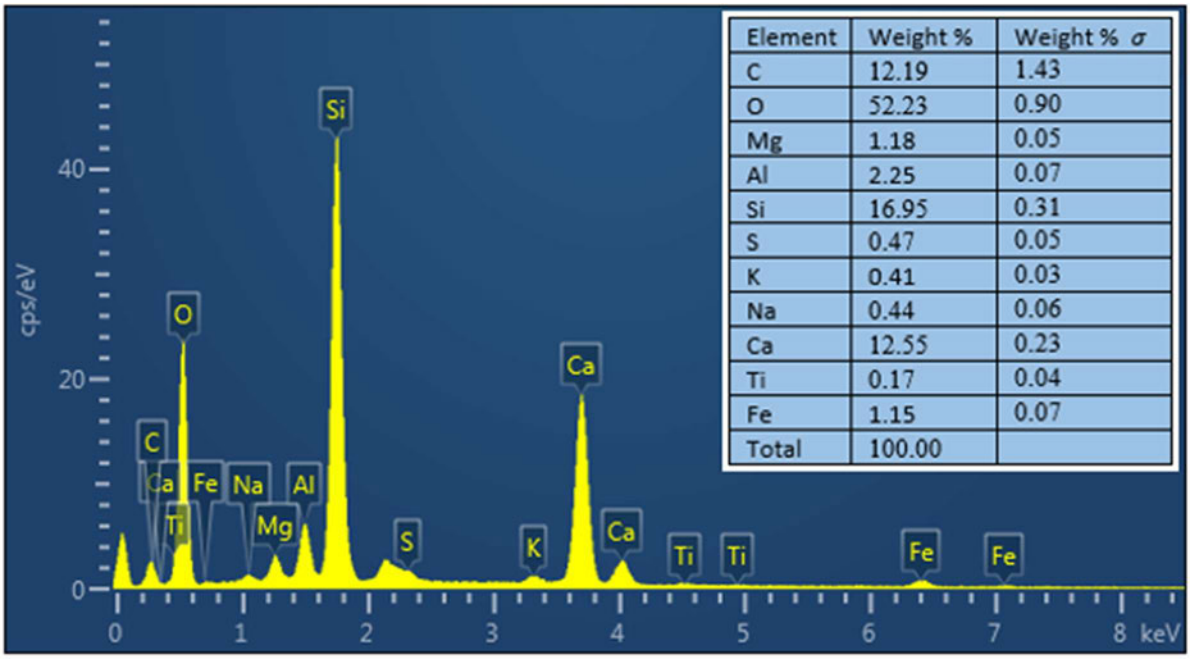


| Element | Weight % | Weight % σ |
|---|---|---|
| C | 12.19 | 1.43 |
| O | 52.23 | 0.90 |
| Mg | 1.18 | 0.05 |
| Al | 2.25 | 0.07 |
| Si | 16.95 | 0.31 |
| S | 0.47 | 0.05 |
| K | 0.41 | 0.03 |
| Na | 0.44 | 0.06 |
| Ca | 12.55 | 0.23 |
| Ti | 0.17 | 0.04 |
| Fe | 1.15 | 0.07 |
| Total | 100.00 | |

Figure 4-38: EDS spectra of an unexposed $PCA_m$ sample

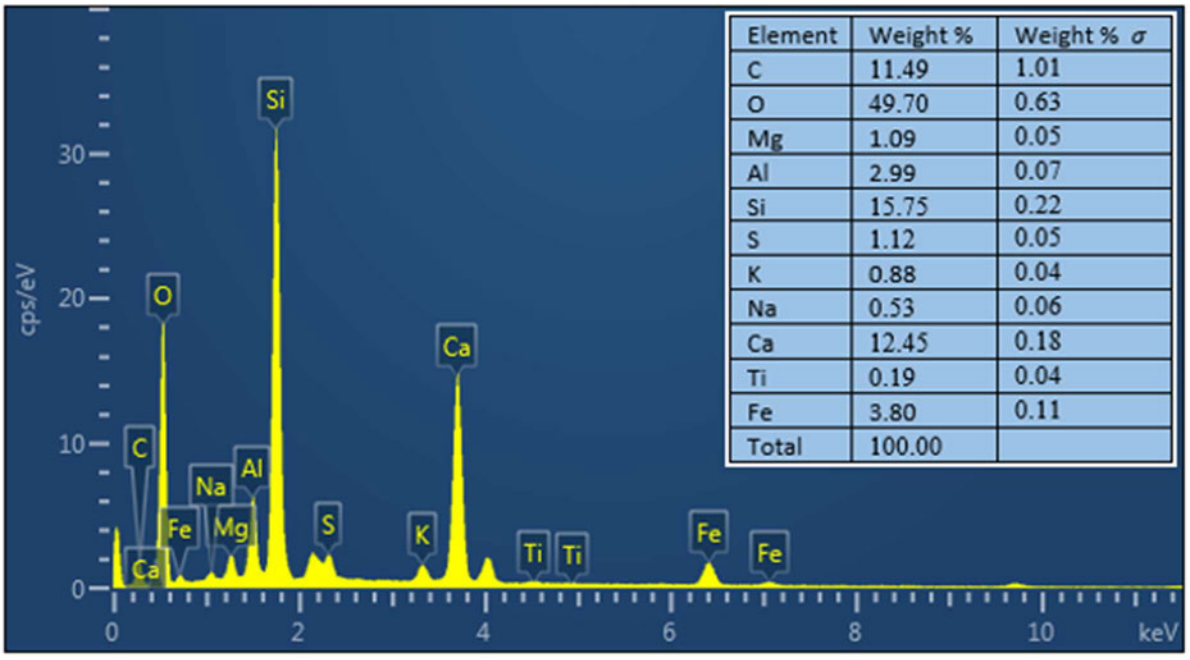


| Element | Weight % | Weight % σ |
|---|---|---|
| C | 11.49 | 1.01 |
| O | 49.70 | 0.63 |
| Mg | 1.09 | 0.05 |
| Al | 2.99 | 0.07 |
| Si | 15.75 | 0.22 |
| S | 1.12 | 0.05 |
| K | 0.88 | 0.04 |
| Na | 0.53 | 0.06 |
| Ca | 12.45 | 0.18 |
| Ti | 0.19 | 0.04 |
| Fe | 3.80 | 0.11 |
| Total | 100.00 | |

Figure 4-39: EDS spectra of an exposed $PCA_m$ sample

The EDS spectra of $PCA_m$ is quite similar to that of $PC_m$ as they are both PC-based mortars, and unlike $CAC_m$, $PCA_m$ (just like $PC_m$) have elemental peaks of $Si, Ca$ and $O$ because of the aggregate and binder (Portland cement).

### 4.6.1.3 Elemental mapping of mortar samples

For elemental mapping, focus was placed on calcium ($Ca$), aluminium ($Al$), silica ($Si$) and sulphur ($S$), as shown in Figure 4-40 to 4-51, for the unexposed sample (the 'a's) and exposed samples (the 'b's).

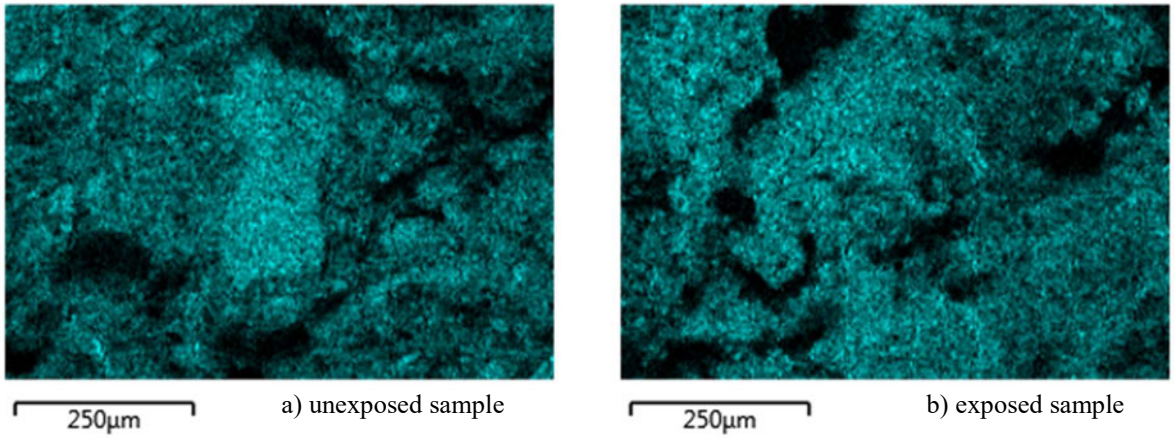


a) unexposed sample b) exposed sample

Figure 4-40: Calcium elemental mapping of $CAC_m$

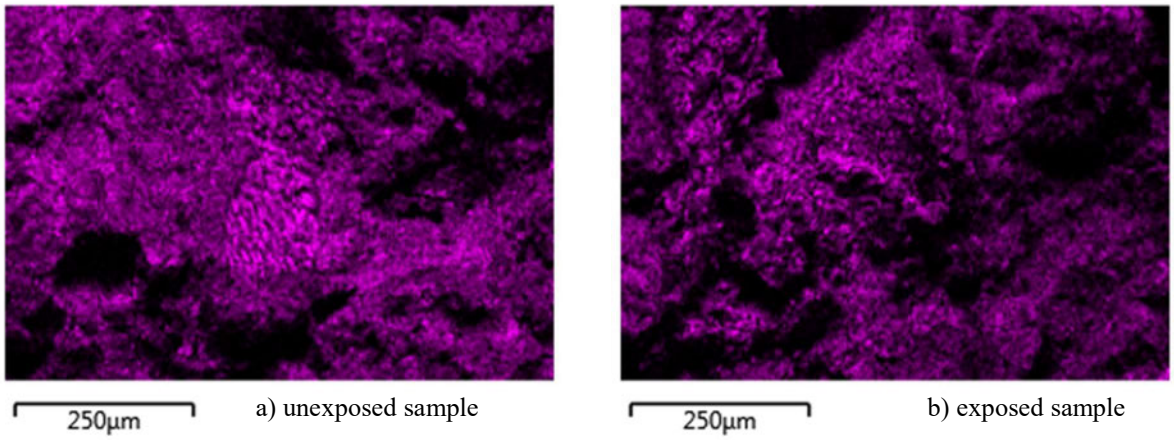


a) unexposed sample b) exposed sample

Figure 4-41: Aluminum elemental mapping of $CAC_m$

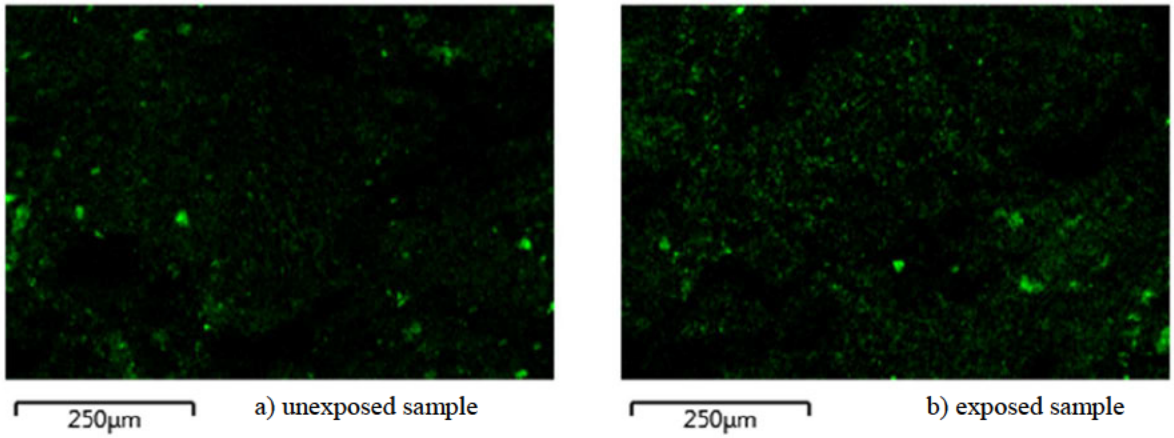


a) unexposed sample b) exposed sample

Figure 4-42: Silica elemental mapping of $CAC_m$

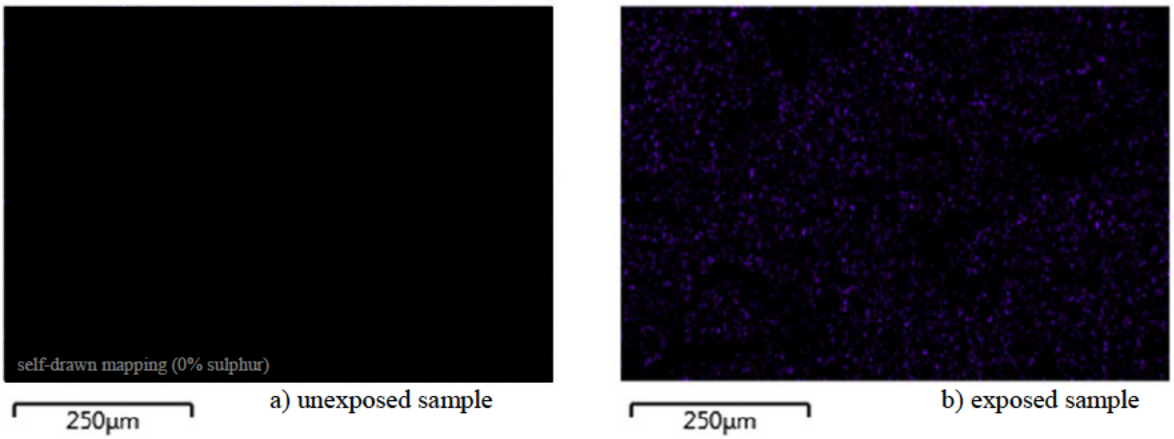


a) unexposed sample b) exposed sample

Figure 4-43: Sulphur elemental mapping of $CAC_m$

Figure 4-40 and Figure 4-41 shows that there is a large amount of $Ca$ and $Al$ respectively, present in $CAC_m$, which is expected as calcium aluminate cement (CAC) is used as binder. Also, the very low quantity of silica, as seen in Figure 4-42, is a reflection of its chemical composition, as given in Table 3-1.

Comparing the elemental mapping of the unexposed and exposed $CAC_m$ side by side, as shown in Figure 4-40(a & b) to 4-43 (a & b), there is not much difference between the $Ca$, $Al$, $Si$ mappings of the two. Sulphur mapping, however, shows a very small amount of sulphur (Figure 4-43b), from zero abundance (Figure 4-43a). This must be due to the biogenic acid attack as expected in such aggressive environment.

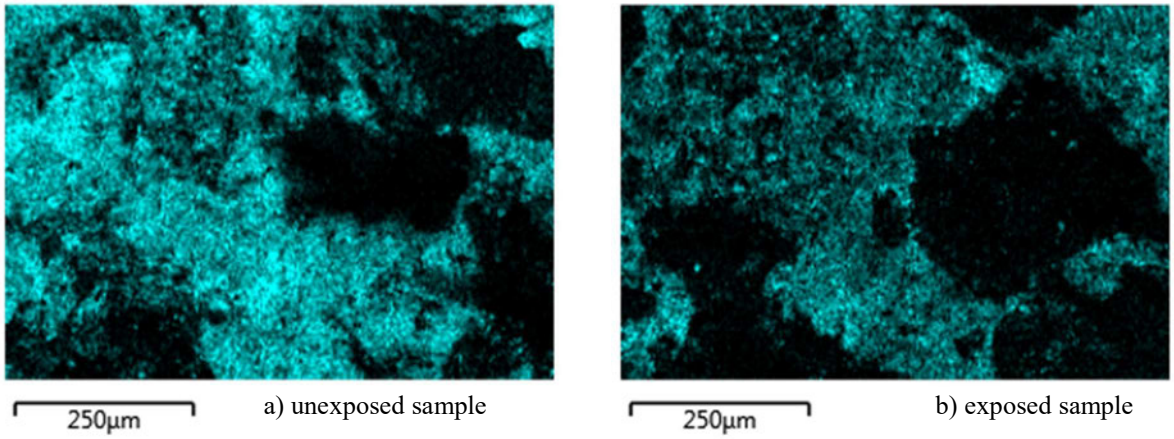


a) unexposed sample b) exposed sample

Figure 4-44: Calcium elemental mapping of $PC_m$

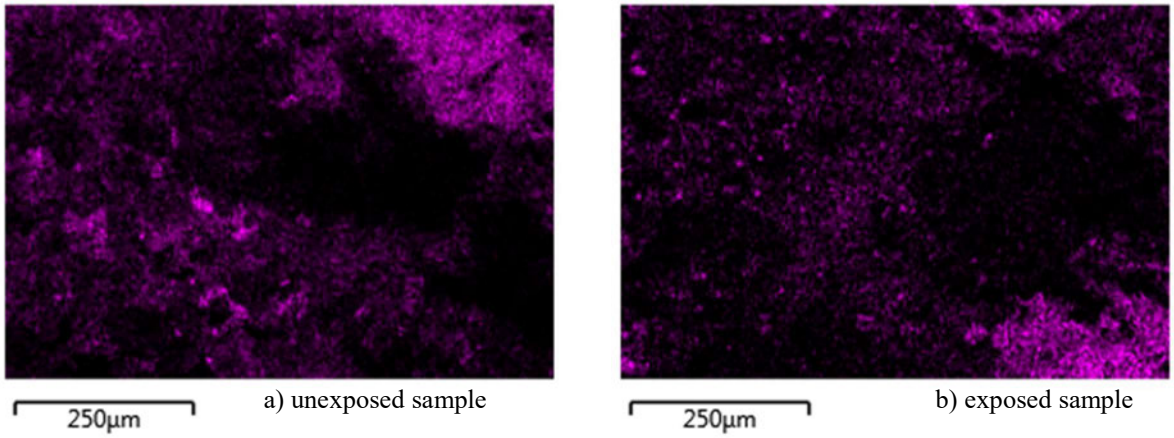


a) unexposed sample b) exposed sample

Figure 4-45: Aluminum elemental mapping of $PC_m$

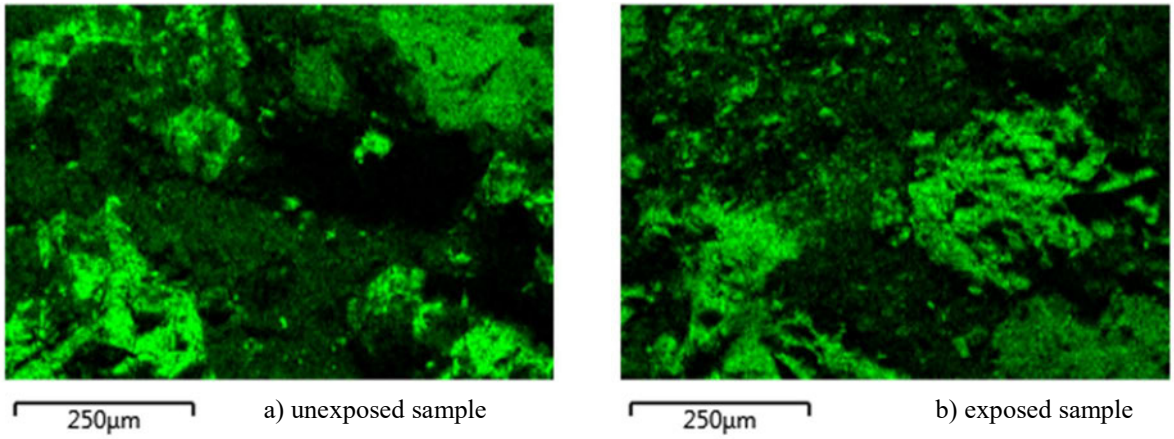


a) unexposed sample b) exposed sample

Figure 4-46: Silica elemental mapping of $PC_m$

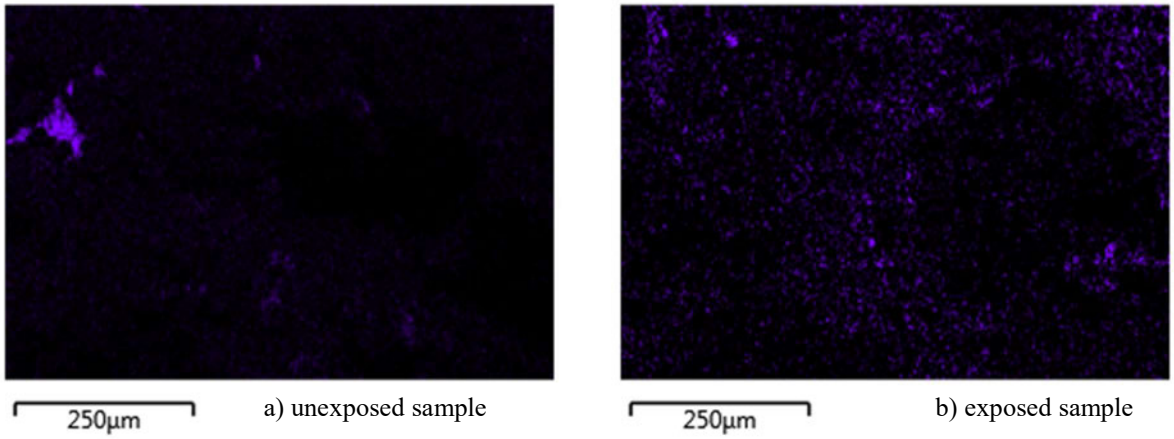


a) unexposed sample b) exposed sample

Figure 4-47: Sulphur elemental mapping of $PC_m$

Among the elements presented in Figure 4-44 to 4-47, $Ca$ (Figure 4-44) shows the highest abundance, followed by $Si$ (Figure 4-46), then $Al$ (Figure 4-45). This is a reflection of the chemical composition of PC. The high abundance of $Si$ can, however, be attributed primarily to the fine aggregate in the mixture, then the cement.

Unlike the mapping for $CAC_m$ (Figure 4-40 to 4-43), a critical examination of the mappings of the unexposed $PC_m$ to the exposed $PC_m$, reveal obvious changes. A decrease in the intensity of the $Ca$ and $Si$ elemental mappings can be seen in the exposed $PC_m$; this is an indication of MICC, as the binding system of the mixture is being attacked. $Al$ and $S$ elemental mapping of exposed $PC_m$ also show a decrease in abundance; however, in the case of sulphur mapping, besides the intensity-drop, it also displays a fair distribution of $S$ compared to the unexposed $PC_m$ $S$ mapping; this is an indication of the presence of thionic or polythionic acids due to the aggressiveness of the environment.

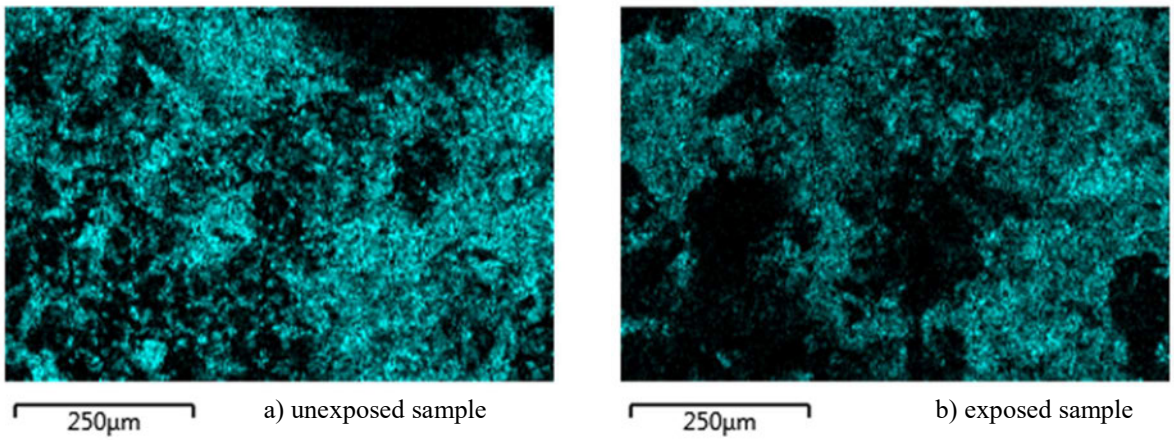


a) unexposed sample b) exposed sample

Figure 4-48: Calcium elemental mapping of $PCA_m$

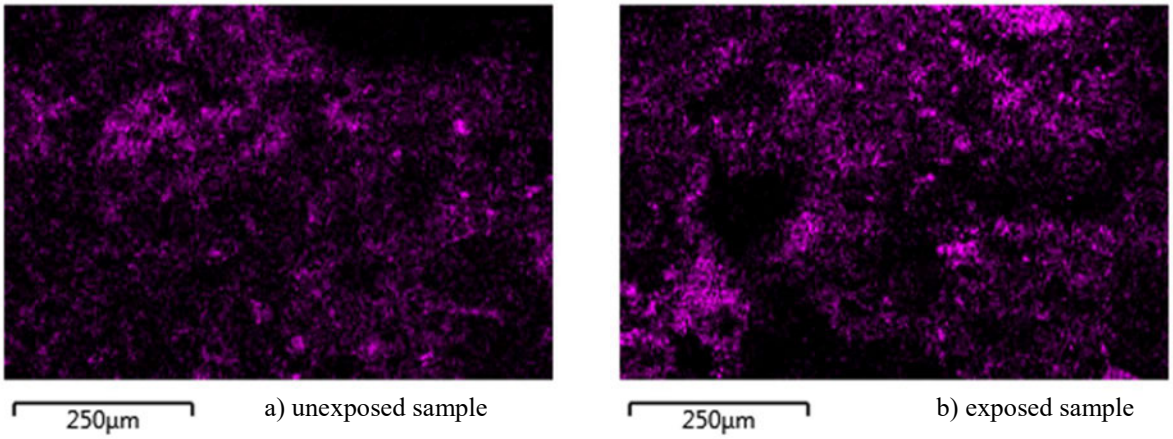


a) unexposed sample b) exposed sample

Figure 4-49: Aluminum elemental mapping of $PCA_m$

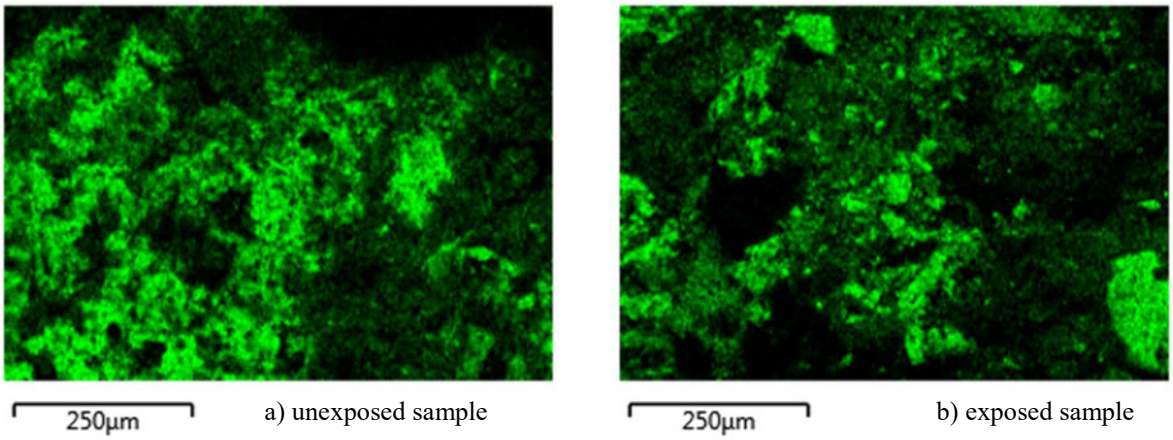


a) unexposed sample b) exposed sample

Figure 4-50: Silica elemental mapping of $PCA_m$

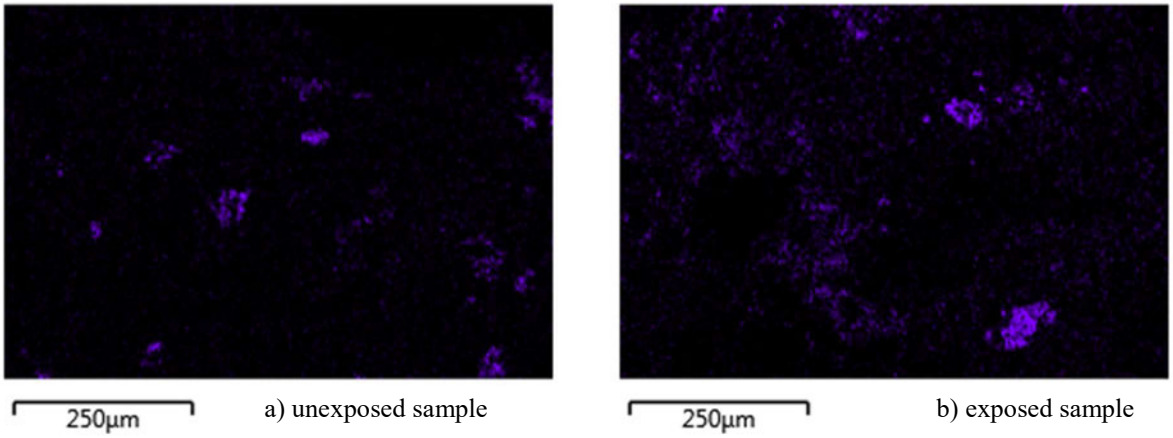


a) unexposed sample b) exposed sample

Figure 4-51: Sulphur elemental mapping of $PCA_m$

Just like the EDS spectra of $PC_m$ and $PCA_m$ (Figure 4-36 to 4-39), their elemental mappings (Figure 4-44 to 4-51) are also similar; this is because PC was used in both mixtures at the same ratio. However, the intensity-drop of $Ca$, $Si$ and $Al$ mappings of exposed $PCA_m$ compared to the mappings of unexposed $PCA_m$ is not as pronounced as in the case of $PC_m$ (Figure 4-44 to 4-47); this may be due to the presence of CWA. The $S$ elemental mapping of unexposed $PCA_m$ also display more spread of the element, due to the presence of thionic compounds induced by the environment.

### 4.6.2 SEM Analysis of corroded concrete

In this section, the EDS spectra and SEM images of different samples of the product of corrosion, obtained from the concrete wall of the sewer facility (MGWWPS) is presented and discussed. Figure 4-52 to 4-55 is a picture showing the area where the corrosion products were taken.

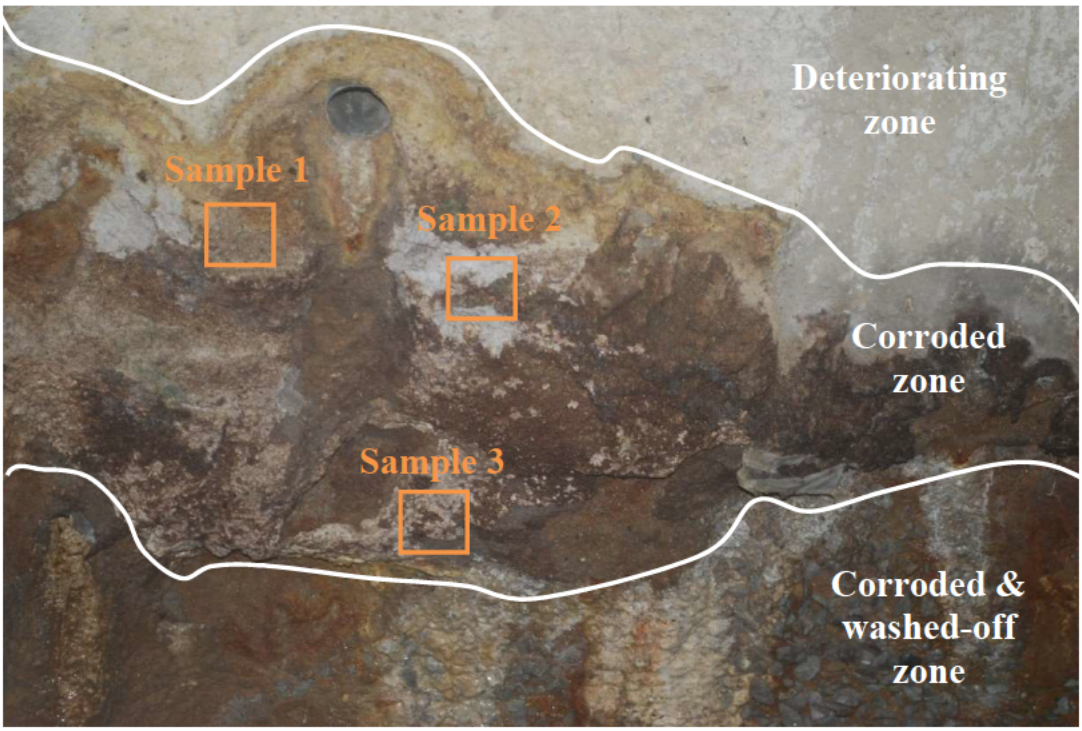


Figure 4-52: Sampling of corroded product on concrete wall

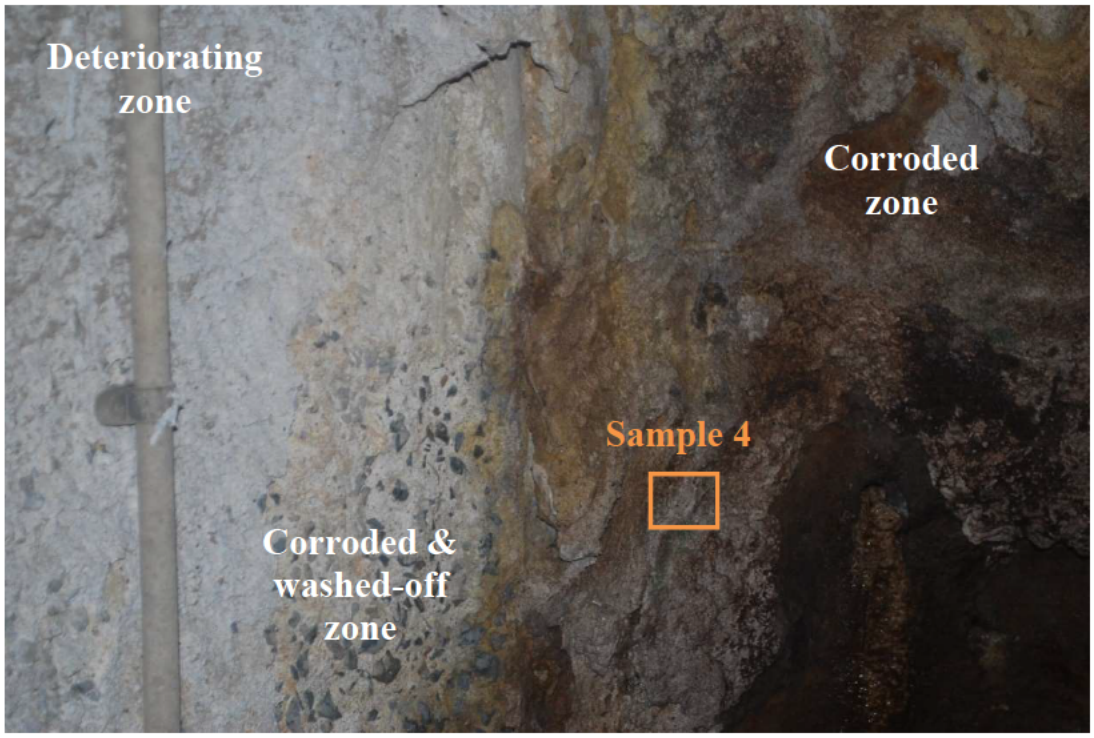


Figure 4-53: Sampling of corroded product on concrete wall

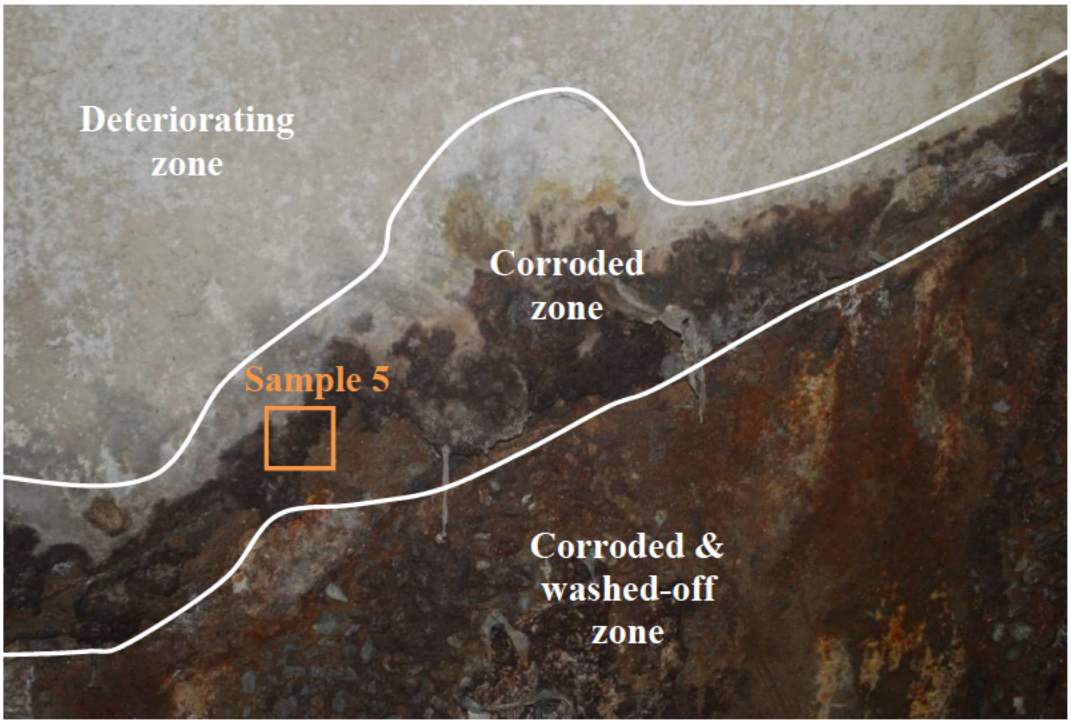


Figure 4-54: Sampling of corroded product on concrete wall

Besides the location of sample 1, sample 2, sample 3, sample 4 and sample 5, Figure 4-52 to 4-54, also shows the three zones identified on the concrete wall—the deteriorating zone, the corroded zone, and the corroded-and-washed-off zone. The deteriorating zone is characterized by weakened concrete cover and cracks, the corroded zone is characterized by mushy substances (gypsum) with no cohesive properties, the corroded-and-wash-off zone is characterized by exposed aggregates; this is due to the washing away of gypsum from the top surface of the concrete wall.

### 4.6.2.1 SEM images of corroded concrete

The SEM image of sample 1, sample 2, sample 3, sample 4 and sample 5, shown in Figure 4-52 to 4-54, is given in Figure 4-55, Figure 4-56, Figure 4-57, Figure 4-58 and Figure 4-59 respectively.

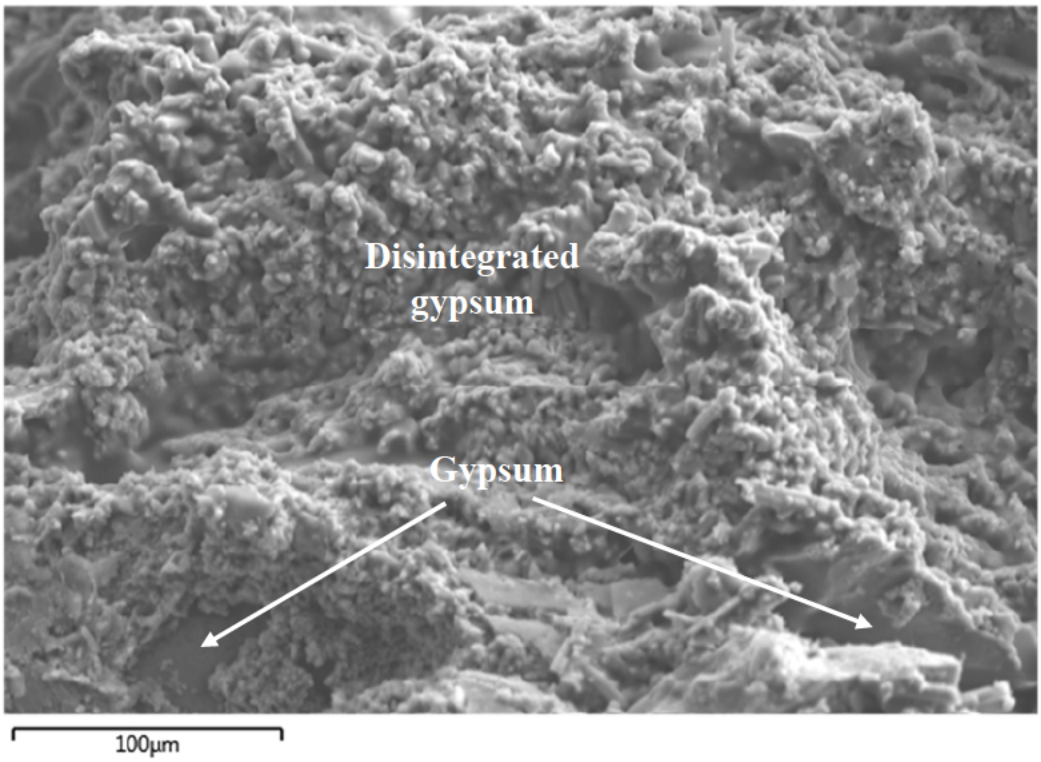


Figure 4-55: SEM image of corrosion product (sample 1)

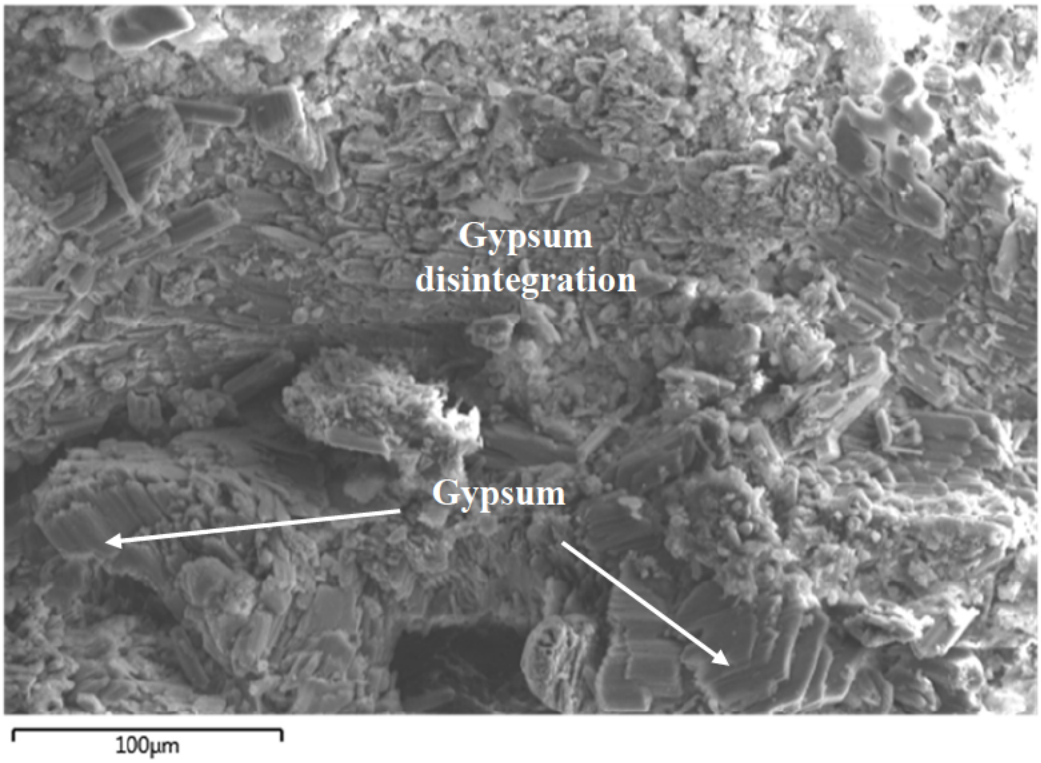


Figure 4-56: SEM image of corrosion product (sample 2)

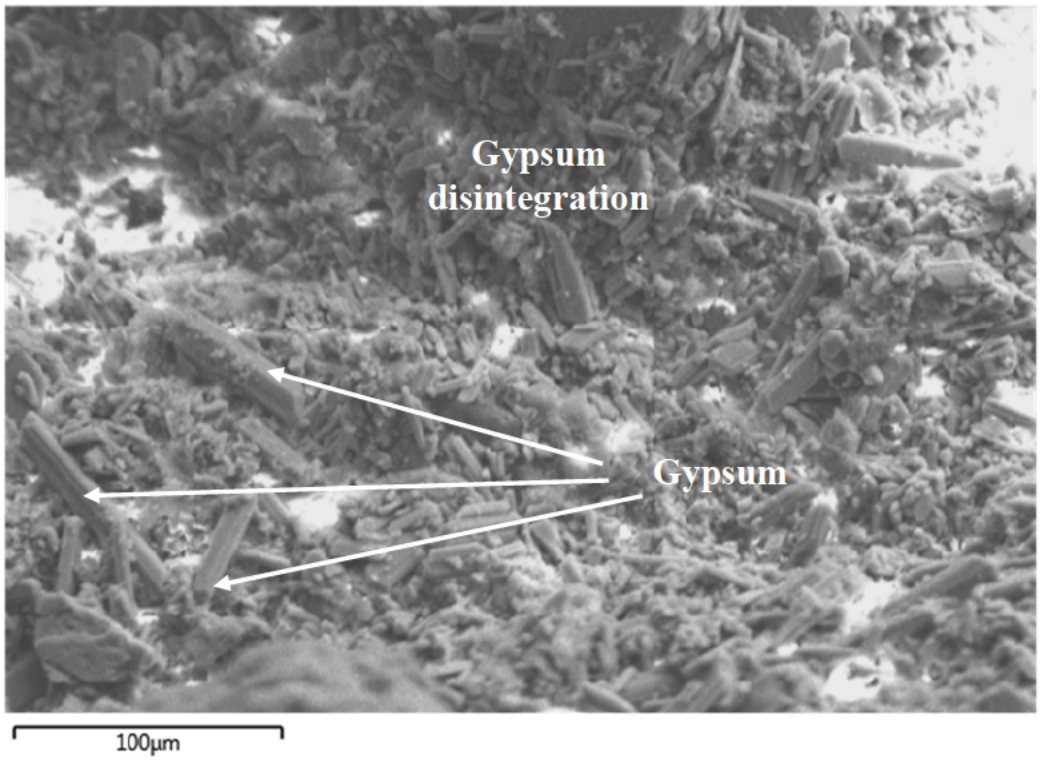


Figure 4-57: SEM image of corrosion product (sample 3)

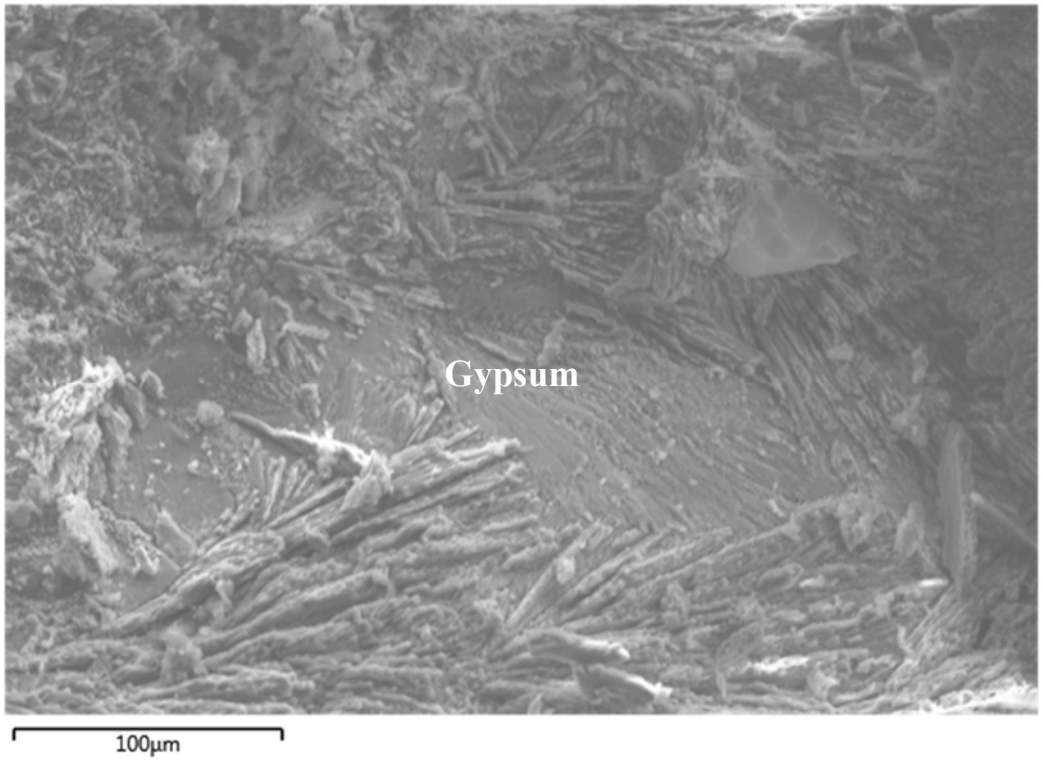


Figure 4-58: SEM image of corrosion product (sample 4)

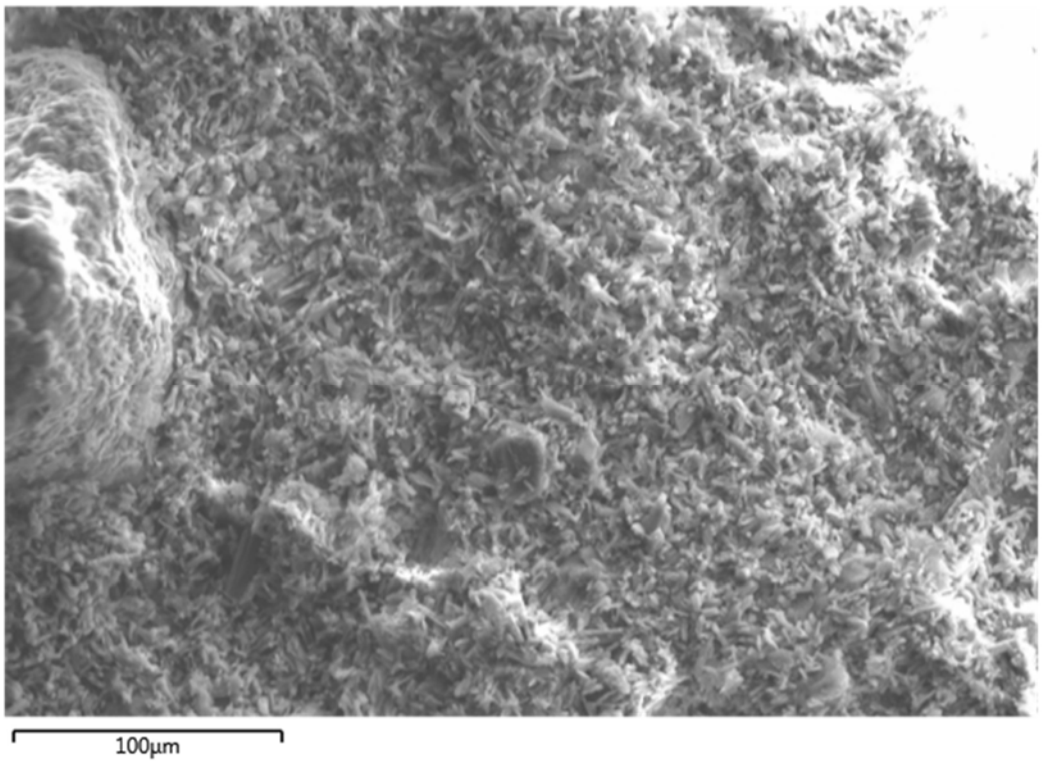


Figure 4-59: SEM image of corrosion product (sample 5)

The above figures (Figure 4-55 to 4-59) are mainly characterized by the presence of expanded gypsum which lack cohesive properties. Figure 4-55 show gypsum in a disintegrated state, Figure 4-56 & Figure 4-57 shows gypsum in a disintegrating state, while Figure 4-58 shows gypsum in a swollen and mushy form. The dominant substance in Figure 4-59 is yet to be identified, but it seems to have developed after the corrosion. This is later discussed in Section 4.6.2.2.

### 4.6.2.2 EDS spectra of corroded concrete

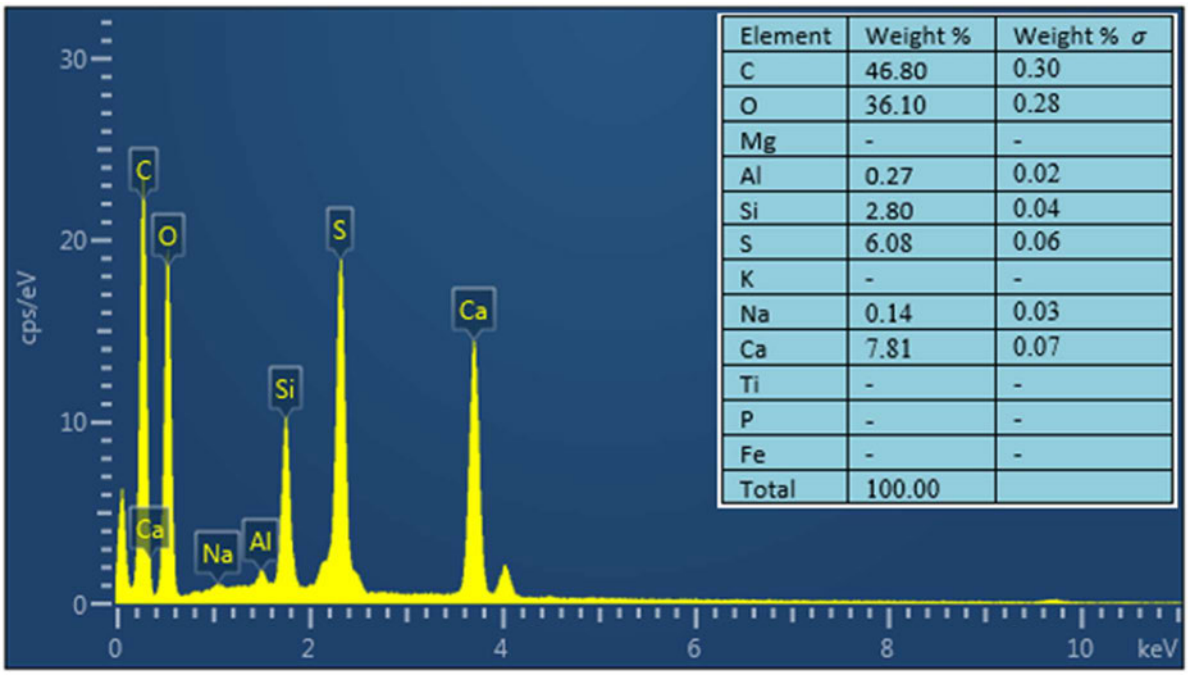


| Element | Weight % | Weight % σ |
|---|---|---|
| C | 46.80 | 0.30 |
| O | 36.10 | 0.28 |
| Mg | - | - |
| Al | 0.27 | 0.02 |
| Si | 2.80 | 0.04 |
| S | 6.08 | 0.06 |
| K | - | - |
| Na | 0.14 | 0.03 |
| Ca | 7.81 | 0.07 |
| Ti | - | - |
| P | - | - |
| Fe | - | - |
| Total | 100.00 | |

Figure 4-60: EDS spectra of corroded product (sample 1)

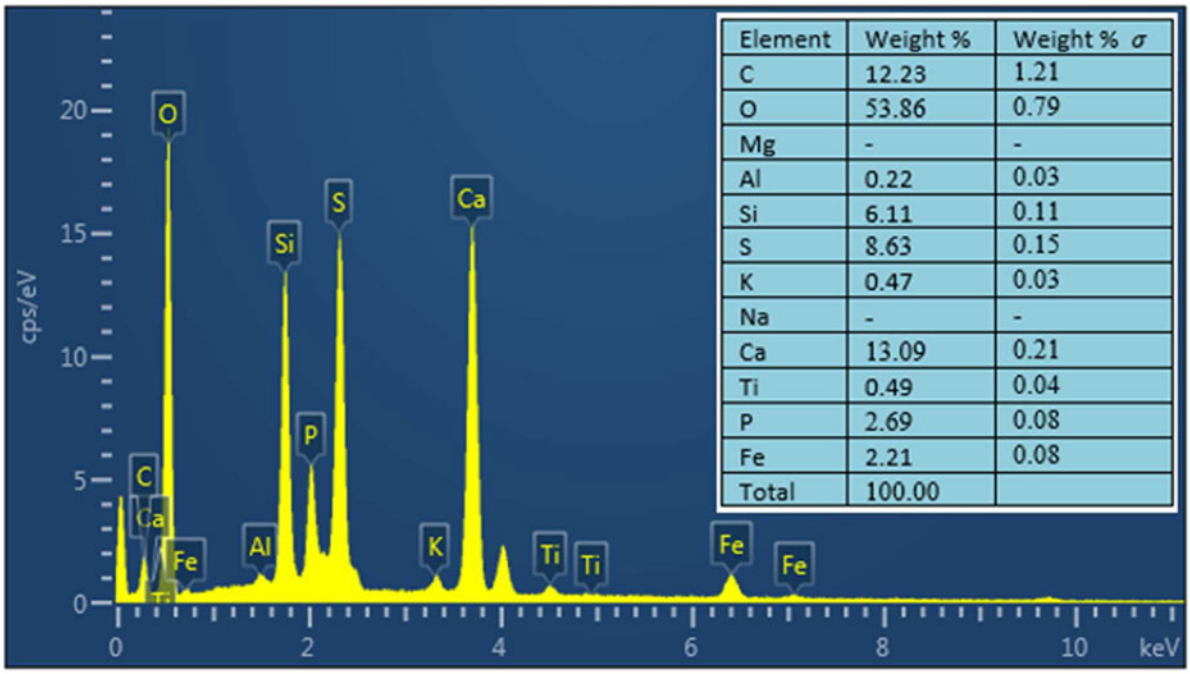


| Element | Weight % | Weight % σ |
|---|---|---|
| C | 12.23 | 1.21 |
| O | 53.86 | 0.79 |
| Mg | - | - |
| Al | 0.22 | 0.03 |
| Si | 6.11 | 0.11 |
| S | 8.63 | 0.15 |
| K | 0.47 | 0.03 |
| Na | - | - |
| Ca | 13.09 | 0.21 |
| Ti | 0.49 | 0.04 |
| P | 2.69 | 0.08 |
| Fe | 2.21 | 0.08 |
| Total | 100.00 | |

Figure 4-61: EDS spectra of corroded product (sample 2)

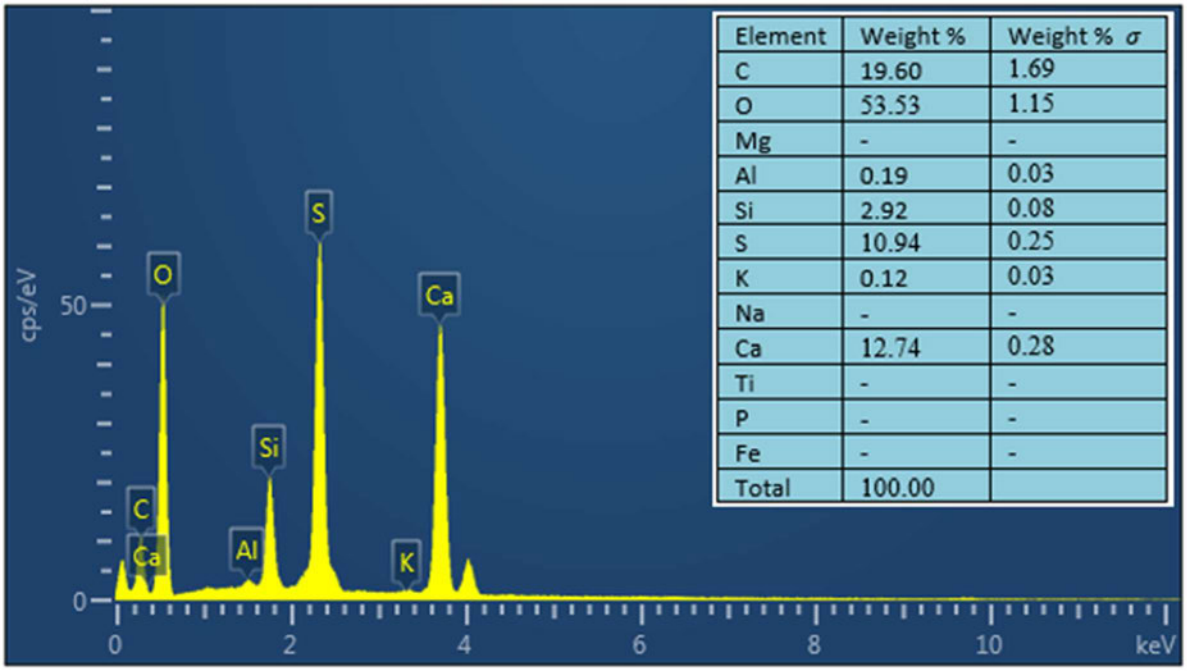


| Element | Weight % | Weight % σ |
|---|---|---|
| C | 19.60 | 1.69 |
| O | 53.53 | 1.15 |
| Mg | - | - |
| Al | 0.19 | 0.03 |
| Si | 2.92 | 0.08 |
| S | 10.94 | 0.25 |
| K | 0.12 | 0.03 |
| Na | - | - |
| Ca | 12.74 | 0.28 |
| Ti | - | - |
| P | - | - |
| Fe | - | - |
| Total | 100.00 | |

Figure 4-62: EDS spectra of corroded product (sample 3)

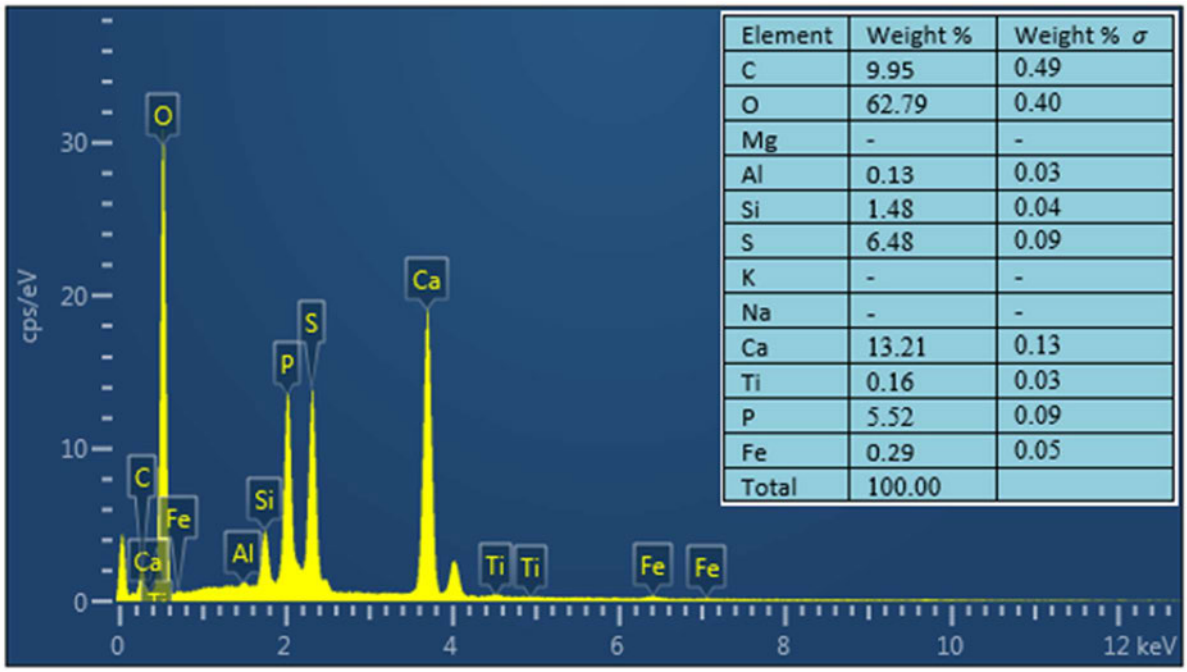


| Element | Weight % | Weight % σ |
|---|---|---|
| C | 9.95 | 0.49 |
| O | 62.79 | 0.40 |
| Mg | - | - |
| Al | 0.13 | 0.03 |
| Si | 1.48 | 0.04 |
| S | 6.48 | 0.09 |
| K | - | - |
| Na | - | - |
| Ca | 13.21 | 0.13 |
| Ti | 0.16 | 0.03 |
| P | 5.52 | 0.09 |
| Fe | 0.29 | 0.05 |
| Total | 100.00 | |

Figure 4-63: EDS spectra of corroded product (sample 4)

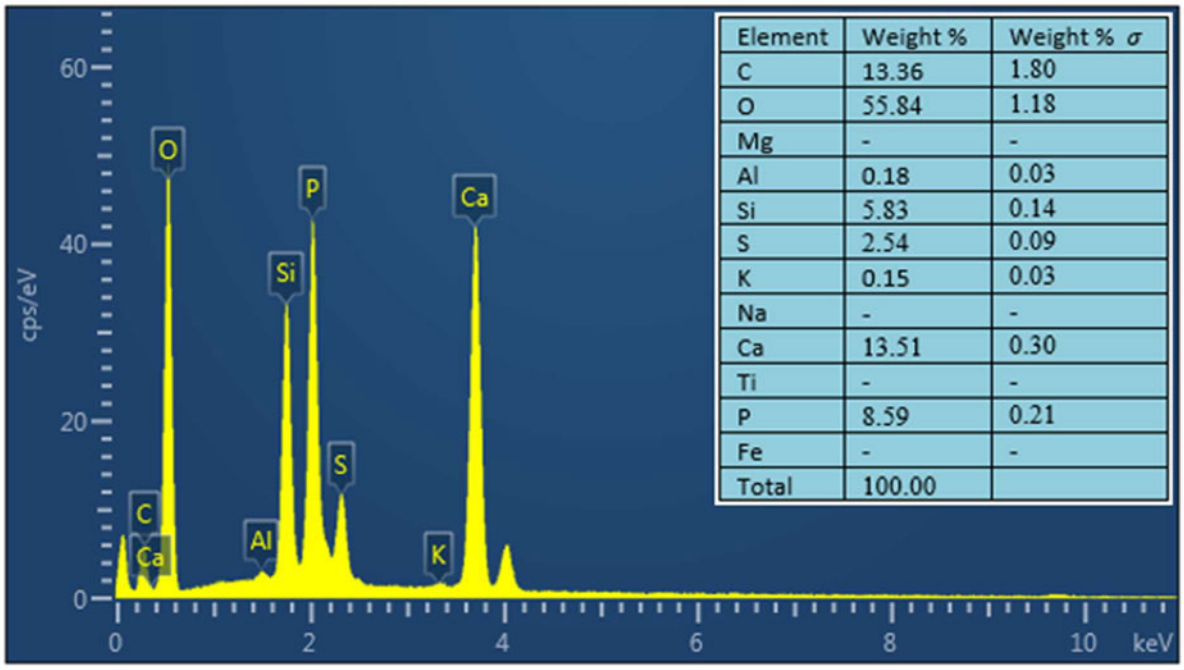


| Element | Weight % | Weight % σ |
|---|---|---|
| C | 13.36 | 1.80 |
| O | 55.84 | 1.18 |
| Mg | - | - |
| Al | 0.18 | 0.03 |
| Si | 5.83 | 0.14 |
| S | 2.54 | 0.09 |
| K | 0.15 | 0.03 |
| Na | - | - |
| Ca | 13.51 | 0.30 |
| Ti | - | - |
| P | 8.59 | 0.21 |
| Fe | - | - |
| Total | 100.00 | |

Figure 4-64: EDS spectra of corroded product (sample 5)

As seen in Figure 4-60 to Figure 4-64, the EDS spectra of the exposed mortar samples (Figure 4-34 to 4-39), especially the exposed $PC_m$ (Figure 4-37) and exposed $PCA_m$ (Figure 4-39), are quite different.

This is due to the difference in exposure duration; the mortar samples ($CAC_m$, $PC_m$ & $PCA_m$) were exposed for a year (12 months) while the concrete wall has been exposed for over 8 years (96 months) since the sewer facility started functioning. It should be noted that the facility concrete walls were constructed using Portland cement, just like $PC_m$ and $PCA_m$.

The EDS spectra of the corrosion products samples (Figure 4-60 to Figure 4-64) indicate peaks of S (sulphur); this was not obvious in the EDS spectra of the mortar samples (Figure 4-34 to Figure 4-39) has it only had $S$ spectrum in its background. Having peaks of $S$ is an indication of MICC, due to the presence of sulphuric acid.

Figure 4-60 to Figure 4-64 also shows peaks of Ca (calcium) which is an indication of the presence of gypsum ($CaSO_4 \cdot 2H_2O$) or/and ettringite ($3CaO \cdot Al_2O_3 \cdot 3CaSO_4 \cdot 32H_2O$) which are the most common product of sulphuric acid attack, as explained in Section 2.4.5. In addition, the EDS spectra of the corrosion products (Figure 4-60 to Figure 4-64) also low peaks of $Si$ (silica) compared to that of the mortar samples (Figure 4-34 to Figure 4-39) which is an indication that most of the fine aggregate have been washed off from the surface of the corroded wall.

Some of the EDS spectra of the corrosion products samples (Figure 4-61, Figure 4-63 & Figure 4-64) also show peaks of $P$ (phosphorous). This was not expected as Portland cement (PC) does not contain any significant amount of $P$, and this has also never been reported in past studies. $P$ (phosphorus) and $P$-based compounds are usually solid; hence, it is very unlikely that it was transferred to the wall through the sewer atmosphere, as was in the case of sulphur ($H_2S_{(g)}$). However, its most likely that the $P$ content in the environment originated from industrial waste added to the body of wastewater which became dissolved phosphorus (liquid phase). It is also possible that the $P$ content emerged from the type of aggregate or admixture used in the construction.

Sample 5 (Figure 4-64) particularly shows high peak of phosphorus and a high % weight compared to the others (Samples 2 & 4). This same sample (Sample 5) has the unidentified substance shown in Figure 4-59, which suggests that the substance contain phosphorus. Nevertheless, further studies are required here.

## 4.7 References

García-Vera, V.E., Tenza-Abril, A.J., Saval, J.M. and Lanzón, M., 2019. Influence of crystalline admixtures on the short-term behaviour of mortars exposed to sulphuric acid. *Materials*, *12*(1), p.82.

Gojević, A., Ducman, V., Netinger Grubeša, I., Baričević, A. and Banjad Pečur, I., 2021. The Effect of Crystalline Waterproofing Admixtures on the Self-Healing and Permeability of Concrete. *Materials*, *14*(8), p.1860.

Hao, O.J., Chen, J.M., Huang, L. and Buglass, R.L., 1996. Sulfate-reducing bacteria. *Critical reviews in environmental science and technology*, *26*(2), pp.155-187.

Okabe, S. and Characklis, W.G., 1992. Effects of temperature and phosphorous concentration on microbial sulfate reduction by Desulfovibrio desulfuricans. *Biotechnology and bioengineering*, *39*(10), pp.1031-1042.

Pazderka, J. and Hájková, E., 2016. Crystalline admixtures and their effect on selected properties of concrete. *Acta Polytechnica*, *56*(4), pp.306-311.

# CHAPTER 5
# CONCLUSIONS & RECOMMENDATIONS

## 5.1 Introduction

The main aims of this research are to study the performance of two cement systems—calcium aluminate cement (CAC)-based system and Portland cement (PC)-based systems—in an aggressive wastewater environment and investigate the effect of a crystalline waterproofing admixture (CWA) in a PC-based mortar exposed to microbially induced concrete corrosion (MICC). To achieve this, mortars were produced using three different mortar mixtures— CAC-based mortars, $CAC_m$, PC-based mortars, $PC_m$, and PC-based mortars with CWA, $PCA_m$.

Microbially induced concrete corrosion (MICC) is the main cause of concrete sewer deterioration, due to the activity of microorganisms—sulphur-reducing bacteria (SRB) and sulphur-oxidizing bacteria (SOB). SRB, which are anaerobes, reduces the sulphate ($SO_4{}^{2-}$) in sewage resulting into the formation of hydrogen sulphide ($H_2S$) within the wastewater. $H_2S$ diffuses through the wastewater and is released into the sewer headspace, as a $H_2S$ gas. The released gas is trapped within moisture condensates on the surface of the concrete walls where it is eventually oxidized, through the activity of SOB, to form sulphuric acid ($H_2SO_4$) which continues to damage the concrete material; where this is not addressed, collapse is imminent.

To achieve the main objective of this study, a suitable site had to be used, one where MICC is active. Mahatma Gandhi Wastewater Pumping Station (MGWWPS) met this criterion and so was used as the exposure site for the mortar mixtures—$CAC_m$, $PC_m$, and $PCA_m$.

## 5.2 Conclusion- sewer environment (MGWWPS)

In order to investigate the sewer environment, wastewater samples were collected and taken through a number of effluent tests—pH, temperature, RDO (Relative Dissolved Oxygen), conductivity, nitrate, ammonia, solids, BOD (Biological Oxygen Demand), COD (Chemical Oxygen Demand), and ICP (Inductively Coupled Plasma) test—as covered in Section 3.3.3.

The average pH of the wastewater was found to be about 7.5 while the average wastewater temperature was found to be 26℃; these are both good conditions for SRB. In addition, the wastewater also had a relatively low DO concentration mostly within the values 0.3 to 1.4 $mg/L$; this results into sulphide build-up within the wastewater, as SRB now have to depend on sulphate as a source of energy. The average standardized conductivity value was found to be about 1142 $\mu S/cm$, while the nitrate ion average concentration and ammonia ion average concentration were found to 4.8 $mg/L$ and 34.3 $mg/L$ respectively. This indicates the decomposition of organic matter within the wastewater. The BOD values (average of 380 $mg/L$) and COD values (average of 420 $mg/L$) also shows that the wastewater contain a good amount of oxidization compounds, which are mostly organic matter.

Results from the solids tests—total solid (TS), volatile solid (VS) and fixed solid (FS)—showed that the wastewater contain 0.12% of TS, which were mostly VS. Results from the ICP analysis, however, revealed an abundance of calcium ($Ca$) and silicon ($Si$) metals, with $Ca$ being 3 to 5 times the abundance of $Si$. The relatively very high concentration of $Ca$ metals in the wastewater suggested the presence of cement hydration products like ettringite ($3CaO.Al_2O_3.3CaSO_4.32H_2O$) and gypsum ($CaSO_4.2H_2O$) within the wastewater due to MICC. The high concentration of $Si$ metals also

suggested the presence of sand particles from the deteriorated concrete mixtures which have been washed down into the liquid phase of the sewer environment.

Besides, the wastewater analysis, site assessment revealed that temperature is the main factor influencing the rate of MICC in the environment, while visual investigations, carried out on the site, confirmed the aggressiveness of the environment. This was evident due to the presence of products of corrosion on the concrete walls, plus the exposure of aggregates, and observed progressive damages on the walls.

## 5.3 Conclusion- CAC-based and PC-based systems

As mentioned in Section 5.1, the main aims of the research are to investigate the performance of three different mortar mixtures—$CAC_m$, $PC_m$, and $PCA_m$—in an aggressive sewer environment; however, these mixtures are made from two cement binding systems—calcium aluminate cement (CAC)-based system and Portland cement (PC)-based systems.

Samples of these mortar mixtures were taken through a strength test, after 28 days curing, and it was found that the CAC-based mortars had a much greater compressive strength of 38.5 $MPa$, which was about three times that of PC-based mortars. The CAC-based mortars also had a greater average density of 2715 $kg/m^3$, while the PC-based mortars had an average densities of 2279 $kg/m^3$ ($PC_m$) and 2353 $kg/m^3$ ($PCA_m$).

After about two months of sample exposure, physical changes were observed on the PC-based mortar which increased over the subsequent months; the CAC-based mortars, however, remained unchanged. After a 12-month exposure, the CAC-based mortar was found to have performed a lot better than the PC-based mortars, in that $CAC_m$ had a 0.87% total mass loss, while the $PC_m$ and $PCA_m$ had a 28.4% and 25.6% total mass loss respectively. The mass loss of each mortar mixture was further used to calculate their average corrosion rate due to MICC; this was found to be 0.02 $mm/year$ for $CAC_m$, 0.7 $mm/year$ for $PC_m$ and 0.6 $mm/year$ for $PCA_m$. These values are a clear indication that CAC-based systems are much more durable than PC-based systems.

SEM images of the exposed samples revealed the microstructural damages that had taken place in the PC-based samples due to acid attack; these damages include the dissociation of C-S-H matrix and the presence of gypsum in the PC-based mixtures. However, the $AH_3$ matrix of the CAC-based sample were not significantly impacted. Although both the PC-based and CAC-based mixtures were exposed to the same aggressive environment, the PC-based mixtures were significantly impacted because of their high calcium hydroxide ($CH$) content, which dissolves—together with the calcium contained in the C-S-H gel—in the presence of acid. This resulted into the opening of the matrix pores, giving room for further acid attack. The CAC-based mixtures, on the other hand, were not significantly impacted as the matrix is predominately alumina-based. As explained in Section 2.7.3, although, some of its hydrates also dissolves, $AH_3$ remains stable down to a pH of about 3 or 4. The dissolution of the other hydrates, however, leads to the formation of more $AH_3$, resulting into greater stability within the binder system.

In addition, the EDS spectra and elemental mappings of the CAC-based mixtures showed no significant difference between exposed and unexposed samples. This was not in case for PC-based mixtures, as noticeable differences were seen in the exposed and unexposed samples, evident by the observed changes in peaks and relative abundance of elements.

## 5.4 Conclusion- effect of crystalline waterproofing admixture (CWA)

Now, focusing on the PC-based mortar mixtures—$PC_m$ and $PCA_m$—which have one difference, which is the inclusion of crystalline waterproofing admixture (CWA) in $PCA_m$ and non-inclusion in $PC_m$. It was found that CWA did not have any significant effect on the compressive strength on $PCA_m$, in that their compressive strengths were close: 13.1 $MPa$ for $PC_m$ and 12.6 $MPa$ for $PCA_m$. A noticeable difference was, however, seen in their performance in the aggressive wastewater environment. $PC_m$ recorded a total mass loss of 28.4% while $PCA_m$ recorded a total mass loss of 25.6%, after 12-month exposure period, resulting into an average corrosion rate 0.7 $mm/year$ for $PC_m$ and 0.6 $mm/year$ for $PCA_m$. Hence, the addition of CWA had a positive effect on the durability of the PC-based mortar $PCA_m$.

The SEM images, EDS spectra and elemental mappings of the two mixtures were found to be quite similar; this is because they have the same cement binder system.

## 5.5 General conclusions

In summary, the following conclusions can be made from the research:

1) CAC-based mortars are much more durable than PC-based mortars, as they showed the greatest resistance to MICC; hence, CAC-based mortars are better alternatives to PC-based mortars for rehabilitation or surface coating of municipal wastewater infrastructures.

2) Crystalline waterproofing admixture (CWA) can be used to improve the performance of PC-based mortars within wastewater infrastructures; however, it should be noted that its addition did not provide a notable resistance to MICC, it only slowed it done slightly.

## 5.6 Recommendations for further work

While this study made some knowledge contributions, the following are recommendations for further work in this area:

1) The research findings were based on a 12-month exposure of the mortar samples within the aggressive environment. However, a long-term study can be done to investigate the long-term performance of the different concrete mixtures.

2) While a wet-dry scenario was considered in this study, as stated in Section 1.5, further similar study can be carried out in consideration of other scenarios such as dry scenario.